THOUSAND CANKERS DISEASE OF EASTERN BLACK WALNUT: ECOLOGICAL INTERACTIONS IN THE HOLOBIONT OF A BARK BEETLE-FUNGAL DISEASE

by

Geoffrey M. Williams

A Dissertation

Submitted to the Faculty of Purdue University

In Partial Fulfillment of the Requirements for the degree of

Doctor of Philosophy

Department of Forestry and Natural Resources

West Lafayette, Indiana

August 2021

THE PURDUE UNIVERSITY GRADUATE SCHOOL
STATEMENT OF COMMITTEE APPROVAL

Dr. Matthew D. Ginzel, Chair
Department of Forestry and Natural Resources
Department of Entomology

Dr. Đenita Hadžiabdić
Department of Entomology and Plant Pathology
University of Tennessee-Knoxville

Dr. John Couture
Department of Forestry and Natural Resources
Department of Entomology

Dr. Michael Jenkins
Department of Forestry and Natural Resources

Approved by:
Dr. Robert Wagner

Dedicated to my teachers, mentors, and peers, past and present, in work and in life.

ACKNOWLEDGMENTS

This work owes many thanks to the guidance, support, encouragement, and intellectual contribution of my committee, Matt Ginzel, Đenita Hadžiabdić, Michael Jenkins and John Couture. On a professional level, the following people also selflessly provided knowledge, wisdom, critical guidance, fresh ideas, assistance, and intangible forms of support: Scott Gula, Matt Ethington, Sara Stack, Tyler Stewart, Kelsey Tobin, Kylle Roy, Holly Wantuch, Justin Schaeffer, Andrew Nelson, Aziz Ebrahimi, Jenny Antonides, Keith Woeste, Rucha Karve, Richard Meilan, Shelly Wischmaier, Samarth Mathur, Jennifer Spitznagel, Theresa Baker, Aaron Onufrak, Sarah Boggess, Hector Urbina, Jorge Ronny Diaz Valderamma, Pedro Pablo Parra Giraldo, Catherine Aime, Stephen Russell, Romina Gazis-Seregina, William Klingeman, Jennifer DeBruyn, Lynn K. Carta, Jamal Faghihi, Veronica Schirm, Lorenzo Cotrozzi, Sylvia Park, James McKenna, Bart Nelson, Reid Nelson, Bob Rupar, Indira Paudel, Robert Swihart, Zhao Ma, Michael Saunders, Douglass Jacobs, Bruce Godfrey, Ashley Howes, Sandy Cho, Colton Prechtel, Taylor Ailes, Sarah Paul, Nick Cazzaniga, Brian Beheler, Sue Cambron, Staci Nugent, Maia Leach, Felix Coronado, Samuel Belteton, Dan Bollock, Dan Cassens, Caleb Kell, Dan Szmanski, Ian Kaplan, Julius Eason, Michael Scharf, Laura Ingwell, Wadih Ghanem, Kevin Hoyt, Tammy Stackhouse, Beant Kapoor, Grace Pietsch, Jeffrey Holland, Diane Warwick, John Conn, Ignazio Carbone, Elisa Lauritzen, Claudia Nischwitz, Teryl Roper, George Newcombe, Mary Ridout, and James White. The following institutions also provided in-kind support: Utah State University, University of Tennessee, University of Idaho, Oak Ridge National Laboratory (ORNL), and the United States Department of Agriculture.

This work was funded by the following sources: Fred M. Van Eck Memorial Foundation, FNR Investments in Excellence Seed Grant, Charles Michler Scholarship, University of Tennessee Department of Entomology and Plant Pathology, the USDA National Institute of Food and Agriculture (NIFA) (Hatch project 1009630: TEN00495), and the Genomic Science Program, U.S. Department of Energy, Office of Science, Biological and Environmental Research, as part of the Plant Microbe Interfaces Scientific Focus Area at ORNL (http://pmi.ornl.gov).

TABLE OF CONTENTS

LIST OF TABLES

LIST OF FIGURES

ABSTRACT

Eastern black walnut (*Juglans nigra* L.) ranks among the most highly valued timber species in the central hardwood forest and across the world. This valuable tree fills a critical role in native ecosystems as a mast bearing pioneer on mesic sites. Along with other *Juglans* spp. (Juglandaceae), *J. nigra* is threatened by thousand cankers disease (TCD), an insect-vectored disease first described in 2009. TCD is caused by the bark beetle *Pityophthorus juglandis* Blackman (Corthylini) and the phytopathogenic fungus *Geosmithia morbida* Kol. Free. Ut. & Tiss. (Bionectriaceae). Together, the *P. juglandis*-*G. morbida* complex has expanded from its historical range in southwest North America throughout the western United States (U.S.) and Europe. This range expansion has led to widespread mortality among naïve hosts *J. nigra* and *J. regia* planted outside their native distributions.

The severity of TCD was previously observed to be highest in urban and plantation environments and outside of the host native range. Therefore, the objective of this work was to provide information on biotic and abiotic environmental factors that influence the severity and impact of TCD across the native and non-native range of *J. nigra* and across different climatic and management regimes. This knowledge would enable a better assessment of the risk posed by TCD and a basis for developing management activities that impart resilience to natural systems. Through a series of greenhouse-, laboratory- and field-based experiments, environmental factors that affect the pathogenicity and/or survival of *G. morbida* in *J. nigra* were identified, with a focus on the microbiome, climate, and opportunistic pathogens. A number of potentially important interactions among host, vector, pathogen and the rest of the holobiont of TCD were characterized. The *holobiont* is defined as the whole multitrophic community of organisms—including *J. nigra*, microinvertebrates, fungi and bacteria—that interact with one another and with the host.

Our findings indicate that interactions among host, vector, pathogen, secondary pathogens, novel microbial communities, and novel abiotic environments modulate the severity of TCD in native, non-native, and managed and unmanaged contexts. Prevailing climatic conditions favor reproduction and spread of *G. morbida* in the western United States due to the effect of wood moisture content on fungal competition. The microbiome of soils, roots, and stems of trees and seedlings grown outside the host native range harbor distinct, lower-diversity communities of

bacteria and fungi compared to the native range, including different communities of beneficial or pathogenic functional groups of fungi. The pathogen *G. morbida* was also associated with a distinct community of microbes in stems compared to *G. morbida*-negative trees. The soil microbiome from intensively-managed plantations facilitated positive feedback between *G. morbida* and a disease-promomting endophytic *Fusarium solani* species complex sp. in roots of *J. nigra* seedlings. Finally, the nematode species *Bursaphelenchus juglandis* associated with *P. juglandis* synergizes with *G. morbida* to cause foliar symptoms in seedlings in a shadehouse; conversely, experiments and observations indicated that the nematode species *Panagrolaimus* sp. and cf. *Ektaphelenchus* sp. could suppress WTB populations and/or TCD outbreaks.

In conclusion, the composition, function, and interactions within the *P. juglandis* and *J. nigra* holobiont play important roles in the TCD pathosystem. Managers and conservationists should be aware that novel associations outside the host native range, or in monocultures, intensive nursery production, and urban and low-humidity environments may favor progression of the disease through the effects of associated phytobiomes, nematodes, and climatic conditions on disease etiology. Trees in higher diversity, less intensively managed growing environments within their native range may be more resilient to disease. Moreover, expatriated, susceptible host species (*i.e., J. nigra*) growing in environments that are favorable to novel pests or pest complexes (*i.e.*, the western U.S.) may provide connectivity between emergent forest health threats (*i.e.*, TCD) and native host populations (*i.e., J. nigra* in its native range).

CHAPTER 1. NATURAL HISTORY OF THE THOUSAND CANKERS DISEASE HOLOBIONT AND SYNTHESIS OF RELEVANT ECOLOGICAL INTERACTIONS

1.1 Introduction

Plant disease and biotic invasions can lead to landscape-scale epidemics, but drivers of such epidemics operate on local scales. At the landscape scale, range expansions of forest pests and emergent diseases of cultivated trees can be understood through the lens of biogeography. Many of the most destructive forest pests affect trees growing outside of their native range. Others involve insects and pathogens that have been introduced to new hosts and geographic areas where they attack native plants that are related to their ancestral hosts (Parker & Gilbert, 2004; Dalin & Björkman, 2008; Paine et al., 2010; Liebhold et al., 2017).

In these novel contexts, pathogens, insects and hosts also interact with and drive the formation of novel communities of plant-associated microorganisms. These communities may have novel function and structure and may form under novel climatic conditions. Interactions within these communities and with the host can function as drivers of plant invasiveness (Baynes et al., 2012; Coats & Rumpho, 2014; Meinhardt et al., 2018; Mamet et al., 2019; Collins et al., 2020; Gornish et al., 2020; Malacrinò et al., 2020; Onufrak et al., 2020). Due to a lack of previous coevolutionary selection on host, vector, and pathogen species in novel holobionts (Margulis et al., 1991; Gordon et al., 2013), the microbiome and the climatic factors that regulate it may have landscape-scale consequences for the resilience of naïve host plants during novel encounters with exotic pests and pathogens. Specifically, these environmental factors may determine the realized range of pests and pathogens, leading to continental-scale differences in the incidence and severity of plant disease or the success of plants within or outside their native range.

Thousand cankers disease (TCD) was discovered and described after recent expansions in the geographic and host range of the bark beetle *Pityophthorus juglandis* Blackman (Curculionidae: Scolytinae) (walnut twig beetle) and its phytopathogenic fungal symbiont *Geosmithia morbida* Kol. Free. Ut. & Tiss. (Sordariomycetes: Hypocreales) (Tisserat et al., 2009, 2011; Kolařík et al., 2011; Seybold et al., 2012, 2019). *Juglans nigra* is native to the eastern U.S., is a novel and evolutionarily naïve host of *P. juglandis*, and is more susceptible to TCD than other *Juglans* spp. (Williams, 1990; Utley et al., 2012; Hefty et al., 2018). The widespread introduction

of *J. nigra* in cultivation west of the Great Plains has provided connectivity between the native range of *J. nigra* in the eastern U.S. and the center of *P. juglandis* and *G. morbida* diversity in the southwest (Tisserat et al., 2011; Hadžiabdić et al., 2014; Zerillo et al., 2014; Rugman-Jones et al., 2015). This novel connectivity between *P. juglandis* and *J. nigra* also coincided geographically with abiotic conditions that are similar to the native range of *P. juglandis* and *G. morbida*. These conditions have favored the development of disease, allowing vector populations to build up, and likely contributed to spillover and spread to the native range of *J. nigra* (Sitz et al., 2021; Chapter 4). This has, in turn, led to widespread mortality of *J. nigra* in the western U.S. However, the impact of TCD on *J. nigra* in the eastern U.S. has been minimal despite repeated introductions of *P. juglands* and *G. morbida* (Hadžiabdić et al., 2014; Zerillo et al., 2014; Rugman-Jones et al., 2015; Seybold et al., 2019). The impact of TCD has also been mostly confined to urban areas, orchards and plantations (Seybold et al., 2019).

In novel encounters between insect-transmitted pathogens and host plants, the development of disease depends jointly on vector fidelity, pathogen virulence, host susceptibility, and environmental factors that include biotic and abiotic conditions (Leach, 1940; Agrios, 2004; Simler et al., 2019). In the context of TCD, host resistance, vector behavior, and pathogen virulence have been studied by others (Utley et al., 2012; Sitz et al., 2017a; Blood et al., 2018; Sitz et al., 2021). Furthermore, disease etiology has been described (Tisserat et al., 2009). Therefore these studies focused on environmental factors that may account for differences in severity of TCD between the native (eastern) and non-native (western) range and between forests and plantations.

To place TCD into a wider ecological and biogeographical context, this overview will first provide a summary background on host, vector, and pathogen natural history. In the later sections of this overview, key findings from this dissertation will be summarized to highlight the abiotic and biotic environmental mechanisms that are likely to contribute to the discrepancy in incidence and severity of TCD between native *vs*. non-native, and plantation *vs*. natural forest contexts. I will briefly discuss the implications of these contextual factors on multipartite interactions among a) phytobiome, climate, and *G. morbida*; b) host, phytobiome, and *G. morbida*; and c) host, *P. juglandis*, *G. morbida*, and nematodes. Finally, all of these interactions will be discussed together. Then the extent to which they can be expected to influence the trajectory of TCD across time and space will be considered from ecological and management perspectives.

1.2 Natural History of *Juglans nigra* and Relatives

Juglans nigra is a long-lived angiosperm, a member of the family Juglandaceae (Fagales), and native to North America. The native range of *J. nigra* extends from the eastern edge of the Great Plains from Texas to South Dakota to the eastern U.S. from Florida to Vermont and Ontario (Williams, 1990). Throughout its range, *J. nigra* can be found regenerating and growing well in disturbed riparian areas and slopes with well drained, nutrient rich soils (Williams, 1990).

Juglans nigra has several adaptations in common with some invasive plants (Blumenthal et al., 2009). The species is shade-intolerant, fast-growing and releases large amounts of the napthoquinone compound juglone into the soil from roots and senescent vegetation (Williams, 1990; McCoy et al., 2018). Juglone is a powerful reducing agent that may interfere with nitrification and the growth of competing vegetation, particularly in poorly aerated soils (Vogel & Dawson, 1986; Ponder Jr, 1987; Thevathasans et al., 1998; Islam & Widhalm, 2020). Perhaps due to its life history strategy as a highly competitive species that exploits resource rich environments including disturbances and alluvial soils, *J. nigra* is not known to form associations with ectomycorrhizal fungi to help it compete for limiting nutrients, unlike other members of the family Juglandaceae (Wang & Qiu, 2006; Corrales et al., 2016, 2018, 2021). *Juglans nigra* has been widely planted throughout western North America and southern Europe (Newton & Fowler, 2009; Moricca et al., 2020). *Juglans* spp. escape from cultivation and have become naturalized in places where animal dispersers of its large, highly-protected seeds are present (Burda & Koniakin, 2018; G. M. Williams, *pers. obs*.).

Escape from coevolved natural enemies in a plant species' range of origin, and resulting competitive advantage in the expanded range over native plant species with their own pathogen associations, can impart invasiveness to species with competitive and resource demanding life histories (Mitchell et al., 2006, Blumenthal et al., 2009; Heger & Jeschke, 2014; Liebhold et al., 2017). In addition to TCD, *J. regia* and *J. nigra* suffer from a number of fungal and nematode root diseases of seedlings, foliar anthracnose, bacterial and fungal cankers, and other infections in their native and introduced ranges (Wilson et al., 1957, 1967; Michler et al., 2004; Chen et al., 2013; Lamichhane, 2014; UC Davis Fruit & Nut Extention, 2021). The decimation of *Juglans* spp., which are otherwise very productive in the western U.S., by a novel insect and pathogen association (*i.e.*, TCD) therefore provides a case study of how plant invasion can be mediated by an evolutionary tradeoff between growth and defense (Stamp, 2003; Mitchell et al., 2006).

Moreover, as elaborated in Chapter 4, TCD provides an example of how novel pathogen assocations may buffer against plant invasions by introduced exotic plants, and even how realized geographic host ranges may be influenced by the geographic limits of favorable environments of potential pests and pathogens.

1.3 Natural History of *P. juglandis* and its Phoretic and Parasitic Associates

The genus *Pityophthorus* Eichoff (Corthylini) is the most diverse in all the Scolytinae and has a worldwide distribution on angiosperm and gymnosperm trees and shrubs (Wood, 1982; Hulcr et al., 2015). The Corthylini are diverse in the western hemisphere and contain multiple lineages of ambrosia beetles (Wood, 1982, 2007). *Pityophthorus juglandis* was recorded historically from California (CA), Arizona (AZ), New Mexico (NM), and Chihuahua, Mexico; in its historic range, *P. juglandis* breeds in *J. californica*, a highly endemic host species, and *J. major*, whose range extends south into central Mexico (Bright, 1981). Like the other destructive coleopteran forest pests in North America *Agrilus auroguttatus*, *A. prionurus*, *Dendroctonus ponderosae* and *D. frontalis*, the geographic range of *P. juglandis* has recently expanded farther north than its previous historical limit (Havill et al., 2019). In its expanded range, *P. juglandis* has come into contact with expatriate populations of *J. nigra* and caused mortality among new host species (Cullingham et al., 2011; Seybold et al., 2012; Rugman-Jones et al., 2015; Lesk et al., 2017).

The lifecycle of *P. juglandis* is relatively short in comparison to many other *Pityopthorus* spp. (Furniss & Kegley, 2018). The beetle can complete one to several generations in a year, typically has overlapping generations, and overwinters as both larvae and adults (Luna et al., 2013; Sitz et al., 2017b). Individual males typically fly ~100 m but can disperse up to 2 km to select branches. Male *P. juglandis* excavate a nuptial chamber and release the mating pheromone 3-methyl-2-buten-1-ol to attract and mate with up to eight females (Seybold et al., 2013; Faccoli et al., 2016; Kees et al., 2017). Over the course of six to eight weeks, the females excavate egg galleries, and larvae hatch, complete three instar stages, eclose, and emerge (Dallara et al., 2012).

When they disperse, males and females carry hydrophobic spores of *G. morbida* which cling to their elytra by hydrostatic adhesion (Seybold et al., 2016). Many individuals also carry phoretic and parasitic mites and nematodes (Seybold et al., 2016; Ryss et al., 2020; G. M. Williams, *pers. obs.*; Chapter 5). At the time of host colonization and gallery initiation, these microorganisms are

shed or actively disperse from vector beetles to colonize the galleries and surrounding host tissue (Massey, 1974; Tisserat et al., 2009; Hofstetter et al., 2015). By the time the lifecycle of *P. juglandis* is complete, *G. morbida* kills, colonizes, and sporulates from surrounding host tissue in the galleries, and nematodes and mites reproduce and aggregate on or inside of larvae and adult beetles. When *P. juglandis* leave the galleries in search of new host material in which to mate and reproduce, they carry the microinvertebrates and fungal spores with them to new trees.

1.4 Natural History of *Geosmithia morbida* and *Geosmithia* spp.

Geosmithia spp. are diverse and found on many substrates, including plant material and soil, but they are most frequently found in the galleries of bark and ambrosia beetles (Kolařík et al., 2008). *Geosmithia* spp. also have a worldwide distribution that includes Asia, central America, and northern Mexico (Wu et al., 2013; Kolařík et al., 2017; Juan Alfredo et al., 2020; Zhang et al., 2021). There is at least one linage of primary ambrosia fungi in the *Geosmithia* genus but pathogenicity has only been known to evolve in *G. morbida* and *Geosmithia* sp. 41 (Schuelke et al., 2016, 2017). *Geosmithia* spp. are known only as mitosporic fungi and have two developmental modes for condiogenesis; persistent chains of cylindrical to ellipsoid conidia produced from phialides on penicilliate conidiophores and yeastlike substrate conidia produced from substrate mycelium (Kolarík et al., 2004; Kolarik et al., 2005; Kolařík et al., 2011); both routes of conidiogenesis occur in *G. morbida*. The production of soluble pigments in the media are also a common feature of the *Geosmithia* genus. In *G. morbida* pigmentation ranges in color from light-yellow to orange; in *G. lavendula* these pigments include three-ringed anthraquinones, but their identity in *G. morbida* has not been confirmed (Stodůlková et al., 2010). Given their affinity for Scolytinae, pigments and modes of conidiogenesis of *Geosmithia* are likely to be adaptations to the bark beetle niche, but their significance in this regard is poorly understood.

Fungi in the genus *Geosmithia* have intimate associations with other fungi and these associations may have consequences for the evolution of pathogenicity and etiology of disease (Pepori et al., 2018). *Geosmithia* has been placed in the family Bionectriaceae, which includes mycoparasites such as *Clonostachys* spp. *Geosmithia* spp. can form mycoparasitic associations with other fungi (Karlsson et al., 2015). It is presumably through mycoparasitism that they have acquired pathogenicity genes through lateral gene transfer with co-occurring, highly virulent

pathogenic associates of bark beetles such as *Ophiostoma* spp. (Bettini et al., 2014; Pepori et al., 2018). In a study of *P. juglandis* galleries in the eastern and western U.S., fungi in the genus *Sporothrix* (=*Ophiostoma*) were found to co-occur with *G. morbida*, raising the possibility of a similar association with *G. morbida* (Gazis et al., 2018). Despite their abundance and diversity as symbionts of bark and ambrosia beetles, the role that *Geosmithia* spp. play in the fitness of scolytine vectors is poorly understood.

Available evidence points to a function of *G. morbida* as a key component of the microbiome of *P. juglandis*. Foremost among this evidence are repeated observations that the tissues that *P. juglandis* larvae consume are first necrotized by *G. morbida* introduced by colonizing adults (Kolarik et al. 2011, Tisserat et al. 2009). *G. morbida* is consistently isolated from *P. juglandis* and *P. juglandis* galleries throughout its native range (Kolarik et al. 2011, Tisserat et al. 2009, Zerillo et al. 2014, Gazis et al. 2017), though the beetle does not have mycangia, a criterion that has been generally used to consider other fungi as primary symbionts of other bark beetle species (Hofstetter et al. 2015). The ecological dependence of the fungus on a close association with the beetle is further suggested by a highly reduced genome compared with other *Geosmithia* species; the inability to utilize mineral nitrogen compared to other *Geosmithia* spp. which grow on minimal media; and selective pathogenicity for suitable hosts of *P. juglandis* (Kolařík et al., 2011; Schuelke et al., 2017, Hefty et al. 2018, Utley et al. 2010). In a cluster analysis of metabolic functional traits across the genus *Geosmithia, G. morbida* clustered with two of the tree ambrosial species in the analysis (Veselká et al., 2019). These features suggest a higher level of dependence and specificity compared to close relatives. However, like other *Geosmithia* spp., the ecological role of *G. morbida* in the beetle lifecycle is not totally clear. Unlike other groups of primary beetle-associated fungi in the Microascales, which contain virulent pathogens, and Ophiostomatales, which cause sap-stain, vascular stress or systemic wilt, *G. morbida* is only known to cause necrosis in the phloem around bark beetle galleries (Ploetz et al., 2013).

Symbioses fall along a spectrum that includes mutualism and parasitism depending on the cost-benefit ratio of associations (Margulis et al., 1991; Douglas, 1994). Most organisms engage in mutualistic interactions (Herre et al., 1999). Mutualistic fungi provide precursors for important metabolites to bark beetles, weaken host defenses to facilitate colonization, or help beetles to acquire nutrients such as nitrogen (Six, 2013). Alternatively, some bark-beetle associated fungi such as *O. minus* are considered antagonists of beetles because they are known to compete with

beetle-mutualistic fungi and beetles for nutrients (Klepzig et al., 2001). In the case of ambrosia beetles, the mutualistic primary ambrosia fungi provide all the nutrition for beetle development. *Geosmithia* spp. have been generalized as commensal associates of bark and ambrosia beetles, but few species are considered to be pathogenic (Zhang et al., 2021). As a pathogen, *G. morbida* must metabolize host defensive chemicals to colonize its substrate (Agrios 2004; Scheulke et al., 2016, 2017). In this capacity, pathogenic *G. morbida* likely provides nutritional or metabolic benefits by making host-derived nutrients more readily available to *P. juglandis,* or helps the beetle to overcome host defenses during colonization (Six & Wingfield, 2010).

1.5 Interactions Among the Microbiome of *J. nigra*, the Abiotic Environment, and *G. morbida*

Direct interactions among fungi in aboveground parts of mature trees may alter the progression of disease (Rodriguez et al., 2009). The range of these interactions can be classified as either antagonism or facilitation.

Fungal competition is dynamic and outcomes are highly dependent on the abiotic environment (Rayner & Boddy, 1988), and this dependence has consequences for the biogeography of TCD. We found that differences in wood moisture content led to contrasting expected outcomes for competition among *G. morbida* and other fungi in walnut wood (Chapter 4). In the western U.S., *G. morbida* is expected to outcompete other fungi and sporulate abundantly, which should lead to passive dispersal by *P. juglandis* and additional disease cycles as *P. juglandis* initiates new galleries in the branches of *J. nigra* trees. In the eastern U.S., *G. morbida* is expected to be outcompeted by other fungi such as *Trichoderma*, *Clonostachys*, and *Aspergillus* spp. that are better adapted to prevailing environmental conditions and may even exploit beetles or other fungi as a food source. Based on this observation, *G. morbida* and *P. juglandis* may not be as competitive with native fungi in the native range of *J. nigra*.

The effect of direct interactions among fungi and primary fungal associates of bark beetles such as *G. morbida* therefore depend on environmental. As has been suggested for other bark beetle-fungal relationships, environmentally-dependent interactions among fungi within the bark beetle holobiont may determine the realized geographic range of destructive forest pests (Hofstetter et al., 2007; Six & Bentz, 2007). Though prevailing climate may currently limit its impact in the eastern U.S. by favoring competing fungi in wood, increases in the severity and

impact of TCD in the eastern U.S. is possible in the future (Chapter 4). Furthermore, plantations and urban areas may be expected to promote *G. morbida* in competition with other fungi due to higher-temperature and low-humidity microclimates (Imhoff et al., 2010).

Juglans nigra also harbors xerophilic fungi in its native range that could antagonize *G. morbida* under conditions that otherwise might favor disease (Chapter 4). Because these fungi have the potential to control TCD, it is worth investigating the potential use of xerophilic fungi that successfully compete with and antagonize *G. morbida* in low-moisture wood. Climate also determines the favorability of environmental conditions for other associates including microinvertabrates that may also have an impact on disease etiology as discussed below in Section 1.7 (Hofstetter et al., 2007; Chapter 5).

1.6 Interactions Among *J. nigra*, its Microbiome, and *G. morbida*

The effect of the microbiome on plant health is likely to be driven by interactions at a higher level of complexity than the bipartite competitive or facilitative interactions discussed above (Porras-Alfaro & Bayman, 2011). The idea of emergent properties—which include metabolic pathways completed by multiple members and the host—are routinely discussed in the study of the microbiome in the context of animal disease (Tataru & David 2021). As has been found in animal microbiomes, emergent properties of plant microbiomes could ultimately impart resilience to hosts. Alternatively, emergent properties could push hosts into a state of dysbiosis where they are unable to maintain their physiological state in equilibrium (Coyte et al., 2015; van der Heijden & Hartmann, 2016). A state of dysbiosis could then precondition the host or result in heightened susceptibility for development of disease (Manion, 1981; Eyles et al., 2010; Vega Thurber et al., 2020).

A number of sources of perturbation or disturbance, including stress, mutualists, and pethogens, have the capacity to push the composition and function of the plant microbiome into alternative stable states conditions (Amor et al., 2020; Jiang et al., 2020; Wang et al. 2021). In the context of TCD, such sources of perturbation include infection with *G. morbida* and/or attack by *P. juglandis* (Chapters 2 & 3), management practices (Chapter 2), the environment in which *J. nigra* seedlings are grown (Chapters 2 & 6), and the feeding of activity of micoinvertebrates (Chen

& Ferris, 1999). Alternative states, including patterns of cooccurrence between taxa, functional groups, or emergent properties in the microbiome may impart equilibrium or dysbiosis to the host.

In support of alternative stable states in the microbiome and their impact on plant disease, the microbiome has differing composition and contrasting potential impacts on TCD between the native and non-native host range (Chapters 2, 3, and 6). A culture-free investigation of the microbiome was conducted in five grafted genotypes and open pollinated *J. nigra* growing in TCD-free IN, an active TCD epicenter in WA, and locations that previous experienced a TCD outbreak in TN (Chapter 2). The microbiome of mature trees differed among the three locations but differed most outside the native range (WA), where communities of potentially beneficial and pathogenic fungi were also found to be unique and novel compared to IN and TN. Evidence for alternative stable states in the microbiome was discovered in WA in association with the stems of *G. morbida*-positive and negative trees.

In TN, evidence was also found for alternative stable states, but it was unclear whether they could be attributed to past perturbation by transient TCD outbreaks (an experimentally-demonstrated possibility—see Amor et al., 2020), or to differences in management histories or initial conditions among sites in TN. Alternative states in the *J. nigra* microbiome could have been an artifact in the study design in TN if management conditions or initial conditions accounted for the appearance of alternative stable states. Clones grew in plantations but "bedrun" (ungrafted, open pollinated) trees were sampled in less intensively managed or unmanaged environments on forest edges. These bedrun trees were more similar to one another between IN and TN than the other trees in the study.

Culture-dependent study of the root endosphere of seedlings provided further evidence that perturbation of the microbiome by pathogens or initial microbial "legacy effects" (Berendsen et al., 2018) can push communities into alternative states (Chapter 6). When seeds were sown in IN and WA, it was observed that a distinct assemblage of fungi were recruited to the roots and shoots of seedlings from the two states. IN- and WA-derived rhizosphere and stem microbiomes also contained distinct facilitators and antagonists of *G. morbida* pathogenicity as determined by positive and negative correlation with necrotic area of cankers and inoculation points. The microbiome from roots of seedlings sown in WA and IN plantations differed substantially from that of nursery-grown seedlings from IN in a prior study (Chapter 3).

Forest management practices have an effect on the plant microbiome that have downstream consequences for susceptibility to disease (Chapter 3). When nursery-grown seedlings were grown in potting media amended with sterile, plantation, or forest soils, the response of a disease synergist, *Fusarium solani* species complex sp. in seedling roots, to *G. morbida* inoculation depended on the soil amendment. Nursery-grown seedlings amended with forest soil had the smallest cankers and experienced the least amount of feedback as measured by changes in the abundance of the most dominant members of microbial communities in roots—*Rhizoctonia* and *Fusarium* spp. Feedback of *G. morbida* inoculation on *Fusarium* in roots was positive and greatest in nursery-grown seedlings amended with plantation soil, suggesting that high host density in plantations accumulates a microbiome that is less resilient to purturbations caused by disease. Nursery-grown seedlings amended with sterile soil were most susceptible to *G. morbida* as measured by the size of necrotic cankers, indicating that nursery practices generate seedlings with unhealthy root microbiomes. By contrast, the buffering effect of the forest soil and its suppression of *Fusarium* spp. in the rhizosphere may have accounted for smaller cankers caused by *G. morbida*.

1.7 Interactions Among *J. nigra, P. juglandis, G. morbida,* and Nematodes

Like those in soils and other environments, fungal communities in plants may be influenced by the presence of microinvertebrates, which are much larger than microbesa, mobile, and feed on fungi, host tissue, and one another (Chen & Ferris, 1999; Yeates, 2003; Wagg et al., 2014). Through their influence on microbial communities and impacts on the host, microinvertebrates can have a top-down effect on plant disease (Busby et al., 2019). Previously, several mite species, which can alter fungal-fungal interactions in the bark beetle holobiont were found in association with Dutch elm disease (Hofstetter & Moser, 2014), and nematode species were found in association with TCD (Chapter 5).

Nematodes were studied broadly in the context of TCD in WA (Chapter 5). *P. juglandis* colonizing *J. nigra* in WA was found to associate with nematodes in three different genera. These included cf. *Ektaphelenchus* sp., internal parasites that potentially reduced fecundity of *P. juglandis* (Massey, 1974). *Bursaphelenchus juglandis* Ryss, Park., Álv., Nad. & Subb., a potential disease synergist, was associated with decline of shade-grown seedlings. The abundance of both of cf. *Ektaphelenchus* and *B. juglandis* associates increased with host density and *B. juglandis*

appeared to be more abundant in trees in later stages of decline that no longer harbored large *P. juglandis* populations. *B. juglandis* was found associated with an ambrosia beetle, *Anisandrus dispar* Fab., which could be a later successor after *P. juglandis* associated with TCD in WA. Both inside and outside of disease epicenters, a third species of nematode, *Panagrolaimus* sp. was also found that antagonizes *G. morbida* and decreases the size of cankers. In two studies it was determined that canker size was most strongly influenced by host genetics, followed by the presence of the nematode.

1.8 Synthesis

In sum, ecological interactions in the TCD pathosystem are consistent with the hypothesis that such interactions partly determine the impact of TCD across time, space, and forest management practices. In urban areas, plantations, dry and hot climates, and within the overlapping expanded ranges of *P. juglandis* and *J. nigra*, environmental conditions and microbiota jointly favor the development of TCD. These factors contribute to disease progression through the influence of low-humidity continental climate and microclimate, the resulting competitive advantage of *G. morbida* over other fungi, the abundance of opportunistic pathogens and novel fungal associations, and emergent properties and associations within the microbiome. Furthermore, nursery practices may impoverish the rhizosphere in *J. nigra* seedlings of beneficial associations that are still not well understood or explored. At the same time, such practices may promote disease synergists such as *Fusarium solani* species complex spp. A wide diversity and distinct community of fungi was also observed from the roots and rhizospheres of black walnut trees amended with forest soil or germinated in the field. The function of these fungi, which include members of the mycorrhizae-rich fungal taxonomic groups Sebacinales, Helotiales, and Cantherellales, in nutrient acquisition and buffering of biotic and abiotic host stress merits further investigation (Chapter 5).

This work expands our understanding of the influence of biotic interactions in the etiology of TCD and novel encounters between host trees, bark beetles and pathogenic fungi. To the classic disease triangle, we have added key natural enemies such as mycoparasitic and antagonistic fungi in branches and freeliving and entomoparasitic nematodes, beneficial fungi and bacteria in the rhizosphere, disease synergists and opportunistic pathogens. This body of work indicates that the potential geographic range of TCD is determined in part by the abiotic environment and its

influence on biotic interactions. From a management perspective, this knowledge may aid in the development of adaptive management practices to manipulate the plant and soil microbiome to promote forest resilience and to bolster host resistance to pests in native and novel environments.

1.9 References

Agrios, G. (2004). *Plant pathology: Fifth edition*. doi:10.1016/C2009-0-02037-6.

Amor, D. R., Ratzke, C., & Gore, J. (2020). Transient invaders can induce shifts between alternative stable states of microbial communities. *Scientific Advances,* 6. doi:10.1126/sciadv.aay8676.

Baynes, M., Newcombe, G., Dixon, L., Castlebury, L., & O'Donnell, K. (2012). A novel plant-fungal mutualism associated with fire. *Fungal Biology,* 116, 133–144. doi:10.1016/j.funbio.2011.10.008.

Berendsen, R. L., Vismans, G., Yu, K., Song, Y., de Jonge, R., Burgman, W. P., et al., (2018). Disease-induced assemblage of a plant-beneficial bacterial consortium. *ISME Journal*, 12, 1496–1507. doi:10.1038/s41396-018-0093-1.

Bettini, P. P., Frascella, A., Kolařík, M., Comparini, C., Pepori, A. L., Santini, A., Scala, F. & Scala, A., (2014). Widespread horizontal transfer of the cerato-ulmin gene between *Ophiostoma novo-ulmi* and *Geosmithia species*. *Fungal Biology,* 118, 663–674. doi:https://doi.org/10.1016/j.funbio.2014.04.007.

Blood, B. L., Klingeman, W. E., Paschen, M. A., Hadžiabdić, Đ., Couture, J. J., & Ginzel, M. D. (2018). Behavioral Responses of *Pityophthorus juglandis* (Coleoptera: Curculionidae: Scolytinae) to Volatiles of Black Walnut and Geosmithia morbida (Ascomycota: Hypocreales: Bionectriaceae), the Causal Agent of Thousand Cankers Disease. *Environmental Entomology,* 47, 412–421. doi:10.1093/ee/nvx194.

Blumenthal, D., Mitchell, C. E., Pyšek, P., & Jarošík, V. (2009). Synergy between pathogen release and resource availability in plant invasion. *PNAS,* 106, 7899–7904. doi:10.1073/pnas.0812607106.

Bright, D. E. (1981). Taxonomic monograph of the genus *Pityophthorus* Eichoff in North and Central Americs (Coleoptera: Scolytidae). *Memoirs of the Entomological Society of Canada*, 113, 1–378. doi:10.4039/entm113118fv.

Burda, R. I., & Koniakin, S. N. (2018). Spontaneous Dispersion of Species of the Genus *Juglans* L. in the Forests and Parks of Kyiv. *Russian Journal of Biological Invasions*, 9, 95–107. doi:10.1134/S2075111718020029.

Busby, P. E., Crutsinger, G., Barbour, M., & Newcombe, G. (2019). Contingency rules for pathogen competition and antagonism in a genetically based, plant defense hierarchy. *Ecology and Evolution,* 9, 6860–6868. doi:https://doi.org/10.1002/ece3.5253.

Chen, J., & Ferris, H. (1999). The effects of nematode grazing on nitrogen mineralization during fungal decomposition of organic matter. *Soil Biology and Biochemistry*, 31, 1265–1279.

Chen, S., Morgan, D. P., Hasey, J. K., Anderson, K., & Michailides, T. J. (2013). Phylogeny, Morphology, Distribution, and Pathogenicity of Botryosphaeriaceae and Diaporthaceae from English Walnut in California. *Plant Disease*, 98, 636–652. doi:10.1094/PDIS-07-13-0706-RE.

Coats, V. C., & Rumpho, M. E. (2014). The rhizosphere microbiota of plant invaders: an overview of recent advances in the microbiomics of invasive plants. *Frontiers in Microbiology*, 5, 368. doi:10.3389/fmicb.2014.00368.

Collins, C. G., Spasojevic, M. J., Alados, C. L., Aronson, E. L., Benavides, J. C., Cannone, N., Caviezel, C., Grau, O., Guo, H., Kudo, G. & Kuhn, N. J. (2020). Belowground impacts of alpine woody encroachment are determined by plant traits, local climate, and soil conditions. *Global Change Biology*, 26, 7112–7127. doi:https://doi.org/10.1111/gcb.15340.

Corrales, A., Henkel, T. W., & Smith, M. E. (2018). Ectomycorrhizal associations in the tropics – biogeography, diversity patterns and ecosystem roles. *New Phytologist*, 220, 1076–1091. doi:https://doi.org/10.1111/nph.15151.

Corrales, A., Mangan, S. A., Turner, B. L., & Dalling, J. W. (2016). An ectomycorrhizal nitrogen economy facilitates monodominance in a neotropical forest. *Ecology Letters*, 19, 383–392. doi:https://doi.org/10.1111/ele.12570.

Corrales, A., Xu, H., Garibay-Orijel, R., Alfonso-Corrado, C., Williams-Linera, G., Chu, C., Truong, C., Jusino, M. A., Clark-Tapia, R., Dalling, J. W. and Liu, Y. (2021). Fungal communities associated with roots of two closely related Juglandaceae species with a disjunct distribution in the tropics. *Fungal Ecology*, 50, 101023. doi:https://doi.org/10.1016/j.funeco.2020.101023.

Coyte, K. Z., Schluter, J., & Foster, K. R. (2015). The ecology of the microbiome: Networks, competition, and stability. *Science* 350, 663–666. doi:10.1126/science.aad2602.

Cullingham, C. I., Cooke, J. E. K., Dang, S., Davis, C. S., Cooke, B. J., & Coltman, D. W. (2011). Mountain pine beetle host-range expansion threatens the boreal forest. *Molecular Ecology*, 20, 2157–2171.

Dalin, P., & BjöRkman, C. (2008). Native insects colonizing introduced tree species—patterns and potential risks. In T. D. Paine (Ed.), *Invasive forest insects, introduced forest trees, and altered ecosystems* (pp. 63–77). Springer.

Dallara, P. L., Flint, M. L., & Seybold, S. J. (2012). An analysis of the larval instars of the walnut twig beetle, *Pityophthorus juglandis* Blackman (Coleoptera: Scolytidae), in northern California black walnut, *Juglans hindsii*, and a new host record for *Hylocurus hirtellus*. *Pan-Pacific Entomologist*, 88, 248–266.

Douglas, A. E. (1994). *Symbiotic interactions*. Oxon, GB: Oxford University Press, 1994.

Eyles, A., Bonello, P., Ganley, R., & Mohammed, C. (2010). Induced resistance to pests and pathogens in trees. *New Phytologist*, 185: 893–908.

Faccoli, M., Simonato, M., & Rassati, D. (2016). Life history and geographical distribution of the walnut twig beetle, *Pityophthorus juglandis* (Coleoptera: Scolytinae), in southern Europe. *Journal of Applied. Entomology*, 140, 697–705. doi:https://doi.org/10.1111/jen.12299.

Furniss, M. M., & Kegley, S. J. (2018). Biology of *Pityophthorus pulchellus tuberculatus* (Coleoptera: Curculionidae: Scolytinae) in Lodgepole Pine in Northern Idaho. *Environmental Entomology*, 47, 775–780. doi:10.1093/ee/nvy058.

Gazis, R., Poplawski, L., Klingeman, W., Boggess, S. L., Trigiano, R. N., Graves, A. D., Seybold, S. J., & Hadžiabdić, Đ.. (2018). Mycobiota associated with insect galleries in walnut with thousand cankers disease reveals a potential natural enemy against *Geosmithia morbida*. *Fungal Biology*, 122, 241–253. doi:10.1016/j.funbio.2018.01.005.

Gordon, J., Knowlton, N., Relman, D. A., Rohwer, F., & Youle, M. (2013). Superorganisms and holobionts. *Microbe*, 8, 152–153.

Gornish, E. S., Franklin, K., Rowe, J., & Barberán, A. (2020). Buffelgrass invasion and glyphosate effects on desert soil microbiome communities. *Biological Invasions*, 22, 2587–2597. doi:10.1007/s10530-020-02268-8.

Hadžiabdić, Đ., Vito, L. M., Windham, M. T., Pscheidt, J. W., Trigiano, R. N., & Kolařík, M. (2014). Genetic differentiation and spatial structure of *Geosmithia morbida*, the causal agent of thousand cankers disease in black walnut (*Juglans nigra*). *Current Genetics*, 60. doi:10.1007/s00294-013-0414-x.

Havill, N. P., Cognato, A. I., Del-Val, E., Rabaglia, R. J., & Garrick, R. C. (2019). New molecular tools for *Dendroctonus frontalis* (Coleoptera: Curculionidae: Scolytinae) reveal an east–west genetic subdivision of early Pleistocene origin. *Insect Systematics and Diversity*, 3(2), 2.

Hefty, A. R., Aukema, B. H., Venette, R. C., Coggeshall, M. V, McKenna, J. R., & Seybold, S. J. (2018). Reproduction and potential range expansion of walnut twig beetle across the Juglandaceae. *Biological Invasions*, 20, 2141–2155. doi:10.1007/s10530-018-1692-5.

Herre, E. A., Knowlton, N., Mueller, U. G., & Rehner, S. A. (1999). The evolution of mutualisms: exploring the paths between conflict and cooperation. *Trends in Ecology and Evolution*, 14, 49–53. doi:https://doi.org/10.1016/S0169-5347(98)01529-8.

Hofstetter, R. W., Dempsey, T., Klepzig, K., & Ayres, M. (2007). Temperature-dependent effects on mutualistic, antagonistic, and commensalistic interactions among insects, fungi and mites. *Community Ecology*, 8, 47–56. doi:10.1556/comec.8.2007.1.7.

Hofstetter, R. W., Dinkins-Bookwalter, J., Davis, T. S., & Klepzig, K. D. (2015). Symbiotic associations of bark beetles. In F. Vega and R. Hofstetter (Eds.), *Bark Beetles: Biology and Ecology of Native and Invasive Species* (pp 209–245). Academic Press.

Hofstetter, R. W., & Moser, J. C. (2014). The Role of Mites in Insect-Fungus Associations. *Annual Review of Entomology*, 59, 537–557. doi:10.1146/annurev-ento-011613-162039.

Hulcr, J., Atkinson, T. H., Cognato, A. I., Jordal, B. H., & McKenna, D. D. (2015). Morphology, taxonomy, and phylogenetics of bark beetles. In F. Vega and R. Hofstetter (Eds.), *Bark Beetles: Biology and Ecology of Native and Invasive Species*, (pp 209–245). Academic Press.

Imhoff, M. L., Zhang, P., Wolfe, R. E., & Bounoua, L. (2010). Remote sensing of the urban heat island effect across biomes in the continental USA. *Remote Sensing of the Environment*, 114, 504–513.

Islam, A. K. M. M., & Widhalm, J. R. (2020). Agricultural Uses of Juglone: Opportunities and Challenges. *Agronomy*, 10. doi:10.3390/agronomy10101500.

Jiang, J., Abbott, K. C., Baudena, M., Eppinga, M. B., Umbanhowar, J. A., & Bever, J. D. (2020). Pathogens and mutualists as joint drivers of host species coexistence and turnover: implications for plant competition and succession. *The American Naturalist*, 195(4), 591-602.

Juan Alfredo, H.-G., Gerardo, C.-R., Nallely Guadalupe, A.-O., Lourdes, V.-T., César, H.-R., & Francisco, A.-T. (2020). Phylogenetic Position of *Geosmithia* spp. (Hypocreales) Living in *Juniperus* spp. Forests (Cupressaceae) with Bark Beetles of *Phloeosinus* spp. (Scolytinae) from the Northeast of Mexico. *Forests*, 11. doi:10.3390/f11111142.

Karlsson, M., Durling, M.B., Choi, J., Kosawang, C., Lackner, G., Tzelepis, G. D., Nygren, K., Dubey, M. K., Kamou, N., Levasseur, A. and Zapparata, A. (2015). Insights on the Evolution of Mycoparasitism from the Genome of *Clonostachys rosea*. *Genome Biology and Evolution*, 7, 465–480. doi:10.1093/gbe/evu292.

Kees, A. M., Hefty, A. R., Venette, R. C., Seybold, S. J., & Aukema, B. H. (2017). Flight Capacity of the Walnut Twig Beetle (Coleoptera: Scolytidae) on a Laboratory Flight Mill. *Environmental Entomology*, 46, 633–641. doi:10.1093/ee/nvx055.

Klepzig, K. D., Moser, J. C., Lombardero, F. J., Hofstetter, R. W., & Ayres, M. P. (2001). Symbiosis and competition: complex interactions among beetles, fungi, and mites. *Symbiosis*, 30, 83–96.

Kolařík, M., Freeland, E., Utley, C., & Tisserat, N. (2011). *Geosmithia morbida* sp. nov., a new phytopathogenic species living in symbiosis with the walnut twig beetle (*Pityophthorus juglandis*) on *Juglans* in USA. *Mycologia*, 103. doi:10.3852/10-124.

Kolařík, M., Hulcr, J., Tisserat, N., De Beer, W., Kostovčík, M., Kolaříková, Z., Seybold, S. J. and Rizzo, D. M. (2017). *Geosmithia* associated with bark beetles and woodborers in the western USA: taxonomic diversity and vector specificity. *Mycologia*, 109, 185–199.

Kolařík, M., Kubátová, A., Hulcr, J., and Pažoutová, S. (2008). *Geosmithia* Fungi are Highly Diverse and Consistent Bark Beetle Associates: Evidence from their Community Structure in Temperate Europe. *Microbial Ecology*, 55, 65–80. doi:10.1007/s00248-007-9251-0.

Kolařík, M., Kubátová, A., Pažoutová, S., & Šrûtka, P. (2004). Morphological and molecular characterisation of *Geosmithia putterillii*, *G. pallida* comb. nov. and *G. flava* sp. nov., associated with subcorticolous insects. *Mycological Research*, 108, 1053–1069. doi:https://doi.org/10.1017/S0953756204000796.

Kolařík, M., Kubatova, A., van Cepicka, I., Pazoutova, S., & Srutka, P. (2005). A complex of three new white-spored, sympatric, and host range limited *Geosmithia* species. *Mycological Research*, 109, 1323–1336. doi:https://doi.org/10.1017/S0953756205003965.

Lamichhane, J. R. (2014). *Xanthomonas arboricola* Diseases of Stone Fruit, Almond, and Walnut Trees: Progress Toward Understanding and Management. *Plant Disease*, 98, 1600–1610. doi:10.1094/PDIS-08-14-0831-FE.

Leach, J. G. (1940). *Insect transmission of plant diseases.* New York, NY: McGraw-Hill.

Lesk, C., Coffel, E., D'Amato, A. W., Dodds, K., & Horton, R. (2017). Threats to North American forests from southern pine beetle with warming winters. *Nature Climate Change,* 7, 713–717. doi:10.1038/nclimate3375.

Liebhold, A. M., Brockerhoff, E. G., Kalisz, S., Nuñez, M. A., Wardle, D. A., & Wingfield, M. J. (2017). Biological invasions in forest ecosystems. *Biological Invasions,* 19, 3437–3458. doi:10.1007/s10530-017-1458-5.

Luna, E. K., Sitz, R. A., Cranshaw, W. S., & Tisserat, N. A. (2013). The effect of temperature on survival of *Pityophthorus juglandis* (Coleoptera: Curculionidae). *Environmental Entomology,* 42, 1085–1091.

Malacrinò, A., Sadowski, V. A., Martin, T. K., Cavichiolli de Oliveira, N., Brackett, I. J., Feller, J. D., Harris, K. J., Combita Heredia, O., Vescio, R. and Bennett, A.E. (2020). Biological invasions alter environmental microbiomes: a meta-analysis. *PLoS One,* 15, e0240996.

Mamet, S.D., Redlick, E., Brabant, M., Lamb, E.G., Helgason, B.L., Stanley, K. and Siciliano, S.D. (2019). Structural equation modeling of a winnowed soil microbiome identifies how invasive plants re-structure microbial networks. *ISME Journal,* 13, 1988–1996. doi:10.1038/s41396-019-0407-y.

Manion, P. D. (1981). Tree disease concepts. Prentice-Hall, Inc.

Margulis, L., & Fester, R. (Eds.) (1991). *Symbiosis as a source of evolutionary innovation: speciation and morphogenesis*. MIT Press.

Massey, C. L. (1974). Biology and taxonomy of nematode parasites and associates of bark beetles in the United States. Agricultural Handbook No. 446. U.S. Department of Agriculture, Forest Service.

McCoy, R. M., Utturkar, S. M., Crook, J. W., Thimmapuram, J., & Widhalm, J. R. (2018). The origin and biosynthesis of the naphthalenoid moiety of juglone in black walnut. *Horticultural Research,* 5, 67. doi:10.1038/s41438-018-0067-5.

Meinhardt, K. A., Gehring, C. A., Meinhardt, K. A., & Gehring, C. A. (2018). Disrupting mycorrhizal mutualisms : a potential mechanism by which exotic tamarisk outcompetes native cottonwoods. *Ecological Applications,* 22, 532–549.

Michler, C. H., Pijut, P. M., Van Sambeek, J. W., Coggeshell, M. V., Seifert, J., Woeste, K., Overton, R., & Ponder, F. J. (2004). Diseases of Intensively Managed Eastern Black Walnut. In C. H. Michler, P. M. Pijut, J. W. Van Sambeek, M. V. Coggeshall, J. Seifert, K. Woeste, R. Overton, & F. J. Ponder (Eds.), *Black Walnut in a New Century, Proceedings of the 6th Walnut Council Research Symposium*. St. Paul, MN: U.S. Department of Agriculture, Forest Service, North Central Research Station, 110–113.

Moricca, S., Bracalini, M., Benigno, A., Ghelardini, L., Furtado, E. L., Marino, C. L., & Panzavolta, T. (2020). Observations on the non-native thousand cankers disease of walnut in Europe's southernmost outbreak. *Global Ecology and Conservation,* 23, e01159. doi:https://doi.org/10.1016/j.gecco.2020.e01159.

Newton, L., & Fowler, G. (2009). Pathway Assessment: *Geosmithia* sp. and *Pityophthorus juglandis* Blackman movement from the western into the eastern United States. In K. A. McManus, K. W. Gottschalk (Eds.), *Proceedings of the 21st U.S. Department of Agriculture interagency research forum on invasive species. January 12-15, Annapolis, MD. General Technical Report NRS-P-75.* U. S. Department of Agriculture, Forest Service, Northern Research Station 112. Available online https://www.uaex.edu/environment-nature/ar-invasives/invasive-diseases/docs/Thousand-Cankers Disease.pdf.

Onufrak, A. J., Williams, G. M., Klingeman, W. E., Cregger, M. A., Klingeman, D. M., DeBruyn, J. M., Ginzel, M. D., & Hadžiabdić, Đ. (2020). Regional Differences in the Structure of *Juglans nigra* Phytobiome Reflect Geographical Differences in Thousand Cankers Disease Severity. *Phytobiomes Journal*, 4: 388–404.

Paine, T. D., Steinbauer, M. J., & Lawson, S. A. (2010). Native and Exotic Pests of Eucalyptus: A Worldwide Perspective. *Annual Review of Entomology,* 56, 181–201. doi:10.1146/annurev-ento-120709-144817.

Parker, I. M., & Gilbert, G. S. (2004). The Evolutionary Ecology of Novel Plant-Pathogen Interactions. *Annual Review of Ecology Evolution and Systematics*, 35, 675–700. doi:10.1146/annurev.ecolsys.34.011802.132339.

Pepori, A. L., Bettini, P. P., Comparini, C., Sarrocco, S., Bonini, A., Frascella, A., Gheraldinia, A., Scala, A., Vannacci, G., & Santini, A. (2018). *Geosmithia-Ophiostoma*: a New Fungus-Fungus Association. *Microbial Ecology,* 75, 632–646. doi:10.1007/s00248-017-1062-3.

Ploetz, R. C., Hulcr, J., Wingfield, M. J., & de Beer, Z. W. (2013). Destructive Tree Diseases Associated with Ambrosia and Bark Beetles: Black Swan Events in Tree Pathology? *Plant Disease*, 97, 856–872. doi:10.1094/PDIS-01-13-0056-FE.

Ponder Jr, F. (1987). Allelopathic interference of black walnut trees with nitrogen-fixing plants in mixed plantings. In Waller, G. (Ed.) *Allelochemicals: Role in Agriculture and Forestry* (pp. 195-204) American Chemical Society.

Porras-Alfaro, A., & Bayman, P. (2011). Hidden Fungi, Emergent Properties: Endophytes and Microbiomes. *Annual Review of Phytopathology,* 49, 291–315. doi:10.1146/annurev-phyto-080508-081831.

Rayner, A. D. M., & Boddy, L. (1988). *Fungal decomposition of wood: its biology and ecology*. Wiley and Sons doi:10.1086/416403.

Rodriguez, R. J., White, J. F., Arnold, A. E., & Redman, R. S. (2009). Fungal endophytes: Diversity and functional roles: Tansley review. *New Phytologist,* 182.

Rugman-Jones, P. F., Seybold, S. J., Graves, A. D., & Stouthamer, R. (2015). Phylogeography of the walnut twig beetle, *Pityophthorus juglandis*, the vector of thousand cankers disease in North American walnut trees. *PLoS One,* 10. doi:10.1371/journal.pone.0118264.

Ryss, A. Y., Parker, C., Álvarez-Ortega, S., Nadler, S. A., & Subbotin, S. A. (2020). *Bursaphelenchus juglandis* n. sp. (Nematoda: Aphelenchoididae), an associate of walnut twig beetle, *Pityophthorus juglandis*, the vector of thousand cankers disease. *Nematology,* 1, 1–30.

Schuelke, T. A., Westbrook, A., Broders, K., Woeste, K., and MacManes, M. D. (2016). *De novo* genome assembly of *Geosmithia morbida*, the causal agent of thousand cankers disease. *PeerJ*. doi:10.7717/peerj.1952.

Schuelke, T. A., Wu, G., Westbrook, A., Woeste, K., Plachetzki, D. C., Broders, K., & McManes, M. D. (2017). Comparative Genomics of Pathogenic and Nonpathogenic Beetle-Vectored Fungi in the Genus *Geosmithia*. *Genome Biology and Evolution*, 9, 3312–3327. doi:10.1093/gbe/evx242.

Seybold, S. J., Coleman, T. W., Dallara, P. L., Dart, N. L., Graves, A. D., Pederson, L. A., & Spichiger, S. (2012). Recent collecting reveals new state records and geographic extremes in the distribution of the walnut twig beetle, *Pityophthorus juglandis* Blackman (Coleoptera: Scolytidae), in the United States. *Pan-Pacific Entomologist*, 88. doi:10.3956/2012-32.1.

Seybold, S. J., Dallara, P. L., Hishinuma, S. M., & Flint, M. L. (2013). Detecting and identifying the walnut twig beetle: Monitoring guidelines for the invasive vector of thousand cankers disease of walnut. University of California-Davis Extension, Agricultural and Natural Resources.

Seybold, S. J., Klingeman III, W. E., Hishinuma, S. M., Coleman, T. W., & Graves, A. D. (2019). Status and Impact of Walnut Twig Beetle in Urban Forest, Orchard, and Native Forest Ecosystems. *Journal of Forestr,y* 117, 152–163. doi:10.1093/jofore/fvy081.

Seybold, S. J., Penrose, R. L., & Graves, A. D. (2016). Invasive bark and ambrosia beetles in California Mediterranean forest ecosystems. In T. D. Paine and F. Lieutier (Eds.), *Insects and Diseases of Mediterranean Forest Systems* (pp, 583–662). Springer.

Simler, A. B., Williamson, M. A., Schwartz, M. W., & Rizzo, D. M. (2019). Amplifying plant disease risk through assisted migration. *Conservation Letters*, 12, e12605. doi:https://doi.org/10.1111/conl.12605.

Sitz, R. A., Luna, E. K., Caballero, J. I., Tisserat, N. A., Cranshaw, W. S., & Stewart, J. E. (2017a). Virulence of Genetically Distinct *Geosmithia morbida* Isolates to Black Walnut and Their Response to Coinoculation with *Fusarium solani*. *Plant Disease*, 101, 116. doi:10.1094/PDIS-04-16-0535-RE.

Sitz, R. A., Luna, E., Ibarra Caballero, J., Tisserat, N., Cranshaw, Whitney S., McKenna, J. R., Stoltz, J., & Stewart, J (2021). Eastern black walnut (*Juglans nigra* L.) originating from native range varies in their response to inoculation with *Geosmithia morbida*. *Frontiers in Forests and Global Change*, 4:12. doi.org/10.3389/ffgc.2021.627911.

Sitz, R., Utley, C., Hall, A., Tisserat, N., & Cranshaw, W. (2017b). Trapping the Walnut Twig Beetle 1 to Determine Flight Patterns in Colorado. *Southwest Entomologist*, 42, 347–356.

Six, D. L. (2013). The Bark Beetle Holobiont: Why Microbes Matter. *Journal of Chemical Ecology*, 39. doi:10.1007/s10886-013-0318-8.

Six, D. L., & Bentz, B. J. (2007). Temperature Determines Symbiont Abundance in a Multipartite Bark Beetle-fungus Ectosymbiosis. *Microbial Ecology*, 54, 112–118. doi:10.1007/s00248-006-9178-x.

Six, D. L., & Wingfield, M. J. (2010). The Role of Phytopathogenicity in Bark Beetle–Fungus Symbioses: A Challenge to the Classic Paradigm. *Annual Review of Entomology*, 56, 255–272. doi:10.1146/annurev-ento-120709-144839.

Stodůlková, E., Man, P., Kolařík, M., & Flieger, M. (2010). High-performance liquid chromatography–off line mass spectrometry analysis of anthraquinones produced by *Geosmithia lavendula*. *Journal of Chromatography, A.,* 1217, 6296–6302. doi:https://doi.org/10.1016/j.chroma.2010.08.009.

Tataru, C. A., & David, M. M. (2020). Decoding the language of microbiomes using word-embedding techniques, and applications in inflammatory bowel disease. *PLoS computational biology*, 16(5), e1007859.

Thevathasans, N. V, Gordon, A. M., & Voroney, R. P. (1998). Juglone (5-hydroxy-1, 4 napthoquinone) and soil nitrogen transformation interactions under a walnut plantation in southern Ontario, Canada. *Agroforestry Systems,* 44, 151–162.

Tisserat, N., Cranshaw, W., Leatherman, D., Utley, C., & Alexander, K. (2009). Black walnut mortality in Colorado caused by the walnut twig beetle and thousand cankers disease. *Plant Health Progress,* 11, 10. doi:10.1094/php-2009-0811-01-rs.

Tisserat, N., Cranshaw, W., Putnam, M. L., Pscheidt, J., Leslie, C. A., Murray, M., Hoffman, J., Barkley, Y., Alexander, K., & Seybold, S. J. (2011). Thousand Cankers Disease is Widespread in Black Walnut in the Western United States. *Plant Health Progress,* 12, 35. doi:10.1094/PHP-2011-0630-01-BR.

UC Davis Fruit & Nut Extention (2021). Walnut Deficiencies and Pests. Available online: http://fruitandnuteducation.ucdavis.edu/fruitnutproduction/Walnut/Walnut_DeficienciesPests/

Utley, C., Nguyen, T., Roubtsova, T., Coggeshall, M., Ford, T. M., Grauke, L. J., Graves, A D., Leslie, C. A., McKenna, J., Woeste, K., Yaghmour, M A., Cranshaw, W., Seybold, S. J., Bostock, R. M., & Tisserat, M. (2013). Susceptibility of Walnut and Hickory Species to *Geosmithia morbida*. *Plant Disease,* 97, 601–607. doi:10.1094/PDIS-07-12-0636-RE.

van der Heijden, M. G. A., & Hartmann, M. (2016). Networking in the plant microbiome. *PLoS Biology*, 14, e1002378.

Vega Thurber, R., Mydlarz, L. D., Brandt, M., Harvell, D., Weil, E., Raymundo, L., Willis, B. L., Langevin, S., Tracy, A. M., Littman, R., Kemp, K. M., Dakins, P., Prager, K. C., Garren, M., & Lamb, J. (2020). Deciphering Coral Disease Dynamics: Integrating Host, Microbiome, and the Changing Environment. *Frontiers in Ecology and Evolution,* 8, 402. doi:10.3389/fevo.2020.575927.

Veselská, T., Skelton, J., Kostovčík, M., Hulcr, J., Baldrian, P., Chudíčková, M., Cajthaml, T., Vojtová, T., Garcia-Fraile, P., & Kolařík, M. (2019). Adaptive traits of bark and ambrosia beetle-associated fungi. Fungal Ecology, 41, 165–176.

Vogel, C. S., & Dawson, J. O. (1986). In vitro growth of five Frankia isolates in the presence of four phenolic acids and juglone. *Soil Biology and Biochemistry,* 18, 227–231.

Wagg, C., Bender, S. F., Widmer, F., & van der Heijden, M. G. A. (2014). Soil biodiversity and soil community composition determine ecosystem multifunctionality. *PNAS,* 111, 5266–5270. doi:10.1073/pnas.1320054111.

Wang, B., & Qiu, Y.-L. (2006). Phylogenetic distribution and evolution of mycorrhizas in land plants. *Mycorrhiza*, 16, 299–363. doi:10.1007/s00572-005-0033-6.

Wang, B., & Allison, S. D. (2021). Drought legacies mediated by trait trade-offs in soil microbiomes. *Ecosphere,* 12(6), e03562.

Williams, G. M. Personal observations. 2017-2021. Walla Walla, WA and West Lafayette, IN.

Williams, R. D. (1990). *Juglans nigra* L., black walnut. In *Silvics of North America Vol 2.* (pp. 391–399). U. S. Department of Agriculture, Forest Service.

Wilson, E. E., Stake, M. P., & Berger, J. A. (1957). Bark canker, a bacterial disease of the Persian Walnut tree. *Phytopathologym,* 47.

Wilson, E. E., Zeitoun, F. M., & Fredrickson, D. L. (1967). Bacterial phloem canker, a new disease of Persian walnut trees. *Phytopathology,* 57, 618–621.

Wood, S. L. (1982). The bark and ambrosia beetles of North and Central America (Coleoptera: Scolytidae), a taxonomic monograph. *Great Basin Naturalist Memoirs,* 6.

Wu, Y., Xu, J., Wang, H., & Zhang, T. (2013). *Geosmithia tibetensis* sp. nov. and new *Gibellulopsis* and *Scopulariopsis* records from Qinghai-Tibet. *Mycotaxon*, 125, 59–64.

Yeates, G. W. (2003). Nematodes as soil indicators: functional and biodiversity aspects. *Biology and Fertility of Soils,* 37, 199–210.

Zerillo, M. M., Ibarra Caballero, J., Woeste, K., Graves, A. D., Hartel, C., Pscheidt, J. W., Tonos, J., Broders, K., Cranshaw, W., Seybold, S. J., & Tisserat, N. (2014). Population structure of *Geosmithia morbida*, the causal agent of thousand cankers disease of walnut trees in the United States. *PLoS ONE*, 9:e112847.

Zhang, X., Li, Y., Dai, M., Si, H., Zhao, G., Kolařík, M., Hulcr, J., Jiang, X., & Chang, R. (2021). *Geosmithia* Species Associated With Bark Beetles From Southern China, With the Description of Four New Species. (Preprint). Available online: https://www.researchsquare.com/article/rs-558245/v1.

CHAPTER 2. REGIONAL DIFFERENCES IN THE STRUCTURE OF *JUGLANS NIGRA* PHYTOBIOME REFLECT GEOGRAPHICAL DIFFERENCES IN THOUSAND CANKERS DISEASE SEVERITY

*** Reprinted from Onufrak, A.J., Williams, G.M., Klingeman III, W.E., Cregger, M.A., Klingeman, D.M., DeBruyn, J.M., Ginzel, M.D. and Hadžiabdić, Đ., 2020. Regional Differences in the Structure of *Juglans nigra* Phytobiome Reflect Geographical Differences in Thousand Cankers Disease Severity. Phytobiomes Journal 4:388-404.**

A. Onufrak (UT-Knoxville) and G. Williams contributed equally to this work

2.1 Introduction

Thousand Cankers Disease (TCD) threatens the ecological and economic sustainability of walnut trees in urban and natural landscapes (Feeley, 2010; Treiman et al., 2010; Treiman & Tuttle, 2009). TCD is caused by the fungal pathogen *Geosmithia morbida* Kolarík, Freeland, Utley and Tisserat (Ascomycota: Hypocreales: Bionectriaceae) and its insect vector, the walnut twig beetle (WTB; *Pityophthorus juglandis* Blackman; Coleoptera: Curculionidae: Scolytinae). Susceptible hosts include *Juglans* spp. and *Pterocarya* spp. important for nut and timber production. The most susceptible host species is *Juglans nigra* L. (Eastern Black Walnut), which is native to most of the central and eastern U.S. (Utley et al., 2013; Williams, 1990). Both the insect vector and fungal pathogen appear to have originated from the arid southwestern U.S. and Mexico and have been detected in 18 U.S. states, including seven states within the native range of *J. nigra*, and Italy (Bright, 1981; Hadžiabdić et al., 2014a; Juzwik et al., 2015; Juzwik et al., 2016; Moore et al., 2019; Moricca et al., 2019; Rugman-Jones et al., 2015; Wood & Bright, 1992; Zerillo et al., 2014).

Incidence and severity of TCD appears to be greatest in the western U.S., where *J. nigra* has been introduced, and widespread decline and massive die-offs have occurred (Tisserat et al., 2009). However, within the native range of *J. nigra*, TCD has been detected in isolated locations (Hadžiabdić et al., 2014b; Juzwik et al., 2015; Juzwik et al., 2016; Oren et al., 2018; Williams, 1990). In the native range, there appear to be two disease outcomes of TCD in *J. nigra*: either tree recovery following initial decline, or gradual decline in health and eventual tree mortality (Griffin, 2015; Seybold et al., 2019). These geographical patterns of TCD incidence and severity may be a

consequence of less favorable climatic conditions for disease establishment in the eastern U.S. For instance, reduced WTB activity and abundance in the eastern U.S. are hypothesized to result from higher levels of precipitation that reduce drought stress on host trees and susceptibility to WTB (Griffin, 2015; Seybold et al., 2019). Host genetics may also influence susceptibility of *J. nigra* to TCD (Blood et al., 2018; Utley et al., 2013).

In addition to the influence of abiotic factors and host genetics, absence of mutualists in the phytobiome of *J. nigra* in its introduced range or presence of microbial antagonists of *G. morbida* in the native range may affect TCD severity (Gazis et al., 2018). Phytobiome composition is largely influenced by host genetics and the physicochemical environment in which plants grow (Bálint et al., 2013; Cregger et al., 2018; Erlandson et al., 2018; Ren et al., 2019; Veach et al., 2019). The phytobiome is known to influence the health of introduced plants (Gundale et al., 2016; Hoffman & Arnold, 2008; Klironomos, 2002; Zhang et al., 2010). Introduced plants can benefit by escaping pathogens and predators from their native ranges, thereby facilitating establishment, range expansion, and invasiveness (van der Putten et al., 2007). Conversely, organisms introduced into novel habitats, including plants, pests, and pathogens, may lose mutualists or encounter novel pathogens or parasites that limit range expansion (Parker et al., 2006; Prider et al., 2008; Stricker et al., 2016; Thompson et al., 2019). In support of this hypothesis, culture-dependent comparison of the *J. nigra* microbiome between the eastern and western U.S. found greater abundance of potential TCD-antagonists (*Trichoderma* spp.) in the native range and potential novel pathogens (*Sporothrix* spp.) in the invaded range (Gazis et al., 2018).

To compare the phytobiomes of diseased vs. healthy, and native vs. introduced *J. nigra*, we chose locations in Indiana, Tennessee, and Washington where TCD severity and incidence varied across each study area, and tested trees for the presence of *G. morbida* with a molecular probe (Oren et al., 2018). We used DNA sequencing methods to characterize bacterial and fungal community composition of *J. nigra* in both the native and introduced ranges of the species. We predicted that the phytobiome of *J. nigra* in its native range would have higher alpha-diversity and differ in composition compared to the introduced range in the western U.S., and that phytobiome composition would vary with host genetics. Fungal functional guild, indicator species and microbial network analyses were used to identify microorganisms associated with disease and geography, and to evaluate the extent to which the presence and absence of mutualists and disease-associated microorganisms differs between the native and introduced ranges.

2.2 Methods

2.2.1 Study Sites, Thousand Cankers Disease Pressure, and Tree Sources

Study areas were selected in Indiana (Tippecanoe Co.) and Tennessee (Polk and Knox Co.) to represent the northern and southern native range of *J. nigra*. An additional study area in Walla Walla Co., Washington (WA), where disease pressure was high and trees were in early to advanced stages of TCD-related decline, was included to represent *J. nigra* in its introduced range in the western U.S.

In Walla Walla, WA, active populations of WTB were detected at both sites as early as 2009 and crown decline is present throughout the county (Zerillo et al., 2014). To date, there has been no record of WTB or *G. morbida* in Tippecanoe Co., IN. In TN, we sampled from Knox Co. a quarantined area where TCD was widespread throughout urban areas and *G. morbida* was detected, and Polk Co., a buffer zone where the transport of walnut products outside of the county is limited and WTB were present at low levels, but *G. morbida* was not detected (Grant et al., 2011; Griffin, 2015; Oren et al., 2018; https://www.tn.gov/; WEK and DH, unpublished data). Tippecanoe Co., IN soils were silt loam and loamy sand Alfisols, Polk Co., TN soils were loam Entisols, Knox Co., TN soils were Ultisols, and Walla Walla Co., WA soils were silt loam Mollisols.

At sites in each state, three grafted clonal trees were selected from the same four scion stock accessions (HTIRC #55, #130, #132, and #272), which originated from a Hardwood Tree Improvement and Regeneration Center (HTIRC) program that is jointly administered by the U.S. Forest Service Northern Research Station and Purdue University (http://www.htirc.org). Grafted clones from each of the four genotypes had been established in each state. Additionally, non-grafted, wild type (WT) trees were sampled from nearby border areas in WA, IN, TCD-positive Knox Co. and TCD-negative Polk Co. GPS coordinates, planting dates, and number of clones and WT trees at each location are presented in Table 2.1.

Table 2.1. Description of field sites and locations of 47 *Juglans nigra* trees used in this study.

Site	Latitude	Longitude	State	County	Habitat Type[a]	Tree Age (years) Clone (WT)	TCD[b]	Planting Year	#55	#130	#132	#272	WT	Total
MCB 1	40.430987	-87.040339	IN	Tippecanoe	P, F	52 (> 35)	N	1968	3	2	1	-	1	7
MCB 2	40.433322	-87.03536	IN	Tippecanoe	P, F	40 (> 35)	N	1980	-	-	-	1	1	2
MCB 9	40.429721	-87.036605	IN	Tippecanoe	P, F	30 (> 35)	N	1990	-	1	2	2	1	6
Delano	35.247163	-84.575997	TN	Polk	P	14 (> 35)	N	2006	3	3	3	3	3	15
Lakeshore	35.9211	-83.9909	TN	Knox	F	(> 35)	Y	2006	-	-	-	-	3	3
BNL	46.015194	-118.29504	WA	Walla Walla	P	11 to 16 (11 to 16)	Y	2004-2009	1	1	3	2	3	10
RN	46.044965	-118.2336	WA	Walla Walla	P	11 to 16	Y	2004-2009	2	1	-	1	-	4
Total	-	-	-	-	-	-	-	-	9	8	9	9	12	**47**

[a] Location Type: P = plantation, F = forest, [b] TCD indicates whether trees in the county have tested positive for the presence of Thousand Cankers Disease (Oren et al., 2018).

2.2.2 Sample Collection Methodology

All samples were collected between April and June of 2017. From each tree, we collected samples from branches (henceforth, the caulosphere) and bulk soil with sterile tools. For the caulosphere microbiome, a total of two to four branches (~6 cm diameter) were collected per tree from different cardinal directions. Branches were sectioned into 30 cm segments, placed into large plastic zipper seal bags, transported to the laboratory on ice, and stored in a walk-in cooler at 4°C for 1 to 4 days until drill shavings could be collected. Drill shavings were taken following Oren et al., (2018), and stored at -80°C until DNA extraction.

For soil microbiome samples, leaf litter and debris were removed from the tree base. A 2 cm diameter stainless steel auger was used to collect a total of eight 20 cm soil cores from four cardinal directions at distances of 20 cm and 30 cm from the base of each tree. All eight cores were pooled by tree and homogenized in the field in paper bags. Coarse debris (e.g., large roots, rocks, etc.) was removed by hand from the pooled sample, labeled, and split into subsamples for soil analysis and DNA extraction. For laboratory DNA extraction, an approximately 10 g subsample was taken from each pooled and homogenized soil sample, immediately placed in liquid nitrogen, and stored at -80°C until further processing. The remaining soil was bulked and stored at 4°C. Soil was air-dried, ground, passed through a 2 mm sieve (No. 10), and sent to Brookside Laboratories (New Bremen, OH) for analysis of pH (1:1), soil organic matter (SOM; loss on ignition 360°C), nitrate (NO_3.N), ammonium (NH_4.N), and Mehlich III extractable aluminum (Al), boron (B), calcium (Ca), copper (Cu), iron (Fe), potassium (K), magnesium (Mg), manganese (Mn), sodium (Na), phosphorus (P), sulfur (S), and zinc (Zn), and total cation exchange capacity (TEC) using standard methods.

2.2.3 DNA Extraction and molecular probe detection of *G. morbida*

We extracted DNA from branch drill shavings following the Qiagen DNA Stool Mini Kit protocol (Qiagen, Germantown, MD, U.S.). DNA was extracted from soil by homogenizing approximately 0.25 g of field-moist soil in a Bead Mill 25 Homogenizer (Omni International, Kennesaw, GA, U.S.) and using the DNeasy Powerlyzer Powersoil Kit protocol (Qiagen). The TCD infection status of sampled trees was tested in triplicate following the protocol of Oren et al., (2018).

2.2.4 Amplicon Library Preparation and Sequencing

ITS1 and ITS2 regions of the fungal internal transcribed spacer (ITS) were amplified from DNA isolated from drill shavings and sequenced at the University of Tennessee Genomics Core (Knoxville, TN). The V4 region of the 16S rRNA for bacteria and archaea was amplified from DNA isolated from drill shavings, and sequenced at Oak Ridge National Laboratory (ORNL; Oak Ridge, TN). DNA isolated from bulk soil was amplified for fungal ITS1, ITS2, and 16s V4 regions and sequenced at ORNL. To maximize coverage of fungal taxa, the ITS1 region was amplified using the ITS1 and ITS2 primer pair and the ITS2 region was amplified using a pool of six ITS3 and two ITS4 primers (Cregger et al., 2018; White et al., 1990). For amplification of the 16s V4 rRNA region, a pool of four 515F and one 806R primers were used to maximize coverage of bacterial taxa (Cregger et al., 2018).

Amplicon metagenomic sequencing libraries were prepared as described in the Illumina 16s metagenomic sequencing library preparation guide (Part 15044223 Rev B). Pooled libraries were validated on an Agilent Bioanalyzer (Agilent, Santa Clara, CA) using a DNA7500 chip, and the final library pool concentration was determined on an Invitrogen Qubit (Waltham, MA) with the broad range double stranded DNA assay. A paired end sequencing run (2x 251x 8x 8) was competed on an Illumina MiSeq instrument (Illumina, San Diego, CA) using v2 chemistry. Raw amplicon sequences are located under the NCBI SRA BioProject PRJNA633586.

2.2.5 Sequence Processing

The resulting 16s and ITS reads were processed in mothur v.1.42.3 (Schloss, 2020). Processing of 16s reads followed the mothur MiSeq SOP (Kozich et al., 2013; https://www.mothur.org/wiki/MiSeq_SOP). We assigned taxonomy to 16s sequences using the naïve-Bayesian classifier trained on the SILVA r.132 reference files with an 80% confidence cut-off. Sequences that either did not classify, or were classified as eukaryotes, mitochondria, or chloroplasts were removed. Additionally, sequences classified as bacteria or archaea with unknown phylum designations were also removed prior to OTU clustering. Sequences were then clustered into OTUs using a 97% similarity threshold using the cluster function. Taxonomy was then assigned to the resulting OTUs using the SILVA r.132 database as reference.

Bulk soil and caulosphere ITS reads were processed separately following a modified version of the mothur MiSeq SOP (Kozich et al., 2013); https://www.mothur.org/wiki/MiSeq_SOP). Only ITS2 contigs were used for analysis. Short (<50 bp) or long (>450 bp) sequences and sequences with homopolymers (>10 bp) were removed. Remaining sequences were pre-clustered with a maximum differences cut-off of 2 bp. Taxonomic assignments were made using the UNITE database v.8.0 (Nilsson et al., 2018); https://unite.ut.ee). ITS2 amplicons of plant origin or unknown phylum designation were removed and distances were calculated from pairwise alignments prior to OTU clustering at 98% sequence similarity following Tedersoo et al., (2014) which assessed global variation in soil fungal communities. All code related to sequence processing and analysis are available in an online repository (https://github.com/readingradio/Juglans.microbiome.github).

2.2.6 Classification of Fungal Functional Guilds

Fungal OTUs were assigned to fungal functional guilds using the online version of the FUNGuild database (http://funguild.org; accessed 26 November, 2019; Nguyen et al., 2016) with a confidence cutoff of "possible". Abundance values for any OTU assigned to multiple functional guilds were divided by the number of functional guilds assigned so that each possible function for that OTU were equally weighted. To visualize differences in potential fungal functions between states, stacked bar plots depicting the relative abundance of each fungal functional guild were created for each state.

2.2.7 Statistical Analyses

All statistical analyses were conducted in R v.3.4.4 or R v.3.6.0 and packages ape, car, stats, and vegan (R Core Team, 2018, 2019; Oksanen et al., 2018; Paradis & Schliep, 2019; Fox et al., 2019). To visualize differences in soil physicochemical properties between states, soil physicochemical properties were scaled and centered and a principal component analysis (PCA) was conducted using the prcomp function. The contribution of state to variation in soil physicochemical properties was evaluated using permutational analysis of variance (PERMANOVA) with 10,000 permutations using the adonis function.

OTU abundances were then rarified based on visual inspection of rarefaction curves and Good's coverage values (Fig. A.1, Table A.1-A.4). We calculated the observed species richness and the Shannon diversity index with the specnumber and diversity functions. Singleton OTUs were then removed from rarefied OTU tables prior to construction of stacked bar plots and beta-diversity analysis. We performed a principal coordinate analysis (PCoA) on Bray-Curtis distances for each habitat using the pcoa and vegdist functions.

To test for regional and clonal differences in fungal and bacterial diversity and richness, we performed analyses of variance (ANOVA) with Type III sum of squares. Additionally, the contribution of state and clone identity to variation in community composition was tested using PERMANOVA with the adonis function with 10,000 permutations. If there was not a significant interaction ($P > 0.05$), a two-way ANOVA or PERMANOVA was performed with state and clone. For non-significant main effects ($P > 0.05$), we report P-values from the simplest two-way ANOVA or PERMANOVA that includes the non-significant terms. For significant main effects ($P < 0.05$) we report the P-value from the ANOVA that only included significant variables. We followed up ANOVA tests with post-hoc Tukey tests to identify pairwise differences between states when variables were significant in the ANOVA.

To assess regional differences in beneficial and pathogenic fungal functional groups from FUNGuild (Nguyen et al., 2016), we also performed alpha- and beta-diversity comparisons for fungal OTUs classified as mycoparasites, plant pathogens, and wood saprotrophs in the caulosphere and OTUs classified as arbuscular mycorrhizae, mycoparasites, or plant pathogens in bulk soils.

2.2.8 Indicator Species Analysis

To identify archaeal/bacterial and fungal OTUs characteristic of the native and introduced ranges, we performed indicator species analyses for caulosphere and soil communities using the multipatt function from the indicspecies package with 10,000 permutations (De Caceres & Legendre, 2009). We report significant indicator OTUs ($P < 0.05$, indicator value > 0.80) for IN, TN, WA, and IN+TN grouping which represents the native range of *J. nigra*. To identify OTUs characteristic of TCD infection, we also performed indicator analysis to identify fungal and bacterial OTUs in the caulosphere characteristic of TCD-positive and TCD-negative trees.

2.2.9 Network Analysis of Hub Taxa and Network Complexity

We used network analysis modified from (Agler et al., 2016) and (Barberán et al., 2012) to a) compare measures of network complexity between states, and b) to identify 'hub taxa' OTUs from merged bacterial and fungal data. OTUs that occurred in less than four caulosphere samples or less than five times in fewer than five soil samples were removed to reduce noise in the dataset from rare taxa. Within each state, Spearman correlation networks were created for absolute value of R > 0.6 or 0.8 and P cutoffs of 5×10^{-2}, 10-2, 5×10^{-3}, and 10-^{3} for caulosphere networks, or three orders of magnitude smaller for the much larger soil networks.

The following measures of network complexity were calculated for each state and tissue type at each combination of R and P cutoffs: Kolmogorov-Chaitin algorithmic complexity (Zenil et al., 2014; Zenil et al., 2015; Soler-Toscano, 2014); entropy sensu Mowshowitz (1968), graph index complexity (Kim & Wilhelm, 2008), and normalized edge complexity (Bonchev & Buck, 2005) as implemented in the R package QuACN (Mueller et al., 2011); and first and second-order Shannon complexity as implemented in the R package acss (Gauvrit et al., 2014). To control for network size (number of OTUs) when comparing relative network complexity among states, we randomly pruned network adjacency matrices to the size of the smallest microbiome network at each P and R cutoff value (i.e., IN, TN, or WA). Bootstrap mean and standard deviation for each complexity measure were then calculated from twenty random submatrices.

Each node in the unpruned networks was analyzed by calculating degree, defined as the number of direct connections to other nodes, and betweenness, which is the proportion of all pairwise node paths that include a node, using the R package tidygraph (Pederson, 2018). After fitting a Weibull function to the degree distribution and an exponential distribution function to the betweenness centrality in each network, we considered to be 'hub taxa' those OTUs that were in the 90th percentile for both degree and betweenness at a given combination of P and R cutoffs.

2.3 Results

2.3.1 Regional Differences in Soil Physicochemical Properties

Soil physicochemical properties significantly differed by state (Fig. A.2; Pseudo-$F_{2,44} = 7.0$, $P < 0.001$, $R^2 = 0.24$). Following PCA, a total of three principal components (PC) were retained that

accounted for 74% of the variation observed within the data. Soil physicochemical properties were largely differentiated by state along PC1, whereas variation within states was accounted for more by PC2 (Fig. A2). PC1 (39.8% variation explained) correlated positively with Al and Fe, and negatively with B, Ca, K, Mg, Na, pH, and TEC. PC1 also correlated positively with sites in TN and negatively with sites in WA. PC2 (20.0% variation explained) correlated positively with Ca, Cu, Mn, Zn, and NO_3.N and negatively with P. PC3 (14.3% variation explained) correlated with Al, Fe, Mg, Mn, S, NH_4.N, pH, and SOM.

2.3.2 Bacterial Sequence Processing

A total of 2.5 million 16s soil sequences and a total of 5 million 16s caulosphere sequences were assembled from paired-end reads to characterize the walnut archaeal/bacterial community. Following sequence processing in mothur, a total of 2.3 million 16s sequences were clustered into 37,604 OTUs in bulk soils and a total of 333,951 sequences were clustered into 4,530 bacterial OTUs in caulosphere samples. In the caulosphere, no archaeal sequences were retained following sequence processing. Prior to downstream analyses for bacterial/archaeal communities, soil 16S samples were rarefied to 37,329 sequences per library with no sample loss; caulosphere 16S samples were rarified to 2,000 sequences, through which three samples from TN and four samples from WA were removed from further analyses. Following rarefaction and singleton removal, caulosphere samples retained a total of 1,791 bacterial OTUs and soil samples retained 21,464 archaeal/bacterial OTUs.

2.3.3 Fungal Sequence Processing

For fungal communities within the phytobiome, a total of 308,000 sequences were assembled from the ITS1 region and 2.5 million sequences were assembled from the ITS2 region for soil samples. In the separate Illumina run for caulosphere samples, a total of 1.6 million paired-end reads were assembled from the ITS1 region and 2.9 million paired-end reads were assembled from the ITS2 region. Following processing in mothur a total of 1.8 million ITS2 sequences clustered into 12,337 OTUs in soils and 629,829 sequences clustered into 4,646 OTUs in the caulosphere. Prior to downstream analyses for fungal communities, soil ITS2 data were rarefied to 25,000 paired-end reads per sample, resulting in the removal of two WA samples from further analyses. Caulosphere

ITS2 data were rarified to 3,400 paired-end reads per sample, resulting in the removal of one sample from IN from the analyses. Following rarefaction and singleton removal, caulosphere samples retained 1,578 fungal OTUs and soil samples retained 6,738 fungal OTUs.

2.3.4 *Geosmithia morbida* Detection

Of the 47 *J. nigra* trees included in the study, eight tested positive for *G. morbida* DNA using the GS004 microsatellite locus. All *G. morbida* positive samples were from WA sites. Additionally, Otu0115, the only *Geosmithia* sp. OTU retained in the data set following rarefaction and singleton removal, was detected in the caulosphere of seven of the same eight trees that tested positive with GS004 markers, except WA_BNL 23_WT. No trees from IN or TN tested positive for *G. morbida* using the GS004 microsatellite locus or contained Otu0115.

2.3.5 Regional and Host Genetic Differences in Alpha Diversity Measures

In both the caulosphere and bulk soil, fungal and bacterial richness and diversity significantly differed by state (Table 2.2). In the caulosphere, bacterial richness and diversity was the highest in IN and lowest in WA (Fig. 2.1A, B; Table 2.2). In soils, the richness and diversity of archaeal/bacterial communities was highest in WA and lower in IN and TN (Fig. 2.1C, 2.1D; Table 2.2). For caulosphere fungal communities, richness and diversity was highest in TN and lower in IN and WA (Fig. 2.1E, 2.1F; Table 2.2). In soils, fungal community richness was higher in IN and TN and lowest in WA (Fig. 2.1G; Table 2.2). Soil fungal diversity did not significantly differ between states (Fig. 2.1H; Table 2.2). Clone and state by clone interactions were non-significant; however, state by clone interaction had a marginally significant effect on fungal richness in the caulosphere (Table 2.2).

2.3.6 Regional and Host Genetic Differences in Microbiome Composition

In both the caulosphere and bulk soil, fungal and bacterial community composition differed by state (Fig. 2.2, Table 2.2). Clone identity only had a significant influence on the composition of caulosphere fungal communities (Fig 2.2C; Table 2.2). The majority of 16s sequences recovered from caulosphere samples were identified as Proteobacteria which comprised 45% of recovered sequences in IN, 48% in TN, and 62% in WA (Fig. A.3). At the class level, the majority of 16s

Table 2.2. Results of statistical tests comparing alpha and beta diversity of the *Juglans nigra* microbiome (significant *P*-values bolded). Unless otherwise stated (†), significant main effects for State were tested using a one-way ANOVA, non-significant effects for Clone were tested in a non-interactive two-way ANOVA, and non-significant interactions were tested in a full two-way model.

Habitat	**Richness**						**Shannon diversity**						**Beta-diversity**			
Organism	**ANOVA**			**Tukey's HSD *P*-value**			**ANOVA**			**Tukey's HSD *P*-value**			**PERMANOVA**			
Analysis	***F***	***df***	***P***	**TN-IN**	**WA-IN**	**WA-TN**	***F***	***df***	***P***	**TN-IN**	**WA-IN**	**WA-TN**	***F****	***df***	***P***	R^2
Caulosphere																
Fungi																
State	58.6	2, 43	**<0.001**	**<0.001**	**<0.001**	**<0.001**	18.5	2, 43	**<0.001**	0.580	**<0.001**	**<0.001**	21.2†	2, 31	**<0.001**	0.46
Clone	0.9	4, 39	0.470				1.6	4, 39	0.205				2.0†	4, 31	**0.006**	0.09
State × Clone	2.0	8, 31	0.079				0.6	8, 31	0.757				1.5†	8, 31	**0.03**	0.13
Bacteria																
State	132.6	2, 37	**<0.001**	**<0.001**	**<0.001**	**<0.001**	35.2	2, 37	**<0.001**	**<0.001**	**<0.001**	**<0.001**	12.2	2,37	**<0.001**	0.40
Clone	2.3	4, 33	0.080				1.0	4, 33	0.414				1.4	4,33	0.090	0.09
State × Clone	1.6	8, 25	0.184				0.9	8, 25	0.510				1.2	8,25	0.109	0.15
Soil																
Fungi																
State	8.3	2, 42	**0.001**	0.941	**0.002**	**0.003**	0.2	2, 42	0.790	0.918	0.777	0.939	6.2	2, 42	**<0.001**	0.23
Clone	1.0	4, 38	0.438				0.3	4, 38	0.848				1.0	4, 38	0.406	0.07
State × Clone	0.6	8, 30	0.802				0.8	8, 30	0.602				1.0	8, 30	0.466	0.15
Bacteria																
State	14.6	2, 44	**<0.001**	0.557	**<0.001**	**<0.001**	26.7	2, 44	**<0.001**	0.462	**<0.001**	**<0.001**	9.5	2, 44	**<0.001**	0.30
Clone	0.1	4, 40	0.971				0.7	4, 40	0.630				0.7	4, 40	0.893	0.04
State × Clone	0.5	8, 32	0.860				0.4	8, 32	0.910				0.7	8, 32	0.938	0.10

*†Results for State, Clone, and interaction presented from full interactive 2-way model. *Pseudo-F statistic.*

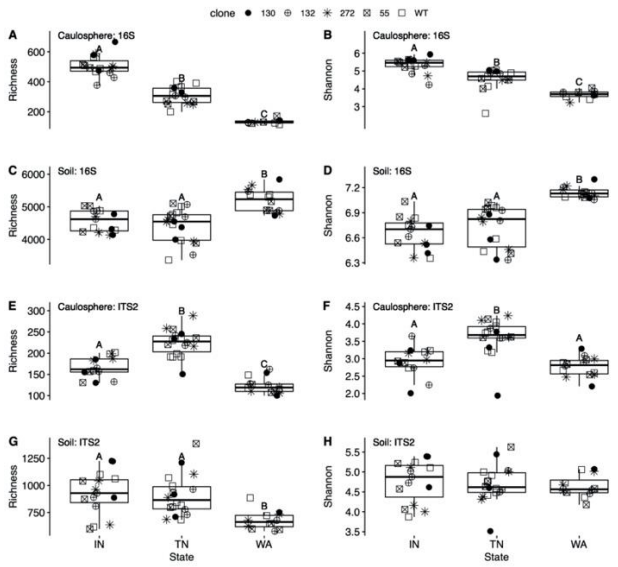

Figure 2.1. Observed richness (A, C, E, G) and Shannon Diversity (B, D, F, H) in *Juglans nigra* trees from Indiana (IN), Tennessee (TN), and Washington (WA) representing caulosphere bacterial communities (A, B), soil bacterial and archaeal communities (C, D), caulosphere fungal communities (E, F) and soil fungal communities (G, H). Letters represent significant mean differences between states based on Tukey's post hoc comparison ($P < 0.05$). Points are shaped by clone identity.

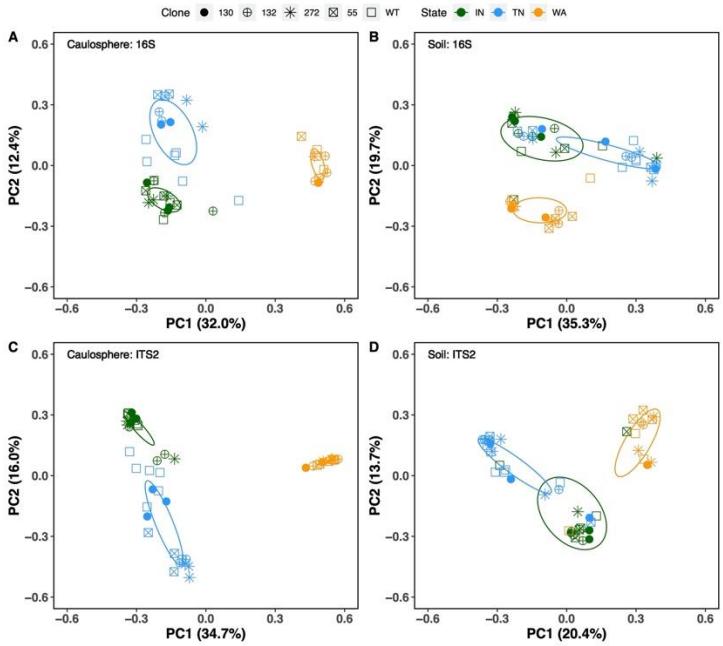

Figure 2.2. Principal Coordinate Analysis of caulosphere (A, C) and soil (B, D), bacterial and archaeal (A, B) and fungal (C, D) communities from *Juglans nigra* trees in Indiana (IN), Tennessee (TN), and Washington (WA). Points and ellipses are colored by state and shaped by clone genotype. Ellipses represent standard deviation of axis scores from the group centroid.

caulosphere sequences in IN and TN were classified as Alphaproteobacteria (Proteobacteria) which comprised 32% of detected sequences in IN and 33% in TN (Fig. 2.3A). In WA, the majority of 16s sequences were identified as Gammaproteobacteria (Proteobacteria) which comprised 27% of detected sequences at the class level (Fig. 2.3A). The dominance of Gammaproteobacteria in the WA caulosphere was driven in part by 15% of 16s sequences in WA being classified to the Burkholderiaceae (Betaproteobacteriales) at the family level, which had less representation in IN (3%) and TN (1%) (Figs. A.4A and A.5).

In soils, the majority of 16s sequences recovered from soils were identified as Proteobacteria from all three states and comprised 24% of detected sequences in IN and TN and 28% in WA (Fig. A.3B). At the class level, Alphaproteobacteria (Proteobacteria) comprised the greatest proportion of soil 16S sequences recovered from TN and WA soils, representing 12% of recovered sequences at the class level in both states. In IN, the majority of soil 16S sequences were identified as Nitrososphaeria (Thaumarchaeota) representing 12% of recovered soil 16S sequences at the class level (Fig. 2.3B).

In the caulosphere the majority of ITS sequences recovered from caulosphere originated from Ascomycota in all three states representing 96% of recovered ITS2 sequences in IN, 98% in TN, and 93% in WA (Fig. A.3C). In the caulosphere, the classes Dothidiomycetes (Ascomycota) and Eurotiomycetes (Ascomycota) dominated the fungal sequences recovered, with the Dothidiomycetes being more abundant in WA (58%), Eurotiomycetes more abundant in IN (50%), and TN intermediate for both Dothidiomycetes (41%) and Eurotiomycetes (27%) (Fig. 2.3C).

Finally, the majority of soil ITS sequences recovered from soils were identified to the Ascomycota in IN (73%), TN (74%), and WA (76%) (Fig. A.3D). Sordariomycetes comprised the greatest proportion of ITS sequences from soil in all three states, representing 32% of recovered ITS sequences in IN, 31% in TN, and 29% in WA (Fig. 2.3D).

2.3.7 Regional and Host Genetic Differences in Fungal Functional Guilds

In caulosphere fungal communities, a total of 632 OTUs out of 1,578 OTUs were assigned to a fungal functional guild. The majority of caulosphere fungal sequences belonging to classifiable OTUs were classified as plant pathogens in IN (27%) and TN (23%) and as undefined saprotrophs

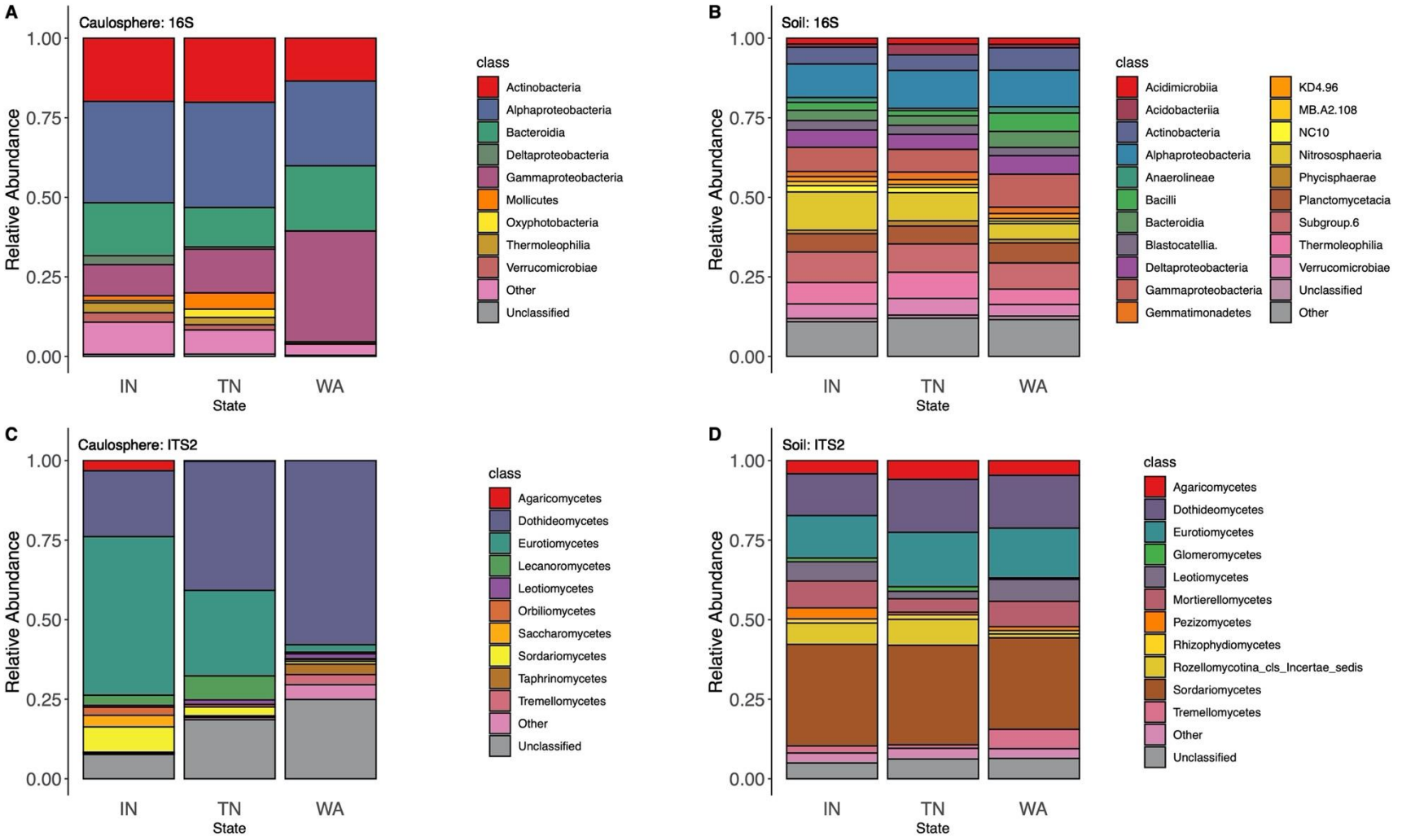

Figure 2.3. Relative abundance of caulosphere (A, C) and soil (B, D) bacterial and archaeal (A, B) and fungal (C, D) classes from *Juglans nigra* trees in Indiana (IN), Tennessee (TN), and Washington (WA). Other represents classes that comprised less than 1% of all bacterial and archaeal sequences or fungal sequences in the study. Unclassified represent OTUs classified at the phylum level but not at the class level.

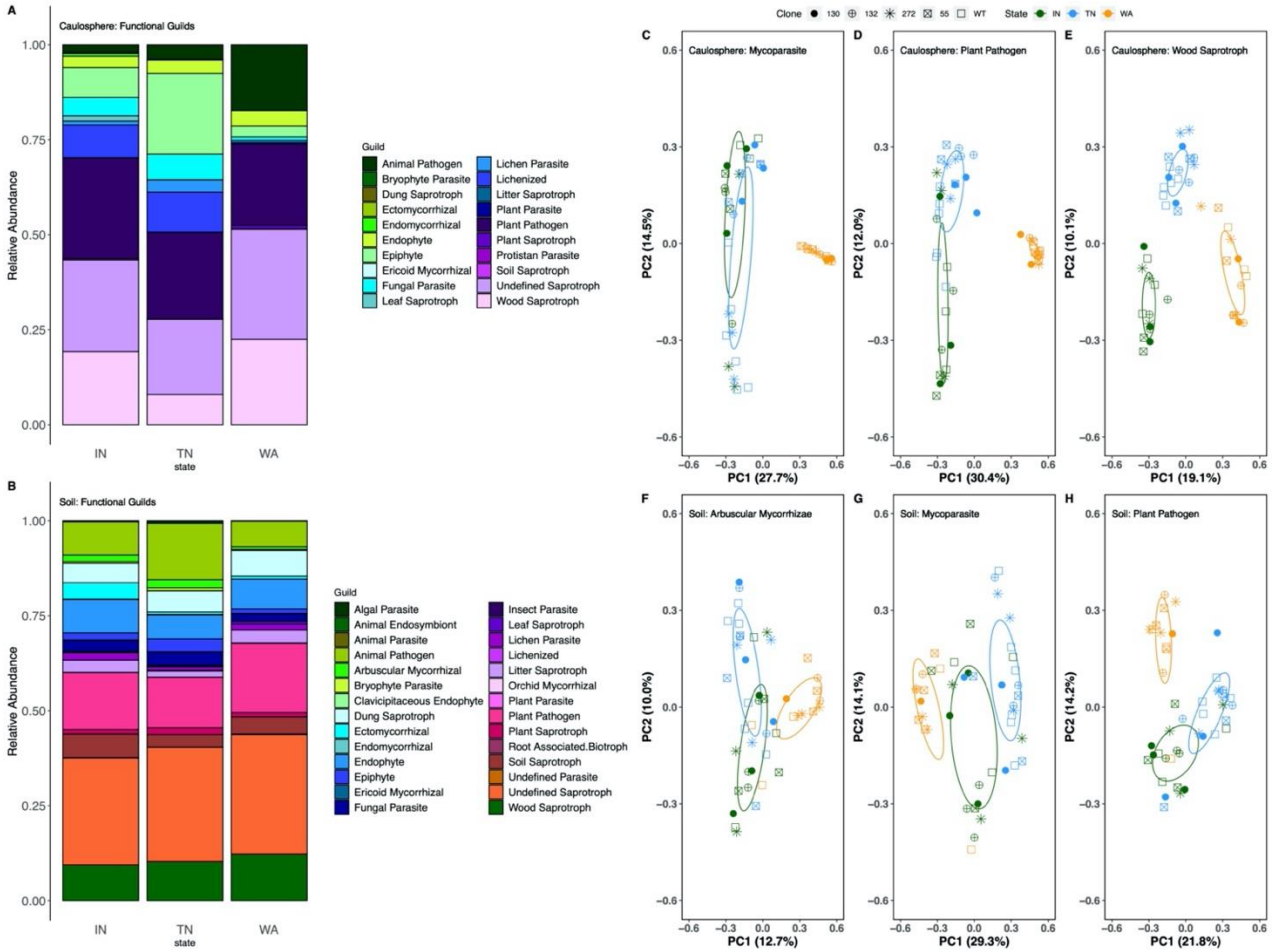

Figure 2.4. Relative abundance of caulosphere (A) and soil (B) fungal functional guilds from *Juglans nigra* trees in Indiana (IN), Tennessee (TN), and Washington (WA). Principal coordinate analyses (PCoA) of caulosphere mycoparasite (C), plant pathogen (D), and wood saprotrophs (E) communities and soil arbuscular mycorrhizae (F), mycoparasite (G), and plant pathogen (H) communities from IN, TN, and WA. Fungal functional guilds were assigned to fungal OTUs using FUNGuild database (accessed 26 November, 2019). In caulosphere fungal communities a total of 632 OTUs out of 1,578 OTUs were assigned to a fungal functional guild. In soil fungal communities a total of 3,836 OTUs out of 6,738 OTUs were assigned to a fungal functional guild.

in WA (29%) (Fig. 2.4A). The richness and composition of caulosphere mycoparasite, plant pathogen, and wood saprotroph communities significantly differed between states (Fig. 2.4C-E; Table 2.3). Mycoparasite richness was highest in IN and TN and lowest in WA; and wood saprotroph richness was highest in IN, followed by TN and WA (Figs. A.6A, E; Table 2.3). Plant pathogen richness was highest in TN and lowest in WA (Figs. A.6C; Table 2.3) with a greater number of potential plant pathogen OTUs from the Dothidiomycetes (e.g. *Helminthosporium* spp.), Sordariomycetes (e.g. *Diaporthe* spp.and *Phaeoacremonium* spp.), and Eurotiomycetes (e.g. *Calciopsis* spp. and *Strelitziana* spp.) in TN. There was also a significant host genetic effect on plant pathogen community composition in the caulosphere (Table 2.3).

In soil fungal communities, a total of 3,836 OTUs out of 6,738 OTUs were assigned to a fungal functional guild. The majority of soil fungal sequences belonging to classifiable OTUs were classified as undefined saprotrophs in IN (28%), TN (30%), and WA (31%) (Fig. 2.4B). Soil arbuscular mycorrhizae, mycoparasites, and plant pathogen richness and community composition significantly differed between states (Fig. 2.4F-H; Table 2.3). The richness of arbuscular mycorrhizae and soil plant pathogens was highest in IN and TN and lowest in WA, and mycoparasite richness was highest in IN and lowest in WA (Fig. A.6B, D, F; Table 2.3).

2.3.8 Indicator Species Analysis

For bacterial communities in the caulosphere, 175 bacterial indicator OTUs were detected across the four potential state groupings of IN (47 OTUs), TN (16 OTUs), WA (23 OTUs), and IN+TN (89 OTUs) (Table A.5). In soils, a total of 448 bacterial indicator OTUs were detected across the four potential state groupings of IN (62 OTUs), TN (60 OTUs), WA (210 OTUs), and IN+TN (116 OTUs). Spirosomaceae and Gemmataceae were common indicator OTUs in the caulosphere and soils, respectively for IN, TN, IN+TN, and TCD negative trees in WA (Fig. 2.5A, Supplementary Table A.5).

For caulosphere fungal communities, a total of 135 fungal indicator OTUs were detected across the four potential state groupings of IN (19 OTUs), TN (43 OTUs), WA (55 OTUs), and IN+TN (18 OTUs) (Table A.7). In the soil, a total of 198 indicator OTUs were detected across the four potential state groupings IN (17 OTUs), TN (42 OTUs), WA (80 OTUs), and IN+TN (59 OTUs) (Table A.8). IN and TN indicator OTUs included many Pleosporales (Dothidiomycetes),

Table 2.3. Results of statistical tests comparing alpha and beta diversity of the *Juglans nigra* fungal functional guilds (significant *P*-values bolded). Unless otherwise stated (†), significant main effects for State were tested using a one-way ANOVA, non-significant effects for Clone were tested in a non-interactive two-way ANOVA, and non-significant interactions were tested in a full two-way model.

Habitat			**Richness**					**Beta-diversity**		
Organism		**ANOVA**		**Tukey's HSD *P*-value**				**PERMANOVA**		
Analysis	***F***	***df***	***P***	**TN-IN**	**WA-IN**	**WA-TN**	***F****	***df***	***P***	R^2
Caulosphere										
Mycoparasites										
State	31.4	2, 43	**<0.001**	0.861	**<0.001**	**<0.001**	16.5	2, 43	**<0.001**	0.43
Clone	28.7	4, 39	0.675				1.3	4, 39	0.195	0.06
State × Clone	0.8	8, 31	0.610				1.3	8, 31	0.144	0.12
Plant Pathogens										
State	6.2	2, 43	**0.004**	0.289	0.159	**0.003**	15.1†	2, 39	**<0.001**	0.40
Clone	0.5	4, 39	0.730				1.63†	4, 39	**0.033**	0.09
State × Clone	1.7	8, 31	0.136				1.3	8, 31	0.098	0.13
Wood Saprotrophs										
State	22.8	2, 43	**<0.001**	**<0.001**	**<0.001**	0.554	11.8	2, 43	**<0.001**	0.36
Clone	0.8	2, 39	0.533				1.4	4, 39	0.082	0.08
State × Clone	0.6	8, 31	0.789				1.2	8, 31	0.114	0.14
Soil										
Arbuscular Mycorrhizae										
State	7.2	2, 42	**0.002**	0.915	**0.003**	**0.006**	3.6	2, 42	**<0.001**	0.15
Clone	0.6	4, 38	0.680				0.9	4, 38	0.742	0.07
State × Clone	1.7	8, 30	0.133				1.1	8, 30	0.200	0.18
Mycoparasite										
State	6.1	2, 42	**0.005**	0.080	**0.004**	0.312	7.9	2, 42	**<0.001**	0.27
Clone	0.9	4, 38	0.493				1.1	4, 38	0.381	0.07
State × Clone	0.5	8, 30	0.880				1.2	8, 30	0.1286	0.16
Plant Pathogens										
State	7.0	2, 42	**0.002**	0.787	**0.003**	**0.010**	6.3	2, 42	**<0.001**	0.23
Clone	1.8	4, 38	0.158				0.8	4, 38	0.788	0.06
State × Clone	0.3	8, 30	0.941				1.0	8, 30	0.563	0.14

†*Results for State and Clone presented from non-interactive 2-way model.* **Pseudo-F statistic.*

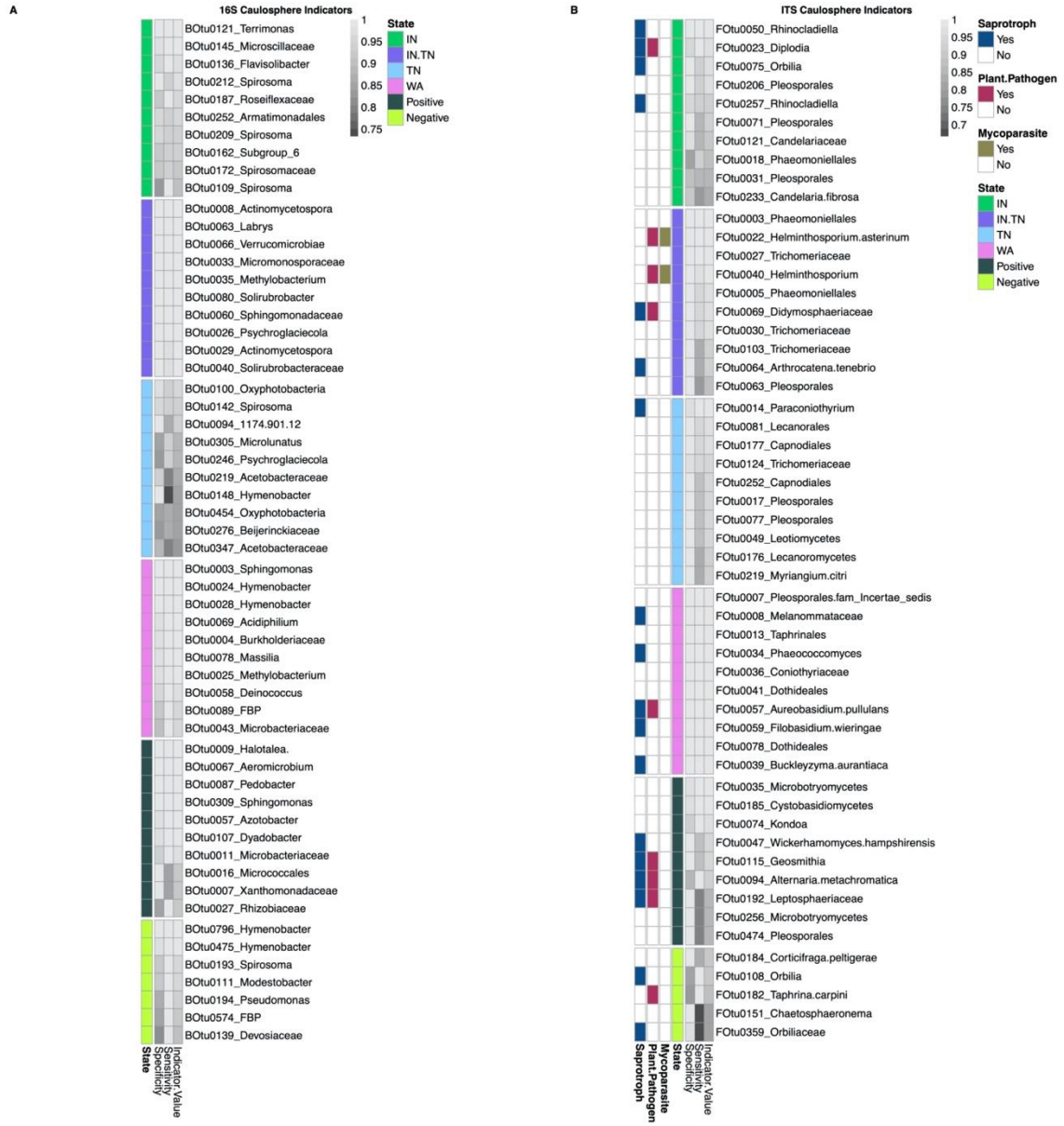

Figure 2.5. Sensitivity, specificity, and indicator values for top 10 bacterial (A) and fungal (B) indicator OTUs for caulosphere of *Juglans nigra* in Indiana (IN), Tennessee (TN), Washington (WA), IN+TN, and TCD positive trees and TCD negative trees in WA. Only top 20 OTUs classified to at least the class level for each group are depicted. Full list of indicator species can be found in supplementary materials (see Table A.7). Left three columns indicate whether the OTU was assigned to the saprotroph, plant pathogen, or mycoparasite functional guilds in FUNGuild database (accessed 26 November, 2019).

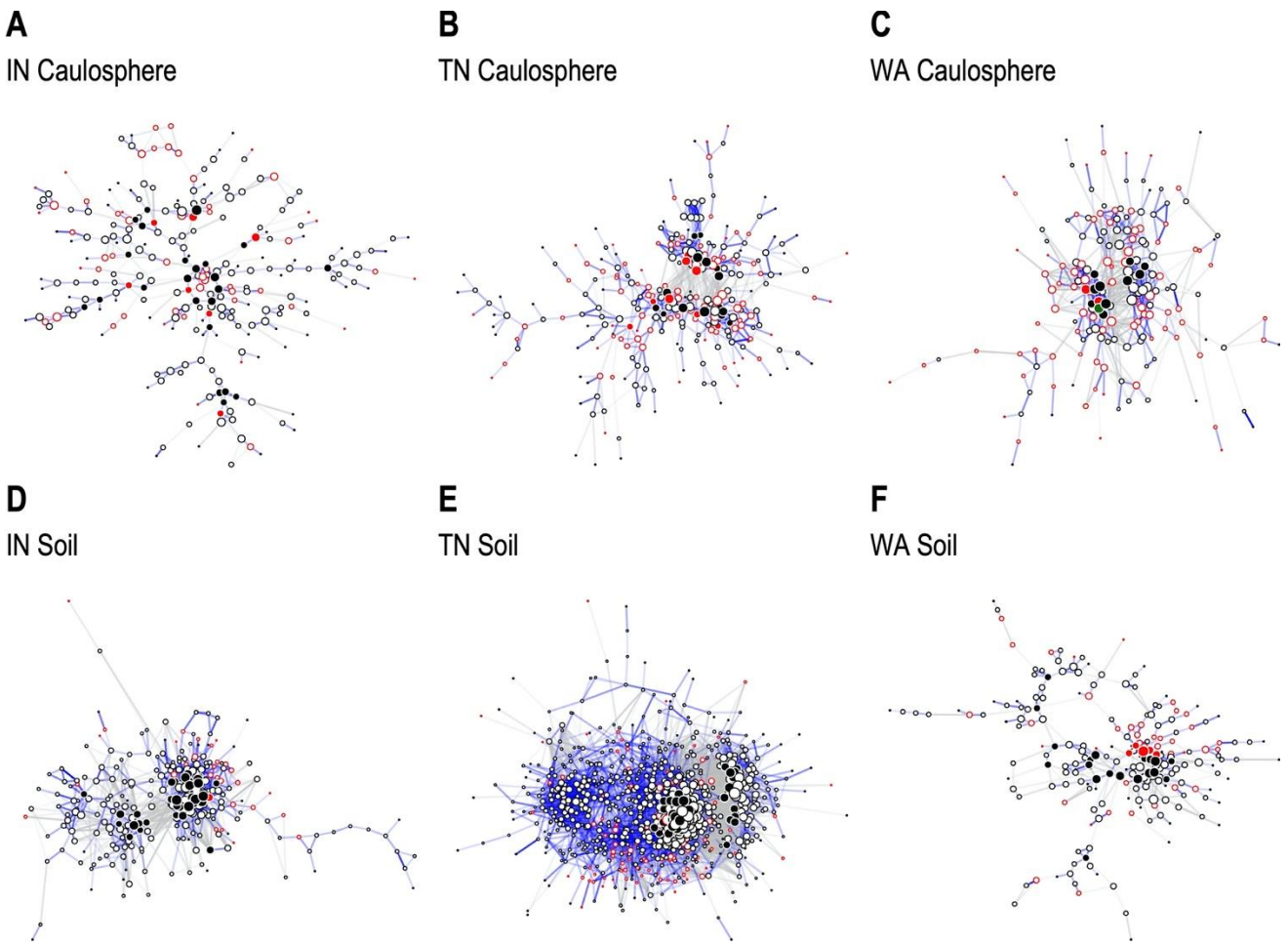

Figure 2.6. Depiction of correlation network for relationships among bacterial (black) and fungal (red) OTUs from the caulosphere (A, B and C) and soil microbiome (D, E, and F) of *Juglans nigra* in Indiana (IN) (A and D), Tennessee (TN) (B and E), and Washington (WA) (C and F), with hub nodes indicated by solid circles, and *Geosmithia morbida* as a green circle (C). Size of node indicates number of connections (degree). Darkness of lines indicate strength of correlation (absolute value of Spearman coefficient > 0.8). *P*-value cutoffs for networks shown < 0.01 for caulosphere (A, B, and C) and < 10^{-5} for soil (D, E, and F). Positive and negative associations are indicated by blue and grey lines, respectively. Independent subnetworks not shown.

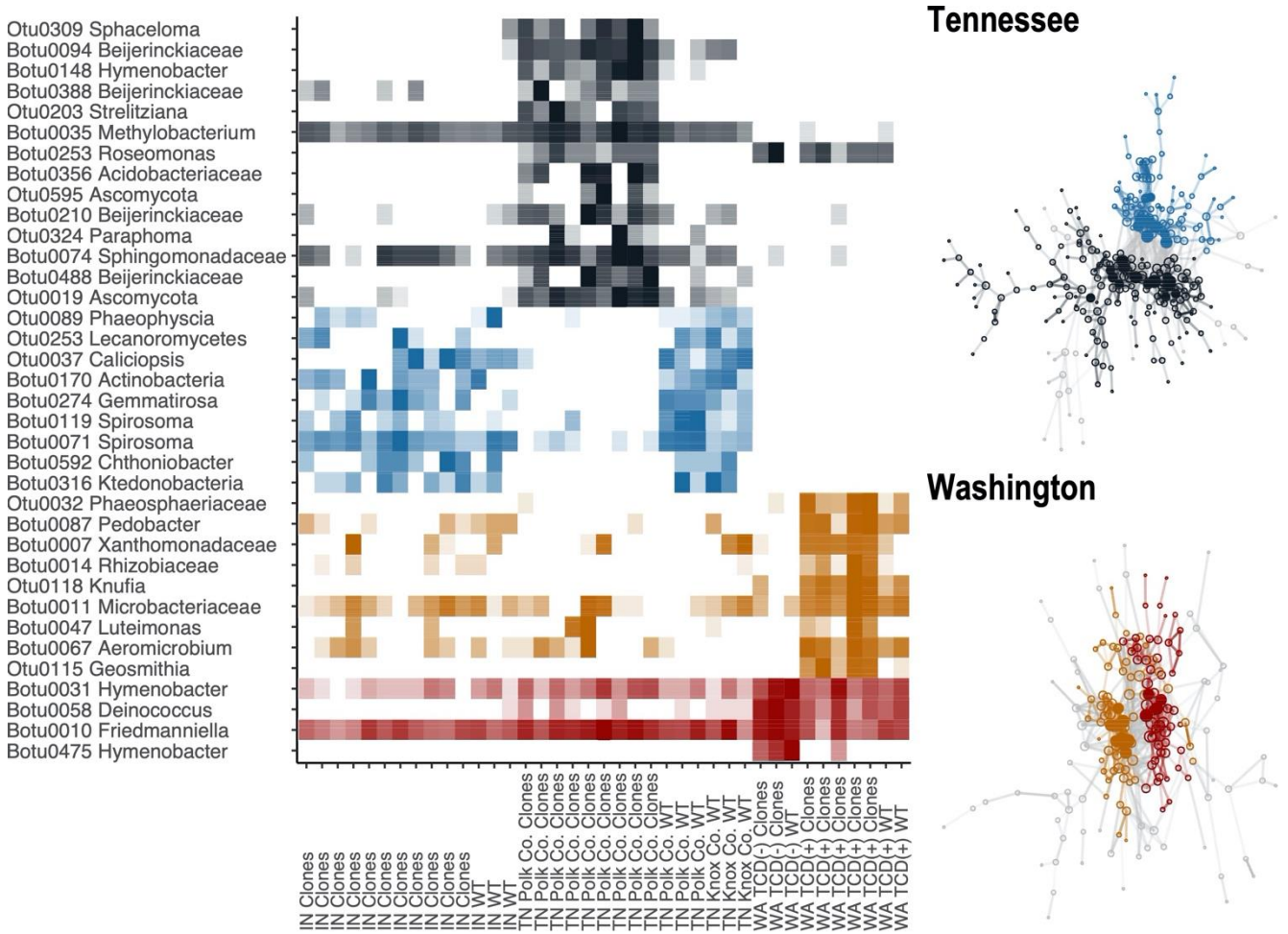

Figure 2.7. Heatmap of the relative abundance of hub taxa from alternative highlighted subnetworks of *Juglans nigra* in Tennessee (TN) (black and blue) and Washington (WA) (orange and red) caulosphere microbiome from merged fungal and bacterial data. Darkness of squares in heatmap represents standardized log transformed abundance of each OTU. Size of nodes indicates number of connections (degree); hub nodes depicted as solid circles; darkness of lines indicates absolute value of Spearman's r (> 0.8); networks are based on associations with $P < 0.01$.

Phaeomoniellales and *Rhinocladiella* (Eurotiomycetes) in caulospheres and entomopathogenic *Metarhizium* spp. (Sordariomycetes) in soils (Figs. 2.5B and A.8, Table A.8). WA had several plant pathogenic indicator OTUs in the caulosphere, such as *Cryptococcus cuniculi* (Tremellomycetes), *Taphrina* spp. (Taphrinomycetes), *Aureobasidium pullulans*, and *Alternaria* spp. (Dothidiomycetes), and in soils, including *Fusarium* spp. (Sordariomycetes) and *Alternaria* spp. (Dothidiomycetes; Fig. 2.5B and Fig. A.8; Table A.7 and Table A.8). In WA, there were 9 fungal indicator OTUs of TCD positive trees, including fungal pathogens such as *Alternaria metachromatica*, and 6 fungal indicator OTUs of TCD negative trees (Fig. 2.5B), including Orbiliaceae, which were also detected in IN and IN+TN (Fig. 2.5B).

2.3.9 Network Analysis of Hub Taxa and Network Complexity

In the caulosphere, TN and IN networks contained two subnetworks. Network analysis detected 174 hub caulosphere OTUs across IN (84 OTUs), TN (67 OTUs), and WA (23 OTUs) (Fig. 2.6A-C; Table A.9). There were common hub OTUs across all three states (Fig. 2.6A-C and Fig. A.9). Hub OTUs from WA included the black yeast *Knufia* spp. (FOtu0118) and a bacterium classified to the Xanthomonadaceae (BOtu0007), a bacterial family containing plant pathogens known to infect walnut (Arrieta et al., 2010). BOtu0007 was also identified as an indicator OTU of TCD-positive trees in WA (Fig. 2.5A and Fig. 2.7). In soils, network analysis detected 185 hub soil OTUs across IN (55 OTUs), TN (60 OTUs), and WA (70 OTUs) (Fig. 2.6D-F and Table A.10). There was overlap in soil hub OTUs between all three states (Fig. A.10).

Overall in the caulosphere, bootstrap mean microbiome network complexity was highest in WA, followed by TN and IN across all *P* and *R* cutoffs for all network complexity measurements (Fig. A.11). In soils, bootstrap mean microbiome network complexity was highest in TN, followed by IN and WA, respectively, for all measures and *P* and *R* cutoffs, with the sole exception of Mowshowitz entropy, which was lowest in IN for $P > 10^{-2}$ (Fig. A.12).

2.4 Discussion

Our study revealed differences in the diversity and composition of the phytobiome within and between the native (i.e. IN, TN) and introduced (WA) ranges of *J. nigra*, an economically and ecologically important tree species. These results support our central hypothesis of regional

differences in the host phytobiome across native and introduced ranges. Furthermore, alpha diversity measures were generally lower in WA compared to the native range, potentially linking observed geographic dependency of TCD incidence and severity to a species-poor phytobiome in the introduced range. We also observed stronger geographical differences in the alpha and beta diversity of the caulosphere compared to bulk soil.

Fungal and bacterial communities in the caulosphere of *J. nigra* within the introduced range had lower species richness and diversity when compared to trees from the native range. This finding is congruent with previous studies that observed differences in the alpha diversity of microbial communities between the native and introduced ranges of plant hosts (Gundale et al., 2016; Lu-Irving et al., 2019). We cannot rule out the possibility that lower species richness and patterns of beta diversity observed in WA caulosphere samples were partly a consequence of TCD infection because all eight TCD-positive trees were located in WA. The microbiome of diseased plants can have lower levels of alpha diversity compared to healthy plants (Koskella et al., 2017; Trivedi et al., 2012; Wei et al., 2018).

While it is possible that WA caulosphere communities were less diverse as a consequence of infection, our data support the hypothesis that the higher levels of alpha diversity recorded from IN and TN caulosphere compared to the introduced range (WA) could potentially function to limit establishment success, severity, and spread of *G. morbida* in the native range of *J. nigra*. Despite the fact that network analysis distinguished distinct microbial communities associated with trees that tested positive and negative for *G. morbida* in WA, overall alpha and beta diversity of WA samples differed dramatically from the native range. Although detected in eastern TN, TCD has not spread very far since its initial detection in 2009 (Tisserat et al., 2009). Apart from the incidental recovery of an adult WTB at a sawmill, no WTB have been detected in IN. Moreover, state-wide surveys have found no evidence of TCD in standing trees, despite the recovery of *G. morbida* from other beetle species (Juzwik et al., 2015; Marshall, 2015; Seybold et al., 2019).

At local scales, diverse communities are often more resistant to invasion than species poor communities (i.e. biotic resistance hypothesis) due to limited resource availability and niche space (Fitzgerald et al., 2016; Knops et al., 1999; Pinto & Ortega, 2016; Stachowicz et al., 1999; van Elsas et al., 2012). In contrast, several studies have found a positive relationship between alpha diversity and invasion success, which may be dependent upon more than just the alpha diversity

of recipient communities but also the phylogenetic relatedness of the invader to its recipient plant communities and the spatial scale under consideration (Fitzgerald et al., 2016; Li et al., 2015).

In addition to potentially limiting the establishment success of *G. morbida*, species-rich microbial communities tend to be more complex and possess greater multifunctionality and functional redundancy than species-poor communities (Wagg et al., 2014; Wagg et al., 2019). We observed the highest levels of network complexity in the WA *J. nigra* caulosphere compared to IN and TN, despite lower levels of species richness in WA caulsophere communities. The higher levels of network complexity in the WA caulosphere could be derived from the presence of two stable community states in WA, one of which contains *G. morbida* (Fig. 2.6). Perturbation of the system by *G. morbida* infection may have pushed the system from one state to the other (Shaw et al., 2019). The hub OTUs in the subnetwork with *G. morbida* also contained four bacterial OTUs (0007, 0011, 0014, and 0087) identified as indicator species that were present at the TCD positive site in Knox Co. and could be involved in disease (Fig. 2.5A and Fig. 2.7). The TN caulosphere also contains two subnetworks, but they segregated between clones and WT trees along with TCD status (Fig. 2.7). The TN subnetwork associated with WT trees was abundant in clones and WT trees in IN (Fig. 2.7, blue), but the subnetwork associated with TN clones was not well represented in IN (Fig. 2.7, black). However, two bacterial OTUs (0010 and 0031) from the presumably healthy (i.e. *G. morbida*-free) WA subnetwork were present in all three states (Fig. 2.7, red) along with Botu0011 from the *G. morbida*-associated WA subnetwork (Fig. 2.7, orange).

Compositional differences identified between IN and TN communities in this study demonstrate that the *J. nigra* phytobiome is highly variable across the host's native range. Even though the TN and WA caulospheres were characterized by the presence of two subnetworks and higher complexity than IN, the caulosphere phytobiomes sampled in the native range (IN and TN) shared more taxa with one another than they did with WA phytobiomes. Despite similarity in subnetwork structure to TN, community membership in WA was dominated by taxa that were either not present or less abundant in the native range. Geographic variation in the phytobiome among populations of individual species is well documented (Agler et al., 2016; Lu-Irving et al., 2019; Ramirez et al., 2019). Variation among regions has been attributed to differences in associated host plant communities, climate and soil differences, and host genetics (Bálint et al., 2015; Bálint et al., 2013; Gundale et al., 2016; Laforest-Lapointe et al., 2016; Ramirez et al., 2019; Wagner et al., 2016). The composition of fungal communities in the caulosphere of *J. nigra*

clones was influenced by host genetics, but the bacterial community composition was not. Our observations build on previous reports that fungal communities may be more sensitive to host plant genetics than bacterial communities (Bergelson et al., 2019).

The mycoparasite and plant pathogen communities that were recovered in the native range of *J. nigra* differed from those found in the introduced range. This observation provides support for the hypothesis that *J. nigra* has encountered novel pathogens and or lacks certain mutualists in its introduced western U.S. range. The greater richness of mycoparasites in the caulosphere of trees in their native range raises the possibility that trees in the native range (IN and TN) benefit from direct antagonism of pathogens (Gazis et al., 2018).

Caulosphere fungal communities in both the native and introduced ranges sampled in this study were dominated by sequences classified to the Ascomycota, which aligns with many studies evaluating phyllosphere endophyte communities (Cregger et al., 2018; Rogers et al., 2018). Caulosphere fungal communities in the introduced range of *J. nigra* (WA) had a greater proportion of sequences identified to the Dothideomycetes and Taphrinomycetes which contain well-known plant pathogens such as *Alternaria* spp. (Belisario et al., 1999) and *Taphrina* spp. (Cissé et al., 2013); the former was identified as an indicator OTU of TCD-positive trees in WA. Fungi in these taxa could act as secondary pathogens that increase severity of TCD in the western U.S (Busby et al., 2016). The Eurotiomycetes, predominantly represented by Phaeomoniellales, had greater representation in IN and TN (Fig. 2.3C and Fig. 2.5B and Fig. A.4C). Phaemoniellales is dominated by endophytes of gymnosperms and pathogens of dicots (Chen et al., 2015). Future effort should be undertaken to articulate the roles of these fungi as potential antagonists to *G. morbida*. Finally, we detected *Sydowia polyspora*, a common bark beetle associate, as an indicator OTU in the WA caulosphere (Muñoz-Adalia et al., 2017).

Interestingly, we did not detect any *Trichoderma* OTUs in the caulosphere despite their prevalence among fungi that were cultured from insect induced galleries and fungal lesions (Gazis et al., 2018). Failure to detect *Trichoderma* could be a product of primer bias which limited the amplification of *Trichoderma* DNA (Tedersoo & Lindahl, 2016), extraction bias, or the fact that sampling in this study did not include the insect galleries themselves. It is also possible that *Trichoderma* spp. were not present in the samples. These results highlight the importance of using culture-dependent methods in tandem with culture-independent screening to provide a more

complete picture of microbial communities that are interacting with infected host plants (Goulart et al., 2019; Pei et al., 2017; Weber et al., 2019).

Caulosphere bacterial communities were dominated by sequences from the Proteobacteria and did not contain archaeal sequences consistent with observations of other hardwood and coniferous tree species (Cregger et al., 2018; Proença et al., 2017; Ren et al., 2019; Rogers et al., 2018). OTUs belonging to Betaproteobacteriales (Gammaproteobacteria) were more abundant in WA than the native range, and mainly classified to the Burkholderiaceae, which were also identified as indicator OTUs for the WA caulosphere. Burkholderiaceae are considered to be ruderal species because they thrive in low-stress, highly disturbed environments and are reported as plant pathogens and endophytes (Bulgari et al., 2012; Fierer, 2017; Kajiwara, 2016). Additionally, members of the Burkholderiaceae are commonly detected in culture-dependent and culture-independent assessments of bark beetles and bark beetle galleries (Cardoza et al., 2009; Mason et al., 2015). The higher relative abundance of Burkholderiaceae in WA may be related to higher levels of disease incidence in this region.

Both soil alpha-diversity and community composition differed between native and introduced ranges of *J. nigra*. However, within-range differences were less distinct in the soil compared to the caulosphere, suggesting that different factors drive community composition in caulosphere and soil environments. Compared to bulk soil, communities directly associated with plant tissues are more strongly influenced by host biology and exclusionary interactions occurring in response to other endophytes (Lagunas et al., 2015; Newcombe et al., 2018; Plett & Martin, 2018; Roy & Kirchner, 2000). In soils, microbial communities are structured in large part by dispersal and edaphic factors (Colin et al., 2017; Erlandson et al., 2018; Fierer, 2017; Fukami, 2015; Glassman et al., 2017). In support of this, the stress-tolerant groups Acidobacteria, Chloroflexi, and Verrucomicrobia were most common in the most highly-weathered soils in TN, followed by IN (Fierer, 2017). Soil physicochemical properties significantly differed between sites, most likely due to differences in soil type and land use history between sites. Higher alpha diversity in the bacterial soil communities was likely driven by higher pH and lower NO_3-N concentrations in WA soils compared to IN and TN soils (Campbell et al., 2010; Zhang et al., 2017). Lower fungal richness in WA soils, compared to IN and TN, could be attributed to differences in the relative ability of native fungal communities to adapt to novel substrates and/or

allelochemicals, such as the root-secreted juglone (Block et al., 2019; Ladino-Orjuela et al., 2016; Lubbers et al., 2019; Meinhardt & Gehring, 2012; Schmidt, 1988).

There were significant differences in the community composition of arbuscular mycorrhizae in the soil within the native and introduced ranges of *J. nigra*. Arbuscular mycorrhizal richness was also greater in IN and TN. Arbuscular mycorrhizae are important plant symbionts that suppress canker diseases of apple (Krishna et al., 2010) and poplar (Tang & Chen, 1994) and thus may contribute to the observed differences in TCD severity. To better understand differences in arbuscular mycorrhizal communities between the native and introduced ranges of *J. nigra*, future studies should evaluate and compare root colonization by arbuscular mycorrhizae.

We also detected significant differences in the composition of plant pathogens in soil communities between the native and introduced ranges of *J. nigra*. In particular, the pathogens *Fusarium redolens* and *Alternaria* spp. were identified as indicator OTUs in WA soils. The presence of *F. redolens* in WA soils is of interest due to previous studies which found co-infection of *G. morbida* and *Fusarium* spp. in *J. nigra* trees (Tisserat et al., 2009). *Fusarium redolens* is a pathogen of chickpea (Jiménez-Fernández et al., 2011) and wheat (Esmaeili Taheri et al., 2011; Moya-Elizondo et al., 2011) in the Pacific Northwest. These two crops are among the most common rotation crops that are planted in southeast WA where our study site is located. *Gibberella zeae*, a common pathogen of wheat, was also detected as an indicator OTU of TCD positive trees providing further support that land-use history may explain some of the observed differences in soil microbiota associating with *J. nigra* trees. We also detected *Clonostachys* sp. as an indicator OTUs in the soils of IN+TN and TCD negative trees in WA; this common mycoparasitic biocontrol fungus and can induce systemic acquired resistance in plant hosts, suggesting a possible role in suppression of TCD (Roberti et al., 2008; Rodríguez et al., 2011).

In additional to regional differences, host genetics influenced fungal community composition in the caulosphere of *J. nigra* trees in this study. Given evidence that host genetics also play a significant role in regulating the severity of TCD infections and the higher severity and incidence of TCD in urban habitats, future efforts to develop practical management approaches for TCD should consider host genetic, environmental, and management factors that could modify susceptibility to disease (Busby et al., 2017).

2.4.1 Conclusion

In this study, we found evidence that genetic and geographic factors lead to differences in the richness, diversity, and composition of the *J. nigra* microbiome across the host's native and introduced ranges. These differences could possibly have a role in the observed geographical differences in TCD severity and incidence; however, additional research employing manipulated controlled experiments is needed to disentangle the effects of disease and geography on the phytobiome and the role of the phytobiome in controlling TCD spread (Busby et al., 2016). It should be noted that the microbiome can provide only a partial explanation for differences in TCD incidence and severity. WTB and *G. morbida* have likely not yet been introduced to north-central Indiana due to successful quarantine protections, thus explaining the absence of these TCD members in our IN study location. Differences in prevailing climate are also likely to be important factors that limit the establishment of both the fungus and its vector, accounting for differences in disease incidence and severity between the native and introduced ranges of *J. nigra*.

2.5 References

Agler, M. T., Ruhe, J., Kroll, S., Morhenn, C., Kim, S.-T., Weigel, D., & Kemen, E. M. (2016). Microbial hub taxa link host and abiotic factors to plant microbiome variation. *PLoS Biology*, 14:e1002352.

Arrieta, A., Díaz, B., & Frutos, D. (2010). Exploration and selection of walnut genotypes (Juglans regia L.) in Asturias with potential tolerance to *Xanthomonas arborícola* pv. *Juglandis* (Xaj). *Spanish Journal of Rural Development* (SJRD), 1:1-6.

Bálint, M., Tiffin, P., Hallström, B., O'Hara, R. B., Olson, M. S., Fankhauser, J. D., Piepenbring, M., & Schmitt, I. (2013). Host genotype shapes the foliar fungal microbiome of balsam poplar (*Populus balsamifera*). *PLoS ONE*, 8:e53987.

Bálint, M., Bartha, L., O'Hara, R. B., Olson, M. S., Otte, J., Pfenninger, M., Robertson, A. L., Tiffin, P., & Schmitt, I. (2015). Relocation, high-latitude warming and host genetic identity shape the foliar fungal microbiome of poplars. *Molecular Ecology*, 24:235-248.

Barberán, A., Bates, S. T., Casamayor, E. O., & Fierer, N. (2012). Using network analysis to explore co-occurrence patterns in soil microbial communities. *The ISME Journal*, 6:343-351.

Belisario, A., Forti, E., Corazza, L., and Van Kesteren, H. (1999). First report of *Alternaria* alternata causing leaf spot on English walnut. *Plant disease* 83:696-696.

Bergelson, J., Mittelstrass, J., & Horton, M. W. (2019). Characterizing both bacteria and fungi improves understanding of the *Arabidopsis* root microbiome. *Scientific Reports* 9:1-11.

Block, A. K., Yakubova, E., & Widhalm, J. R. (2019). Specialized naphthoquinones present in *Impatiens glandulifera* nectaries inhibit the growth of fungal nectar microbes. *Plant Direct* 3:e00132.

Blood, B. L., Klingeman, W. E., Paschen, M. A., Hadžiabdić, Đ., Couture, J. J., & Ginzel, M. D. (2018). Behavioral responses of *Pityophthorus juglandis* (Coleoptera: Curculionidae: Scolytinae) to volatiles of black walnut and *Geosmithia morbida* (Ascomycota: Hypocreales: Bionectriaceae), the causal agent of thousand cankers disease. Environmental *Entomology* 47:412-421.

Bonchev, D., & Buck, G. A. (2005). Quantitative measures of network complexity. In D. Bonchev & D. H. Rouvray (Eds.), *Complexity in Chemistry, Biology, and Ecology* (pp 191-235). Springer.

Bright, D. E. (1981). Taxonomic monograph of the genus *Pityophthorus* Eichhoff in North and Central America (Coleoptera: Scolytidae). *The Memoirs of the Entomological Society of Canada* 113:1-378.

Bulgari, D., Bozkurt, A. I., Casati, P., Çağlayan, K., Quaglino, F., & Bianco, P. A. (2012). Endophytic bacterial community living in roots of healthy and '*Candidatus* Phytoplasma mali'-infected apple (*Malus domestica*, Borkh.) trees. *Antonie Van Leeuwenhoek* 102:677-687.

Busby, P. E., Ridout, M., & Newcombe, G. (2016). Fungal endophytes: modifiers of plant disease. *Plant Molecular Biology* 90:645-655.

Busby, P. E., Soman, C., Wagner, M. R., Friesen, M. L., Kremer, J., Bennett, A., Morsy, M., Eisen, J. A., Leach, J. E., & Dangl, J. L. (2017). Research priorities for harnessing plant microbiomes in sustainable agriculture. *PLoS Biology* 15:e2001793.

Campbell, B. J., Polson, S. W., Hanson, T. E., Mack, M. C., & Schuur, E. A. (2010). The effect of nutrient deposition on bacterial communities in Arctic tundra soil. *Environmental Microbiology* 12:1842-1854.

Cardoza, Y. J., Vasanthakumar, A., Suazo, A., & Raffa, K. F. (2009). Survey and phylogenetic analysis of culturable microbes in the oral secretions of three bark beetle species. *Entomologia Experimentalis et Applicata* 131:138-147.

Chen, K.-H., Miadlikowska, J., Molnár, K., Arnold, A. E., U'Ren, J. M., Gaya, E., Gueidan, C., & Lutzoni, F. (2015). Phylogenetic analyses of eurotiomycetous endophytes reveal their close affinities to Chaetothyriales, Eurotiales, and a new order–Phaeomoniellales. *Molecular Phylogenetics and Evolution* 85:117-130.

Cissé, O. H., Almeida, J. M., Fonseca, Á., Kumar, A. A., Salojärvi, J., Overmyer, K., Hauser, P. M., & Pagni, M. (2013). Genome sequencing of the plant pathogen *Taphrina deformans*, the causal agent of peach leaf curl. *MBio* 4:e00055-00013.

Colin, Y., Nicolitch, O., Van Nostrand, J. D., Zhou, J. Z., Turpault, M. P., & Uroz, S. (2017). Taxonomic and functional shifts in the beech rhizosphere microbiome across a natural soil toposequence. *Scientific Reports* 7:9604.

Cregger, M., Veach, A., Yang, Z., Crouch, M., Vilgalys, R., Tuskan, G., & Schadt, C. (2018). The *Populus* holobiont: dissecting the effects of plant niches and genotype on the microbiome. *Microbiome* 6:31.

De Caceres, M., & Jansen, F. (2016). Package 'indicspecies' relationship between species and groups of sites. Page Functions to assess the strength and statistical significance of the relationship between species occurrence/abundance and groups of sites.

Erlandson, S., Wei, X., Savage, J., Cavender-Bares, J., & Peay, K. (2018). Soil abiotic variables are more important than Salicaceae phylogeny or habitat specialization in determining soil microbial community structure. *Molecular Ecology* 27:2007-2024.

Esmaeili Taheri, A., Hamel, C., Gan, Y., & Vujanovic, V. (2011). First report of Fusarium redolens from Saskatchewan and its comparative pathogenicity. *Canadian Journal of Plant Pathology* 33:559-564.

Feeley, T. (2010). Emerging threats to Iowa's forests, communities, wood industry, & economy thousand cankers disease. Iowa Department of Natural Resources Forestry Bureau.

Fierer, N. (2017). Embracing the unknown: disentangling the complexities of the soil microbiome. *Nature Reviews Microbiology* 15:579.

Fitzgerald, D. B., Tobler, M., & Winemiller, K. O. (2016). From richer to poorer: successful invasion by freshwater fishes depends on species richness of donor and recipient basins. *Global Change Biology* 22:2440-2450.

Fox, J., Weisberg, S., Price, B., Adler, D., Bates, D., Baud-Bovy, G., Bolker, B., & Ellison, S. (2018). Car: Companion to Applied Regression. The CRAN R Project. Retrieved 21 March, 2019.

Fukami, T. (2015). Historical contingency in community assembly: integrating niches, species pools, and priority effects. *Annual Review of Ecology, Evolution, and Systematics* 46:1-23.

Gauvrit, N., Singmann, H., Soler-Toscano, F., & Zenil, H. (2016). Algorithmic complexity for psychology: a user-friendly implementation of the coding theorem method. *Behavior Research Methods* 48:314-329.

Gazis, R., Poplawski, L., Klingeman, W., Boggess, S. L., Trigiano, R. N., Graves, A. D., Seybold, S. J., & Hadžiabdić, Đ.. (2018). Mycobiota associated with insect galleries in walnut with thousand cankers disease reveals a potential natural enemy against *Geosmithia morbida*. *Fungal Biology* 122:241-253.

Glassman, S. I., Wang, I. J., & Bruns, T. D. (2017). Environmental filtering by pH and soil nutrients drives community assembly in fungi at fine spatial scales. *Molecular Ecology* 26:6960-6973.

Goulart, M. C., Cueva-Yesquén, L. G., Hidalgo Martinez, K. J., Attili-Angelis, D., and Fantinatti-Garboggini, F. (2019). Comparison of specific endophytic bacterial communities in different developmental stages of *Passiflora incarnata* using culture-dependent and culture-independent analysis. *MicrobiologyOpen* 8:e896.

Grant, J. F., Windham, M. T., Haun, W. G., Wiggins, G. J., & Lambdin, P. L. (2011). Initial assessment of thousand cankers disease on black walnut, *Juglans nigra*, in eastern Tennessee. *Forests* 2:741-748.

Griffin, G. (2015). Status of thousand cankers disease on eastern black walnut in the eastern United States at two locations over 3 years. *Forest Pathology* 45:203-214.

Gundale, M. J., Almeida, J. P., Wallander, H., Wardle, D. A., Kardol, P., Nilsson, M. C., Fajardo, A., Pauchard, A., Peltzer, D. A., & Ruotsalainen, S. (2016). Differences in endophyte communities of introduced trees depend on the phylogenetic relatedness of the receiving forest. *Journal of Ecology* 104:1219-1232.

Hadžiabdić, Đ.., Vito, L. M., Windham, M. T., Pscheidt, J. W., Trigiano, R. N., and Kolarik, M. 2014a. Genetic differentiation and spatial structure of *Geosmithia morbida*, the causal agent of thousand cankers disease in black walnut (*Juglans nigra*). *Current Genetics* 60:75-87.

Hadžiabdić, Đ.., Windham, M., Baird, R., Vito, L., Cheng, Q., Grant, J., Lambdin, P., Wiggins, G., Windham, A., and Merten, P. J. P. d. 2014b. First report of *Geosmithia morbida* in North Carolina: The pathogen involved in thousand cankers disease of black walnut. *Plant Disease* 98:992-992.

Hoffman, M. T., & Arnold, A. E. (2008). Geographic locality and host identity shape fungal endophyte communities in cupressaceous trees. *Mycological Research* 112:331-344.

Jiménez-Fernández, D., Navas-Cortés, J. A., Montes-Borrego, M., Jiménez-Díaz, R. M., & Landa, B. B. (2011). Molecular and pathogenic characterization of *Fusarium redolens*, a new causal agent of *Fusarium* yellows in chickpea. *Plant Disease* 95:860-870.

Juzwik, J., McDermott-Kubeczko, M., Stewart, T., & Ginzel, M. (2016). First report of *Geosmithia morbida* on ambrosia beetles emerged from thousand cankers-diseased *Juglans nigra* in Ohio. *Plant Disease* 100:1238-1238.

Juzwik, J., Banik, M. T., Reed, S. E., English, J. T., & Ginzel, M. D. (2015). *Geosmithia morbida* found on weevil species *Stenomimus pallidus* in Indiana. *Plant Health Progress* 16:7-10.

Kajiwara, H. (2016). Direct detection of the plant pathogens *Burkholderia glumae*, *Burkholderia gladioli* pv. *gladioli*, and *Erwinia chrysanthemi* pv. *zeae* in infected rice seedlings using matrix assisted laser desorption/ionization time-of-flight mass spectrometry. *Journal of MIcrobiological Methods* 120:1-5.

Klironomos, J. N. (2002). Feedback with soil biota contributes to plant rarity and invasiveness in communities. *Nature* 417:67-70.

Knops, J. M., Tilman, D., Haddad, N. M., Naeem, S., Mitchell, C. E., Haarstad, J., Ritchie, M. E., Howe, K. M., Reich, P. B., & Siemann, E. (1999). Effects of plant species richness on invasion dynamics, disease outbreaks, insect abundances and diversity. *Ecology Letters* 2:286-293.

Koskella, B., Meaden, S., Crowther, W. J., Leimu, R., & Metcalf, C. J. E. 2017. A signature of tree health? Shifts in the microbiome and the ecological drivers of horse chestnut bleeding canker disease. *New Phytologist* 215:737-746.

Kozich, J. J., Westcott, S. L., Baxter, N. T., Highlander, S. K., & Schloss, P. D. (2013). Development of a dual-index sequencing strategy and curation pipeline for analyzing amplicon sequence data on the MiSeq Illumina sequencing platform. *Applied and Environmental Microbiology* 79:5112-5120.

Krishna, H., Das, B., Attri, B. L., Grover, M., & Ahmed, N. (2010). Suppression of *Botryosphaeria* canker of apple by arbuscular mycorrhizal fungi. *Crop Protection* 29:1049-1054.

Ladino-Orjuela, G., Gomes, E., da Silva, R., Salt, C., & Parsons, J. R. (2016). Metabolic pathways for degradation of aromatic hydrocarbons by bacteria. *Reviews of Environmental Contamination and Toxicology* 237. Springer.

Laforest-Lapointe, I., Messier, C., & Kembel, S. W. (2016). Host species identity, site and time drive temperate tree phyllosphere bacterial community structure. *Microbiome* 4:27.

Lagunas, B., Schäfer, P., & Gifford, M. (2015). Housing helpful invaders: the evolutionary and molecular architecture underlying plant root-mutualist microbe interactions. *Journal of Experimental Botany* 66:2177-2186.

Li, S. p., Cadotte, M. W., Meiners, S. J., Hua, Z. s., Shu, H. y., Li, J. t., & Shu, W. S. 2015. The effects of phylogenetic relatedness on invasion success and impact: deconstructing Darwin's naturalisation conundrum. *Ecology Letters* 18:1285-1292.

Lu-Irving, P., Harenčár, J. G., Sounart, H., Welles, S. R., Swope, S. M., Baltrus, D. A., & Dlugosch, K. M. (2019). Native and invading yellow starthistle (*Centaurea solstitialis*) microbiomes differ in composition and diversity of bacteria. *mSphere* 4:e00088-00019.

Lubbers, R. J., Dilokpimol, A., Visser, J., Mäkelä, M. R., Hildén, K. S., and de Vries, R. P. (2019). A comparison between the homocyclic aromatic metabolic pathways from plant-derived compounds by bacteria and fungi. *Biotechnology Advances* 37(7): 107396.

Marshall, P. (2015). Walnut twig beetle detected in Indiana. Indiana Department of Natural Resources.

Mason, C. J., Hanshew, A. S., & Raffa, K. F. (2015). Contributions by host trees and insect activity to bacterial communities in *Dendroctonus valens* (Coleoptera: Curculionidae) galleries, and their high overlap with other microbial assemblages of bark beetles. *Environmental Entomology* 45:348-356.

Meinhardt, K. A., & Gehring, C. A. (2012). Disrupting mycorrhizal mutualisms: a potential mechanism by which exotic tamarisk outcompetes native cottonwoods. *Ecological Applications* 22:532-549.

Moore, M., Juzwik, J., Miller, F., Roberts, L., & Ginzel, M. D. (2019). Detection of *Geosmithia morbida* on numerous insect species in four eastern states. *Plant Health Progress* 20:133-139.

Moricca, S., Bracalini, M., Benigno, A., Ginetti, B., Pelleri, F., & Panzavolta, T. (2019). Thousand cankers disease caused by Geosmithia morbida and its insect vector *Pityophthorus juglandis* first reported on *Juglans nigra* in Tuscany, Central Italy. *Plant Disease* 103:369-369.

Mowshowitz, A. (1968). Entropy and the complexity of graphs: II. The information content of digraphs and infinite graphs. The Bulletin of Mathematical Biophysics 30:225-240.

Moya-Elizondo, E. A., Rew, L. J., Jacobsen, B. J., Hogg, A. C., & Dyer, A. T. (2011). Distribution and prevalence of *Fusarium crown* rot and common root rot pathogens of wheat in Montana. *Plant Disease* 95:1099-1108.

Mueller, L. A., Kugler, K. G., Dander, A., Graber, A., & Dehmer, M. (2011). QuACN: an R package for analyzing complex biological networks quantitatively. *Bioinformatics* 27:140-141.

Muñoz-Adalia, E. J., Sanz-Ros, A. V., Flores-Pacheco, J. A., Hantula, J., Diez, J. J., Vainio, E. J., & Fernández, M. (2017). *Sydowia polyspora* dominates fungal communities carried by two Tomicus species in pine plantations threatened by *Fusarium circinatum*. *Forests* 8:127.

Newcombe, G., Harding, A., Ridout, M., & Busby, P. E. (2018). A hypothetical bottleneck in the plant microbiome. *Frontiers in Microbiology* 9:1645.

Nguyen, N. H., Song, Z., Bates, S. T., Branco, S., Tedersoo, L., Menke, J., Schilling, J. S., & Kennedy, P. G. (2016). FUNGuild: An open annotation tool for parsing fungal community datasets by ecological guild. *Fungal Ecology* 20:241-248.

Nilsson, R. H., Larsson, K.-H., Taylor, A. F. S., Bengtsson-Palme, J., Jeppesen, T. S., Schigel, D., Kennedy, P., Picard, K., Glöckner, F. O., & Tedersoo, L. (2018). The UNITE database for molecular identification of fungi: handling dark taxa and parallel taxonomic classifications. *Nucleic Acids Research* 47:D259-D264.

Oksanen, J., Blanchet, F. G., Friendly, M., Kindt, R., Legendre, P., McGlinn, D., Minchin, P. R., O'Hara, R. B., Simpson, G. L., Solymos, P., Henry, M., Stevens, H., Szoecs, E., & Maintainer, H. W. (2019). Package 'vegan' community ecology package.

Oren, E., Klingeman, W., Gazis, R., Moulton, J., Lambdin, P., Coggeshall, M., Hulcr, J., Seybold, S. J., & Hadžiabdić, Đ. (2018). A novel molecular toolkit for rapid detection of the pathogen and primary vector of thousand cankers disease. PLoS ONE 13:e0185087.

Paradis, E., & Schliep, K. (2019). ape 5.0: an environment for modern phylogenetics and evolutionary analyses in R. *Bioinformatics* 35:526-528.

Parker, M. A., Malek, W., & Parker, I. M. (2006). Growth of an invasive legume is symbiont limited in newly occupied habitats. *Diversity and Distributions* 12:563-571.

Pedersen, T. (2019). tidygraph: A Tidy API for Graph Manipulation. 2018.

Pei, C., Mi, C., Sun, L., Liu, W., Li, O., & Hu, X. (2017). Diversity of endophytic bacteria of Dendrobium officinale based on culture-dependent and culture-independent methods. *Biotechnology & Biotechnological Equipment* 31:112-119.

Pinto, S. M., & Ortega, Y. K. (2016). Native species richness buffers invader impact in undisturbed but not disturbed grassland assemblages. *Biological Invasions* 18:3193-3204.

Plett, J. M., & Martin, F. M. (2018). Know your enemy, embrace your friend: using omics to understand how plants respond differently to pathogenic and mutualistic microorganisms. *The Plant Journal* 93:729-746.

Prider, J., Watling, J., & Facelli, J. M. (2008). Impacts of a native parasitic plant on an introduced and a native host species: implications for the control of an invasive weed. *Annals of Botany* 103:107-115.

Proença, D. N., Francisco, R., Kublik, S., Schöler, A., Vestergaard, G., Schloter, M., & Morais, P. V. (2017). The microbiome of endophytic, wood colonizing bacteria from pine trees as affected by pine wilt disease. *Scientific Reports* 7:4205.

Ramirez, K. S., Snoek, L. B., Koorem, K., Geisen, S., Bloem, L. J., Ten Hooven, F., Kostenko, O., Krigas, N., Manrubia, M., & Caković, D. (2019). Range-expansion effects on the belowground plant microbiome. *Nature Ecology & Evolution* 3:604.

Ren, F., Kovalchuk, A., Mukrimin, M., Liu, M., Zeng, Z., Ghimire, R. P., Kivimäenpää, M., Holopainen, J. K., Sun, H., & Asiegbu, F. O. (2019). Tissue microbiome of Norway spruce affected by *Heterobasidion*-induced wood decay. *Microbial Ecology* 77:640-650.

Roberti, R., Veronesi, A., Cesari, A., Cascone, A., Di Berardino, I., Bertini, L., & Caruso, C. (2008). Induction of PR proteins and resistance by the biocontrol agent *Clonostachys rosea* in wheat plants infected with *Fusarium culmorum. Plant Science* 175:339-347.

Rodríguez, M. A., Cabrera, G., Gozzo, F., Eberlin, M., & Godeas, A. (2011). *Clonostachys rosea* BAFC3874 as a *Sclerotinia sclerotiorum* antagonist: mechanisms involved and potential as a biocontrol agent. *Journal of Applied Microbiology* 110:1177-1186.

Rogers, T. J., Leppanen, C., Brown, V., Fordyce, J. A., LeBude, A., Ranney, T., Simberloff, D., & Cregger, M. A. (2018). Exploring variation in phyllosphere microbial communities across four hemlock species. *Ecosphere* 9:e02524.

Roy, B., & Kirchner, J. (2000). Evolutionary dynamics of pathogen resistance and tolerance. *Evolution* 54:51-63.

Rugman-Jones, P. F., Seybold, S. J., Graves, A. D., & Stouthamer, R. (2015). Phylogeography of the walnut twig beetle, *Pityophthorus juglandis*, the vector of thousand cankers disease in North American walnut trees. *PLoS ONE* 10:e0118264.

Schloss, P. D. (2020). Reintroducing mothur: 10 years later. Applied and Environmental *Microbiology* 86.

Schmidt, S. (1988). Degradation of juglone by soil bacteria. *Journal of Chemical Ecology* 14:1561-1571.

Seybold, S. J., Klingeman, W. E., III, Hishinuma, S. M., Coleman, T. W., & Graves, A. D. (2019). Status and impact of walnut twig beetle in urban forest, orchard, and native forest ecosystems. *Journal of Forestry* 117:152-163.

Shaw, L. P., Bassam, H., Barnes, C. P., Walker, A. S., Klein, N., & Balloux, F. (2019). Modelling microbiome recovery after antibiotics using a stability landscape framework. *The ISME Journal* 13:1845-1856.

Soler-Toscano, F., Zenil, H., Delahaye, J.-P., & Gauvrit, N. (2014). Calculating Kolmogorov complexity from the output frequency distributions of small Turing machines. *PloS ONE* 9:e96223.

Stachowicz, J. J., Whitlatch, R. B., & Osman, R. W. (1999). Species diversity and invasion resistance in a marine ecosystem. *Science* 286:1577-1579.

Stricker, K. B., Harmon, P. F., Goss, E. M., Clay, K., and Luke Flory, S. (2016). Emergence and accumulation of novel pathogens suppress an invasive species. *Ecology Letters* 19:469-477.

Tang, M., & Chen, D. (1994). The effect of vesicular-arbuscular mycorrhizas on the resistance of poplar to a canker fungus (*Dothiorella gregaria*). *Mycorrhizas for Plantation Forestry in Asia* 92:67.

Tedersoo, L., Bahram, M., Põlme, S., Kõljalg, U., Yorou, N.S., Wijesundera, R., Ruiz, L.V., Vasco Palacios, A.M., Thu, P.Q., Suija, A., Smith, M.E. 2014. Global diversity and geography of soil fungi. *Science* 346:6213.

Tedersoo, L., & Lindahl, B. (2016). Fungal identification biases in microbiome projects. *Environmental Microbiology Reports* 8:774-779.

Thompson, B. M., Bodart, J., & Gruner, D. S. (2019). Community resistance to an invasive forest insect–fungus mutualism. *Ecosphere* 10:e02609.

Tisserat, N., Cranshaw, W., Leatherman, D., Utley, C., & Alexander, K. (2009). Black walnut mortality in Colorado caused by the walnut twig beetle and thousand cankers disease. *Plant Health Progress* 11, 10. doi:10.1094/php-2009-0811-01-rs.

Treiman, T., & Tuttle, J. (2009). Thousand cankers disease of black walnut: how much will it hurt Missouri's pocketbook? *Notes for Forest Managers* 16.

Treiman, T., Atchison, B., McDonnell, T., Barden, C., & Moser, W. K. (2010). Economic loss associated with the introduction of thousand cankers disease of black walnut to Kansas. Kansas State University Agricultural Experiment Station and Cooperative Extension Service.

Trivedi, P., He, Z., Van Nostrand, J. D., Albrigo, G., Zhou, J., & Wang, N. (2012). Huanglongbing alters the structure and functional diversity of microbial communities associated with citrus rhizosphere. *The ISME Journal* 6:363-383.

Utley, C., Nguyen, T., Roubtsova, T., Coggeshall, M., Ford, T. M., Grauke, L. J., Graves, A D., Leslie, C. A., McKenna, J., Woeste, K., Yaghmour, M A., Cranshaw, W., Seybold, S. J., Bostock, R. M., & Tisserat, M. (2013). Susceptibility of Walnut and Hickory Species to *Geosmithia morbida*. *Plant Disease* 97, 601–607. doi:10.1094/PDIS-07-12-0636-RE.

van der Putten, W. H., Kowalchuk, G. A., Brinkman, E. P., Doodeman, G. T. A., van der Kaaij, R. M., Kamp, A. F. D., Menting, F. B. J., & Veenendaal, E. M. (2007). Soil feedback of exotic savannah grass relates to pathogen absence and mycorrhizal selectivity. *Ecology* 88:978-988.

van Elsas, J. D., Chiurazzi, M., Mallon, C. A., Elhottovā, D., Krištůfek, V., & Salles, J. F. (2012). Microbial diversity determines the invasion of soil by a bacterial pathogen. *PNAS* 109:1159-1164.

Veach, A. M., Morris, R., Yip, D. Z., Yang, Z. K., Engle, N. L., Cregger, M. A., Tschaplinski, T. J., & Schadt, C. W. (2019). Rhizosphere microbiomes diverge among *Populus trichocarpa* plant-host genotypes and chemotypes, but it depends on soil origin. *Microbiome* 7:76.

Wagg, C., Bender, S. F., Widmer, F., and van der Heijden, M. G. (2014). Soil biodiversity and soil community composition determine ecosystem multifunctionality. *PNAS* 111:5266-5270.

Wagg, C., Schlaeppi, K., Banerjee, S., Kuramae, E. E., and van der Heijden, M. G. (2019). Fungal-bacterial diversity and microbiome complexity predict ecosystem functioning. *Nature Communications* 10:1-10.

Wagner, M. R., Lundberg, D. S., Tijana, G., Tringe, S. G., Dangl, J. L., and Mitchell-Olds, T. (2016). Host genotype and age shape the leaf and root microbiomes of a wild perennial plant. *Nature Communications* 7:1-15.

Weber, M., Liedtke, J., Plattes, S., & Lipski, A. (2019). Bacterial community composition of biofilms in milking machines of two dairy farms assessed by a combination of culture-dependent and–independent methods. *PLoS ONE* 14.

Wei, Z., Hu, J., Yin, S., Xu, Y., Jousset, A., Shen, Q., and Friman, V.-P. 2018. *Ralstonia solanacearum* pathogen disrupts bacterial rhizosphere microbiome during an invasion. *Soil Biology and Biochemistry* 118:8-17.

White, T. J., Bruns, T., Lee, S., & Taylor, J. (1990). Amplification and direct sequencing of fungal ribosomal RNA genes for phylogenetics. In M. Innis, D. Gelfand, J. Sninsky, & T. White, (Eds.), *PCR Protocols: a guide to methods and applications* (pp. 282–287). New York, NY: Academic Press

Williams, R. D. (1990). *Juglans nigra* L., black walnut. *Silvics of North America* 2:391-399.

Wood, S. L., & Bright, D. E. (1992). A Catalog of Scolytidae and Platypodidae (Coleoptera), Part 2: Taxonomic Index. Volume B. Great Basin Naturalist Memoirs. 13:835-1557.

Zenil, H., Soler-Toscano, F., Dingle, K., & Louis, A. A. (2014). Correlation of automorphism group size and topological properties with program-size complexity evaluations of graphs and complex networks. *Physica A: Statistical Mechanics and its Applications* 404:341-358.

Zenil, H., Soler-Toscano, F., Delahaye, J.-P., & Gauvrit, N. (2015). Two-dimensional Kolmogorov complexity and an empirical validation of the Coding theorem method by compressibility. *PeerJ Computer Science* 1:e23.

Zerillo, M. M., Ibarra Caballero, J., Woeste, K., Graves, A. D., Hartel, C., Pscheidt, J. W., Tonos, J., Broders, K., Cranshaw, W., Seybold, S. J., & Tisserat, N. (2014). Population structure of *Geosmithia morbida*, the causal agent of thousand cankers disease of walnut trees in the United States. *PLoS ONE* 9:e112847.

Zhang, Q., Yang, R., Tang, J., Yang, H., Hu, S., & Chen, X. (2010). Positive feedback between mycorrhizal fungi and plants influences plant invasion success and resistance to invasion. *PLoS ONE* 5(8):e13280.

Zhang, Y., Shen, H., He, X., Thomas, B. W., Lupwayi, N. Z., Hao, X., Thomas, M. C., & Shi, X. (2017). Fertilization shapes bacterial community structure by alteration of soil pH. *Frontiers in Microbiology* 8:e1325.

CHAPTER 3. FOREST AND PLANTATION SOIL MICROBIOMES DIFFER IN THEIR CAPACITY TO SUPPRESS FEEDBACK BETWEEN GEOSMITHIA MORBIDA AND RHIZOSPHERE PATHOGENS OF *J. NIGRA* SEEDLINGS

*** In press as: Williams, G.M. and Ginzel, M.D., 2021. Forest and Plantation Soil Microbiomes Differ in their Capacity to Suppress Feedback Between Geosmithia morbida and Pathogens of *J. nigra* seedlings. Phytobiomes Journal.**

3.1 Introduction

The etiology of tree diseases can be best understood within a framework of predisposing conditions, proximate or primary agents, and ultimate causes of mortality that includes both biotic and abiotic factors (Manion, 1981; Tainter & Baker, 1996). This framework is particularly relevant when considering diseases where severity is highly variable across environmental conditions, such as thousand cankers disease (TCD) of eastern black walnut (*Juglans nigra* L.). The proximate cause of TCD, an emergent disease of *J. nigra* and other *Juglans* and *Pterocarya* spp., is attack by the walnut twig beetle *Pityophthorus juglandis* Blackman and necrosis caused by its primary fungal symbiont, *Geosmithia morbida* Kol. Free. Ut. & Tiss. (Tisserat et al., 2009; Ploetz et al., 2013).

Additional factors, including site quality or the activity of other microorganisms, can predispose hosts to disease or contribute to later stages of decline and ultimate mortality. TCD appears to be most severe in urban forests and managed plantations, whereas natural forest populations of *J. nigra* in its native range have remained relatively unaffected, even in areas where the pathogen and vector have been detected (Seybold et al., 2019; Juzwik et al., 2020). Urban forests are frequently subject to invasive pest outbreaks due to predisposing factors such as connectivity with transportation pathways, higher ambient and soil temperatures, increased wind and drought exposure, and physical damage (Klein & Perkins, 1987; Tello et al., 2005). Natural forest landscapes are likely to be more resilient to disease compared to managed plantations due to higher biological and structural diversity (Coyle et al., 2005; Ennos, 2015; Wingfield et al., 2015; Jactel et al., 2021).

Environmental differences among managed plantations, urban and natural forests can also include dissimilarites in the composition and function of the bulk soil microbiome and host

phytobiome. Such differences in the microbiome may include the relative abundance of other pathogens or beneficial endophytes that could play roles in the etiology of disease (Carroll, 1988; Arnold et al., 2000; Porras-Alfaro & Bayman, 2011). Pathogens other than *G. morbida* are frequently found in soil around TCD-symptomatic walnut trees or in tissues surrounding subdermal cankers (Kasson et al., 2014; Gazis et al., 2018; Lauritzen, 2018; Onufrak et al., 2020). In fact, a role for *Fusarium solani* species complex *sensu* Summerell (2019) (FSSC; Sordariomycetes: Hypocreales: Nectriaceae) in the etiology of later stages of TCD was recognized in the first description of the disease (Tisserat et al., 2009). FSSC spp. were frequently isolated by Tisserat et al., (2009) from the boles of trees in the later stages of decline, indicating that these generalist pathogens might contribute to the ultimate causes of mortality of trees with TCD. Culture-based studies of TCD-symptomatic trees have since uncovered a diversity of *F. solani*, *F. fujikuroi*, *F. lateritium*, and *F. tricinctum* species complexes *sensu* Summerell (2019) associated with cankers (Kasson et al., 2014; Gazis et al., 2018; Lauritzen, 2018). In particular, FSSC sp. 25 is found in close association with *G. morbida* in TCD-symptomatic walnut trees in the U.S. and Italy, but does not increase the size of cankers when coinoculated with *G. morbida*, nor does it cause larger cankers alone compared to water controls (Kasson et al., 2014; Montecchio et al., 2015; Sitz et al., 2017; Juzwik et al., 2020). Thus, the impact of these and other canker-causing pathogens on the etiology of TCD remains unclear. Nevertheless, other studies suggest that multitrophic interactions between the host and primary and secondary pathogens lead to the development of plant disease and are regulated by the microbiome (Lamichhane & Venturi, 2015; Van Gils et al., 2017).

Trees in urban and plantation forests exist in a state of heightened physiological stress due to abiotic factors, management activities, and contrasting levels of herbivory and disease (Van Loon, 1997; Durrant & Dong, 2004; Coyle et al., 2005; Yuan et al., 2018). This stress may also condition the host microbiome and susceptibility to disease. In particular, limited genetic and species diversity in plantations and orchards might lead to the accumulation of pests and secondary pathogens (Coyle et al., 2005; Yang et al., 2012; Ennos, 2015). These same secondary pathogens, including *Fusarium*, related Nectriaceae and *Rhizoctonia* spp. (Agaricomycetes: Cantharellales: Ceratobasidiaceae) are thought to be major contributors to plant-soil feedbacks, in which plants condition soil biota to the benefit (positive feedback) or detriment (negative feedback) of conspecifics (McKenry, 1999; Klironomos, 2002; Bennett & Klironomos, 2019). These negative

feedbacks are also responsible for replant diseases of orchard crops in the western U.S. where TCD is severe (Mazzola, 1998; Browne et al., 2006; Schmidt et al., 2010). Plant-soil feedbacks and belowground pests and pathogens can also promote aboveground herbivores, including bark beetles (Hertert et al., 1975; Aukema et al., 2010; Van Gils et al., 2017; Kaplan et al., 2018). Therefore, it is possible that feedbacks between *G. morbida* and soil-dwelling microbiota such as FSSC spp. play a role in TCD etiology as predisposing factors and/or ultimate causes of mortality.

In natural forests where TCD has been slower to establish, *J. nigra* might benefit from favorable associations that contribute to host resilience such as mycorrhizal or other mutualistic fungi and bacteria (Jung et al., 2012; Pineda et al., 2017; Gazis et al., 2018). For example, *Trichoderma* spp. have been employed as biological control for plant diseases, and were found in higher abundance and diversity in *P. juglandis* galleries in the eastern compared with the western U.S. (Gazis et al., 2018). Accumulation of pathogens may also lead to recruitment of beneficial, antagonistic microbiota (Schlatter et al., 2017). In addition to build-up of pathogens like *Gibberella zeae* (Schwein.) Petch (syn. *F. graminearum* Schwabe) in soils around TCD-infected trees, beneficial fungi such as mycoparasites were found in soils around non-infected trees (Onufrak et al., 2020). The extent to which beneficial microbes and feedback between aboveground pathogens such as *G. morbida* and soil biota influence host susceptibility to and severity of bark beetle-fungal diseases such as TCD has not been explored. Basic knowledge of these processes could be translated to management strategies to improve interactions of trees with pests and pathogens in their environment (Busby et al., 2017).

We conducted two experiments to test the hypothesis that the soil microbiome modifies susceptibility or resistance of *J. nigra* seedlings to *G. morbida* under greenhouse conditions. In our first experiment, untreated potting mix was amended with live or steam-treated soil, a) to determine the extent to which forest and plantation soil microbiomes affect the size and healing of cankers caused by *G. morbida*; and b) to assess the effect of live and steam-treated soil amendments on feedback between aboveground *G. morbida* infection and the microbiome of seedling roots. We were particularly interested in the response of *Fusarium* and *Rhizoctonia* spp., soilborne pathogens associated with negative soil feedback (Cesarano et al., 2017), to inoculation with *G. morbida*. In a second experiment, we treated seeds with two endophytic fungi isolated from roots in the first experiment to determine the extent to which they affected canker growth after seedlings were inoculated with *G. morbida*. One isolate FSSC sp., was a putative disease

synergist, and the other *Trichoderma* sp., a putative biological control fungus. We hypothesized that FSSC sp. would increase the size and decrease healing of cankers and that *Trichoderma* sp. would limit root colonization by FSSC sp. and/or canker growth.

3.2 Materials and Methods

3.2.1 Live Soil Amendment Experiment

Soil Collection

Soils were collected on May 21, 2018 from four 3 x 3 m plots: two located in two different plantations of *J. nigra* of ages 50 (40°25'51.6"N, 87°02'25.2"W) and 28 years (40°25'60.0"N, 87°02'07.3"W) at Martell experimental forest (West Lafayette, IN); and two plots that were each located below two different 100+ year old *J. nigra* growing in mixed hardwood stands adjacent to each of the two plantations. Approximately 500 L (bulk volume) of soil was removed from the top ~8 cm of the plots, sifted through 1.5-cm wire mesh to remove debris, and mixed by type (forest and plantation) to obtain a composite sample of each type. A subsample of ~ 120 L (bulk volume) of each soil type was kept at 4°C for three to five days prior to planting.

Potting of Bare-Root Seedlings with Live Soil Amendments

On May 22, 2018, we planted 120 one-year-old *J. nigra* seedlings grown at Vallonia nursery (IN-DNR) from mixed, open-pollinated seed collected in Indiana. The nursery beds at Vallonia nursery are fumigated with methyl bromide (336 kg/ha) and chloropicrin (56 kg/ha; James McKenna, *personal communication*). Prior to planting, root systems were trimmed to stimulate root growth and remove damaged roots and washed with water and antimicrobial dish soap to remove nursery soil. We planted seedlings in Metro-Mix 560 Sun-Coir (560SC) tree potting media (Sun Gro Horticulture, Agawam, MA) in new 9.6 L TP818 Treepots (Stuewe and Sons, Corvallis, OR). We chose not to sterilize the 560SC potting mix because it would result in the loss of nutrients and soil structure, and can lead to misleading inferences (Trevors, 1996; Van Gils et al., 2017). To ensure a sufficient amount of live soil inoculum and substrate were present to transfer potential disease suppressiveness (Schlatter et al., 2017), potting mix was amended 20% by bulk volume with live

soil from forest (n = 40) or plantation soil (n = 40). As a control soil amendment, we used a 50-50 mixture of forest and plantation soil that had been heat-pasteurized in a 54 Soil Steamer (Hummert International, Topeka, KS) twice for 5 hours with steam at 30 PSIG and 274° C with an intervening 24-hour cooling period. The steam-treated soil mixture was also added to pots at a 20% bulk volume ratio like the other treatments (n = 40). Seedlings were grown in the Entomology Environmental Laboratory greenhouses at Purdue University, West Lafayette, IN, USA. Greenhouse temperatures ranged from 20° to 40° C. No supplemental fertilization was provided beyond what was available in the amended 560SC tree potting media and soil amendments. All plants were watered to saturatation as needed over the course of the growing period.

Inoculation of Seedlings with G. morbida and Measurement of Necrosis and Healing

In the greenhouse, seedlings were inoculated with *G. morbida* forty-three days after transplanting (July 4) following the methods of Utley et al., (2012). Cultures of isolate IN-66 from Brown Co., IN (Juzwik et al., 2015) were grown for one week on 1/8-strength potato dextrose agar (4.9 g PDA powder + 13.1 g agar per 1 L H_2O; Thermo Fisher Scientific, Waltham MA). A 6-mm diameter corkborer was used to remove the outer bark and phloem 20 cm above the root collar. In the resulting wound, seedlings from each soil amendment treatment received a 6 mm diameter plug of either *G. morbida* (n = 30 per soil amendment treatment), or sterile 1/8-strength PDA (control inoculation, n = 10). Across the three soil treatments, a total of 90 seedlings were inoculated with *G. morbida*, and 30 were inoculated with sterile 1/8-strength PDA alone as a control. After inoculation, wounds were sealed with parafilm and duct tape.

Seedlings were harvested between Sept. 18 and 30, 2018 (76 to 88 days post-inoculation). Bark and phloem were carefully removed from the outer sapwood, and inner phloem was imaged with a flatbed scanner to allow precise quantification of necrotic area by manually tracing canker margins using ImageJ 1.51 (U.S. National Institute of Health). To collect data on host response, canker healing was scored on an ordinal scale (Fig. 3.1A).

Isolation of Fungi from Roots

Roots were harvested from 10 *G. morbida*-inoculated and 10 agar-only control plants within each soil amendment treatment. A total sample of ~80 root sections (~ 2 cm ea.) were harvested at

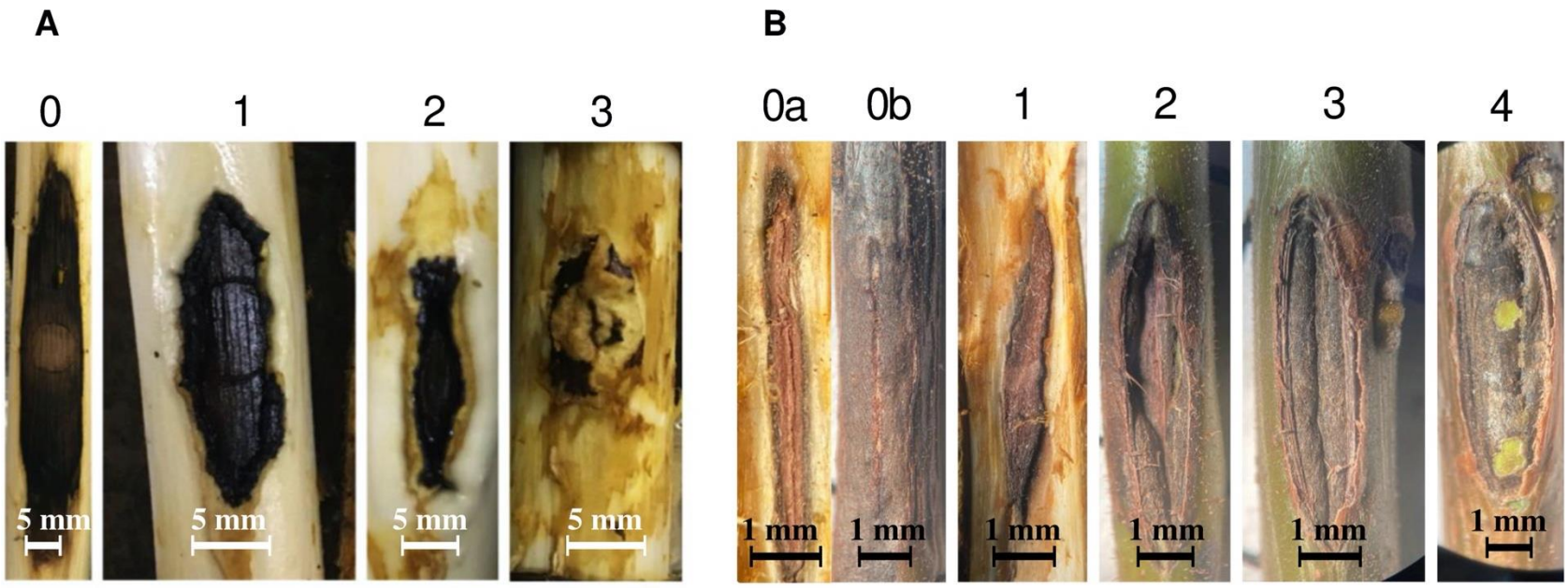

Figure 3.1. Key to ratings of inoculation wound healing. The amount of reactive host tissue response and healing of wounds increases from left to right in each panel. Different scoring systems were used to score healing of wounds after inoculation with *G. morbida* in the live soil amendment experiment, which employed 6-mm plugs to inoculate 1-year old seedlings (A), and the endophyte inoculation experiment which employed spore suspensions to inoculate 3-month old seedlings (B).

A. Canker healing scale for plug inoculations in live soil amendment experiment (sapwood shown): 0), no raised reactive sapwood border around canker margin; 1), raised boundary around canker margin without covering original wound; 2), wound partly covered by reactive tissue; 3), wound is completely healed.

B. Canker healing scale for spore suspension inoculations in endophyte inoculation experiment (outer bark shown unless otherwise indicated): 0), no raised reactive sapwood border around canker margin, (a) sapwood and (b) outer bark shown; 1), raised boundary around canker margin without covering original wound (sapwood shown); 2), wound partly covered by reactive tissue; 3), sides of wound closed but not joined by new tissue; 4), sides of closed wound joined by formation of healing scar.

random from 10 primary or secondary lateral roots of each plant. Our root surface sterilization procedure was modified from Arnold et al., (2000) and consisted of three successive 30 sec washes in sterile distilled water (SDW) with a vortex, followed by rinsing with agitation in 70% EtOH (15 sec), 2% NaOCl (2 min), 70% EtOH (15 sec), a final rinse in SDW, and air drying on sterile paper towel. Ten surface-sterilized root segments per plant were plated onto each of the following five types of media: 1) 1/2-strength PDA++ (Tisserat et al., 2009); 2) 2.5 ppm malachite green agar (Castellá et al., 1997); 3) glucose yeast extract rose bengal agar (Newhouse & Hunter, 1983); 4) "Modified PDA" formulated as described in Vargas Gil et al., (2009); and 5) 5 mg/L natamycin-ampicillin-rifampicin-pentochloronitrobenzene cornmeal agar (Jeffers & Martin, 1986). In total, a subset of 1,000 root pieces (n = 50 per plant) were plated onto five different selective growth media (n = 10 per media per plant). The latter four selective media were chosen to promote the growth of known seedling pathogens or beneficial fungi, *Fusarium*, *Cylindrocladium*, *Trichoderma*, and *Phytophthora-Pythium*, respectively (Michler et al., 2004). To verify the effectiveness of the surface-sterilization procedure, imprint plates were made on 1/4-strength PDA from root samples collected from eight seedlings from each soil treatment for a total of 24 imprint plates (Ridout et al., 2017). All plates were checked semiweekly for two months and all fungal colonies from plated roots were subcultured on 1/4-strength PDA until pure cultures were obtained to be used for extraction of DNA.

PCR and Bioinformatics

To obtain molecular-based taxonomic assignments of fungal isolates from root subcultures, DNA was extracted from subcultures following Lee and Taylor (1990) and subjected to PCR amplification of the internal transcribed spacer (ITS) region. 25-μL PCR reactions contained $MgCl_2$ (1.5 mM), forward and reverse primers ITS5 and ITS4 (White et al., 1990) and dNTPs (0.2 μM each), PlatinumTaq DNA Polymerase (0.1 μL), DNA template (1 μL), and PlatinumTaq buffer (1X). A touchdown thermocycle profile was employed with denaturation at 94° C (4 min); 5 cycles of 94° C (30 sec), 48° C (30 sec) and 72° C (1 min); 5 cycles of 94° C (30 sec), 47° C (30 sec), and 72° C (30 sec); 20 cycles of 94° C (30 sec), 46.3° C (30 sec) and 72° C (30 sec); and final extension at 72° C (10 min). PCR products were cleaned with a PureLink Pro 96 PCR Purification

Kit (Invitrogen, Waltham, MA) and sequenced with standard protocols at the Purdue Genomics Facility (West Lafayette, IN) on an 3730XL DNA Analyzer (Applied Biosystems, Waltham, MA).

Assembly of forward and reverse sequences, quality control, and trimming were performed with the Chromaseq package and base tools in Mesquite (Edgar, 2004; Maddison and Maddison 2019a, 2019b). Trimmed assembled sequences were pairwise-aligned, furthest-neighbor clustered at 95% similarity and assigned to taxonomy concepts from the UNITE database version 02.02.2019 in mothur 1.39.3 (Schloss et al., 2009; Nilsson et al., 2019, http://unite.ut.ee). Sequences of interest were also aligned via basic local alignment (BLAST) to the National Center for Biotechnology Information (Altschul, 1990, https://blast.ncbi.nlm.nih.gov/Blast.cgi). Sequences have been deposited to GenBank under accessions **MW301139** and **MW326227**-**MW326432**.

Statistical Analyses

All statistical analyses were performed in R 3.6.1 (R Core Team, 2019). Pathogenicity of *G. morbida* isolate IN-66 relative to agar-only control inoculation was confirmed separately within soil treatment groups with one-way analyses of variance (ANOVA) on Box-Cox transformed necrotic area (Venables & Ripley, 2002). Subsequent analyses of canker necrotic area and healing across soil treatments were performed for *G. morbida*-inoculated plants only.

The effect of soil amendment on canker growth was analyzed with ANOVA after a Box-Cox transformation and removing outliers with Cook's distance > 4/n (Fox & Weisberg, 2019). Among the 30 control seedlings that were inoculated with PDA alone (n = 10 per soil treatment), one seedling in the sterile soil treatment died. Among the *G. morbida*-inoculated seedlings (n = 30 per soil amendment treatment), ten seedlings were left out of the analysis: two outliers from the plantation soil, two from the forest soil amendment groups and six seedlings that died, leaving a total of n = 80 *G. morbida*-inoculated seedlings. This removal resulted in a slightly unbalanced number of *G. morbida*-inoculated seedlings between the steam-treated (n = 27), plantation (n = 26), and forest soil (n = 27) amendment groups for analysis of necrotic area among soil treatments. Marginal and conditional R^2 were calculated (Nakagawa et al., 2017). Pairwise group comparisons of necrotic area among treatments were performed with a Tukey post-hoc test. The effect of soil amendment on canker healing rating was tested with proportional-odds logistic regression (*i.e.*,

ordinal regression) and drop-in-deviance Wald χ^2 tests (ANODEV). Healing was compared among groups with unadjusted regression contrasts (Venables & Ripley, 2002).

Effects of soil amendment, stem inoculation treatments and their interaction on community composition were tested with 9999-permutational multivariate analysis of variance on Jaccard distances (ADONIS; Oksanen et al., 2018). For the ADONIS, rare OTUs represented by five or fewer isolates were removed from the dataset along with samples rendered empty by the removal of the rare OTUs, resulting in a slightly unbalanced design. Since ADONIS uses marginal sum of squares, the analysis was repeated for both possible orders of main effects to ensure robust inferences.

For individual taxa, isolation and reisolation colony counts of fungi from soil and plant tissues were analyzed with quasipoisson log-link generalized linear models and ANODEV with overdispersion-adjusted contrasts. Colony counts of isolates assigned to the genera *Fusarium* (*sensu* O'Donnell et al., 2020) and *Rhizoctonia* were considered as a function of *G. morbida* inoculation, soil treatment, and their interaction. R^2 for all ordinal and quasipoisson regressions were calculated with the drop-in-deviance method (McFadden, 1974).

3.2.2 Endophyte Inoculation Experiment

Inoculation of Seedlings with Root Endophytes and G. morbida

On April 12, 2019, stratified half-sibling seeds from Hardwood Tree Improvement and Regeneration Center *J. nigra* accession #288 (n = 31) were sown in steam-treated potting mix. Once seeds germinated, they were inoculated with isolates of a *Fusarium* sp. (Rh-217) and a *Trichoderma* sp. (Rh-366) from the first experiment. These isolates were chosen because they were identified as potentially pathogenic or pathogen-antagonistic endophytic fungal species, respectively. Seeds were washed thoroughly in water followed by 2% NaOCl (2 min). Seeds were germinated in 12-cm pots containing potting media (560SC) with 3.125 g per L bulk soil (g/L) Osmocote® fertilizer (Scotts Co., Marysville, OH) and 11.25 g/L lime that had been autoclaved three times for two hours with two intervening days of cool-down between cycles. Seeds were inoculated with fungi at ~60% germination, 25 days after sowing (May 7) with isolates of *F. solani* (Mart.) Sacc. (Rh-217) and *Trichoderma* sp. (Rh-366) from the previous experiment grown in 2% malt extract broth at 30º C for 25 days. Cultures were homogenized in a blender and 75 mL was

added to each pot. To control for the potential effects of waste, mycotoxins, and/or residual nutrients from liquid cultures of each fungus on the soil microbiomes and/or plant physiology, we added 75 mL filtrate obtained by passing homogenate through a 22-micron filter (Nalgene Nunc, Rochester, NY) to each pot from the other fungus treatment (Table 3.1). Absence of viable fungal propagules was verified by spreading 10 μL filtrate on five 1/4-strength PDA plates.

Table 3.1. Design of endophyte inoculation experiment.

Treatment	**Homogenate**	**Filtrate**	**No. of replicates***
FSSC[1]	FSSC Rh-217	*Trichoderma* Rh-366	5
Trichoderma[2]	*Trichoderma* Rh-366	FSSC Rh-217	5
FSSC + *Trichoderma*	FSSC Rh-217 + *Trichoderma* Rh-366	None	7
Control	None	FSSC Rh-217 + *Trichoderma* Rh-366	4
Non-sterile[3]	None	None	3

*[1]Isolate Rh-217 has an ITS sequence (GenBank Acc. **MW300971**) 99% similar to FSSC sp. 25 (GenBank Acc. **KP696749**) and its concatenated ITS+TEF1a grouped with FSSC spp. 25a & b (NRRL 31169 & 25101) and 35c (NRRL 46707) (Fig. 3.6). [2]Isolate Rh-366 sequence (GenBank Acc. **MW301139**) that was 97.4% similar to T. asperellum Samuels, Lieckf. & Nirenberg (GenBank Acc. **MH744738**). [3]As a control to determine if Fusarium solani present in nonsterile potting mix promotes G. morbida canker growth, seeds were also germinated in untreated potting media. *Variable germination resulted in an unbalanced design with regard to the number of plants in each treatment.*

Seedlings were moved to 6.2 L TP616 Treepots (Stuewe and Sons, Corvallis, OR) 29 days after soil inoculations and inoculated with *G. morbida* 34 days after transplanting (July 8), at an age of ~ 3 months. Seedlings were inoculated with spore suspensions because seedling stem diameters were too small for the use of agar plugs. The spore suspension was prepared from 60-day-old cultures of IN-66 grown on 1/8-strength PDA and adjusted to 100,000 μL^{-1} in a 1:10,000 volume solution of Tween 20 and SDW. The spore suspension (5 μL) was pipetted into three rectilinear wounds (5 mm) made by a utility knife in the phloem, until the wounds were filled and overflowing, at 5, 10, and 15 cm above the root collar on the north side of the stem, and sealed with parafilm.

Seedlings were harvested 80-87 days after inoculation (Sept 26 – Oct 3). To measure necrosis and healing at the conclusion of the experiment, outer bark was shaved away with a utility

knife to expose maximum phloem necrosis, which was imaged on a flatbad scanner and measured with ImageJ as described above. Canker healing was scored on an ordinal scale (Fig. 3.1B).

Reisolation of Fusarium and Trichoderma

From each plant, forty 2-cm root segments were collected, surface sterilized as described above, and placed on selective *Fusarium* agar (SFA; n = 20 pieces per plant; Leslie & Summerell, 2008) and *Trichoderma* selective media (n = 20 pieces per plant; Vargas Gil et al., 2009). Cultures from roots were checked semiweekly for 30 days and all fungal colonies that grew from root pieces were classified to morphospecies and counted. From identified morphospecies, two colonies were subcultured as vouchers within each morphospeices, plant, and media type. For quantification of FSSC, soil was collected from each pot with a sterile 50 mL Falcon tube and a subsample of 3.75 g was serially diluted to a final concentration of 15 g/L in a 1:100,000 volume solution of Tween 20 and SDW. We plated 800 μL aliquots of the resulting soil dilution on four plates of peptone-pentonitrochlorobenzene agar (Leslie & Summerell, 2008) per plant. After 7 days, colonies that grew from soil dilutions were counted, classified to morphospecies within sets of plates from five plants at a time, and two colonies were subcultured as vouchers for each morphospecies for molecular-based taxonomic assignments. To reisolate and quantify FSSC and *G. morbida* from cankers, a total of 120 ~10-mm^2 sections of necrotic phloem (n = four to six per plant) were washed briefly in 70% EtOH (10 sec) followed by SDW (10 sec), and placed on 1/2-strength PDA++. Fungi were maintained on 1/4-strength PDA or SFA and examined under a light microscope at 400X (roots and soil) or as a slide mount at 1000X (necrotic lesions) magnification, and classified as *F. solani*, other *Fusarium* spp., *Trichoderma* sp., *G. morbida*, or "other" prior to DNA extraction.

PCR and Bioinformatics

DNA was extracted from cultures as described above. To identify *Fusarium* species from the endophyte inoculation experiment, the translation elongation factor 1-alpha (TEF-1a) gene was also amplified with primers EF-1a-EF1 and EF-1a-EF2 (O'Donnell et al., 1998) in addition to amplification of the ITS region as described above. TEF1 reactions were 30 mL with the same concentrations of reagents to ITS reactions described above but with modification to MgCl (2.5

mM), forward and reverse primer (0.25 μM), and template (2 μL). For TEF, thermocycle profile included denaturation at 94° C (1 min); 35 cycles of 94° C (30 sec), 59° C (45 sec) and 72° C (1 min); and final extension at 72° C (10 min). Products from the endophyte inoculation experiment were purified and sequenced at GeneWiz corporation (South Plainfield, NJ).

Sequences were processed and aligned as described above and deposited to GenBank under accessions **MW300958**-**MW301040** and **MW456941**-**MW457023**. Sequences of interest were also aligned via basic local alignment (BLAST) to the *Fusarium*-ID database (Geiser et al., 2004, http://isolate.fusariumdb.org). To identify putative *Fusarium* isolates recovered in the endophyte inoculation experiment and determine their relationship to the isolate Rh-217 used in inoculations and other species, we built a phylogenetic tree that included vouchered accessions from the *Fusarium* multilocus sequence typing database (O'Donnell et al., 2012, https://fusarium.mycobank.org). A majority-rule consensus tree was made in PAUP from 1000 bootstrap trees generated from concatenated ITS-TEF-1a alignments in RAxML under a GTR+CAT model, and visualized in R 3.6.1 (Swafford, 2003; Stamatakis, 2014; R Core Team, 2019).

Statistical Analyses

Generalized linear mixed models (GLMM) of canker necrosis and healing were fit with random effects for plant nested within treatment. Apart from the inclusion of random effects, the GLMMs were fit as described above for the ANOVA on necrosis and proportional odds logistic regression on healing. Marginal and conditional R^2 were calculated for fixed and fixed + random effects (Nakagawa et al., 2017). To test for the effect of endophyte treatment on reisolation rate of *Fusarium* morphotypes with identical ITS+TEF1 voucher sequences to Rh-217, separate quasipoisson and ANODEV analyses were performed as described above at the level of each substrate from which isolates were obtained (*i.e.*, cankers, roots, and soil).

3.3 Results

3.3.1 Live Soil Amendment Experiment

Effect of Soil Amendment on Necrosis and Healing

In our live soil amendment experiment, amending potting mix with forest-associated soil biota led to smaller cankers caused by *G. morbida* in seedlings; however, the effects of plantation soil on necrotic area were intermediate and nonsignificant (Fig. 3.2A). Soil amendment had a significant effect on area of necrosis caused by *G. morbida* (p = 0.011; $df_{1,2}$ = 2, 77; R^2 = 0.11). Amending seedlings with forest soil reduced the size of cankers by 17.2 ± 5.6% (5.8 ± 1.9 mm^2; Tukey p = 0.008; 1 SE denoted by ±) relative to the steam-treated soil amendment treatment (Fig. 3.2A). Necrotic area for seedlings that received the plantation soil amendment was intermediate and not significantly different from those that were amended with steam-treated soil (Tukey p = 0.202) or forest soil (Tukey p = 0.385). *Geosmithia morbida* inoculation led to an increase in necrotic area compared to agar-only control inoculations among seedlings that were amended with forest (10.4 ± 3.7 mm^2; p = 0.007; df = 37), plantation (13.6 ± 3.2 mm^2; p < 0.001; df = 36), and steam-treated soil (18.3 ± 3.3 mm^2; p < 0.001; df = 34).

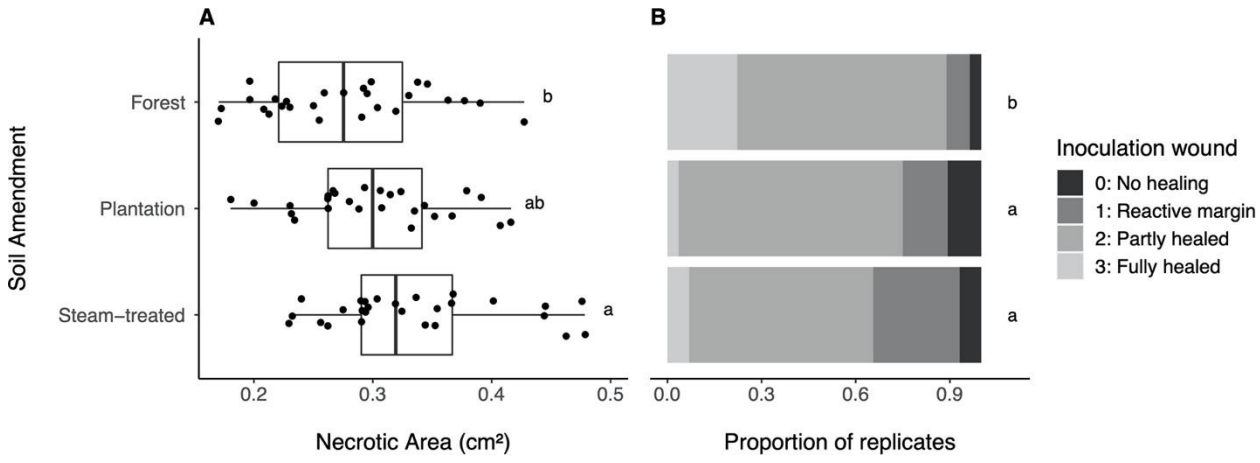

Figure 3.2. Necrotic area (A) and healing (B) of cankers caused by *Geosmithia morbida* in seedlings that received forest, plantation, and steam-treated soil amendments. Different letters in plot (A) denote significant Tukey-adjusted contrasts from a Box-Cox (λ = 0.9) transformed linear model. Outliers not shown. Different letters in plot (B) denote significant unadjusted contrasts from a log-link proportional odds model.

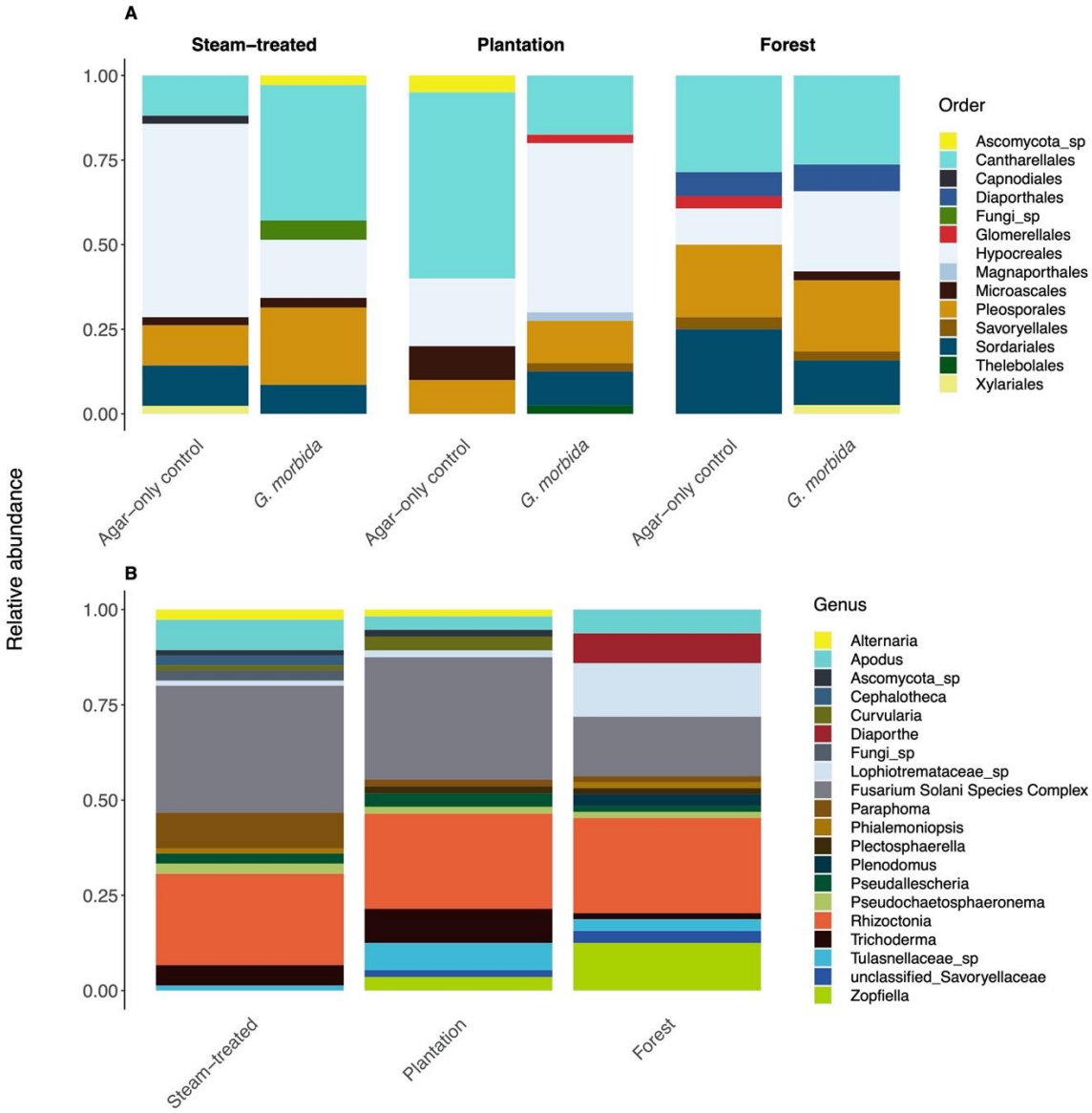

Figure 3.3. Composition of microbiome by soil amendment and *Geosmithia morbida* inoculation treatment. A) Relative abundance of UNITE database fungal order assignments of isolated endophyte OTUs based on internal transcribed spacer (ITS) sequences from roots of seedlings grown in potting mix amended with steam-treated, plantation, and forest soil and inoculated with *G. morbida* or agar-only control. B) Relative abundance of UNITE database fungal genus assignments based on internal transcribed spacer (ITS) sequences of non-singleton (n > 1) endophytes isolated from roots of seedlings grown in potting mix amended with steam-treated, plantation, and forest soil.

Soil amendment also had a significant effect on healing of inoculation wounds ($p = 0.024$; $df = 2$; $R^2 = 0.04$) and seedlings amended with forest soil had the highest probability of healing (Fig. 3.2B). On average, seedlings that were amended with forest and plantation soil had 4.5-fold (95% CI [1.3, 14.6]; $p = 0.014$) and 3.7-fold (95% CI [1.1, 12.3]; $p = 0.032$) higher odds, respectively, of being in a higher healing rating category relative to those that received steam-treated soil (Fig. 3.2B).

Effects of Soil Amendment and G. morbida Inoculation on Rhizosphere Fungal Community

We recovered full-length ITS sequences for 203 fungal isolates from roots of *J. nigra* seedlings across all treatments and media types: forest (n = 66); plantation (n = 60); and steam-treated (n = 77) soil amendments (GenBank Accs. **MW326227**-**MW326432**). Bacteria grew on 9 out of 24 (37.5%) imprint plates, but only one imprint plate (4%) had fungal growth. Isolates from roots of seedlings grown with forest, plantation and steam-treated soil amendments clustered into 18, 20, and 18 OTUs, respectively. In total, 39 OTUs were classified to at least 20 genera and 24 families across 15 known orders of Fungi (Fig. 3.3A). Only 9 OTUs occurred in all three treatments.

The influence of aboveground inoculation on belowground community structure depended on soil amendment treatment (Fig. 3.3A). The composition of the fungal rhizosphere microbiome of seedlings that received plantation or steam-treated soil amendments shifted in response to inoculation with *G. morbida*. By contrast, the fungal rhizosphere microbiome of seedlings grown with forest soil was relatively stable regardless of *G. morbida* inoculation (Fig. 3.3A). Overall, isolates assigned to Hypocreales, including *Fusarium solani* species complex and *Trichoderma* were less abundant in the trees grown in soil amended with forest soil than the other treatments (Figs. 3.3A & 3.3B). Within the plantation soil amendment treatment however, Hypocreales were more abundant and Cantherellales less abundant in *G. morbida*-inoculated seedlings than the control-inoculated seedlings. In contrast, within the steam-treated soil amendment Hypocreales were less abundant and Cantherellales more abundant in the *G. morbida*-inoculated seedlings than the control-inoculated seedlings (Fig. 3.3A). These observations suggest that Cantherellales and Hypocreales in our experiment may have antagonized each other and that their abundance depended on both *G. morbida* inoculation and soil amendments.

Regardless of the order of main effect terms in ADONIS, neither soil amendment ($df_1 = 2$) nor *G. morbida* inoculation ($df_1 = 1$) significantly accounted for variation in community composition of culturable root endophytes ($p > 0.6$; $df_2 = 38$; *Pseudo*-$R^2 < 0.05$), nor did they have a significant interaction ($p = 0.19$; $df_{1,2} = 2, 36$; *Pseudo*-$R^2 = 0.06$). Removal of rare species (n < 6) from the dataset left only eight OTUs for ADONIS, which were assigned by UNITE to FSSC sp. (OTU1), *Rhizoctonia* sp. (OTU2), Lophiotremataceae sp. (OTU3), *Apodus* sp. (OTU4), *Paraphoma* sp. (OTU5), *Zopfiella* sp. (OTU6), Tulasnellaceae sp. (OTU7) and *Trichoderma* sp. (OTU8). Isolates assigned to *Zopfiella* were most abundant in the seedlings amended with forest soil and least abundant in those amended with plantation soil; by contrast, isolates belonging to FSSC spp. were least abundant in those amended with forest soil (Fig. 3.3B).

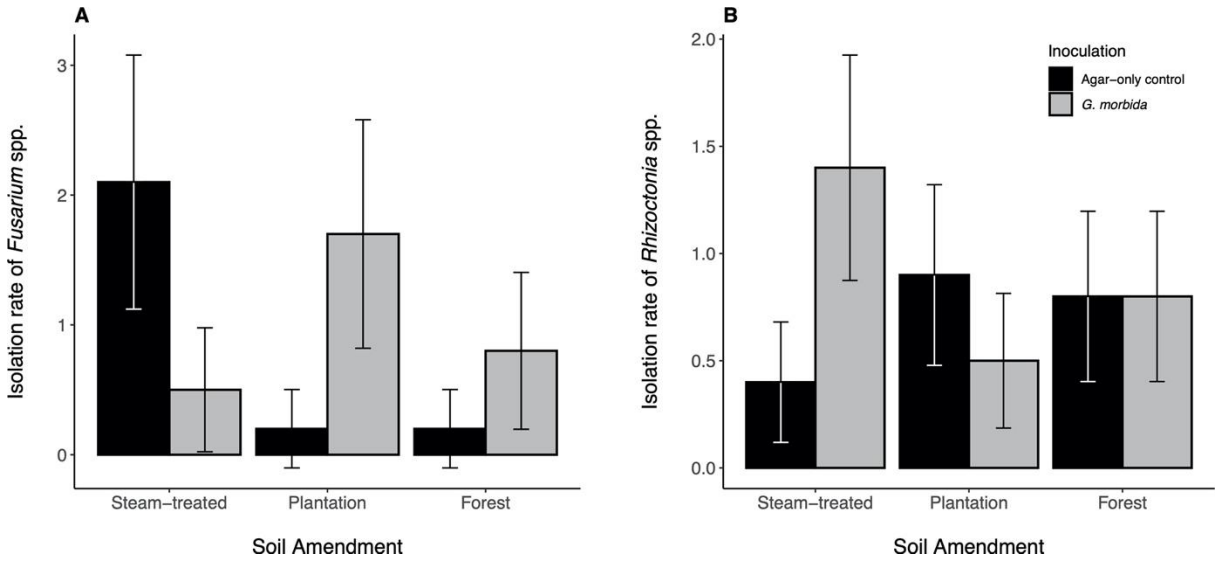

Figure 3.4. Isolation rates (mean ± overdispersion-adjusted SE number of colonies per plant) of (A) *Fusarium* spp. and (B) *Rhizoctonia* spp. from roots of walnut seedlings after being amended with steam-treated, plantation, and forest soil and inoculated with *Geosmithia morbida* or agar-only control.

Aboveground inoculation of stems with *G. morbida* influenced the colonization of roots by *Fusarium* and *Rhizoctonia* spp. (Fig. 3.4). In particular, in the presence of plantation-associated soil biota, aboveground *G. morbida* facilitated colonization by belowground *Fusarium* spp. (Fig. 3.4A). Whether *Fusarium* and *Rhizoctonia* spp. increased or decreased in abundance in the rhizosphere in response to inoculation with *G. morbida* depended on the soil amendment given to

the seedlings, as shown by a significant interaction effect on *Fusarium* spp. infection ($p = 0.049$; $df = 2$). Though the interaction effect on *Rhizoctonia* spp. was non-significant ($p = 0.203$; $df = 2$), above-ground *G. morbida* inoculation led to positive feedback on the infection of roots by *Rhizoctonia* spp. in the steam-treated amendment seedlings and negative feedback on *Rhizoctonia* spp. in the plantation soil-amended seedlings. This observation contrasts with negative feedback on *Fusarium* spp. in the steam-treated amendment seedlings and positive feedback on *Fusarium* spp. in the plantation soil-amended seedlings. Moreover, in the rhizospheres of forest soil-amended seedlings, feedback on *Fusarium* was diminished compared to the other treatments and there was no difference in *Rhizoctonia* spp. between seedlings inoculated with *G. morbida* and PDA alone (Figs. 3.4A & 3.4B).

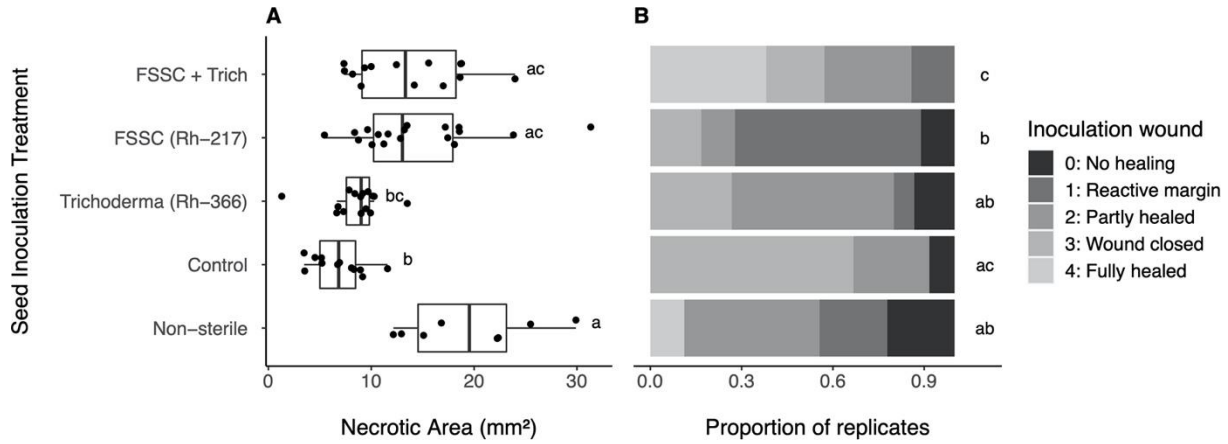

Figure 3.5. Necrotic area (A) and healing of cankers (B) caused by *G. morbida* in seedlings grown in untreated potting mix (Non-sterile) or inoculated with filtrate only (Control), *Trichoderma* sp. isolate Rh-366, FSSC sp. isolate Rh-217, or both Rh-366 and Rh-217 together (FSSC + Trich). Different letters in plot (A) denote significant Tukey-adjusted contrasts from a Box-Cox ($\lambda = 0.4$) transformed linear model. Outliers not shown. Different letters in plot (B) denote significant unadjusted contrasts from a log-link proportional odds model.

Pairwise contrasts were not significant after accounting for substantial overdispersion. However, in the rhizospheres of seedlings amended with plantation soil, *Fusarium* was isolated 8.5 ± 13.6 times more frequently from roots of *G. morbida*-inoculated seedlings compared to agar-only controls. This difference was less pronounced for seedlings amended with forest soil, where *Fusarium* was isolated only 4.0 ± 6.8 times more frequently from roots of *G. morbida*-inoculated plants than controls incolulated with agar only (Fig. 3.4A). In seedlings with steam-treated soil,

Fusarium spp. were isolated 4.2 ± 4.5 times more frequently from roots of agar-only control-inoculated plants compared to those inoculated with *G. morbida*.

3.3.2 Endophyte Inoculation Experiment

Effect of FSSC sp. and Trichoderma sp. on Necrosis and Canker Healing

Fusarium solani species complex sp. isolate Rh-217 appeared to originate from potting mix and predisposed seedlings to greater damage from the pathogen *Geosmithia morbida*. Upon inoculation with *G. morbida*, prior inoculation with FSSC Rh-217 facilitated increased necrotic area and suppression of canker healing (Figs. 3.5A & 3.5B). The area of necrosis caused by *G. morbida* depended on seed treatment ($p < 0.001$; $df = 4$; $R^2_{fix} = 0.43$; $R^2_{fix+rand} = 0.57$). Necrotic area was greater in stems of plants that had been inoculated with FSSC Rh-217 (Fig. 3.5A). Necrotic area was 112.5 ± 35.7% higher in FSSC-inoculated plants than sterile control plants that received filtrates only (7.66 ± 2.43 mm^2; Tukey $p = 0.011$). Necrotic canker area was 163.2 ± 42.2% higher in the plants grown in non-sterile soil without treatment relative to the sterile control plants (11.1 ± 2.9 mm^2; Tukey $p < 0.001$). Overall canker size did not differ between the plants grown in non-sterile soil without FSSC treatment and those that received the FSSC inoculation treatment (Tukey $p = 0.337$). Coinoculation of germinating seedlings with both FSSC Rh-217 and *Trichoderma* Rh-366 together did not result in smaller cankers compared to FSSC Rh-217 alone (Tukey $p = 0.997$).

Trichoderma increased healing of inculation wounds, while healing was decreased by *Fusarium*. Endophyte treatment also had a significant effect on canker healing ($p = 0.013$; $df = 4$; $R^2_{fix} = 0.10$; $R^2_{fix+rand} = 0.17$). On average, inoculation wounds of control seedlings had 27.4 fold (95% CI [1.5, 509.3]; $p = 0.026$) higher odds of being in a more advanced healing category relative to those inoculated with FSSC Rh-217 (Fig. 3.5B). Control plants had 24.1 fold higher odds of healing relative to plants grown in non-sterile soil and not inoculated (95% CI [0.7, 796.2]; $p = 0.075$). Although inoculation with FSSC Rh-217 alone or with *Trichoderma* Rh-366 resulted in similarly sized cankers, coinoculation with *Trichoderma* Rh-366 increased the odds of being in a higher healing category 70.6-fold (95% CI [4.9, 1016.8]; $p = 0.002$) compared to seedlings inoculated with FSSC Rh-217 alone. Eight out of 21 (38%) of coinoculations with FSSC Rh-217

Figure 3.6. (Next page). Likelihood-based multilocus placement of *Fusarium* spp. encounctered while reisolating FSSC sp. isolate Rh-217 from endophyte inoculation experiment. Majority-rules consensus (1000 bootstrap RAxML trees, GTR+CAT model, all nodes > 50%) of concatenated ITS and TEF-1a alignments (561 alignment patterns) from *Fusarium* cultures. Branch lengths proportional to substitutions per site estimated via GTR+I+G in PAUP; node values denote percent of supporting bootstrap replicates. Vouchers isolated in this study are given in red along with isolation source (roots, cankers, or soil), and treatment code (Non-sterile, Control, Trichoderma, FSSC, and FSSC + Trichoderma) in dark green, followed by GenBank accession numbers (ITS & TEF-1) in black. Isolates from the Fusarium Multilocus Sequence Typing database (O'Donnell et al., 2012) are given in bold. *Isolates with identical ITS+TEF-1a sequences.

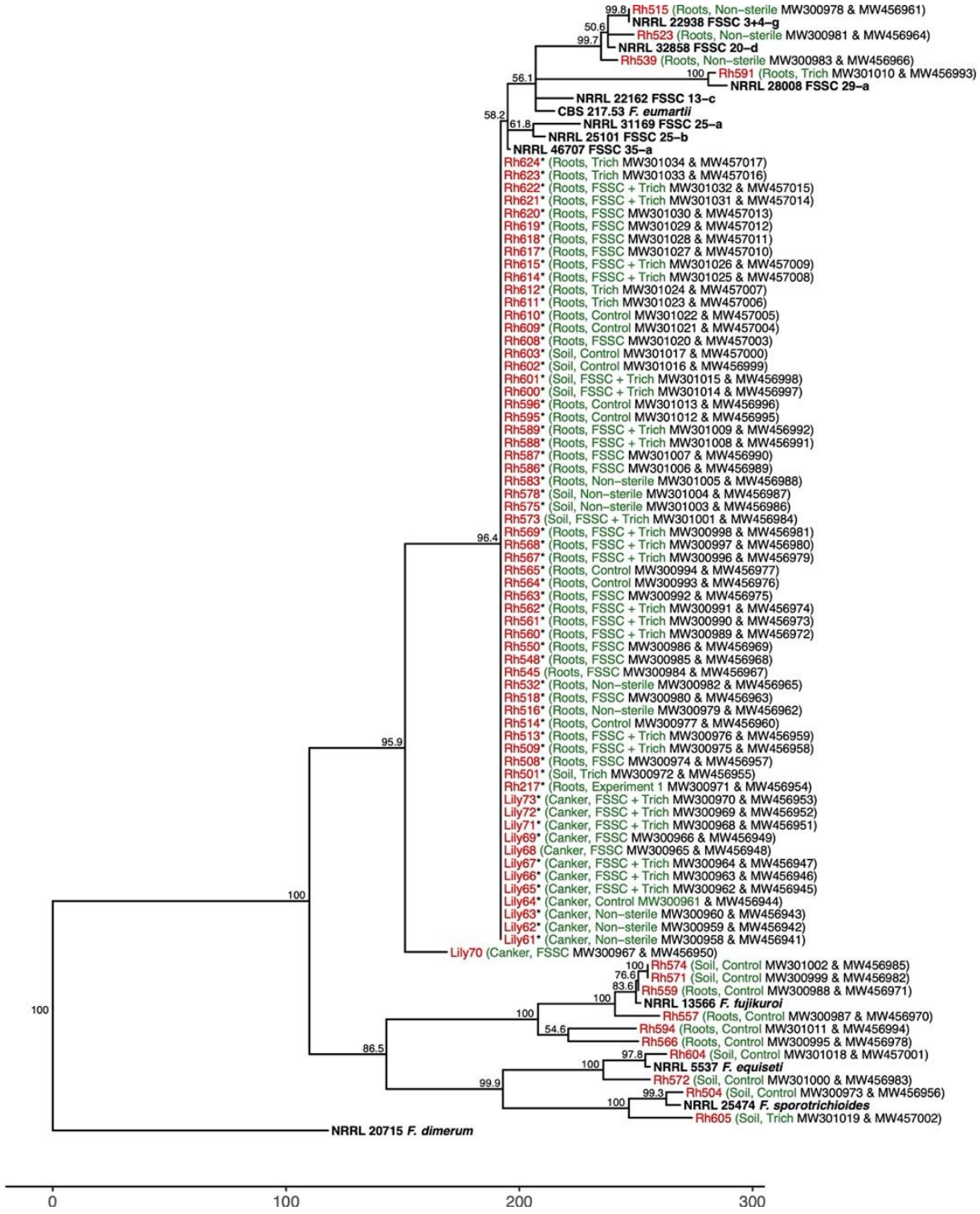
Rh515 (Roots, Non−sterile MW300978 & MW456961)
NRRL 22938 FSSC 3+4−g
Rh523 (Roots, Non−sterile MW300981 & MW456964)
NRRL 32858 FSSC 20−d
Rh539 (Roots, Non−sterile MW300983 & MW456966)
Rh591 (Roots, Trich MW301010 & MW456993)
NRRL 28008 FSSC 29−a
NRRL 22162 FSSC 13−c
CBS 217.53 F. eumartii
NRRL 31169 FSSC 25−a
NRRL 25101 FSSC 25−b
NRRL 46707 FSSC 35−a
Rh624* (Roots, Trich MW301034 & MW457017)
Rh623* (Roots, Trich MW301033 & MW457016)
Rh622* (Roots, FSSC + Trich MW301032 & MW457015)
Rh621* (Roots, FSSC + Trich MW301031 & MW457014)
Rh620* (Roots, FSSC MW301030 & MW457013)
Rh619* (Roots, FSSC MW301029 & MW457012)
Rh618* (Roots, FSSC MW301028 & MW457011)
Rh617* (Roots, FSSC MW301027 & MW457010)
Rh615* (Roots, FSSC + Trich MW301026 & MW457009)
Rh614* (Roots, FSSC + Trich MW301025 & MW457008)
Rh612* (Roots, Trich MW301024 & MW457007)
Rh611* (Roots, Trich MW301023 & MW457006)
Rh610* (Roots, Control MW301022 & MW457005)
Rh609* (Roots, Control MW301021 & MW457004)
Rh608* (Roots, FSSC MW301020 & MW457003)
Rh603* (Soil, Control MW301017 & MW457000)
Rh602* (Soil, Control MW301016 & MW456999)
Rh601* (Soil, FSSC + Trich MW301015 & MW456998)
Rh600* (Soil, FSSC + Trich MW301014 & MW456997)
Rh596* (Roots, Control MW301013 & MW456996)
Rh595* (Roots, Control MW301012 & MW456995)
Rh589* (Roots, FSSC + Trich MW301009 & MW456992)
Rh588* (Roots, FSSC + Trich MW301008 & MW456991)
Rh587* (Roots, FSSC MW301007 & MW456990)
Rh586* (Roots, FSSC MW301006 & MW456989)
Rh583* (Roots, Non−sterile MW301005 & MW456988)
Rh578* (Soil, Non−sterile MW301004 & MW456987)
Rh575* (Soil, Non−sterile MW301003 & MW456986)
Rh573 (Soil, FSSC + Trich MW301001 & MW456984)
Rh569* (Roots, FSSC + Trich MW300998 & MW456981)
Rh568* (Roots, FSSC + Trich MW300997 & MW456980)
Rh567* (Roots, FSSC + Trich MW300996 & MW456979)
Rh565* (Roots, Control MW300994 & MW456977)
Rh564* (Roots, Control MW300993 & MW456976)
Rh563* (Roots, FSSC MW300992 & MW456975)
Rh562* (Roots, FSSC + Trich MW300991 & MW456974)
Rh561* (Roots, FSSC + Trich MW300990 & MW456973)
Rh560* (Roots, FSSC + Trich MW300989 & MW456972)
Rh550* (Roots, FSSC MW300986 & MW456969)
Rh548* (Roots, FSSC MW300985 & MW456968)
Rh545 (Roots, FSSC MW300984 & MW456967)
Rh532* (Roots, Non−sterile MW300982 & MW456965)
Rh518* (Roots, FSSC MW300980 & MW456963)
Rh516* (Roots, Non−sterile MW300979 & MW456962)
Rh514* (Roots, Control MW300977 & MW456960)
Rh513* (Roots, FSSC + Trich MW300976 & MW456959)
Rh509* (Roots, FSSC + Trich MW300975 & MW456958)
Rh508* (Roots, FSSC MW300974 & MW456957)
Rh501* (Soil, Trich MW300972 & MW456955)
Rh217* (Roots, Experiment 1 MW300971 & MW456954)
Lily73* (Canker, FSSC + Trich MW300970 & MW456953)
Lily72* (Canker, FSSC + Trich MW300969 & MW456952)
Lily71* (Canker, FSSC + Trich MW300968 & MW456951)
Lily69* (Canker, FSSC MW300966 & MW456949)
Lily68 (Canker, FSSC MW300965 & MW456948)
Lily67* (Canker, FSSC + Trich MW300964 & MW456947)
Lily66* (Canker, FSSC + Trich MW300963 & MW456946)
Lily65* (Canker, FSSC + Trich MW300962 & MW456945)
Lily64* (Canker, Control MW300961 & MW456944)
Lily63* (Canker, Non−sterile MW300960 & MW456943)
Lily62* (Canker, Non−sterile MW300959 & MW456942)
Lily61* (Canker, Non−sterile MW300958 & MW456941)
Lily70 (Canker, FSSC MW300967 & MW456950)
Rh574 (Soil, Control MW301002 & MW456985)
Rh571 (Soil, Control MW300999 & MW456982)
Rh559 (Roots, Control MW300988 & MW456971)
NRRL 13566 F. fujikuroi
Rh557 (Roots, Control MW300987 & MW456970)
Rh594 (Roots, Control MW301011 & MW456994)
Rh566 (Roots, Control MW300995 & MW456978)
Rh604 (Soil, Control MW301018 & MW457001)
NRRL 5537 F. equiseti
Rh572 (Soil, Control MW301000 & MW456983)
Rh504 (Soil, Control MW300973 & MW456956)
NRRL 25474 F. sporotrichioides
Rh605 (Soil, Trich MW301019 & MW457002)
NRRL 20715 F. dimerum
99.8
50.6
99.7
100
56.1
58.2
61.8
96.4
95.9
100
100
76.6
83.6
100
100
54.6
86.5
97.8
100
99.9
99.3
100
0
100
200
300

and *Trichoderma* Rh-366 led to full healing of the *G. morbida* inoculation wound, compared to just one across all other treatments.

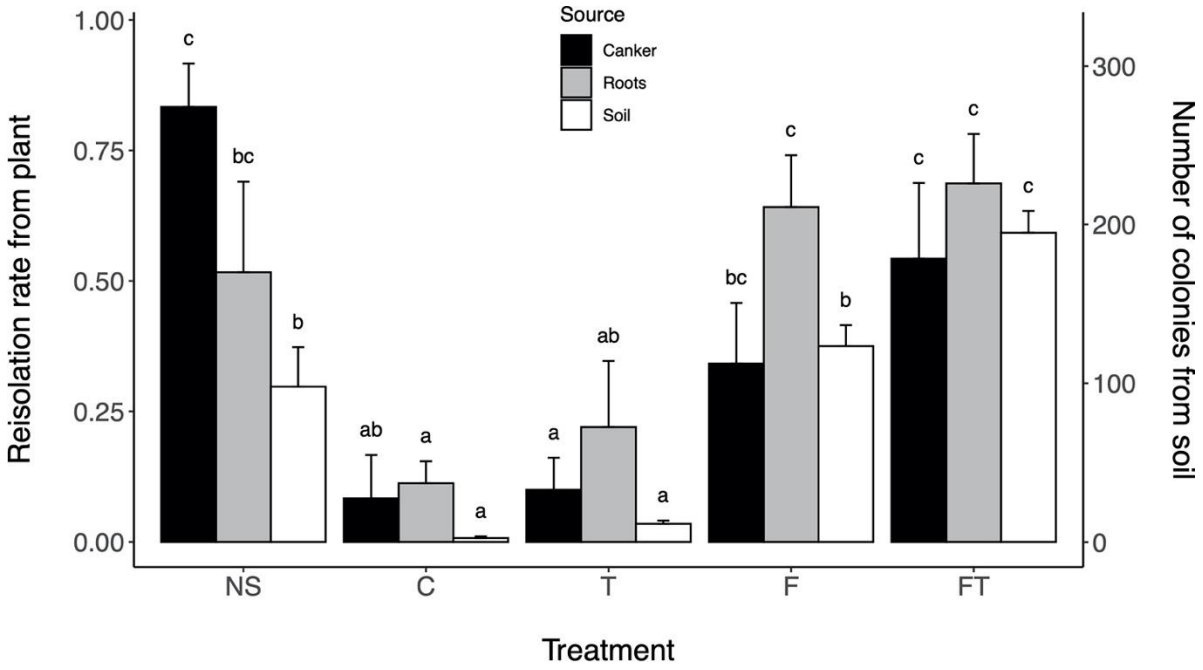

Figure 3.7. Reisolation rates (mean + adjusted SE number of colonies per plant) of FSSC sp. isolate Rh-217 from cankers, roots (left axis), and soil (right axis) of walnut seedlings grown in untreated potting mix (NS) or in sterilized potting mix inoculated with filtrate only (C), Trichoderma asperellum Rh-366 (T), FSSC Rh-217 (F), or both Rh-217 and Rh-366 together (FT). Counts are of colonies whose morphological vouchers had 100% identity to the ITS+TEF-1a sequence of FSSC sp. isolate Rh-217. Groups with different letters had significantly different re-isolation rates within cankers, roots, or soil.

Reisolation of fungi used in inoculations

Isolate Rh-217 was found to be most closely related to FSSC sp. 35-a, 25-a, or 25-b (Fig. 3.6) and its ITS sequence differed by only one base insertion from FSSC sp. 25 isolated from TCD-symptomatic trees in Italy (Montecchio et al., 2015). Fifty-nine isolates from cankers (n = 11), roots (n = 40), and soil (n = 8) were 100% identical to *Fusarium solani* species complex sp. isolate Rh-217 across the merged ITS+TEF1 alignment (Figs. 3.6 & 7). Fungi that were classified to the same morphospecies as these molecular vouchers, which we inferred to be FSSC sp. isolate Rh-217, were isolated at significantly different rates across treatments (Fig. 3.7; $p \leq 0.001$; $df = 4$). FSSC sp. isolate Rh-217 was reisolated more frequently from FSSC, FSSC + *Trichoderma* and

non-sterile treatments than from the control seedlings ($p < 0.05$). *Trichoderma* sp. isolate Rh-366 (GenBank Accs. **MW301039** and **MW301040**) was also reisolated, but from very few plants.

Reisolation rates of *G. morbida* IN-66 from cankers differed significantly among treatments ($p = 0.028$; $df = 4$). *Geosmithia morbida* was isolated from the *Trichoderma* treatment 6.0 ± 5.2 times more frequently than the non-sterile treatment ($p = 0.037$), 2.1 ± 0.9 times more frequently than the FSSC treatment ($p = 0.056$), and 3.2 ± 1.5 times more frequently than the FSSC + *Trichoderma* treatment ($p = 0.010$).

3.4 Discussion

Our findings support the hypothesis that the soil microbiome in natural forests can indirectly enhance the resistance of walnut trees to *G. morbida*. Plant-mediated feedback between primary aboveground pathogens and above- and belowground latent endophytic pathogens may predispose *J. nigra* seedlings to successful infection by *G. morbida*, leading to larger cankers around inoculation points. These findings are consistent with previous work which also demonstrated that the microbiome associated with aboveground woody tissues of mature eastern black walnut trees shifts in response to colonization by *G. morbida* (Onufrak et al., 2020). This feedback appears to be dampened by forest soil microbiota, protecting seedlings from disease. In particular, forest soil microbiota suppressed the abundance of cosmopolitan FSSC spp. Suppression of *Fusarium* pathogens with fungi from forest soil has been demonstrated in annual crops and conifer nursery systems (Sylvia & Sinclair, 1983; Chakravarty & Unestam, 1987; Chakravarty & Hwang, 1991; Chakravarty et al., 1991; Ridout & Newcombe, 2016).

With live soil amendment and endophyte inoculation experiments, we observed plant-mediated positive feedback between *G. morbida* and FSSC spp. Fungi in the FSSC have the ability to asymptomatically colonize root cortical cells of seedlings during a latent period before producing phytotoxins and switching to a necrotrophic habit (Bacon & Yates, 2006; Swett et al., 2016). By contrast, *G. morbida* caused immediate necrosis in our experiments, and likely exploits oxdidative defenses to feed on dead tissue (Govrin & Levine, 2000). Thus, prior colonization by *Fusarium* spp. could have led to a physiological state of hypersensitivity or systemic induced susceptibility to *G. morbida* (Eyles et al., 2010; Plett & Martin, 2018). However, our findings also suggest that interactions between *Fusarium*, *J. nigra*, and *G. morbida* are further regulated by the

entire soil microbiome and/or substrate availability and suitability. This dependence of aboveground-belowground feedback on the soil microbiome and substrate is similar to the findings of Van Gils et al., (2017) for aphids and *Rhizoctonia* in an annual crop. When soil amendments were steam-treated in our study, aboveground inoculation with *G. morbida* inhibited belowground colonization by *Fusarium* and promoted *Rhizoctonia* spp. In contrast, in seedings grown with plantation soil amendments, *Fusarium* was promoted and *Rhizoctonia* was suppressed by aboveground *G. morbida* inoculation; this feedback was suppressed by the addition of live forest soil. Thus, forest soil amendments appear to impart greater resilience to the perturbation of the rhizosphere caused by aboveground pathogen infection.

In our study, legacy effects of forest management in the soil microbiome may have contributed to the susceptibility of seedlings to *G. morbida*. Plantation trees are grown at high density and low diversity and are likely to experience heavy pressue from insects and physical damage (Coyle et al., 2005). Therefore, plantations in our study may have been enriched in the rhizosphere with host-adapted biotrophs or hemibiotrophs like *Fusarium* spp. that heightened host susceptibility to necrotrophic attack by *G. morbida*. Similarly, the annual plant *Arabidopsis thaliana* accumulated necrotrophs when grown in soils conditioned by plants infected aboveground by a biotroph (Yuan et al., 2018). If woody plants similarly condition their soils in response to attack by bark beetles and their necrotrophic fungal symbionts, a corresponding accumulation of specialist biotrophs in the rhizosphere could have important ecological implications for forest regeneration and diversity. The microbiome of seedlings grown in fumigated nursery beds possibly induced a heightened state of defense against *Fusarium* but heightened susceptibility to necrotrophs such as *Rhizoctonia* and *G. morbida* that exploit oxidative defenses (Foley et al., 2016; Govrin & Levine, 2000). This physiological state could have been reversed by *G. morbida* inoculation or forest soil amendments, leading to responses in belowground community structure.

Despite the importance of phytobiomes in plant disease, their interactions with forest management practices and forest health are seldom explored (Busby et al., 2017). Here, we provide evidence suggesting that infection with FSSC spp., high host density, and low genetic diversity in plantations are predisposing factors that could increase the susceptibility of *J. nigra* to *G. morbida*, the primary fungal symbiont of *P. juglandis*, which together cause TCD. Our findings are consistent with the hypotheses that a) some endophytes function as latent pathogens, and b) plant

diseases of forest trees might be attributed to consortia of multiple pests and pathogens and/or disease synergists and secondary pathogens (Carroll, 1988; Mazzola, 1998; Lamichhane & Venturi, 2015; Busby et al., 2016). Disease synergists such as FSSC spp. are both abundant as fungal endophytes and in the natural environment, and frequently encountered as secondary pathogens in TCD-symptomatic trees (Tisserat et al., 2009; Kasson et al., 2014). However, they might be less abundant in forests (Ridout & Newcombe, 2016).

Intensively managed forest agroecosystems might be predisposed to disease, in part due to accumulation of opportunistic pathogens like *Fusarium* spp. In this study, FSSC spp. could have come from potting mix, from the fumigated nursery beds, or as a vertically-transmitted endophyte in seeds (Belisario et al., 2002; Liu et al., 2010; Dalling et al., 2020; Newcombe et al., 2018). Management scenarios that make use of these vectors and substrates could favor *Fusarium* spp. as a first colonizer in the endosphere of seedlings and young trees. If *Fusarium* spp. then persist as dominant members of the microbiome, cultivation and/or intensive orchard seed production of *J. nigra* seedlings may predispose trees to TCD. The extent to which first colonizers, such as FSSC Rh-217 which we used to inoculate germinating seeds, persist in the tissues of mature trees and propagate in plant communities remains poorly understood and is a critical knowledge gap in the field of forest pathology (Newcombe, 2011). Further study should aim to build an understanding of the influence that common soil and seed-dwelling pathogens in orchards and nurseries have on the productivity of hardwood plantations and their susceptibility to disease.

In addition to possible enrichment with secondary pathogens, soil microbiomes in urban forests and plantations, like those in the non-native range of *J. nigra*, are possibly depauperate in beneficial microbiota relative to forests (Onufrak et al., 2020). Our culture-based study design did not permit the detection of arbuscular mycorrhizal fungi (AMF), which cannot be grown in nutrient media, nor did we investigate plant-growth-promoting rhizobacteria (PGPR). AMF and PGPR could have induced resistance to *G. morbida* (Clear & Hom, 2019). AMF might have been more abundant or beneficial to black walnut in forest soils than plantation soils, and could have suppressed *Fusarium* spp. in roots (Ponder et al., 1990; Eke et al., 2016). *Zopfiella* spp., which were predominantly found in forest soil treatments, have been identified as potential biological control agents and implicated in suppression of soilborne disease (Zhao et al., 2018; Liu et al., 2019). In contrast, *Trichoderma* Rh-366, which is related to a putative biological control for other *Fusarium* spp. (*F. oxysporum* and *F. graminearum*; Patel & Saraf, 2017; He et al., 2019), did not

decrease canker size or the amount of infection by FSSC Rh-217 when coinoculated. Nevertheless, *Trichoderma* sp. isolate Rh-366 stimulated more advanced healing of inoculation wounds, which is consistent with findings in other pathosystems, including the application of *Trichoderma* spp. to protect seedlings from aboveground herbivores (Pineda et al., 2017). Further research could investigate whether *Trichoderma* spp. are effective as seed pretreatments to block subsequent *Fusarium* colonization.

Advanced knowledge of the contextual factors of nursery, plantation, and urban forest management and their collective effect on the host microbiome will have important implications for the management of pests and pathogens. Our findings suggest that the microbiome of long-lived hosts in mixed hardwood stands without groundcover management might protect trees from disease by suppressing negative soil feedbacks (Pineda et al., 2017; Schlatter et al., 2017). Therefore, further study should be conducted to explore the role of soil feedbacks in TCD and other tree diseases caused by pathogens and insect vectors. Foresters and funding agencies may consider that a better understanding of microbial legacy effects of prior land use and nursery practices, higher species and genetic diversity, and holistic soil, groundcover, and forest plantation management will lead to improvements in yield, quality, and resilience to biotic disturbance.

3.5 Supporting Material

Data, sequences, and R and mothur scripts are available in a downloadable repository at https://github.com/readingradio/WilliamsGinzel.JnGmFusarium.2021. Voucher cultures of *G. morbida* isolate IN-66, *F. solani* species complex sp. isolate Rh-217, and *Trichoderma* sp. isolate Rh-366 used for inoculations, along with representatives of the most commonly isolated OTUs are held in long-term storage collections at Purdue University, Department of Forestry and Natural Resources and can be made available upon request.

3.6 References

Altschul, S. (1990). Basic Local Alignment Search Tool. Journal of Molecular Biology 215: 403–410.

Arnold, A.E., Maynard, Z., Gilbert, G. S., Coley, P. D., & Kursar, T. A. (2000). Are tropical fungal endophytes hyperdiverse? *Ecology letters* 3: 267–274.

Aukema, B. H., Zhu, J., Møller, J., Rasmussen, J. G., & Raffa, K. F. (2010). Predisposition to bark beetle attack by root herbivores and associated pathogens: Roles in forest decline, gap formation, and persistence of endemic bark beetle populations. *Forest Ecology and Management* 259: 374–382.

Bacon, C. W., & Yates, I. E. (2006). Endophytic root colonization by *Fusarium* species: histology, plant interactions, and toxicity. In B. Schultz, B. Boyle, & T. Sieber (Eds.), *Microbial Root Endophytes*. Germany: Springer, 133–152.

Belisario, A., Maccaroni, M., Corazza, L., Balmas, V., & Valier, A. (2002). Occurrence and etiology of brown apical necrosis on Persian (English) walnut fruit. *Plant Disease* 86: 599–602.

Bengtsson-Palme, J., Ryberg, M., Hartmann, M., Branco, S., Wang, Z., Godhe, A., De Wit, P., Sánchez-García, M., Ebersberger, I., de Sousa, F. et al., 2013. Improved software detection and extraction of ITS1 and ITS2 from ribosomal ITS sequences of fungi and other eukaryotes for analysis of environmental sequencing data. Methods in *Ecology and Evolution* 4: 914–919.

Bennett, J. A., & Klironomos, J. (2019). Mechanisms of plant–soil feedback: interactions among biotic and abiotic drivers. *New Phytologist* 222: 91–96.

Blackman, M. W. (1928). The genus *Pityophthorus* Eichh. North America: a revisional study of the Pityophthori, with descriptions of two new genera and seventy-one species. *Bull New York State College of Forestry*, 1(3-6), 183.

Browne, G., Lee, R., Mclaughlin, S., Connell, J., Schneider, S., & Bulluck, R. (2006). Investigating associations between culturable soilborne fungi and replant disease of stone fruits in California. *Phytopathology* 96: S166.

Busby, P. E., Ridout, M., & Newcombe, G. (2016). Fungal endophytes: modifiers of plant disease. *Plant Molecular Biology* 90: 645–655.

Busby, P. E., Soman, C., Wagner, M. R., Friesen, M. L., Kremer, J., Bennett, A., Morsy, M., Eisen, J. A., Leach, J. E., & Dangl, J. L. (2017). Research priorities for harnessing plant microbiomes in sustainable agriculture. *PLoS Biology* 15: e2001793.

Carroll, G. (1988). Fungal endophytes in stems and leaves: from latent pathogen to mutualistic symbiont. *Ecology* 69: 2–9.

Castellá, G., Bragulat, M. R., Rubiales, M. V., & Cabañes, F. J. (1997). Malachite green agar, a new selective medium for *Fusarium* spp. *Mycopathologia* 137: 173–178.

Cesarano, G., Zotti, M., Antignani, V., Marra, R., Scala, F., & Bonanomi, G. (2017). Soil sickness and negative plant-soil feedback: A reappraisal of hypotheses. *Journal of Plant Pathology* 99: 545–570.

Chakravarty, P., & Hwang, S. F. (1991). Effect of an ectomycorrhizal fungus, *Laccaria laccata*, on *Fusarium* damping-off in *Pinus banksiana* seedlings. *European Journal of Forest Pathology* 21: 97–106.

Chakravarty, C., Peterson, R. L., & Ellis, B. E. (1991). Interaction between the ectomycorrhizal fungus *Paxillus involutus*, damping-off fungi and *Pinus resinosa* seedlings. *Journal of Phytopathology* 132: 207–218.

Chakravarty, P., & Unestam, T. (1987). Differential influence of ectomycorrhizae on plant growth and disease resistance in *Pinus sylvestris* seedlings. *Journal of Phytopathology* 120: 104–120.

Clear, M. R., & Hom, E. F. Y. 2019. The evolution of symbiotic plant-microbe signalling. *Annual Plant Reviews Online* 2. doi: 10.1002/9781119312994.apr0684

Coyle, D. R., Nebeker, T. E., Hart, E. R., & Mattson, W. J. (2005). Biology and Management of Insect Pests in North American Intensively Managed Hardwood Forest Systems. *Annual Review of Entomology* 50: 1–29.

Dalling, J. W., Davis, A. S., Arnold, A. E., Sarmiento, C., & Zalamea, P-C. 2020. Extending Plant Defense Theory to Seeds. *Annual Review of Ecology, Evolution, and Systematics* 51: 123–141.

Durrant, W. E., & Dong, X. (2004). Systemic acquired resistance. *Annu. Rev. Phytopathol*. 42: 185–209.

Edgar, R. C. (2004). MUSCLE: a multiple sequence alignment method with reduced time and space complexity. BMC bioinformatics 5: 113.

Eke, P., Chatue, G., Wakam, L. N., Kouipou, R. M. T., Fokou, P. V. T., & Boyom, F. F. (2016). Mycorrhiza consortia suppress the fusarium root rot (*Fusarium solani* f. sp. *Phaseoli*) in common bean (*Phaseolus vulgaris* L.). *Biological Control* 103: 240–250.

Ennos, R. A. (2015). Resilience of forests to pathogens: an evolutionary ecology perspective. *Forestry: An International Journal of Forest Research* 88: 41–52.

Eyles, A., Bonello, P., Ganley, R., & Mohammed, C. (2010). Induced resistance to pests and pathogens in trees. *New Phytologist* 185: 893–908.

Fox, J., & Weisberg, S. (2019). An R Companion to Applied Regression. Thousand Oaks, CA: Sage.

Foley, R. C., Kidd, B. N., Hane, J. K., Anderson, J. P., & Singh, K. B. (2016). Reactive oxygen species play a role in the infection of the necrotrophic fungi, *Rhizoctonia solani* in wheat. *PLoS One*. 11.

Gazis, R., Poplawski, L., Klingeman, W., Boggess, S. L., Trigiano, R. N., Graves, A. D., Seybold, S. J., & Hadžiabdić, Đ. (2018). Mycobiota associated with insect galleries in walnut with thousand cankers disease reveals a potential natural enemy against *Geosmithia morbida*. *Fungal Biology* 122: 241–253.

Geiser, D. M., del Mar Jiménez-Gasco, M., Kang, S., Makalowska, I., Veeraraghavan, N., Ward T. J., Zhang, N., Kuldau, G. A., & O'donnell, K. 2004. FUSARIUM-ID v. 1.0: a DNA sequence database for identifying *Fusarium*. *European journal of plant pathology* 110: 473–479.

Van Gils, S., Tamburini, G., Marini, L., Biere, A., Van Agtmaal, M., Tyc, O., Kos, M., Kleijn, D., & Van Der Putten, W. H. (2017). Soil pathogen-aphid interactions under differences in soil organic matter and mineral fertilizer. *PLoS ONE* 12: 1–15.

Govrin, E. M., & Levine, A. (2000). The hypersensitive response facilitates plant infection by the necrotrophic pathogen *Botrytis cinerea*. *Current biology* 10: 751–757.

He, A., Liu, J., Wang, X., Zhang, Q., Song, W., & Chen, J. (2019). Soil application of *Trichoderma asperellum* GDFS1009 granules promotes growth and resistance to *Fusarium graminearum* in maize. *Journal of Integrative Agriculture* 18: 599–606.

Hertert, H. D., Miller, D. L., & Partridge, A. D. (1975). Interaction of bark beetles (Coleoptera: Scolytidae) and root-rot pathogens of grand-fir in northern Idaho. *The Canadian Entomologist* 107: 899–904.

Jactel, H., Moreira, M., and Castageneyrol, B. Tree Diverstiy and Forest Resistance to Insect Pests: Patterns, Mechanisms, and Prospects. *Annual Review of Entomology* 66: 277-296.

Jeffers, S. N., & Martin, S. B. (1986). Comparison of two media selective for *Phytophthora* and *Pythium* species. *Plant Disease* 70: 1038–1043.

Jung, S. C.., Martinez-Medina, A., Lopez-Raez, J. A., & Pozo, M. J. (2012). Mycorrhiza-Induced Resistance and Priming of Plant Defenses. *Journal of Chemical Ecology* 38: 651–664.

Juzwik, J., Banik, M. T., Reed, S. E., English, J. T., & Ginzel, M. D. (2015). *Geosmithia morbida* Found on Weevil Species *Stenomimus pallidus* in Indiana. *Plant Health Progress* 16. doi: 10.1094/PHP-RS-14-0014.

Juzwik, J., Moore, M., Williams, G., & Ginzel, M. (2020). Assessment and etiology of thousand cankers disease within the native range of black walnut (*Juglans nigra*). In K. M. Potter, & B. L. Conkling (Eds.), *Forest health monitoring: national status, trends, and analysis 2019* (pp. 169–178). Gen. Tech. Rep. SRS-250. Asheville, NC: US Department of Agriculture, Forest Service, Southern Research Station.

Kaplan, I., Pineda, A., & Bezemer, M. (2018). Application and Theory of Plant-Soil Feedbacks on Aboveground Herbivores. In T. Ohgushi, S. Wurst, & S. N. Johnson (Eds.), *Aboveground-Belowground Community Ecology* (pp. 319–343). Springer International Publishing.

Kasson, M., Griffin, G., Geiser, D., O'Neal, E., Juzwik, J., Reed, S., Tisserat, N., Turcotte, R., Martin, D., Davis, D., Fenstermacher, K., & O'Donnel, K. 2014. New perspectives on thousand cankers disease of walnut. *Phytopathology* 104 (S11), 148–148.

Kolařík, M., Freeland, E., Utley, C., & Tisserat, N. (2011). *Geosmithia morbida* sp. nov., a new phytopathogenic species living in symbiosis with the walnut twig beetle (*Pityophthorus juglandis*) on *Juglans* in USA. *Mycologia*, 103, 325-332.

O'donnell, K. H., Kistler, C., Cigelnik, E., & Ploetz, R. (1998). Multiple evolutionary origins of the fungus causing Panama disease of banana: Concordant evidence from nuclear and mitochondrial gene genealogies. *PNAS*, 95: 2044.

Klein, R. M., & Perkins, T. D. (1987). Cascades of causes and effects of forest decline. *Ambio*, 16: 86–93.

Klironomos, J. N. (2002). Feedback with soil biota contributes to plant rarity and invasiveness in communities. *Nature*, 417: 67–70.

Lamichhane, J. R., & Venturi, V. (2015). Synergisms between microbial pathogens in plant disease complexes: A growing trend. *Frontiers in Plant Science*, 6: 1–12.

Lauritzen, J. E. (2018). Characterization of Black Walnut Genotypes for Resistance to Thousand Cankers Disease, Frost Hardiness and Other Desirable Horticultural Traits. PhD Thesis. Utah State University, Logan, UT.

Lee, S. B., & Taylor, J. W. (1990). Isolation of DNA from fungal mycelia and single spores. In M. Innis, D. Gelfand, J. Sninsky, & T. White, (Eds.), *PCR Protocols: a guide to methods and applications* (pp. 282–287). New York, NY: Academic Press

Leslie, J. F., & Summerell, B. A. (2008). *The Fusarium laboratory manual*. Denver, CO: John Wiley & Sons.

Liu,. L, Huang, X., Zhao, J., Zhang, J., & Cai, Z. (2019). Characterizing the Key Agents in a Disease-Suppressed Soil Managed by Reductive Soil Disinfestation. *Applied and Environmental Microbiology*, 85: e02992-18.

Liu, B., Sun, J., Rivard, C., Welker, R., & Louws, F. (2010). Comparison of fumigation, mustard meal amendments and grafting on bulk soil microbial communities in tomato fields. *Phytopathology*, 100: S73.

Van Loon, L. C. (1997). Induced resistance in plants and the role of pathogenesis-related proteins. *European Journal of Plant Pathology* 103: 753–765.

Maddison, W. P., and Maddison, D. R. 2019a. Mesquite: a modular system for evolutionary analysis. Version 3.61 [WWW document] URL http://mesquiteproject.org. [accessed 29 November 2020].

Maddison, D. R., and Maddison, W. P. 2019b. Chromaseq: a Mesquite package for analyzing sequence chromatograms. Version 1.51 [WWW document] URL http://mesquiteproject.org/http://mesquiteproject.org/packages/chromaseq/. [accessed 29 November 2020].

Manion, P. D. (1981). *Tree disease concepts*. Prentice-Hall, Inc.

Mazzola, M. (1998). Elucidation of the Microbial Complex Having a Causal Role in the Development of Apple Replant Disease in Washington. *Phytopathology* 88: 930–938.

McFadden, D. (1974). The measurement of urban travel demand. *Journal of public economics* 3: 303–328.

McKenry, M. (1999). *The replant problem and its management*. Fresno, CA: Catalina Pubilshing.

Michler, C. H., Pijut, P. M., Van Sambeek, J. W., Coggeshell, M. V., Seifert, J., Woeste, K., Overton, R., & Ponder, F. J. (2004). Diseases of Intensively Managed Eastern Black Walnut. In C. H. Michler, P. M. Pijut, J. W. Van Sambeek, M. V. Coggeshall, J. Seifert, K. Woeste, R. Overton, & F. J. Ponder (Eds.), *Black Walnut in a New Century, Proceedings of the 6th Walnut Council Research Symposium*. St. Paul, MN: U.S. Department of Agriculture, Forest Service, North Central Research Station, 110–113.

Montecchio, L., Faccoli, M., Short, D. P. G., Fanchin, G., Geiser, D. M., & Kasson, M. T. (2015). First report of *Fusarium* solani phylogenetic species 25 associated with early stages of thousand cankers disease on *Juglans nigra* and *Juglans regia* in Italy. *Plant Disease* 99: 1183.

Nakagawa, S., Johnson, P. C. D., & Schielzeth, H. (2017). The coefficient of determination R^2 and intra-class correlation coefficient from generalized linear mixed-effects models revisited and expanded. *Journal of the Royal Society Inte*rface 14: 20170213.

Newcombe, G. (2011). Endophytes in forest management: four challenges. In A. M. Pirttilä, A. C. Frank (Eds.), *Endophytes of Forest Trees* (pp. 251–262). Springer.

Newcombe, G., Harding, A., Ridout, M., & Busby, P. E. (2018). A Hypothetical Bottleneck in the Plant Microbiome. *Frontiers in Microbiology* 9: 1–10.

Newhouse, J. R., and Hunter B. B. 1983. Selective Media for Recovery of *Cylindrocladium* and *Fusarium* Species from Roots and Stems of Tree Seedlings. *Mycologia* 75: 228–233.

Nilsson, R. H., Larsson, K-H., Taylor, A. F. S., Bengtsson-Palme, J., Jeppesen, T. S., Schigel, D., Kennedy, P., Picard, K., Glöckner, F. O., Tedersoo, L., et al., 2019. The UNITE database for molecular identification of fungi: handling dark taxa and parallel taxonomic classifications. *Nucleic Acids Research* 47: D259–D264.

O'Donnell, K., Al-Hatmi, A. M. S., Aoki, T., Brankovics, B., Cano-Lira, J. F., Coleman, J. J., de Hoog, G. S., Di Pietro, A., Frandsen, R. J. N., Geiser, D. M., et al., 2020. No to *Neocosmospora*: Phylogenomic and Practical Reasons for Continued Inclusion of the *Fusarium solani* Species Complex in the Genus. *mSphere* 5: e00810-20.

O'Donnell, K., Humber, R. A., Geiser, D. M., Kang, S., Park, B., Robert, V., Crous, P. W., Johnston, P. R., Aoki, T., Rooney, A. P., et al., 2012. Phylogenetic diversity of insecticolous fusaria inferred from multilocus DNA sequence data and their molecular identification via FUSARIUM-ID and *Fusarium* MLST. Mycologia 104: 427–445.

Oksanen, J., Blanchet, F. G., Friendly, M., Kindt, R., Legendre, P., McGlinn, D., Minchin, P. R., O'Hara, R. B., Simpson, G. L., Solymos, P., et al., 2018. vegan: Community Ecology Package. [WWW document] URL https://cran.r-project.org/web/packages/vegan/index.html. [accessed 29 November 2020].

Onufrak, A. J., Williams, G. M., Klingeman, W. E., Cregger, M. A., Klingeman, D. M., DeBruyn, J. M., Ginzel, M. D., & Hadžiabdić, Đ. (2020). Regional Differences in the Structure of *Juglans nigra* Phytobiome Reflect Geographical Differences in Thousand Cankers Disease Severity. *Phytobiomes Journal* 4: 388–404.

Patel, S., & Saraf, M. (2017). Biocontrol efficacy of *Trichoderma asperellum* MSST against tomato wilting by *Fusarium oxysporum* f. sp. *lycopersici*. *Archives of Phytopathology and Plant Protection* 50: 228–238.

Pineda, A., Kaplan, I., & Bezemer, T. M. (2017). Steering Soil Microbiomes to Suppress Aboveground Insect Pests. *Trends in Plant Science* 22: 770–778.

Plett, J. M., & Martin, F. M. (2018). Know your enemy, embrace your friend: using omics to understand how plants respond differently to pathogenic and mutualistic microorganisms. *Plant Journal* 93: 729–746.

Ploetz, R. C., Hulcr, J., Wingfield, M. J., de Beer, Z. W. (2013). Destructive Tree Diseases Associated with Ambrosia and Bark Beetles: Black Swan Events in Tree Pathology? *Plant Disease* 97: 856–872.

Ponder, F. (1979). Soil structure and mycorhizae encourage black walnut growth on old fields. Res. Note NC-249. St. Paul, MN: U.S. Department of Agriculture, Forest Service, North Central Forest Experimental Station.

Porras-Alfaro, A., & Bayman, P. (2011). Hidden Fungi, Emergent Properties: Endophytes and Microbiomes. *Annual Review of Phytopathology* 49: 291–315.

R Core Team. 2019. R: A Language and Environment for Statistical Computing. [Available online] URL https://cran.r-project.org. [accessd 29 November 2020].

Rice, P., Longden, I., & Bleasby, A. (2000). EMBOSS: the European molecular biology open software suite. *Trends in Genetics* 16: 276–277.

Ridout, M., Houbraken, J., & Newcombe, G. (2017). Xerotolerance of *Penicillium* and *Phialocephala* fungi, dominant taxa of fine lateral roots of woody plants in the intermountain Pacific Northwest, USA. *Rhizosphere* 4: 94–103.

Ridout, M., & Newcombe, G. (2016). Disease suppression in winter wheat from novel symbiosis with forest fungi. *Fungal Ecology* 20: 40–48.

Ridout, M. E., Schroeder, K. L., Hunter, S. S., Styer, J., & Newcombe, G. (2019). Priority effects of wheat seed endophytes on a rhizosphere symbiosis. *Symbiosis* 78: 19–31.

Samuels, G. J., Lieckfeldt, E., & Nirenberg, H. I. (1999). *Trichoderma asperellum*, a new species with warted conidia, and redescription of *T. viride*. *Sydowia* 51, 71-88.

Schlatter, D., Kinkel, L., Thomashow, L., Weller, D., & Paulitz, T. (2017). Disease Suppressive Soils: New Insights from the Soil Microbiome. *Phytopathology* 107: 1284-1297.

Schloss, P. D., Westcott, S. L., Ryabin, T., Hall, J. R., Hartmann, M., Hollister, E. B., Lesniewski, R. A., Oakley, B. B., Parks, D. H., Robinson, C. J., et al., 2009. Introducing mothur: Open-source, platform-independent, community-supported software for describing and comparing microbial communities. *Applied and Environmental Microbiology* 75: 7537-7541.

Schmidt, L., Bhat, R., & Browne, G. (2010). Culture-independent examination of microbial community shifts associated with replant disease of almond. *Phytopathology* 100: S115.

Seybold, S. J., Klingeman, W. E., Hishinuma, S. M., Coleman, T. W., & Graves, A. D. (2019). Status and Impact of Walnut Twig Beetle in Urban Forest, Orchard, and Native Forest Ecosystems. *Journal of Forestry* 117: 152–163.

Sievers, F., Wilm, A., Dineen, D., Gibson, T. J., Karplus, K., Li, W., Lopez, R., McWilliam, H., Remmert, M., Söding, J., et al., 2011. Fast, scalable generation of high-quality protein multiple sequence alignments using Clustal Omega. *Molecular Systems Biology* 7. doi: 10.1038/msb.2011.75.

Sitz, R. A., Luna, E. K., Caballero, J. I., Tisserat, N. A., Cranshaw, W. S., & Stewart, J. E. (2017). Virulence of Genetically Distinct *Geosmithia morbida* Isolates to Black Walnut and Their Response to Coinoculation with *Fusarium solani*. *Plant Disease* 101: 116.

Stamatakis, A. (2014). RAxML version 8: a tool for phylogenetic analysis and post-analysis of large phylogenies. *Bioinformatics* 30: 1312–1313.

Summerell, B. A. (2019). Resolving *Fusarium* : Current Status of the Genus. *Annual Review of Phytopathology* 57: 323–339.

Swofford, D. L. (2003). PAUP*. Phylogenetic Analysis Using Parsimony (*and Other Methods). Version 4. Sinauer Associates, Sunderland, Massachusetts.

Swett, C. L., Kirkpatrick, S. C., & Gordon, T. R. (2016). Evidence for a hemibiotrophic association of the pitch canker pathogen fusarium circinatum with *Pinus radiata*. *Plant Disease* 100: 79–84.

Sylvia, D. M., & Sinclair, W. A. (1983). Suppressive influence of *Laccaria laccata* on *Fusarium oxysporum* and on Douglas-fir seedlings. *Phytopathology* 73: 384–389.

Tainter, F. H., & Baker, F. A. (1996). *Principles of forest pathology*. John Wiley & Sons.

Tello, M-L., Tomalak, M., Siwecki, R., Gáper, J., Motta, E., & Mateo-Sagasta, E. (2005). Biotic urban growing conditions—threats, pests and diseases. In C. Konijnendijk, K. Nilsson, T. Randrup & S. Jasper (Eds.), *Urban forests and trees* (pp. 325–365). Springer.

Tisserat, N., Cranshaw, W., Leatherman, D., Utley, C., & Alexander, K. (2009). Black walnut mortality in Colorado caused by the walnut twig beetle and thousand cankers disease. *Plant Health Progress* 11, 10. doi:10.1094/php-2009-0811-01-rs.

Trevors, J. T. (1996). Sterilization and inhibition of microbial activity in soil. *Journal of Microbiological Methods* 26: 53–59.

Utley, C., Nguyen, T., Roubtsova, T., Coggeshall, M., Ford, T. M., Grauke, L. J., Graves, A D., Leslie, C. A., McKenna, J., Woeste, K., Yaghmour, M A., Cranshaw, W., Seybold, S. J., Bostock, R. M., & Tisserat, M. (2013). Susceptibility of Walnut and Hickory Species to *Geosmithia morbida*. *Plant Disease* 97, 601–607. doi:10.1094/PDIS-07-12-0636-RE.

Vargas Gil, S., Pastor, S., & March, G. J. (2009). Quantitative isolation of biocontrol agents *Trichoderma* spp., *Gliocladium* spp. and actinomycetes from soil with culture media. *Microbiological Research* 164: 196–205.

Venables, W. N., & Ripley, B. D. (2002). *Modern Applied Statistics with S*. New York: Springer.

White, T., Bruns, T., & Lee, T. (1990). Amplification and direct sequencing of fungal ribosomal RNA genes for phylogenetics. In M. Innis, D. Gelfand, J. Sninsky, & T. White, (Eds.), *PCR Protocols: a guide to methods and applications* (pp. 282–287). New York, NY: Academic Press

Wingfield, M. J., Brockerhoff, E. G., Wingfield, B. D., & Slippers, B. (2015). Planted forest health: the need for a global strategy. *Science* 349: 832–836.

Yang, J., Ruegger, P. M., McKenry, M. V., Becker, J. O., & Borneman, J. (2012). Correlations between Root-Associated Microorganisms and Peach Replant Disease Symptoms in a California Soil. *PLOS ONE* 7: 1–10.

Yuan, J., Zhao, J., Wen, T., Zhao, M., Li, R., Goossens, P., Huang, Q., Bai, Y., Vivanco, J. M., Kowalchuk, G. A., et al., 2018. Root exudates drive the soil-borne legacy of aboveground pathogen infection. *Microbiome* 6: 156.

Zhao, J., Zhou, X., Jiang, A., Fan, J., Lan, T., Zhang, J., & Cai, Z. (2018). Distinct impacts of reductive soil disinfestation and chemical soil disinfestation on soil fungal communities and memberships. *Applied Microbiology and Biotechnology* 102: 7623–7634.

CHAPTER 4. COMPETITIVE ADVANTAGE OF *GEOSMITHIA MORBIDA* IN LOW-MOISTURE WOOD MAY EXPLAIN HISTORICAL OUTBREAKS OF THOUSAND CANKERS DISEASE AND PREDICT THE FUTURE FATE OF *JUGLANS NIGRA* WITHIN ITS NATIVE RANGE

*** Submitted for review to Frontiers in Forests and Global Change, section Pest, Pathogens, and Invasions for special topic: Forest Pathology in Changing Climate.**

4.1 Introduction

Range expansions of native pests caused by climate change are a major threat to the health and productivity of forest ecosystems (Ramsfield et al., 2016, Pureswaran et al., 2018). In particular, abiotic factors are known to influence dispersal and reproduction of scolytine beetles (Coleoptera: Curculionidae) and primary symbiotic fungi (Wood, 1982; Six & Bentz, 2007). Beetles and fungi mutualistically rely upon one another for successful host colonization and to satisfy metabolic requirements (Hofstetter et al., 2007, 2015, Six & Bentz, 2007; Mitton & Ferrenberg, 2012). Physicochemical conditions in bark and wood, including nutrient availability, temperature, and moisture, determine the outcome of competition between the primary mutualist of a beetle species and other fungi, and consequently, affect reproductive success and dispersal (Rayner & Boddy, 1988; Ranger et al., 2018).

Co-dispersal of the walnut twig beetle (*Pityophthorus juglandis* Blackman) and its primary mutualist, the pathogenic fungus *Geosmithia morbida* Kol. Free. Ut. & Tiss. to new walnut trees (*Juglans* spp.) is contingent on physicochemical conditions that favor competitive success and sporulation of *G. morbida* in walnut wood. Many species of scolytine beetles have evolved specialized structures, glands, and behaviors that maximize favorability of growth conditions for successful colonization of wood by their mutualistic fungi (Francke-Grosmann, 1967; Weed et al., 2015, Nuotclà et al., 2019). Other species, including *P. juglandis,* lack specialized structures, but rather rely on passive co-dispersal of fungi (Bright, 1981). The hydrophobic spores of *G. morbida* are borne on conidiophores inside beetle galleries and picked up by static adhesion to the cuticle of *adult P. juglandis* as they emerge (Tisserat et al., 2009, Kolařík et al., 2011, Seybold et al., 2016).

Geographic variation in severity and impact of thousand cankers disease (TCD) and establishment of *P. juglandis* and *G. morbida* across North America suggest that climatic factors such as temperature and humidity may be important in determining environmental favorability for development and spread of the disease (Tisserat et al., 2011; Griffin, 2015; Juzwik et al., 2020). TCD is caused by mass attack of *P. juglandis* that introduce *G. morbida* to the inner bark of *Juglans* and *Pterocarya* spp., which causes necrotic cankers in the phloem and outer sapwood that interfere with the translocation of nutrients and photosynthate from distal branches and leaves to other parts of the plant (Tisserat et al., 2009).

G. morbida is evolutionarily adapted to the seasonally dry climate of the western U.S. (Williams & Newcombe, 2017). Both *P. juglandis* and *G. morbida* are native to semiarid southwest North America where the range of their ancestral host, *Juglans major* (Torr.) A. Heller, crosses into the U.S. from Mexico (Little, 1976; Seybold et al., 2012; Hadžiabdić et al., 2014; Zerillo et al., 2014; Rugman-Jones et al., 2015). Large-scale tree mortality attributed to TCD has been restricted to other native and introduced *Juglans* spp. west of the Great Plains (Seybold et al., 2019). *G. morbida* is thermophilic and xerotolerant, and commonly found sporulating inside *P. juglandis* galleries in black walnut (*Juglans nigra* L.) in the western, both not the eastern U.S. (Kolařík et al., 2011; Williams & Newcombe, 2017; Đ. Hadžiabdić, *pers. comm.*). In eastern states including Tennessee, fungal antagonists such as *Trichoderma* spp. are frequently found instead of *G. morbida* in *P. juglandis* galleries. Native populations of *J. nigra* in the eastern U.S. have been largely unaffected by TCD despite detections of the beetle or fungus in nine states (Moore et al., 2019; Seybold et al., 2019; Juzwik et al., 2020; Stepanek, 2020), and moribund trees recovered in disease epicenters in VA and TN (Griffin, 2015).

Climatic differences between the eastern and western U.S. provide one possible explanation for geographical difference in the prevalence and spread of TCD within the native and non-native range of *J. nigra*. In particular, intracontinental differences in prevailing climatic conditions may lead to differences in moisture content of senescent woody tissues around *P. juglandis* galleries and affect the relative competitive success and sporulation of *G. morbida*. When wood dries, its equilibrium moisture content (EMC) is determined by air temperature and relative humidity, which are variable across North America (Simpson, 1973). Largely due to variation in humidity, EMC in spring, summer, and autumn typically falls below 10% in locations in the western U.S. where TCD has been severe, but remains above 10% throughout much of the native

range of *J. nigra* (Eckelman, 1998; Simpson, 1998, Seybold et al., 2019). For example, in Tippecanoe Co., IN, summer moisture content of *J. nigra* wood was much higher, at 14.9 ± 0.20% (n = 156) for air-dried lumber and 20.1 ± 0.29% (n = 180) for retail firewood, the predominant vector for the movement of invasive wood-boring pests (G. M. Williams, *unpublished data*; Newton & Fowler, 2009; Jacobi et al., 2012). Furthermore, peak flight of *P. juglandis* typically occurs in the spring (Sitz et al., 2017; Chen et al., 2020), coinciding with high levels of precipitation in the Midwest.

Geographical variation in TCD incidence and severity could be partly explained by a competitive advantage for *G. morbida* over other xylotropic fungi in the western U.S.; however, colonization and spread of *G. morbida* may be inhibited by competition with other fungi that are better adapted to higher prevailing MC in the eastern U.S. (Eckelman, 1998). *G. morbida* could be recovered after 133 days from wood dried to a moisture content of 7% and grew on 25% glycerol agar with a water potential of –20 MPa (Ridout et al., 2017; Williams & Newcombe, 2017). These moisture levels fall below known limits for fungal wood decomposition (–4 MPa), between limits for biological activity in soils (–14 MPa) and surface litter (–36 MPa), and between limits for soil-dwelling *Fusarium* (–10 MPa) and extremely xerophilic *Penicillium* spp. (–40 MPa) (Griffin, 1977; Harris, 1981, Manzoni et al., 2012). Water potential supporting growth of *G. morbida* are similar to those that support *Penicillium* and *Phialocephala* from roots of conifers that withstand seasonal droughts in the western U.S. (Ridout et al., 2017). To our knowledge, the role of temperature and wood moisture content in determining the outcome of competition between *G. morbida* and other fungi in walnut wood has not yet been investigated.

Understanding the environmental parameters that favor TCD is essential for risk assessments to help predict the future threat to *J. nigra* in a changing climate. Wood moisture content may have historically limited the spread of TCD in the native range of *J. nigra*. Nevertheless, conditions could still become favorable for TCD in the eastern U.S. if prevailing temperature, precipitation, and humidity change as predicted by climate models (USGCRP 2018).

We hypothesized that the success of *G. morbida* and *P. juglandis* is limited by competition between *G. morbida* and other native fungi better adapted to the prevailing temperature and humidity regimes in the native range of *J. nigra.* To test this hypothesis, we first carried out a series of competition experiments in wood that had been naturally or artificial colonized by *G. morbida* and other fungi. We used lethal and nonlethal heat treatments to create fungal wood

microcosms where only a few native fungi survived in the wood and then inoculated the wood with *G. morbida*. In another experiment, competition was observed in nontreated wood that was naturally infested with *G. morbida* and other fungi. We calibrated the incubation conditions of the experiments to a range of EMC corresponding to climatic conditions across the U.S. (Eckelman, 1998; Simpson, 1998). We predicted that *G. morbida* would have a competitive advantage over other fungi that occur in wood that equilibrated to extremely low moisture content, but would be increasingly outcompeted by other fungi in wood that equilibrated to intermediate and high moisture content. We validated our interpretation of the results from our competition experiments by first extrapolating expected survival of *G. morbida* across the U.S. based on historical climate data, and then comparing inferred TCD severity with historical observations. Finally, we extrapolated the model to climate change scenarios based on high- and low-carbon emission to predict the portions of the native range of *J. nigra* that will be threatened by TCD ten and fifty year into the future.

4.2 Materials and Methods

4.2.1 Collection of Branches and *G. morbida* Isolates

Branches (6- to 8-cm diameter) of black walnut (*Juglans nigra*) were collected in 2018 and 2019, cut into 20- to 25-cm lengths and brought or shipped to an authorized quarantine facility at Purdue University (West Lafayette, IN). All branches were cut laterally into discs with a thickness of 4 mm. *G. morbida* (Gm-10) used in experiments 1, 2, and 3 was originally isolated from TCD-symptomatic trees in Tennessee (Hadžiabdić et al., 2014) and obtained courtesy of the laboratory collection of Dr. Đenita Hadžiabdić (UT-Knoxville). To inoculate wood discs with *G. morbida*, they were placed on cultures of Gm-10 growing on 1/8-strength potato dextrose agar (4.9 g PDA powder + 13.1 g agar per 1 L H_2O) in vented, high profile dimension polystyrene petri dishes (100-mm diameter 26-mm deep, Thermo Fisher Scientific, Waltham MA). Cultures of *G. morbida* were allowed to grow until colony diameter matched the diameter of the wood discs (8 to 21 days).

4.2.2 Humidity Chambers

Four fungal competition experiments were conducted in the dark. Humidity chambers with different expected equilibrium relative humidity and wood moisture content were constructed by preparing supersaturated salt solutions in 250-mL beakers and placing one beaker of each solution inside of a tightly-sealed 6-quart plastic storage container (Simpson, 1973; Greenspan, 1977). Wood discs were placed inside of sterile standard-size (100-mm diameter by 17-mm deep) polystyrene petri dishes, which were placed inside of the humidity chambers with the beakers containing the salt solutions. In all experiments, wood discs that were from the same parts of the same branch were distributed equally and randomly among humidity treatments to obtain independent data on survival of fungi from each portion of the branch or branches for each treatment. Temperature was maintained at 30°C by keeping the plastic storage containers containing the petri dishes and beakers with salt solutions inside a Precision 818 Low-Temperature Incubator (Thermo Fischer), or at 22°C by keeping the containers in a laboratory cabinet.

4.2.3 Experiment 1: High-Heat Pretreatment of Wood Discs and Inoculation with *G. morbida*

Branches were collected from Purdue University Martell Forest in West Lafayette, IN (40°25'60.0"N, 87°02'07.3"W), where neither *G. morbida* or *P. juglandis* have been detected, and allowed to dry on a lab bench for approximately 30 days prior to cutting them into discs. Indiana walnut branch discs were wrapped in aluminum foil and placed in an oven at 90°C to dry and kill most fungi for 48 hours. The heat-treated discs were then transferred to cultures of *G. morbida*. After 24 hours, discs with visible growth of fungi other than *G. morbida* were discarded, and the remaining inoculated discs were transferred to sterile plastic petri dishes. Discarding discs with substantial growth of other fungi left a slightly unbalanced sample size across treatments: LiCl (n = 11 inoculated wood discs); KOAc (n = 9); $MgNO_3$ (n = 9); and NH_4Cl (n =11). Discs were then allowed to equilibrate and incubate in the chambers at 30°C for 48 days.

At the conclusion of the incubation period, discs were weighed to record wet mass (m_i) and fungal growth was examined under a stereomicroscope (*e.g.*, Figure 4.1B & 4.1F). Fungi growing on the surface of each wood disc were categorized into morphospecies while examining them under 400X magnification. Presence and absence of each morphospecies were recorded for each

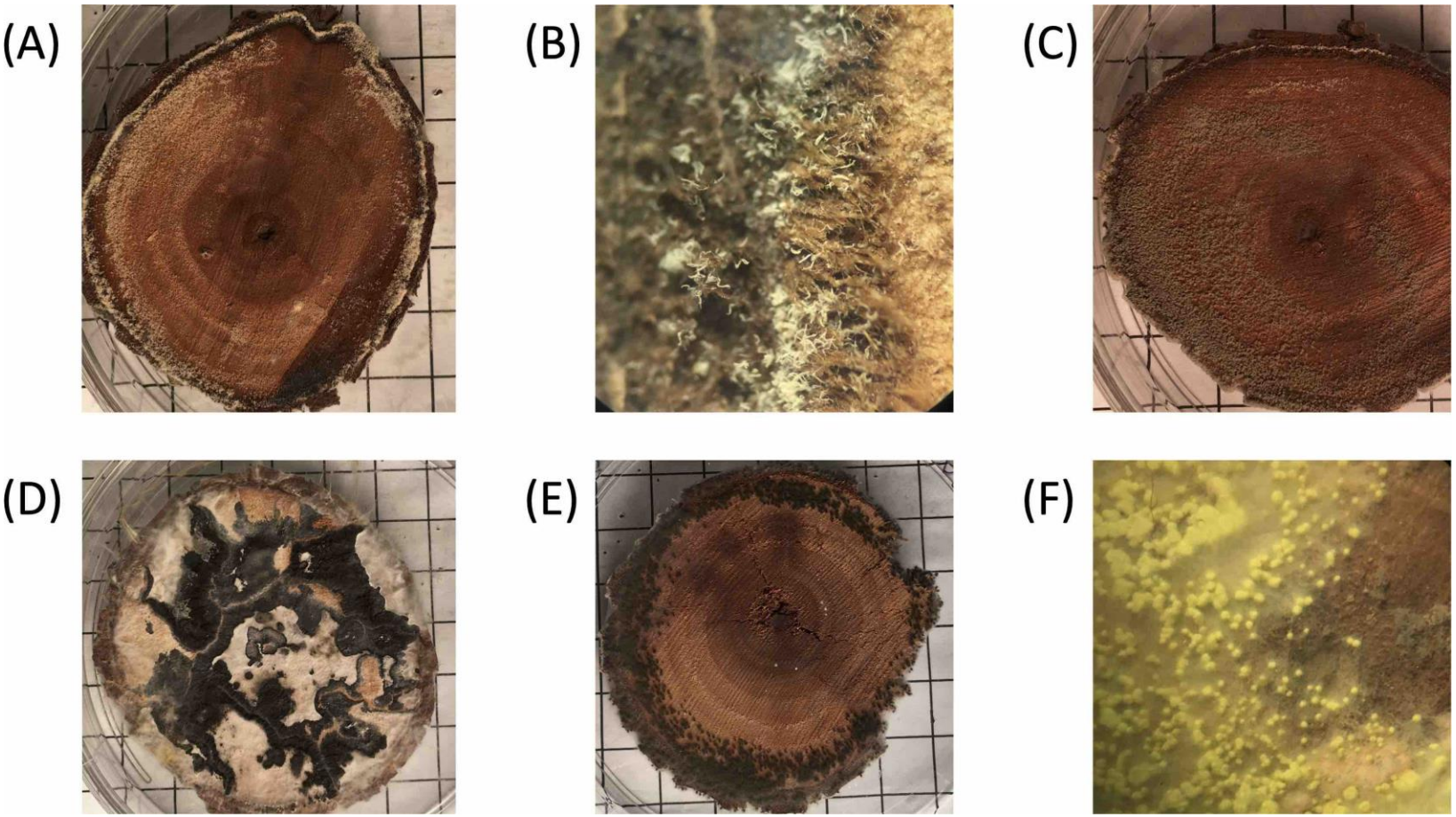

Figure 4.1. Representative images of wood discs colonized by fungi from Experiments 1 (A, C, D & E) and 4 (B & F). Wood disc colonized by *G. morbida* (A & B), *Aspergillus* sp. and *G. morbida* (C), Xylariaceae sp. (D), *Trichoderma* sp. (E), and *Aspergillus* (both anamorph and *Eurotium* sexual stage) sp. and *Clonostachys* sp. (F). Each grid line is 1 cm^2 (A, C, D & E).

disc (Figure 4.1). Mycelia or spores from the most frequently encountered and dominant morphospecies were collected directly into tubes with buffer to extract DNA or cultured to obtain voucher samples. If present, white-to-pink penicilliate conidiophores that resembled those of *G. morbida* (Figure 4.1A, 4.1B & 4.1C) were mounted on slides and examined at 1000X to confirm their identity. *G. morbida* was also cultured from conidiophores to verify viability of the spores across the range of final abiotic conditions. All wood discs were then dried at 70°C for at least 96 hours and weighed again to record dry mass (m_f). Final wood moisture content (MC) of each individual wood disc was calculated gravimetrically according to Eckelman (1998): $\boldsymbol{MC = \frac{m_i - m_f}{m_f}}$.

4.2.4 Experiment 2: Low-Heat Pretreatment of Wood Discs and Inoculation with *G. morbida*

Wood discs were collected, dried, inoculated, and incubated as described for Experiment 1 with the following exceptions. A less intense heat treatment (70°C for 24 h) and longer incubation period in humidity chambers (88 days) was employed to allow more fungal endophytes to persist in the wood prior to being challenged with *G. morbida* and a longer period to compete in humidity chambers. The final number of discs in each treatment was balanced (n = 8 per saturated salt solution). Fungi were counted and sampled and wood moisture content was determined gravimetrically as described above.

4.2.5 Experiment 3: Lethal Heat Pretreatment of Wood Discs and Inoculation with *G. morbida*

A control experiment was designed to demonstrate that fungi capable of growing and competing with *G. morbida* could be completely removed from the wood at sufficiently high temperature. Growth and survival of *G. morbida* at all moisture contents in the absence of other fungi would suggest the low survival of *G. morbida* at higher moisture levels in Experiments 1, 2, and 4 was due to competition with other fungi. To ensure full removal of other fungi that had already colonized the wood discs, they were heat-treated at 105°C for 2 days. To ensure colonization by *G. morbida*, discs were left on cultures for 10 days before being transferred to humidity chambers. Two *G. morbida*-inoculated discs and four control discs were included in each of the four humidity chamber treatments to verify *G. morbida* survival and the absence of other fungi. The saturated

salt solutions, temperature, and incubation times employed were LiCl, NaCl, or no salt, incubated for 57 days at 30°C. An additional no salt treatment was incubated at room temperature (22°C), and expected to result in higher relative humidity and final moisture content. Fungi were sampled and wood moisture content was determined as described above.

4.2.6 Experiment 4: Fungal Competition In wood Naturally Colonized by *G. morbida*

Branches that were already naturally colonized with *G. morbida* were collected from a TCD disease epicenter. The trees grew on a privately-owned plantation of black walnut in Walla Walla, WA. Six branches were collected from six TCD-symptomatic trees and shipped to Purdue University under permit (17-IN-20-007). Two freshly cut discs from each branch were placed directly in sterile petri dishes inside of each of the humidity chambers (n = 18 per treatment). Salt solutions and temperatures employed were the same as described above for Experiment 3. Fully saturated wood discs were allowed to incubate for 111 day to reach their equilibrium moisture content. Fungi were sampled and wood moisture content determined by drying discs at 100°C for 72 hours.

4.2.7 Molecular Identification of Fungi

DNA extraction, polymerase chain reaction (PCR) of the ITS region, and sequence assembly were performed as described previously (Williams and Ginzel, *in press*). ITS sequences were extracted with ITSX and assigned to genera through TBAS (Tree-Based Assignment Selector, Miller et al., 2015; Carbone et al., 2019) on DeCIFR public high-performance computing clusters (Center for Integrated Fungal Research, North Carolina State University; decifr.hpc.ncsu.edu). For high-level classification, all sequences were first aligned to a reference tree for all fungi. Isolates assigned to Ascomycetes were then aligned to the tree Pezizomyctonia 2.1, whereas Basidiomycetes were assigned taxonomy with the RDP Bayesian classifier with the Warcup database (Deshpande et al., 2016). Sequences were submitted to GenBank under accession numbers MW584687-MW584698.

4.2.8 Logistic Regressions

To test the hypothesis that the presence or absence of *G. morbida* and other fungi in each wood disc was significantly correlated to final MC, logistic regression and accompanying analytics were

performed in R v 3.6.0 (R Core Team, 2019) using the function *glm* and tools from the package *ROCR* (Sing et al., 2005). Because we expected survival rate of each fungus to peak at an optimum MC, we also fit models that included second-order terms for MC. Second-order terms were only retained in the model if they were significant ($p < 0.05$). Drop-in-deviance χ^2 tests and area under the receiver-operator curve (AUC) were used to assess overall regression significance and fit, respectively.

4.2.9 Geographical Prediction of *G. morbida* Survival

To create maps of expected *G. morbida* survival across the U.S. for historical and future prevailing climates, we used climate layers from Multivariate Constructed Analogs (MACA) statistical downscaling method, Version 2 (Abatzoglou, 2013). We derived a map of expected EMC from MACA by first calculating monthly average humidity and temperatures from monthly minimums and maximums for five months (*i.e.*, May, June, July, August, and September) between 1995-2004. This time period from late spring to early fall corresponds to the time when *P. juglandis*, the vector of *G. morbida*, is most active. Next, we inputted monthly averages into Simpson's (1973) model for wood moisture sorption with parameters estimated by Glass and Zelinka (2010). The Glass and Zelinka (2010) sorption isotherm model used to calculate equilibrium wood moisture content (*EMC*) as a function of ambient air temperature (*t*, °C) and relative humidity (*h*, decimal) is given by the following system of equations with constants from Simpson (1973):

$$\boldsymbol{EMC = \frac{18}{W}\left(\frac{Kh}{1-Kh} + \frac{KK_1h + 2K_1K_2K^2h^2}{1 + KK_1h + K_1K_2K^2h^2}\right)}$$

$$\boldsymbol{W = 349 + 1.29t + 0.0135t^2}$$

$$\boldsymbol{K = 0.805 + 0.000736t - 0.00000273t^2}$$

$$\boldsymbol{K_1 = 6.27 - 0.00938t - 0.000303t^2}$$

$$\boldsymbol{K_2 = 1.91 + 0.0407t - 0.000293t^2}$$

For each year between 1995-2004, expected *G. morbida* survival from May-September was calculated from the best logistic model fit to Experiment 4 as a function of EMC from the Glass and Zelinka (2010) model. Expected survival rates for each month (between 0 and 1) were then

multiplied across all five months to obtain a conservative, cumulative expected probability of survival for each year. Finally, cumulative probabilities of survival for each year were averaged across ten years (1995-2004) for historical analysis. For future climate, we used MACA data generated by the Geophysical Fluids Dynamic Laboratory Earth System Models II (GFDL-ESM2M) under the Representative Concentration Pathway low- (RCP4.5) and high-emission (RCP8.5) scenarios for ten (2031) and fifty years (2071) into the future. RCP scenarios are coded by the amount of thermal radiation (*i.e.*, 4.5 *vs.* 8.5 Watts per m^2) that is expected to be absorbed and retained by the atmosphere in year 2100. According to the U.S. National Oceanic and Atmospheric Administration (NOAA), the atmosphere held ~400 ppm CO_2 as of 2019 (www.climate.gov), and RCP4.5 projects ~500 ppm CO_2 and RCP8.5 projects ~600 ppm CO_2 in 2071 (IPCC, 2014).

Table 4.1. Model statistics for logistic regression of survival of fungi on final wood moisture content.

Experiment	Species	p_{MC} (1st)[1]	p_{MC} (2nd)[2]	p (χ^2)†	AUC‡
1	*G. morbida*	0.037	0.005	< 0.001	0.863
4	*G. morbida*	< 0.001	-	< 0.001	0.957
4	*Aspergillus* sp.	0.199	0.020	< 0.001	0.721
4	*Trichoderma* sp. 1	0.111	0.025	< 0.001	0.826
4	*Trichoderma* sp. 2	< 0.001	0.054	< 0.001	0.800
4	*Clonostachys* sp.	0.001	-	< 0.001	0.859

1,2 P-values for first- (1) and second-order (2) terms for moisture content.† P-value for overall regression from a drop-in-deviance chi-square test. ‡ Area under reciever-operator curve goodness-of-fit statistic for overall regression

4.3 Results

4.3.1 Competition Experiments

Competition with other fungi limited the survival of *G. morbida* at higher wood moisture levels (Fig. 4.2). *G. morbida* was released from competition at low wood moisture levels (Experiments 1 & 4, Figs. 2A & 2D) or in the absence of other fungi (Experiment 3, Fig. 4.2C). In general, when other fungi were present in wood discs, *G. morbida* was most successful at < 5% final MC and did not grow or sporulate > 30% final MC. Saturated salt solutions were effective at bringing wood discs incubated in the humidity chambers to the target range of MC.

Table 4.2. Final moisture content (MC) range, molecularly- and/or morphologically-inferred taxonomy, and GenBank accession numbers for DNA extracted directly (D) and/or from cultures (C) from fungi growing on wood discs in competition experiments.

MC (%)		Experiment	Locale	TBAS / Warcup Determination			DNA Sample (C= Culture, D= Direct)	GenBank Acc. #
Low	High			Phylum*	Family	Genus (sp)		
0	26.8	1, 2 & 4	E. WA	A	Bionectriaceae	*Geosmithia morbida***	C, D	MG008828
2.7	26.7	4	E. WA	A	Aspergilliaceae	*Aspergillus* sp.†	-	-
3.1	85.0	4	E. WA	A	Hypocreaceae	*Trichoderma* sp. 1	C, D	MW584687
4.7	34.1	1 & 2	IN	A	Aspergilliaceae	*Aspergillus* sp.	C	MW584688
5.5	65.8	2	IN	A	Xylariaceae	*Kretzshmaria* sp.	C	MW584689
6.0	6.0	1 & 2	IN	A	Didymellaceae	*Nothophoma* sp.	C	MW584690
14.3	39.4	4	E. WA	A	Hypocreaceae	*Trichoderma* sp. 2	C	MW584691
16.4	58.4	4	E. WA	A	Aspergilliaceae	*Aspergillus* sp.†	-	-
16.7	16.7	4	E. WA	A	Hyaloschyphaceae	*Hyaloscypha* sp.	D	MW584692
17.2	86.6	4	E. WA	A	Bionectriaceae	*Clonostachys* sp.	C, D	MW584693
17.9	52.9	4	E. WA	B	Tremellaceae	*Cryptococcus* sp.	D	MW584694
23.3	23.3	4	E. WA	B	Schizophyllaceae	*Schizophyllum* sp.	C, D	MW584695
25.6	25.6	4	IN	A	Botryosphaeriaceae	*Diplodia* sp.	C	MW584696
56.1	56.1	4	E. WA	A	Xylariaceae	*Rosellinia* sp.	D	MW584697
56.2	62.8	4	E. WA	B	Steccherinaceae	*Steccherinum* sp.	D	MW584698

** Ascomycota (A) and Basidiomycota (B). **G. morbida reisolated from wood discs were BLAST-aligned to sequences from original cultures used for inoculations. † Isolate taxonomy determined by morphology without the aid of molecular data.*

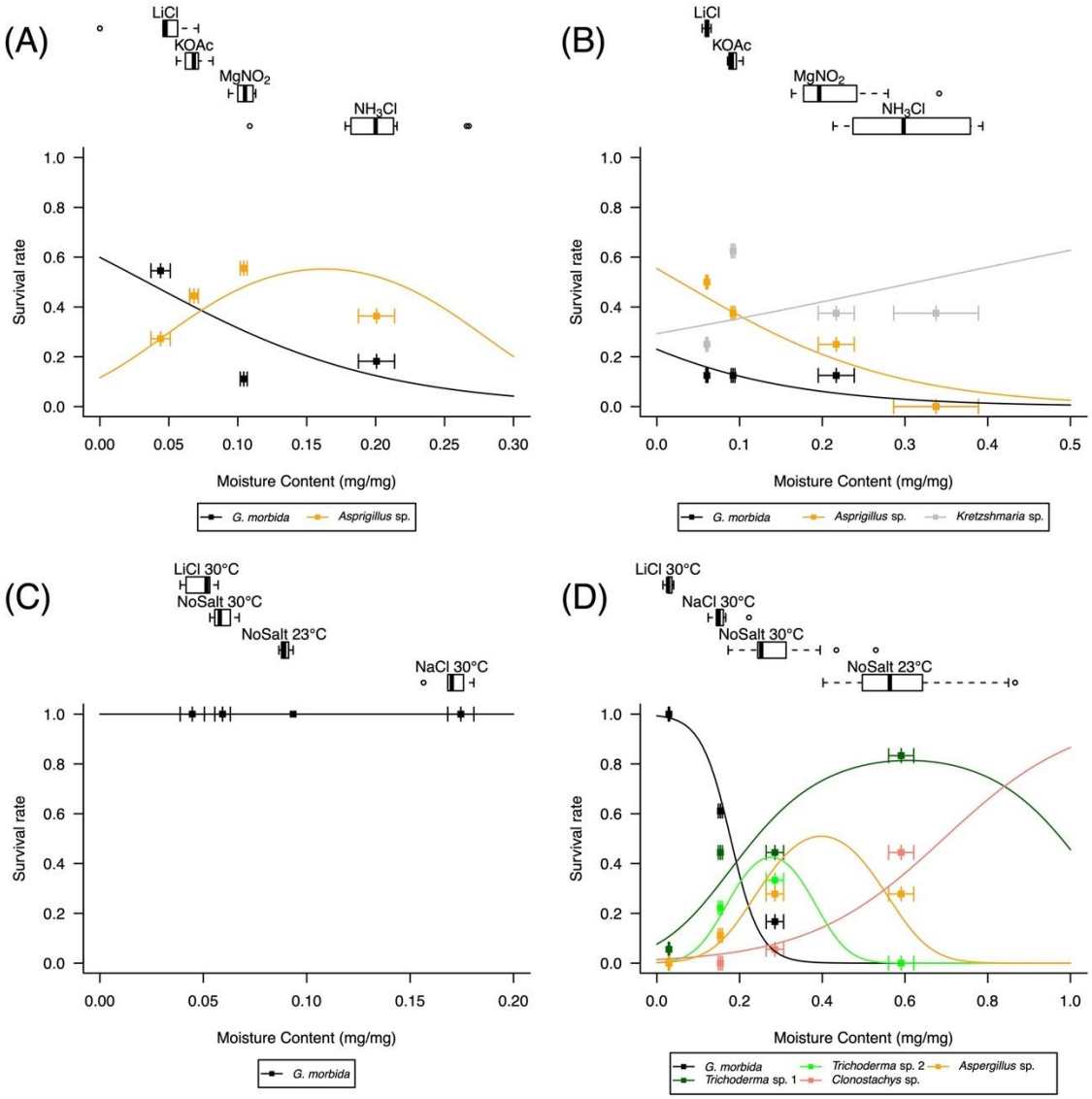

Figure 4.2. Wood moisture content by treatment (top panels) and observed and predicted survival of fungal species as a function of wood moisture content from best-fit logistic regressions (bottom panels) in Experiments 1 (A), 2 (B), 3 (C), and 4 (D). For each saturated salt solution treatment, boxes-and-whiskers show percentiles of final wood moisture content, and points and error bars in the plotting area give observed mean survival ± SE final moisture content.

In Experiment 1, when wood from Indiana was pretreated at a high (90°C) non-lethal temperature prior to inoculation with *G. morbida*, final MC significantly accounted for the survival and sporulation of *G. morbida* (Fig. 4.2A, Table 4.1). Control discs that were not inoculated with *G. morbida* supported growth of other fungi at all final MC levels.

When wood from Indiana was pretreated at a lower (70°C) non-lethal temperature (Experiment 2), final MC did not significantly account for survival of *G. morbida* ($p > 0.05$) due to the growth of other fungi at low final MC (Fig. 4.2B). Fungi from Indiana wood samples in Experiments 1 & 2 included *Aspergillus* sp. (Eurotiomycetes: Eurotiales), *Nothophoma* sp. (Dothidiomycetes: Pleosporales), and *Kretzschmaria* sp. (Sordariomycetes: Xylariales) at low final MC, and *Diplodia* sp. (Dothidiomycetes: Botryosphaeriales) at intermediate final MC (Table 4.2).

However, the higher temperature and duration (105°C for 2 days) treatment was sufficient to remove fungi from the wood from Indiana prior to inoculation (Experiment 3). In the absence of other fungi, *G. morbida* grew and sporulated on all inoculated wood discs regardless of final MC (Fig. 4.2C). Other fungi were not found growing on control or *G. morbida*-inoculated wood discs (*data not shown*).

In Experiment 4, final MC accounted for the survival and sporulation of *G. morbida* in naturally-infested wood from TCD-symptomatic trees from Washington (Table 4.1; Fig. 4.2D). Fungi from Washington wood samples were represented by *Aspergillus*, *Trichoderma* and *Clonostachys* spp. (Sordariomycetes: Hypocreales) at low and intermediate MC and *Rosellinia* spp. (Sordariomycetes: Xylariales) and Basidiomyctoa including *Cryptococcus* (Tremellomycetes: Tremellales), *Schizophyllum* and *Steccherinum* spp. (Agaricomycetes: Polyporales) at higher final MC (Table 4.2). The best-fit model for probability of *G. morbida* survival (*P*) as a function of final MC was:

$$\boldsymbol{P = \frac{1}{1 + e^{2.2457 - 2.1217MC}}}$$

4.3.2 Geographical Trends in Expected *G. morbida* Survival.

When predicting survival using the model above from equilibrium wood moisture content (EMC) calculated from climate models, survival for the ten-year period from 1995 to 2004 closely followed geographical patterns of TCD severity observed from that time to the present (Figure

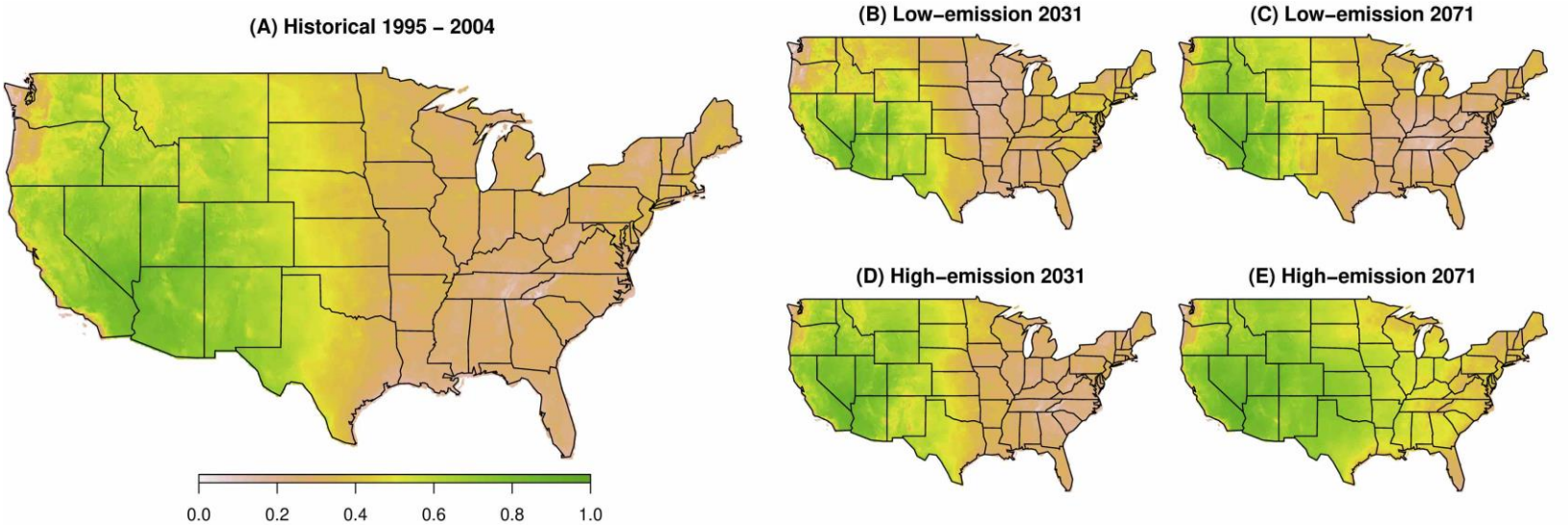

Figure 4.3. Modelled survival of *G. morbida* as a function of equilibrium moisture content (EMC) for average historical (A) and future low- (B & C, RCP4.5) and high-emission (D & E, RCP8.5) climate scenarios twenty (B & D) and fifty years (C & E) into the future. Survival for each year was obtained by multiplying monthly survival estimates from a logistic regression fit to results from Experiment 4 for May through September. For historical survival (A), yearly survival estimates were averaged across the ten-year timespan. Monthly average EMC was calculated using the model of Glass and Zelinkas (2010) as a function of monthly average temperature and humidity averaged from Multivariate Constructed Analogs (MACA) statistical downscaling method, Version 2 (Abatzoglou, 2013) and Geophysical Fluids Dynamic Laboratory Earth System Models II (GFDL-ESM2M) under the Representative Concentration Pathway scenarios (IPCC, 2014).

4.3A). West of the Great Plains and east of the Cascades, predicted survival generally ranged from 50 to 80%. TCD epicenters in WA, UT, ID, and the native range of *P. juglandis* in AZ and NM exceeded 70% expected *G. morbida* survival. TCD epicenters in OR, CA, and CO were predicted to support ~60% expected *G. morbida* survival.

In the native range of *J. nigra*, expected survival for *G. morbida* was generally below 20% (Figure 4.3A). However, known TCD epicenters along the north Atlantic seaboard in eastern PA, MD, and VA are located in some of the only pockets in the east where expected *G. morbida* survival reached ~50% according to our model. By contrast, in Knox and Polk Cos., TN where TCD caused a local and transient outbreak, suitability for *G. morbida* fell to 20% or below.

Under RCP 4.5, the geographical envelope in where *G. morbida* survival rates exceed 50% in the U.S. is expected to remain relatively stable from 2021-2071 (Fig. 4.3B). However, this envelope would expand across the Great Plains and Mississippi Valley into the midwestern and southeastern states under RCP 8.5 (Figure 4.3C).

4.4 Discussion

4.4.1 Wood Moisture, Fungal Competition, and TCD

Our research demonstrates that fungal competition mediated by abiotic conditions limits the potential geographic range of *G. morbid*a, and adds to a growing body of evidence that environmental conditions, including abiotic factors and the host microbiome, account for the lower severity of TCD in the native range of *J. nigra* (Griffin, 2015; Seybold et al., 2019; Onufrak et al., 2020). There were also notable differences in *G. morbida* competition and survival between branches from WA and those from IN, where xerophilic-thermotolerant fungi, including Xylariaceae and *Aspergillus* spp., outcompeted *G. morbida* at low moisture. These fungi survived temperatures up to 70° and even 90°C (*Aspergillus* sp.) for 48 hours. Prior colonization of the substrate by these fungi could have prevented *G. morbida* from colonizing wood discs at lower moisture levels. These findings raise the possibility that other fungi in walnut wood inhibit colonization and growth of *G. morbida* under climatic conditions that would otherwise favor the development of disease, and could have important management implications under future climate.

In ambrosia beetle galleries, *Aspergillus* spp. are known to be parasites of beetle-fungal mutualisms, where they outcompete symbiotic fungi, decrease fecundity, or cause disease of

beetles (Moore, 1971, 1973, Nuotclà et al., 2019). This exploitation is more successful when physicochemical conditions favor *Aspergillus* spp. over ambrosia fungi (Ranger et al., 2018). *Aspergillus* sp. outcompeted *G. morbida* in our experiments, suggesting it could also interfere with the mutualism between *G. morbida* and *P. juglandis.*

The ability of *G. morbida* to outcompete *Trichoderma* spp. and other fast-growing fungi at low wood moisture has potentially important implications for efforts to employ them as biological control (Gazis et al., 2018). Both *Trichoderma* spp. from Washington grew well and partly outcompeted *G. morbida* at 15% MC, which is equivalent to levels in air-dried walnut wood in the Midwest (G. M. Williams, *unpublished data*). However, *G. morbida* was still observed successfully growing and sporulating more frequently than either *Trichoderma* spp. on wood discs at 15% MC (*cf.* Gazis et al., 2018). Our findings support exercising caution when drawing biological inferences from competition assays conducted in standard laboratory media to inform management decisions. When the target organism is a specialist, stress-tolerant, or ruderal species, such laboratory assays are likely to favor competitive, resource-demanding putative antagonists when the target organism would otherwise outcompete them under realistic field conditions (Newcombe, 2011; Fierer, 2017, Whitaker & Bakker, 2019).

Mapping expected survival of *G. morbida* across the U.S. based on EMC reproduced with high fidelity well-known historical geography of TCD epicenters which have been reviewed elsewhere (Seybold et al., 2019). Our experiments suggest that the higher EMC in walnut wood in the Midwest, Appalachia and Atlantic U.S. limits the successful establishment of *G. morbida* due to competition with other fungi. In MD, VA, PA, OH and IN, expected survival of *G. morbida* was higher than the rest of the native range of *J. nigra*, but below 50%. In these locations, *P. juglandis* and/or *G. morbida* have been detected transiently or incidentally since the early to mid-2010s, suggesting failure to establish long-term populations. We infer that areas of transient TCD outbreaks in eastern TN and western NC that occurred following years of below-average precipitation (Griffin, 2015) have nevertheless been historically unfavorable for *G. morbida.*

Drought and above-average temperatures may have increased host stress and susceptibility as suggested by Griffin (2015). Even though expected survival of *G. morbida* is extremely low in Appalachia, TN and neighboring parts of NC experienced severe and extreme drought starting in March of 2007 that persisted in Knoxville until November 2008 (Palmer drought severity index, Palmer, 1965, NOAA 2020). During this time, there was also a massive drought in CA that

persisted into the end of 2009 (NOAA 2020). These conditions likely led to physiological stress and could have facilitated low bark moisture and heightened susceptibility of *Juglans* spp. to attack in the years leading up to outbreaks of TCD that were detected in these areas in 2010.

The dependence of *G. morbida* on low-moisture wood for competitive success over other wood-inhabiting fungi may also partly explain the severity of TCD in urban and periurban forests and plantations (Seybold et al., 2019). Closed canopies provide a cool, humid microclimate, which may favor natural competitors of *G. morbida* in walnut wood. By comparison, the canopies of trees in plantations are likely to provide a more diminished effect on moisture retention compared to naturally-generating forests. In urban areas humidity would be expected to be even lower because trees are even more widely spaced and heat islands generate higher temperatures (Imhoff et al., 2010). Forest diversity, management activities, buildup of other host-specific biotic disturbance agents, or abundance of opportunistic pathogens (Williams and Ginzel, *in review*) could also partly account for the higher incidence of TCD in plantations and urban forests. Nevertheless, wood moisture content is not the only abiotic factor likely to limit the potential geographic range of *G. morbida* and *P. juglandis* in *J. nigra* (Kolařík et al., 2011, Luna et al., 2013, Sitz et al., 2017, Chen et al., 2020). Within the native range of black walnut, it is also possible that xerophilic and thermotolerant fungi such as Xylariaceae and *Aspergillus* spp. from this study might outcompete *G. morbida* and thereby limit the spread of TCD.

4.4.2 Key Assumptions and Other Factors Influencing TCD Severity

Linking the geographical limitations of the potential range of *G. morbida* in the native range of *J. nigra* to the limited reproduction and dispersal of *P. juglandis* rests on the assumptions that the symbiosis is truly mutualistic. Evidence for a causal link between moisture content and TCD severity would be further strengthened if this mutualism were found to be obligate. Primary symbiotic fungi not only weaken hosts to facilitate mass attack by bark beetles, but also provide nutritional and/or detoxifying functions and/or supplement primary and secondary metabolic processes by producing or providing precursors to bark beetle pheromones and hormones (Six, 2003, 2013). For these reasons, bark beetles typically have greatly decreased fecundity or fail to reproduce without their primary fungal symbiont (Six, 2003). If *G. morbida* provided such benefits to *P. juglandis*, the beetle would be expected to have lower establishment success in areas where

G. morbida is unable to compete with other locally-adapted fungi unless alternative symbionts were available (Six & Bentz, 2007).

Our mapping of expected survival of *G. morbida* across historic and future climatic conditions also rests on the additional key assumption that moisture content of inner bark and outer sapwood fully equilibrate to ambient conditions within the timeframe of the *P. juglandis* lifecycle. Woody tissues lose moisture quickly following successful attacks by bark beetles and other wood-boring insects (Nikolov & Encev, 1967, Pinard & Huffman, 1997, Magnussen & Harrison, 2008, Negi & Joshi, 2009, Lawes et al., 2011). Under constant environmental conditions, EMC of bark also reflects that of the wood (Martin, 1967) across angiosperms and gymnosperms (Reeb & Brown, 2007, Glass & Zelinka, 2010). Compared to other woody tissues, bark is by far the fastest to equilibrate its moisture level to ambient conditions (Negi & Joshi, 2009). Furthermore, humidity is low and vapor pressure deficit is high during spring and summer in the western U.S., and senescent bark tissues are therefore likely to dry faster west of the Great Plains.

4.4.3 Natural History and Implications for Forest Health in a Changing Climate

P. juglandis and *G. morbida* have a co-evolved history in native forest ecosystems of the western and southwestern U.S., where they would be presumed to be coadapted with their ancestral host, *J. major* (Seybold et al., 2012, Hadžiabdić et al., 2014, Zerillo et al., 2014, Rugman-Jones et al., 2015). An ancestral *Juglans* sect. *Rhysocaryon* sp. diverged into *J. major*, *J. nigra*, and other species during a climatologically cooler period 2.6 to 5.3 Ma (Stone et al., 2009, Mu et al., 2020, Song et al., 2020). *J. nigra* would then have radiated across humid eastern North America during interglacial periods. Over the last 10,000 years, *J. major*, *P. juglandis*, and *G. morbida* were restricted to moist canyons and cooler montane regions of the arid Southwestern U.S. and Mexico (Little, 1976) and TCD was likely precluded from the current range of *J. nigra* by a lack of connectivity in host populations as well as an unfavorable moisture regime for the fungus. Across the state of Kansas alone, relative humidity varies twofold from ~40% near the Colorado border in the West to ~80% along the Missouri river, which corresponds to ~7.5 and 15.6% EMC at the thermal optimum for *G. morbida* growth at 30°C (Kolarik et al., 2010, Glass & Zelinka, 2010).

However, in the far western portion of its range, *J. nigra* is a riparian species, much like its western relatives including *J. microcarpa* in TX and OK. This adaptation for riparian areas, along

with the activities of humans who used black walnut for food, fiber, and fuel, likely permitted eastern-western connectivity between *J. nigra*, *J. major* and *J. microcarpa* over the last 10,000 years. Evidence that western populations of *J. nigra* have the greatest resistance to *G. morbida* provides support for interceding periods of genetic connectivity with *J. major* and periodic pressure from TCD in western *J. nigra* (Sitz et al., 2021). Transient periods of connectivity favored by shifting climatic conditions may have facilitated gene flow through hybridization zones and provided a corridor for pest-pathogen complexes such as TCD to reach far-western *J. nigra* populations in the Great Plains.

During the last 200 years, the introduction of evolutionarily naïve (Ploetz et al., 2013) eastern *J. nigra* families to regions where environmental conditions remain favorable to the development of TCD may have led to runaway mortality in urban forests and plantations in the western U.S. (Tisserat et al., 2011, Seybold et al., 2019, Moricca et al., 2020). Moreover, the failure of *P. juglandis* to successfully establish in the native range of *J. nigra*, despite incidental introductions and high host susceptibility, may be due to unfavorable conditions for its symbiont (Utley et al., 2013, Moore et al., 2019).

4.5 Conclusions

The geographical and realized host ranges of destructive, native and non-native forest insects will continue to expand as global temperatures rise and climates shift in future decades (Cullingham et al., 2011, Ramsfield et al., 2016, Pureswaran et al., 2018). Such expansions are strongly determined by the environmental conditions that support the growth and reproduction of beetles and their symbiotic fungi (Six & Bentz, 2007). Based on our findings, these conditions include moisture content and its influence on competition between *G. morbida* and secondary fungi in walnut wood.

J. nigra is among the most valuable hardwood species native to the eastern U.S (Duval et al., 2013), with an estimated value of over USD500 billion in merchantable timber alone (Newton & Fowler, 2009). Our study of fungal competition in walnut wood indicates that TCD presents a risk to the long-term sustainability of *J. nigra* within its native range. In light of these findings, investigations of bark beetle-fungal mutualisms will be critical to build a better understanding of

the joint influence that climate and biotic interactions have on the reproductive success of pathogens and their vectors and forest disease epidemiology.

4.6 References

Abatzoglou, J. T. (2013). Development of gridded surface meteorological data for ecological applications and modelling. *International Journal of Climatology* 33, 121–131. doi:https://doi.org/10.1002/joc.3413.

Biedermann, P. H. W., & Vega, F. E. (2020). Ecology and Evolution of Insect–Fungus Mutualisms. *Annual Review of Entomology* 65, 431–455. doi:10.1146/annurev-ento-011019-024910.

Bright, D. E. (1981). Taxonomic monograph of the genus *Pityophthorus* Eichoff in North and Central Americs (Coleoptera: Scolytidae). *Memoirs of the Entomological Society of Canada* 113, 1–378. doi:10.4039/entm113118fv.

Carbone, I., White, J. B., Miadlikowska, J., Arnold, A. E., Miller, M. A., Magain, N., U.Ren, Jana M., & Lutzoni, F. (2019). T-BAS version 2.1: Tree-Based Alignment Selector toolkit for evolutionary placement of DNA sequences and viewing alignments and specimen metadata on curated and custom trees. *Microbiology Resource Announcements* 8.

Chen, Y., Aukema, B. H., & Seybold, S. J. (2020). The Effects of Weather on the Flight of an Invasive Bark Beetle, *Pityophthorus juglandis. Insects* 11. doi:10.3390/insects11030156.

Cullingham, C. I., Cooke, J. E. K., Dang, S., Davis, C. S., Cooke, B. J., & Coltman, D. W. (2011). Mountain pine beetle host-range expansion threatens the boreal forest. *Molecular Ecology* 20, 2157–2171.

Deshpande, V., Wang, Q., Greenfield, P., Charleston, M., Porras-Alfaro, A., Kuske, C. R., Cole, J. R., Midgley, D. J., and Tran-Dinh, N. (2016). Fungal identification using a Bayesian classifier and the Warcup training set of internal transcribed spacer sequences. *Mycologia* 108. doi:10.3852/14-293.

Duval, R. P., McConnell, T. E., & Hix, D. M. (2013). Annual change in Ohio hardwood stumpage prices, 1960 to 2011. *Forest Products Journal* 64. doi:10.13073/FPJ-D-13-00075.

Eckelman, C. A. (1998). The shrinking and swelling of wood and its effect on furniture. Purdue University Cooperative Extension Service. FNR 163. Available online: https://www.extension.purdue.edu/extmedia/fnr/fnr-163.pdf.

Fierer, N. (2017). Embracing the unknown: Disentangling the complexities of the soil microbiome. *Nature Reviews Microbiology* 15, 579–590. doi:10.1038/nrmicro.2017.87.

Francke-Grosmann, H. (1967). Ectosymbiosis in wood-inhabiting insects. In S. M. Henry (Ed.), *Symbiosis* (pp. 141–205). New York: Academic Press.

Gazis, R., Poplawski, L., Klingeman, W., Boggess, S. L., Trigiano, R. N., Graves, A. D., Seybold, S. J., & Hadžiabdić, Đ.. (2018). Mycobiota associated with insect galleries in walnut with thousand cankers disease reveals a potential natural enemy against *Geosmithia morbida*. *Fungal Biology* 122, 241–253. doi:10.1016/j.funbio.2018.01.005.

Glass, S. V, & Zelinka, S. L. (2010). Moisture relations and physical properties of wood. In *Wood handbook : wood as an engineering material*. General Technical Report 190 (pp. 4.1-4.19). Madison, WI. U. S. Department of Agriculture, Forest Service, Forest Products Laboratory.

Greenspan, L. (1977). Humidity fixed points of binary saturated aqueous solutions. *Journal of Research of the National Bureau of Standards* 81, 89–96.

Griffin, D. M. (1977). Water Potential and Wood-Decay Fungi. *Annual Review of Phytopathology* 15. doi:10.1146/annurev.py.15.090177.001535.

Griffin, G. J. (2015). Status of thousand cankers disease on eastern black walnut in the eastern United States at two locations over 3 years. *Forest Pathology* 45, 203–214. doi:10.1111/efp.12154.

Hadžiabdić, Đ.., Vito, L. M., Windham, M. T., Pscheidt, J. W., Trigiano, R. N., & Kolarik, M. (2014). Genetic differentiation and spatial structure of *Geosmithia morbida*, the causal agent of thousand cankers disease in black walnut (*Juglans nigra*). *Current Genetics* 60. doi:10.1007/s00294-013-0414-x.

Harris, R. F. (1981). Effect of water potential on microbial growth and activity. In J. F. Parr, W. R. Gardner & L. F. Elliot (Eds.), *Water Potential Relations Soil Microbiology* Vol. 9 (pp. 23–95). Soil Science Society of America. doi: 10.2136/sssaspecpub9.

Hofstetter, R. W., Dempsey, T., Klepzig, K., & Ayres, M. (2007). Temperature-dependent effects on mutualistic, antagonistic, and commensalistic interactions among insects, fungi and mites. *Community Ecology* 8, 47–56. doi:10.1556/comec.8.2007.1.7.

Hofstetter, R. W., Dinkins-Bookwalter, J., Davis, T. S., & Klepzig, K. D. (2015). Symbiotic associations of bark beetles. In F. Vega and R. Hofstetter (Eds.), *Bark Beetles: Biology and Ecology of Native and Invasive Species* (pp 209–245). Academic Press.

Imhoff, M. L., Zhang, P., Wolfe, R. E., & Bounoua, L. (2010). Remote sensing of the urban heat island effect across biomes in the continental USA. *Remote Sensing of the Environment* 114, 504–513.

Jacobi, W. R., Hardin, J. G., Goodrich, B. A., & Cleaver, C. M. (2012). Retail firewood can transport live tree pests. *Journal of Economic Entomology* 105, 1645–1658.

Juzwik, J., Moore, M., Williams, G., & Ginzel, M. (2020). Assessment and etiology of thousand cankers disease within the native range of black walnut (Juglans nigra). In K. M. Potter & B. L. Conkling (Eds.), *Forest health monitoring: national status, trends, and analysis 2019. Gen. Tech. Rep. SRS-250.* (Vol. 2020, pp. 169–178). Asheville, NC: US Department of Agriculture, Forest Service, Southern Research Station.

Kolařík, M., Freeland, E., Utley, C., & Tisserat, N. (2011). *Geosmithia morbida* sp. nov., a new phytopathogenic species living in symbiosis with the walnut twig beetle (*Pityophthorus juglandis*) on *Juglans* in USA. *Mycologia* 103. doi:10.3852/10-124.

Lawes, M. J., Richards, A., Dathe, J., & Midgley, J. J. (2011). Bark thickness determines fire resistance of selected tree species from fire-prone tropical savanna in north Australia. *Plant Ecology* doi:10.1007/s11258-011-9954-7.

Little, E. L. (1976). Atlas of United States trees. Volume 3. Minor western hardwoods. Washington, DC: U.S. Department of Agriculture, Forest Service.

Luna, E. K., Sitz, R. A., Cranshaw, W. S., & Tisserat, N. A. (2013). The effect of temperature on survival of *Pityophthorus juglandis* (Coleoptera: Curculionidae). *Environmental Entomology*. 42, 1085–1091.

Magnussen, S., & Harrison, D. (2008). Temporal change in wood quality attributes in standing dead beetle-killed lodgepole pine. *Forestry Chronicle.* doi:10.5558/tfc84392-3.

Manzoni, S., Schimel, J. P., & Porporato, A. (2012). Responses of soil microbial communities to water stress: Results from a meta-analysis. *Ecology* 93. doi:10.1890/11-0026.1.

Martin, R. E. (1967). Interim equilibrium moisture content values of bark. *Forest Products Journal* 17, 30–31.

Sitz, R. A., Luna, E., Ibarra Caballero, J., Tisserat, N., Cranshaw, Whitney S., McKenna, J. R., Stoltz, J., & Stewart, J (2021). Eastern black walnut (*Juglans nigra* L.) originating from native range varies in their response to inoculation with *Geosmithia morbida*. *Frontiers in Forests and Global Change* 4:12. doi.org/10.3389/ffgc.2021.627911.

Miller, M. A., Schwartz, T., Pickett, B. E., He, S., Klem, E. B., Scheuermann, R. H., Passarotti, M., Kaufman, S., & O'Leary, M. A. (2015). A RESTful API for Access to Phylogenetic Tools via the CIPRES Science Gateway. *Evolutionary Bioinformatics Online* 11, 43–48. doi:10.4137/EBO.S21501.

Mitton, J. B., & Ferrenberg, S. M. (2012). Mountain pine beetle develops an unprecedented summer generation in response to climate warming. *American Naturalist* 179.

Moore, G. E. (1971). Mortality factors caused by pathogenic bacteria and fungi of the southern pine beetle in North Carolina. *Journal of Invertebrate Pathology* 17, 28–37.

Moore, G. E. (1973). Pathogenicity of three entomogenous fungi to the southern pine beetle at various temperatures and humidities. *Environmental Entomology* 2, 54–57.

Moore, M., Juzwik, J., Miller, F., Roberts, L., & Ginzel, M. D. (2019). Detection of *Geosmithia morbida* on Numerous Insect Species in Four Eastern States. *Plant Health Progress* 20, 133–139. doi:10.1094/php-02-19-0016-rs.

Moricca, S., Bracalini, M., Benigno, A., Ghelardini, L., Furtado, E. L., Marino, C. L., & Panzavolta, T. (2020). Observations on the non-native thousand cankers disease of walnut in Europe's southernmost outbreak. *Global Ecology and Conservation* 23, e01159. doi:https://doi.org/10.1016/j.gecco.2020.e01159.

Mu, X.-Y., Tong, L., Sun, M., Zhu, Y.-X., Wen, J., Lin, Q.-W., & Liu, B. (2020). Phylogeny and divergence time estimation of the walnut family (Juglandaceae) based on nuclear RAD-Seq and chloroplast genome data. *Molecular Phylogenetics and Evolution* 147, 106802. doi:https://doi.org/10.1016/j.ympev.2020.106802.

National Oceanic and Atmospheric Administration (NOAA) (2020). Historical Palmer Drought Indices. Available at: https://www.ncdc.noaa.gov/temp-and-precip/drought/historical-palmers/ [Accessed February 11, 2020].

Negi, S., & Joshi, V. D. (2009). Role of moisture content in rendering the sal tree component susceptible to the borer (*Hoplocerambyx spinicornis*) attack. *Asian Journal of Animal Science* 3, 190–192.

Newcombe, G. (2011). Endophytes in forest management: four challenges. In A. M. Pirttilä, A. C. Frank (Eds.), *Endophytes of Forest Trees* (pp. 251–262). Springer.

Newton, L., & Fowler, G. (2009). Pathway Assessment: *Geosmithia* sp. and *Pityophthorus juglandis* Blackman movement from the western into the eastern United States. In K. A. McManus, K. W. Gottschalk (Eds.), *Proceedings of the 21st U.S. Department of Agriculture interagency research forum on invasive species. January 12-15, Annapolis, MD. General Technical Report NRS-P-75.* U. S. Department of Agriculture, Forest Service, Northern Research Station 112. Available online https://www.uaex.edu/environment-nature/ar-invasives/invasive-diseases/docs/Thousand-Cankers Disease.pdf.

Nikolov, S., & Encev, E. (1967). *Moisture content of green wood*. Sofia, Bulgaria: Zemizdat.

Nuotclà, J. A., Biedermann, P. H. W., & Taborsky, M. (2019). Pathogen defence is a potential driver of social evolution in ambrosia beetles. *Proceedings of the Royal Society B.* 286, 20192332.

Onufrak, A. J., Williams, G. M., Klingeman, W. E., Cregger, M. A., Klingeman, D. M., DeBruyn, J. M., DeBruyn, J. M., Ginzel, M. D., & Hadžiabdić, Đ.. (2020). Regional Differences in the Structure of *Juglans nigra* Phytobiome Reflect Geographical Differences in Thousand Cankers Disease Severity. *Phytobiomes Journal* 4, 388–404. doi:10.1094/PBIOMES-05-20-0044-R.

Palmer, W. C. (1965). Meteorologic drought. U.S. Weather Bureau Research Paper No. 45.

Pinard, M. A., & Huffman, J. (1997). Fire resistance and bark properties of trees in a seasonally dry forest in eastern Bolivia. *Journal of Tropical Ecology* doi:10.1017/S0266467400010890.

Ploetz, R. C., Hulcr, J., Wingfield, M. J., and de Beer, Z. W. (2013). Destructive Tree Diseases Associated with Ambrosia and Bark Beetles: Black Swan Events in Tree Pathology? *Plant Disease* 97, 856–872. doi:10.1094/PDIS-01-13-0056-FE.

Pureswaran, D. S., Roques, A., & Battisti, A. (2018). Forest insects and climate change. *Current Forestry Reports* 4, 35–50.

R Core Team (2019). R: A Language and Environment for Statistical Computing. Available at: https://www.r-project.org/.

Ramsfield, T. D., Bentz, B. J., Faccoli, M., Jactel, H., & Brockerhoff, E. G. (2016). Forest health in a changing world: effects of globalization and climate change on forest insect and pathogen impacts. *Forestry: An International Journal of Forestry Research* 89, 245–252. doi:10.1093/forestry/cpw018.

Ranger, C. M., Biedermann, P. H. W., Phuntumart, V., Beligala, G. U., Ghosh, S., Palmquist, D. E., et al., (2018). Symbiont selection via alcohol benefits fungus farming by ambrosia beetles. *PNAS* 115, 201716852. doi:10.1073/pnas.1716852115.

Rayner, A. D. M., & Boddy, L. (1988). *Fungal Decomposition of Wood: Its Biology and Ecology*. Wiley and Sons doi:10.1086/416403.

Reeb, J., & Brown, T. (2007). Air- and Shed-drying Lumber. Oregon State University Extension EM 8612-E. Available at: https://catalog.extension.oregonstate.edu/sites/catalog/files/project/pdf/em8612.pdf.

Ridout, M., Houbraken, J., & Newcombe, G. (2017). Xerotolerance of *Penicillium* and *Phialocephala* fungi, dominant taxa of fine lateral roots of woody plants in the intermountain Pacific Northwest, USA. *Rhizosphere* 4, 94–103. doi:https://doi.org/10.1016/j.rhisph.2017.09.004.

Rugman-Jones, P. F., Seybold, S. J., Graves, A. D., & Stouthamer, R. (2015). Phylogeography of the walnut twig beetle, *Pityophthorus juglandis*, the vector of thousand cankers disease in North American walnut trees. *PLoS One* 10. doi:10.1371/journal.pone.0118264.

Seybold, S. J., Coleman, T. W., Dallara, P. L., Dart, N. L., Graves, A. D., Pederson, L. A., & Spichiger, S. (2012). Recent collecting reveals new state records and geographic extremes in the distribution of the walnut twig beetle, *Pityophthorus juglandis* Blackman (Coleoptera: Scolytidae), in the United States. *Pan-Pacific Entomologist* 88. doi:10.3956/2012-32.1.

Seybold, S. J., Klingeman III, W. E., Hishinuma, S. M., Coleman, T. W., & Graves, A. D. (2019). Status and Impact of Walnut Twig Beetle in Urban Forest, Orchard, and Native Forest Ecosystems. *Journal of Forestry* 117, 152–163. doi:10.1093/jofore/fvy081.

Seybold, S. J., Penrose, R. L., & Graves, A. D. (2016). Invasive bark and ambrosia beetles in California Mediterranean forest ecosystems. In T. D. Paine and F. Lieutier (Eds.), *Insects and Diseases of Mediterranean Forest Systems* (pp, 583–662). Springer.

Simpson, W. T. (1973). Predicting equilibrium moisture content of wood by mathematical models. *Wood Fiber Science*. 5, 41–49.

Simpson, W. T. (1998). Equilibrium moisture content of wood in outdoor locations in the United States and worldwide. Forest Products Laboratory Research Note FPL-RN-0268. U. S. Deptartment of Agriculture, Forest Service, Forest Products Research Laboratory.

Sing, T., Sander, O., Beerenwinkel, N., & Lengauer, T. (2005). ROCR: visualizing classifier performance in R. Bioinformatics 21, 7881. Available at: http://rocr.bioinf.mpi-sb.mpg.de.

Sitz, R., Utley, C., Hall, A., Tisserat, N., & Cranshaw, W. (2017). Trapping the Walnut Twig Beetle to Determine Flight Patterns in Colorado. *Southwest Entomologist* 42, 347–356.

Six, D. L. (2003). Bark beetle-fungus symbioses. *Insect symbiosis* 1, 97–114.

Six, D. L. (2013). The Bark Beetle Holobiont: Why Microbes Matter. *Journal of Chemical Ecology* 39. doi:10.1007/s10886-013-0318-8.

Six, D. L., & Bentz, B. J. (2007). Temperature Determines Symbiont Abundance in a Multipartite Bark Beetle-fungus Ectosymbiosis. *Microbial Ecology* 54, 112–118. doi:10.1007/s00248-006-9178-x.

Song, Y.-G., Fragnière, Y., Meng, H.-H., Li, Y., Bétrisey, S., Corrales, A., Manchester, S., Deng, M., Jasińska, A. K., Văn Sâm, H., & Kozlowski, G. (2020). Global biogeographic synthesis and priority conservation regions of the relict tree family Juglandaceae. *Journal of Biogeography* 47, 643–657.

Stepanek, L. (2020). Walnut Twig Beetle & Thousand Cankers Disease. Lincoln, NE. https://nfs.unl.edu/publications/walnut-twig-beetle-nebraska. [Accessed June 13, 2021].

Stone, D. E., Oh, S.-H., Tripp, E. A., & Manos, P. S. (2009). Natural history, distribution, phylogenetic relationships, and conservation of Central American black walnuts (*Juglans* sect. *Rhysocaryon*). *Journal of the Torrey Botanical Society* 136, 1–25.

Tisserat, N., Cranshaw, W., Leatherman, D., Utley, C., & Alexander, K. (2009). Black walnut mortality in Colorado caused by the walnut twig beetle and thousand cankers disease. *Plant Health Progress* 11, 10. doi:10.1094/php-2009-0811-01-rs.

Tisserat, N., Cranshaw, W., Putnam, M. L., Pscheidt, J., Leslie, C. A., Murray, M., Hoffman, J., Barkley, Y., Alexander, K., & Seybold, S. J. (2011). Thousand Cankers Disease is Widespread in Black Walnut in the Western United States. *Plant Health Progress* 12, 35. doi:10.1094/PHP-2011-0630-01-BR.

USGCRP (2018). Impacts, Risks, and Adaptation in the United States: Fourth National Climate Assessment, Volume II. Eds. D. R. Reidmiller, C. W. Avery, D. R. Easterling, K. E. Kunkel, K. L. M. Lewis, T. K. Maycock, and B. C. Stewart. Washington, DC, USA doi:10.7930/NCA4.2018.

Utley, C., Nguyen, T., Roubtsova, T., Coggeshall, M., Ford, T. M., Grauke, L. J., Graves, A D., Leslie, C. A., McKenna, J., Woeste, K., Yaghmour, M A., Cranshaw, W., Seybold, S. J., Bostock, R. M., & Tisserat, M. (2013). Susceptibility of Walnut and Hickory Species to *Geosmithia morbida*. *Plant Disease* 97, 601–607. doi:10.1094/PDIS-07-12-0636-RE.

Weed, A. S., Ayres, M. P., & Bentz, B. J. (2015). Population Dynamics of Bark Beetles. In F. Vega and R. Hofstetter (Eds.), *Bark Beetles: Biology and Ecology of Native and Invasive Species* Academic Press. doi:10.1016/B978-0-12-417156-5.00004-6.

Whitaker, B. K., & Bakker, M. G. (2019). Bacterial endophyte antagonism toward a fungal pathogen in vitro does not predict protection in live plant tissue. *FEMS Microbial Ecology* 95, fiy237.

Williams, G. M., & Newcombe, G. (2017). Xerotolerance of *Geosmithia morbida*. In *Proceedings of the 2016 Society of American Foresters National Convention* (Madison, WI). doi:10.5849/jof.2016-108.

Wood, S. L. (1982). The bark and ambrosia beetles of North and Central America (Coleoptera: Scolytidae), a taxonomic monograph. *Great Basin Naturalist Memoirs* 6.

Zerillo, M. M., Ibarra Caballero, J., Woeste, K., Graves, A. D., Hartel, C., Pscheidt, J. W., Tonos, J., Broders, K., Cranshaw, W., Seybold, S. J., & Tisserat, N. (2014). Population structure of *Geosmithia morbida*, the causal agent of thousand cankers disease of walnut trees in the United States. *PLoS ONE* 9:e112847.

CHAPTER 5. FUNCTIONAL ROLES OF NEMATODES ASSOCIATED WITH *PITYOPHTHORUS JUGLANDIS* NLACKMAN (COLEOPTERA: CURCULIONIDAE) AND *JUGLANS NIGRA* L. (FAGALES: JUGLANDACEAE) IN THE INLAND NORTHWEST, U.S.A.

5.1 Introduction

Thousand cankers disease (TCD) is an emergent threat to the health and productivity of eastern black walnut (*Juglans nigra* L.), a high-value hardwood species, and other *Juglans* and *Pterocarya* spp., including the agriculturally important Persian walnut (*J. regia* L.) (Newton & Fowler, 2009, Utley et al., 2013). When the walnut twig beetle (WTB, *Pityophthorus juglandis* Blackman) successfully attacks and colonizes a susceptible host, it introduces the fungal pathogen *Geosmithia morbida* Kol. Free. Ut. & Tiss. (Hypocreales) into the inner bark, which in turn causes necrosis in the phloem (Tisserat et al., 2009). Mass attack by *P. juglandis* and subsequent infection by *G. morbida* cause numerous necrotic lesions in the phloem and outer sapwood of branches and the tree trunk (Tisserat et al., 2009).

Symptoms of TCD are highly variable across its range. In original observations in Colorado, TCD symptoms progressed from flagging to early senescence of leaves on branches, dieback and thinning of the crown, epicormic sprouting, and mortality within three years (Tisserat et al., 2009, 2011). As TCD spread across North America, others subsequently noted persistent morbidity including quiescent dormancy of parts of the crown that can last longer and even give way to recovery of previously symptomatic trees (Griffin, 2015, Juzwik et al., 2020, Seybold et al., 2019). Mortality was conventionally attributed to the coalescence of cankers (Tisserat et al., 2009), but this is not always observed *in situ* (Montecchio et al., 2015). To date, a causal relationship has not been experimentally demonstrated between *P. juglandis* feeding, associated phloem necrosis caused by *G. morbida*, and the classic symptoms of flagging, senescence, and rapid mortality of mature trees. However, it has been suggested that other agents including secondary fungal pathogens may play a role in disease progression during the more advanced stages of decline (Juzwik et al., 2020, Kasson et al., 2014; Lauritzen, 2018, Onufrak et al., 2020, Tisserat et al., 2009, Chapter 3). Thus, a unified understanding of the pathology and etiology of this disease is critically incomplete.

In addition to primary and secondary fungi, the bark beetle holobiont and host tree phytobiomes together comprise a diverse, multitrophic community of microbes and microinvertebrates (Hofstetter et al., 2015; Six, 2013). In particular, the holobiont includes nematodes that interact with fungi, bacteria, beetles, and host plants. This suite of interactions could impact the etiology of decline diseases attributed to beetle-fungal associations (Hofstetter et al., 2015, Hofstetter & Moser, 2014, Klepzig et al., 2001; Six, 2013). In some Coleoptera-associated plant diseases, such as Dutch elm disease (DED) and southern pine beetle (*Dendroctonus frontalis*) outbreaks, mites are important vectors for plant pathogenic fungi but can also interfere with insect-fungal mutualisms (Hofstetter et al., 2007, Hofstetter & Moser, 2014, Moser et al., 2010). In others, such as pine wilt disease, multiple partners including fungi, nematodes, and bacteria all contribute to decline (L. Zhao et al., 2014). Such cross-kingdom consortia, including *Geosmithia* and *Ophiostoma* spp. have even shared pathogenicity genes with one another via lateral gene transfer, providing strong evidence of tight, multi-partner associations (Bettini et al., 2014, Lamichhane & Venturi, 2015, Pepori et al., 2018, L. Zhao et al., 2014).

Recently, Ryss et al., (2020) described a new nematode species, *Bursaphelenchus juglandis* associated with *J. regia*, *J. hindsii* and their hybrids, *J. major*, and *P. juglandis* in California, Arizona, and New Mexico, USA. The genus *Bursaphelenchus* (Aphelenchoididae) contains many *ectophoretic* (*i.e.*, travelling outside the body, especially under elytra) and *endophoretic* nematodes that are associates of Scolytines and wood-boring Cerambycids (Kanzaki, 2008), including two of the most virulent and economically important nematode phytopathogens of both managed and unmanaged forest systems worldwide (Kanzaki & Giblin-Davis, 2018). *Bursaphelenchus* spp. are also found in association with numerous beetle-fungal disease complexes in hardwoods, including DED (Ryss et al., 2015, Tomalak & Filipiak, 2018), sudden aspen decline (SAD; Tomalak et al., 2013), and beetle-attacked *Fagus* (Tomalak & Filipiak, 2014, Tomalak et al., 2017) and *Tilia* spp. (Tomalak & Malewski, 2014), but their significance in the etiology of associated diseases has not been well-characterized.

More information on the full range of potential interactions between nematodes, scolytine vectors, fungi, and host trees could be important for understanding emergent plant diseases. Either as pathogens of host trees, parasites of vectors, or consumers of fungi, nematodes may play a role in the etiology of bark beetle-fungal diseases. Nearly all Scolytinae spp. investigated in North America are vectors of phoretic nematodes and/or have intimate associations with endoparasitic

nematodes (Massey, 1974). When bark and ambrosia beetles emerge in search of a host, juvenile nematodes called *dauerlarvae* travel in a quiescent state on the inside or outside of beetles and disperse to new trees where they reproduce. In response to beetle hormones, their progeny disperse and aggregate in synchrony with stages of the lifecycles of host or vector beetles (Massey, 1974, L. Zhao et al., 2014, 2007). Many phoretic species can be cultured on the primary mutualistic fungi of their scolytine vectors (Cardoza et al., 2006, Carta et al., 2010), raising the possibility that they could alter fungal-fungal and beetle-fungal relationships and disease etiology through feeding activity and/or feeding preferences (e.g., Baynes et al., 2012), as has been found for phoretic mites (Cardoza et al., 2008, Carta et al., 2010; Fukushige, 1991, Klepzig et al., 2001, Tomalak & Filipiak, 2011). Some phoretic nematodes, including *Bursaphelenchus* spp., stimulate the formation of specialized structures called *nematangia* on wings or elytra of over-wintering adult beetles (Cardoza et al., 2006, Čermák et al., 2012, Kanzaki et al., 2008, Penas et al., 2006, Shimizu et al., 2013).

Free-living nematodes, including those in the genera *Panagrolaimus*, are common in the bark of trees. Like the phoretic nematodes, many free-living nematodes are also fungal feeders. Primarily free-living nematodes are frequently found in association with fungal and bacterial cankers, butt and root rot diseases of hardwood trees, as well as healthy and diseased leaves and bark (Carta et al., 2016, Ewing et al., 2019, Self & Bernard, 1994, Tomalak & Filipiak, 2011; Tomalak, Worrall, & Filipiak, 2013, Tóth et al., 2013). Feeding by these mycophagous nematodes could potentially suppress fungal plant diseases (*e.g.*, García De la Cruz et al., 2018). In forests, the free-living and phoretic species *Aphelenchoides hylurgi* can carry hypovirulent *Cryphonectria parasitica*, a potential biological control of virulent *C. parasitica*, the cause of chestnut blight, and they have also been speculated to play a role in assisting dispersal of the hypovirulent fungus within the tree (Griffin et al., 2009). Some species of free-living nematodes are capable of *anhydrobiosis* (Aroian et al., 1993; Shannon, 2005)—the ability to persist for long periods in a dehydrated form between ephemeral episodes of rehydration. A survey of cortical nematode communities of *J. nigra* in West Virginia found that the community of free-living nematodes was vertically stratified between lower, middle, and upper portions of the stem and canopy (Eisenback & Paes-Takahashi, 2015).

In addition to phoretic and free-living species, endoparasitic nematodes are hypothesized to play a role in preventing outbreaks of bark beetles (Furniss, 1967; Massey, 1966, McCambridge

& Knight, 1972; Thorne, 1935, Tomalak et al., 1989). These endoparasitic nematodes can occupy the haemocoel and internal organs of larvae and adult beetles and cause moderate reductions in fat body content, gonad mass, and fecundity or complete castration (Lieutier, 1982, Macguidwin et al., 1980; Oldham, 1930; Reid, 1958, Thong & Webster, 1975b, Tomalak et al., 1988). Significant reduction in reproductive capacity caused by nematode endoparasitism is evident from severe reductions in the size, length, and number of scolytine larval galleries (e.g., Massey, 1974, Thong & Webster, 1975a). However, despite their ubiquity and a diversity of potential functional roles, the full ecological significance of nematodes in the lifecycles of economically important bark and ambrosia beetle species and their associated fungi and diseases remains largely unexplored.

Between 2015-2019 we conducted a preliminary investigation of the functional roles of nematodes associated with *P. juglandis* and *J. nigra* in the inland northwest, USA where TCD exerts a severe and persistent impact on the health of planted and naturalized populations of *J. nigra*. In the present study, we addressed a need for information on incidence and distribution of nematodes within and between stands as well as their potential to interact with disease etiology. Our specific objectives were: 1) to employ single- and multilocus sequence typing (Enright & Spratt, 1999) to gather baseline data on the diversity, abundance, distribution, and taxonomic placement of nematodes associated with *J. nigra* and *P. juglandis* and generate barcodes for their future identification; 2) to elucidate nematode-fungal interactions in culture; and 3) to characterize the effects of inoculating trees and seedlings with *Bursaphelenchus* and *Panagrolaimus* spp. on the amount of necrotic area caused by *G. morbida* in *J. nigra* and easily observable foliar symptoms. We hypothesized that: *P. juglandis* would harbor endoparasites and phoretic associates whose abundance would increase with host density; that *B. juglandis* is an opportunistic pathogen and contributes to foliar symptoms; that *Panagrolaimus* spp. could function as disease antagonists; and that nematode communities in *J. nigra* trees in the western U.S. would differ from those previously observed in the eastern U.S.

5.2 Methods

5.2.1 Determining the Identity, Distribution, and Culturability of Nematodes

Sample Collection and Nematode Cultures

Collections of free-living nematodes were obtained from a single individual of *J. nigra* near the University of Idaho Arboretum and Botanical Garden in Moscow, ID in 2015, 2016 and 2017 (46°43'21.1"N, 117°00'49.5"W) and from multiple trees from walnut plantations in Walla Walla, WA in 2017 and 2019 (46°02'41.9"N, 118°14'01.0"W). To isolate free-living nematodes, ~1.9-cm cross sections were cut from branches, placed in moist incubation chambers, and inspected for nematode activity on a weekly basis for up to 100 days. Typically, nematode activity began within the first 10 to 20 days of the incubation period. When nematodes were observed, approximately 10-20 adults were transferred using an ethanol-rinsed human eyelash to 10- to 20-day old cultures of *G. morbida* isolate Gm-A (GenBank Accession No. MZ425965; from TCD-symptomatic trees with active *P. juglandis* populations in Asotin, WA; 2015 and 2016) or RN2 (from Walla Walla, WA; *coll*. D. Hadizabdic; all other years) growing on 1/4-strength potato dextrose agar (9.75 g PDA powder + 11.25 g agar per L H_2O). All incubations of wood and cultures occurred at room temperature (~23°C).

Phoretic and parasitic nematodes were isolated from *P. juglandis* in the State of Washington in 2017 and 2019. Sections of a single branch, ranging in length from 20- to 24-cm and from 4 to 7.5 cm in diameter were collected from TCD-symptomatic trees, sealed with paraffin wax, and placed inside of emergence chambers made from sealed ventilated transparent plastic boxes (Anderbrant, 1990) or opaque buckets (Mayfield et al., 2014). Emergence chambers were checked semiweekly for 100 days, and any live *P. juglandis* that emerged from the branches were inspected for nematodes under a stereomicroscope. Elytra were removed from the beetle and those that contained daurlarvae (Cardoza et al., 2006, Čermák et al., 2012, Kanzaki et al., 2008, Ryss et al., 2020) were transferred to 20- or 30-day old cultures of *G. morbida* isolate RN2. *P. juglandis* were then dissected by pulling apart the abdomen. Nematode eggs, larvae, or juveniles from each dissected beetle were counted under a stereomicroscope. All incubations of cultures and branch material occurred at room temperature.

To collect data on spatial and seasonal variation in abundance of parasitic, phoretic, and free-living nematodes from *P. juglandis* and *J. nigra*, branches were collected over the course of twelve months along a 150-km stretch of U.S. Hwy 12 from Walla Walla, WA to Lewiston, ID, including multiple locations in Walla Walla, Dayton and Pomeroy, WA. Branches were collected from a total of 26 trees in September 2018 (n = 2), and May (n = 10), June (n = 6), and August (n = 8) of 2019 Five sections were collected from one to two branches from each tree as above. *P.*

juglandis were emerged in ventilated transparent plastic boxes and screened for nematodes as described above. Nematodes were also isolated from moist-incubated branch cross-sections as described above.

In prior work, phoretic and free-living nematodes found on *P. juglandis* and in *J. nigra* bark could be grown on cultures of *G. morbida*, but not on sterile growth media (G. M. Williams, *pers. obs.*). Simple laboratory assays were conducted to obtain approximate data on nematode reproduction on different fungal food sources, as well as the survival of different fungi after nematode feeding and reproduction. A 4-cm^2 piece of agar was transferred from cultures of *G. morbida* containing ~30 nematodes cm^{-2} (*Panagrolaimus* or *Bursaphelenchus* sp.) to five plates of either sterile 1/4-strength PDA, 20-day old cultures on 1/4-strength PDA of *Gibberella fujikuroi* species complex sp. isolate GW-4 (GenBank Accession No. MZ425964), *Epicoccum nigrum* isolate GW-2 (GenBank Accession No. MZ425962) or *Trichoderma* sp. isolate GW-1 (GenBank Accession No. MZ425961) from branches of *J. nigra* in ID and WA (*P. multidentatus* only), or *E. nigrum* isolate TCK 82 (*coll*. T. Kijpornyongpan) from *Solidago* sp. in IN (*Panagrolaimus* sp.). After 20 days, plates were observed and checked for the reproduction of nematodes and the growth of fungi and bacteria. If nematodes were observed, they were counted and transferred again to a new 20-day old culture of the same fungal species, and the entire process was repeated. The fungus was considered an adequate food source if nematodes continued to reproduce on at least some plates through more than two successive transfers to fresh fungal cultures. The fungi from cultures with nematodes were considered viable if they could grow from agar from the mixed cultures with nematodes when transferred to 1/4-strength PDA.

Molecular-Based Identification of Nematodes

We developed a barcoding approach to identify nematodes associated with *J. nigra* and *P. juglandis*. Following techniques in community ecology for fungi and bacteria (Carbone et al., 2017, Schloss et al., 2009, U'Ren et al., 2009, Zalamea et al., 2021), we used 1) a clustering approach to distinguish operational nematode taxa and 2) phylogenetic approach to place the operational taxa into accepted nematode generic concepts and to infer relationships with other species from publicly-available sequence data. In 2015, 2017, and 2018, vouchers from representative nematode variants were imaged using light microscopy for high-level taxonomic

determination (family or order) with the help of available references (Mai et al., 1996; Massey, 1974, Ryss et al., 2015, M Tomalak et al., 1989; http://nemaplex.ucdavis.edu), including the key character of buccal denticles prior to DNA extraction and PCR. In some cases, nematodes were identified to genus or species with the help of experts (USDA-ARS Mycology and Nematology Laboratory, Beltsville, MD).

To extract DNA, individual nematodes were picked into lysis buffer (Williams, 1992) from cultures, dissected *P. juglandis* or moist-incubated *J. nigra* branch cross-sections. Partial small subunit (18S SSU primers 965 and 1537), large subunit (28S LSU primers D2A and D3B), and a short segment of internal transcribed spacer (ITS primer F194 and specific primer ITS-jugR2) rDNA and cytochrome *c* oxidase subunit I-alpha (COI-α M13 primer cocktail) mtDNA regions were amplified (Kanzaki et al., 2012, Prosser et al., 2013, Ryss et al., 2020). 25-uL PCR reactions contained: 18S, 0.05-0.5 ng template, 1.5 mM $MgCl_2$, 0.25 uM each forward and reverse primer, 0.2 mM each dNTP, 0.1 uL PlatinumTaq DNA Polymerase, 20 mM Tris-Cl, and 50 mM KCl; 28S and ITS, 0.1-1 ng template, 5 uL Q solution, 0.6 uM each primer and dNTP, 0.1 uL Taq DNA Polymerase (Qiagen Core Kit), 1X PCR Buffer (Qiagen Core Kit); COI-α, 0.5-5 ng template, 1.5 mM $MgCl_2$, 0.2 uM each primer and dNTP, 0.1 uL PlatinumTaq DNA Polymerase, 20 mM Tris-Cl, and 50 mM KCl. For 18S thermocycle profile was hot start at 94ºC (1 min); 45 cycles 94ºC (30 sec), 53ºC (30 sec), and 0.5 ºC /sec ramp from 53 ºC to 72 ºC (1 min); and final extension at 72ºC (4 min). For 28S touchdown thermocycle profile was hot start at 94ºC (4 min); 15 cycles 94ºC (1 min), 1ºC decrease/cycle from 65 ºC to 55ºC (1.5 min), 72ºC (2 min); 30 cycles 94ºC (1 min), 57ºC (1.5 min), 72ºC (2 min); and final 72ºC (10 min). For ITS touchdown thermocycle profile was hot start at 94ºC (4 min); 10 cycles 94ºC (1 min), 1ºC decrease/cycle from 69 ºC to 59ºC (45 sec), 72ºC (45 sec); 30 cycles 94ºC (1 min), 59ºC (45 sec), 72ºC (45 sec); and final 72ºC (10 min). For COI thermocycle profile was hot start at 94ºC (1 min); 40 cycles of 94ºC (40 sec), 55ºC (1 min), 72ºC (1 min); final extension at 72ºC (10 min). BigDye reactions and sequencing were performed with the same primers (18S, 28S, and ITS) or original Messing (1993) COI-α primers M13F and M13R on an ABI 3730XL sequencing machine (ThermoFisher Scientific) at the Genomics Core Facility, College of Agriculture, Purdue University, West Lafayette, IN and GeneWiz Co. (Cambridge, MA). Base-calling, and assembly of forward and reverse reads, sequence trimming and editing and MUSCLE alignment were performed in Mesquite with the package Chromaseq v. 1.31 (Maddison & Maddison, 2018).

To identify putative *B. juglandis* in this study in addition to the specific ITS preimer reaction a ~1.2kb overlapping region between a previously published long rDNA sequence (>3.7kb SSU-ITS-LSU; MK292121) obtained from *Bursaphelenchus* sp. isolate WA112717-7 from this study (Carta & Li, 2019) were aligned to Ryss et al.'s (2020) SSU-ITS-LSU rDNA sequence (MN759734) from *B. juglandis* using BLAST (Altschul, 1990). All sequences obtained in this study were submitted to GenBank (National Center for Biotechnology Information) under accession numbers MZ423521-MZ423525, MZ425177-MZ425201, MZ425249-MZ425303, and MZ425426- MZ425435.

To delimit operational taxonomic units, we computed and visualized a UPGMA tree in R from total pairwise nucleotide distances computed in MEGA-X (Kumar et al., 2018) from the short 18S and COI-α primers obtained over the course of the study. Operational taxonomic units were delimited at 97 and 99% sequence similarity by superimposing cutoffs on the UPGMA tree. To place nematodes taxonomically, phylogenetic trees were built with 18S, 28S, and COI-α sequences from representative samples from our study along with publicly available sequences from GenBank. Based on NCBI-BLAST results, nematodes recovered in this study represented the superfamilies Diplogasteroidea, Panagrolaimoidea, and Aphelenchoidea, but only the Aphelenchoidea were represented adequately in the database for COI-α markers, and we did not obtain 28S sequences from isolates of *Rhabditolaimus* (Panagrolaimoidea) or *Ditylenchus* (Diplogasteroidea). Therefore, three separate phylogenies were built: Aphelenchoididae analyzed with 18S, 28S, and COI-α in a partitioned dataset; *Panagrolaimus* sp. with 18S and 28S along with publicly available sequences from all three superfamilies in a partitioned dataset; and Panagrolaimoidea and Diplogasteroidea from our study and publicly available sequences with 18S only. Outgroups were *Litylenchus crenatae* for Aphelenchoididae and *Steinernema carpocapsae* for the rest of Rhabditida. Bayesian trees were computed in MrBayes v. 3.2.6 (Ronquist & Huelsenbeck, 2003) with four independent chains of 10^7 generations diagnosed every 10^3 generations with a burn in of the first 25% of each generation and separate GTR+I+G model parameters and rates of evolution among partitions. Maximum likelihood trees were computed with the same partitioned model scheme in RAxML (Stamatakis, 2014) and support values were calculated from 10^4 bootstrap replicates.

5.2.2 Effects of Nematodes on Necrotic Area of Cankers

2016 Inoculations of Trees with Panagrolaimus multidentatus

G. morbida and nematodes were co-inoculated in mature *J. nigra* trees in ID to determine the effect of *Panagrolaimus* sp. from ID on the total area of phloem necrosis caused by *G. morbida* (Table 5.1). Inoculations were performed in June 2016 at a germplasm plantation that is part of the Cyril Reed Funk Research Farm (Dayton, ID) that included a variety of interspecific hybrids. Trees included 5- to 12-year old *J. nigra* and *J. nigra* x *J. regia* but data were not available on individual tree pedigrees. *Juglans* species, provenances, half-sibling families, and individuals are known to vary in their resistance to *G. morbida* (Sitz et al., 2021, Utley et al., 2012). Therefore, to control for expected variation in necrotic area due to host resistance in measuring the effect of nematodes on canker area, individual trees served as experimental units (Table 5.1): each treatment was replicated twice on the same branch, with different treatments on different branches to minimize the chances of different treatments on the same tree affecting one another. One 13- to 46-mm-diameter branch was chosen at random for each treatment on each tree.

Table 5.1. Experimental designs of three nematode inoculation experiments

Species (GenBank No.)	Year	Volume, nema/inoc.	Treatments & Design	
P. multidentatus MSC-A	2016	10 uL ~10 uL^{-1} 80-120 nema	i) Gm-A + nems ii) Gm-A + STW[1] iii) ¼ PDA + nematodes iv) ¼ PDA + STW	n = 64 (blocked by tree)
Panagrolaimus RNC081117	2018	20 uL ~25 uL^{-1} 500 nema	i) Gm-RN2 + nems ii) Gm-RN2 + eluate[2] iii) Gm-RN2 + FTW[3]	n = 18 (blocked by tree)
Bursaphelenchus WA112717-7	2018	20 uL 250 uL^{-1} 5000 nema	i) Gm-RN2 + nems ii) Gm-RN2 + eluate iii) Gm-RN2 + FTW	n = 16 n = 16 n = 16

[1] Sterile tap water (autoclaved); [2]The nematode-free eluate in which nematodes were extracted from cultures of G. morbida *using modified Baermann funnels filled with filtered tap water; [3]Filtered tap water*

P. multidentatus (*det*. L. Carta, USDA-ARS) isolate MSC-A were maintained at 20-day intervals by serial transfer of agar pieces as described above to 20-day cultures of *E. nigrum* isolate GW-2 growing on 1/4-strength PDA. To prepare inocula, 20-day old cultures of nematodes growing on *E. nigrum* isolate GW-2 were placed in modified Baermann funnel traps with sterile tap water for 18-36 hours, eluted, and the nematodes were allowed to settle and adjusted to the desired concentration.

An 8-mm corkborer was used to remove outer bark from the branches and to cut an agar plug of *G. morbida* isolate Gm-A growing on 1/4-strength PDA with 25 mg/L chloramphenicol and 25 mg/L streptomycin, or from sterile media of the same formulation. In treatment (i), nematodes were pipetted onto the agar plug of Gm-A before placing it face-down into the wound made with the corkborer so that the liquid droplet came into contact with the exposed phloem and sapwood; in treatments (ii) and (iv), sterile tap water took the place of the nematodes; in treatments (iii) and (iv), the agar plug was sterile and did not contain *G. morbida* (Table 5.1). All inoculation points were sealed with a piece of parafilm and a piece of duct tape to prevent the plug from falling from the inoculation wound or drying out.

Incubation period between inoculation and destructive sampling was 5 months. Necrotic area was assessed in the field by shaving away outer bark to expose the phloem and measuring the width and length of cankers with calipers. Area was estimated by calculating the area of an ellipse with diameters equal to largest and smallest measured diameters of the canker. Branch diameter was recorded as a covariate for necrotic area. The effect of *Panagrolaimus* inoculation on box-cox transformed necrotic area was analyzed with a linear mixed effects model and ANOVA that included individual tree as a random blocking factor. The significance of branch diameter was tested by including it as a covariate in the regression and comparing model fit to the base model with ANOVA. All statistics were performed in R.

2018 Inoculations of Trees with Panagrolaimus sp.

In a second experiment, *G. morbida* and nematodes were co-inoculated in mature *J. nigra* trees in WA to determine the effect of *Panagrolaimus* sp. from WA on the total area of phloem necrosis caused by *G. morbida* (Table 5.1). Ten- to 12-year-old, open-pollinated and grafted clones of *J. nigra* from the Hardwood Tree Improvement and Regeneration Center (HTIRC) tree improvement

program growing in Walla Walla, WA were inoculated with *Panagrolaimus* sp. isolate RNC081117 and *G. morbida* isolate RN2. *Panagrolaimus* sp. (*det.* G. M. Williams) isolate RNC081117 was maintained at 20-day intervals by extracting them from cultures using the modified Baermann funnels filled with sterile tap water (Van Bezooijen, 2006), counting nematodes under a stereomicroscope, and pipetting 20 adults in 10 uL onto cultures of *G. morbida* isolate RN2 growing on 1/4-strength PDA.

Branches selected for the inoculations were the same diameter as in the previous experiment with *Panagrolaimus* sp. in ID. Inoculation treatments in 2018 were blocked by tree and performed as described above, except that a 6.5-mm corkborer was used with *G. morbida* isolate RN2, 1/4-strength PDA did not contain antibiotics, and tap water that had been passed through a home Britta (Taunusstein, Germany) filter was used as a control for nematodes instead of sterile water because an autoclave was not readily available in the field. To test the effect of nematode secretions on necrotic area, the eluate in which nematodes were extracted was included as a treatment. In treatments (ii) and (iii), the nematodes were replaced by nematode eluate or sterile tap water, respectively; treatments were blocked by tree as described for the previous experiment in ID (Table 5.1). In 2016, branch diameter did not have a significant effect on the size of cankers in the experiment after accounting for treatment. Therefore, branch diameter was not recorded in the 2018 experiment with *Panagrolaimus* RNC081117.

After three months, branch sections that contained the inoculations were cut from the tree, placed in plastic bags and shipped on water ice to West Lafayette, IN under permit (17-IN-20-007). Cankers were photographed and area quantified following as described in Chapter 3. Briefly, bark and phloem were removed from the outer sapwood and cankers were imaged by photographing the sapwood side of the bark on a flatbed scanner and manually tracing canker margins using ImageJ 1.51 (U.S. National Institute of Health). Data were analyzed as described above for 2016 inoculations with *P. multidentatus*.

To reisolate nematodes from inoculated plant tissues, harvested branches were placed in both modified Baermann funnels and moist incubation chambers after canker measurement. Briefly, phloem (4.0 g fresh weight) and sapwood (2.0 g fresh weight) were taken from branch tissues that included the inoculation point from each branch, cut into ~ 1 cm^3 pieces, wrapped in paper towel, and placed in a Baermann funnel filled with sterile distilled water. After 12, 24, and 36 hours, ~ 2 mL was eluted from the funnels, allowed to settle, and checked for nematodes with

a stereomicroscope. For moist incubation chambers, the same or a similar amount of material was placed in a glass petri dish with moist paper towel, and the petri dish was wrapped in parafilm, stored in the dark and checked periodically for nematode activity with a stereomicroscope over the course of 30 days.

2018 Inoculations of Seedlings with Bursaphelenchus juglandis

In a third experiment, *G. morbida* and nematodes were co-inoculated in *J. nigra* seedlings to determine the effect of *Bursaphelenchus* spp. on phloem necrosis, foliar symptoms, and their interaction. The effect of *Bursaphelenchus* sp. (*det*. L. Carta, USDA-ARS) isolate WA112717-7 on area of necrosis caused by *G. morbida* and vascular wilt symptoms were assessed in 1-year-old seedlings of randomly-selected HTIRC-improved families from Vallonia Nursery (Indiana Department of Forestry and Natural Resources, Vallonia, IN). On June 17-18, bare-root seedlings (n = 48) were planted in Metro-mix 560SC (Sun Gro Horticulture, Agawam, MA) in new 9.6 L TP818 Treepots (Stuewe and Sons, Corvallis, OR) and placed on drip irrigation in Walla Walla, WA. Seedlings were allowed to leaf out for one week prior to inoculation with fungi and nematodes. The experiment was conducted under 50% shade to protect seedlings from the heat and high transpiration rates and to limit light and/or water stress that can influence many weakly or opportunistically phytopathogenic *Bursaphelenchus* spp. (Kanzaki & Giblin-Davis, 2018).

Inoculation treatments included fungus with nematodes (n = 16 seedlings), eluate to test for the effect of nematode secretions or nematode-associated microbes on necrotic area and seedling foliar symptoms (n = 16), or filtered water as a control (n = 16). Seedlings were inoculated in a non-random treatment blocked design to minimize potential cross-contamination of nematodes migrating through the soil between plants (Table 5.1). *B. juglandis* isolate WA112717-7 was maintained by serial transfer as described for 2018 experiments with *Panagrolaimus* sp. A 4-mm cork borer was used to remove bark from each seedling and to cut a plug of *G. morbida* isolate RN2. A sterile piece of cotton was placed in the wound, and filtered tap water, eluate, or nematodes was pipetted onto the cotton followed by the plug of *G. morbida*. Inoculation points were sealed with parafilm and duct tape. After 3 months, stems were harvested and shipped to West Lafayette, canker area was measured, and nematodes were incubated for reisolation as described for the above 2018 experiment with *Panagrolaimus* sp.

Wilting symptoms were assessed on a five-point scale by three independent observers just before harvesting seedlings. Crowns of seedlings were rated as follows: 0) healthy; 1) some proximal leaflets wilted or yellow; 2) 25-75% of leaves with some partial leaflet wilting or yellowing; 3) > 50% of leaves fully wilted or > 75% of leaves with some partial leaflet wilting or yellowing; or 4) entire tree wilted with all leaves dead. Consensus scores between the three independent observations were determined by selecting the score chosen by at least two observers, or the middle score if all three observers had different scores. In instances where three observers assigned different scores, scores differed by only one or less.

The effect of *Bursaphelenchus* inoculation on box-cox transformed necrotic area was analyzed with a linear model with fixed effects only. The effects of inoculation treatment, untransformed necrotic area, and their interaction on crown rating was analyzed with a proportional-odds logistic (ordinal) regression using the "polr" function in the package "MASS". To account for small sample sizes that resulted in a low number of degrees of freedom for an interactive model, separate ordinal regressions were also employed to analyze the relationship between canker necrotic area and crown rating with only the seedlings from each treatment group. Model fit for ordinal regressions was assessed with marginal likelihood-based R^2 and area under the receiver operator curve. All statistical analyses were performed in R.

5.3 Results

5.3.1 Identity, Distribution, and Culturability of Nematodes

Based on UPGMA clustering (Fig. 5.1) and phylogenetic analyses (Figs. 5.2-4), we recovered seven unique 18S barcodes from five genera in five (97% sequence similarity) or six (99% similarity) operational taxonomic units (OTUs) of nematodes. The nematodes were closest to *Bursaphelenchus*, *Panagrolaimus*, *Rhabditolaimus*, *Ditylenchus*, and an unknown endoparasite found in the haemocoel of *P. juglandis* that grouped with *Ektaphelenchus* spp. in sequence typing. Juveniles morphologically resembled juvenile *Ektaphelenchus* sp. (*det*. L. Carta, USDA-ARS). UPGMA clustering of the more variable COI-α sequences corresponded to the same clusters obtained from 18S barcodes while revealing subpopulation clusters within 18S OTUs (Fig. B.1).

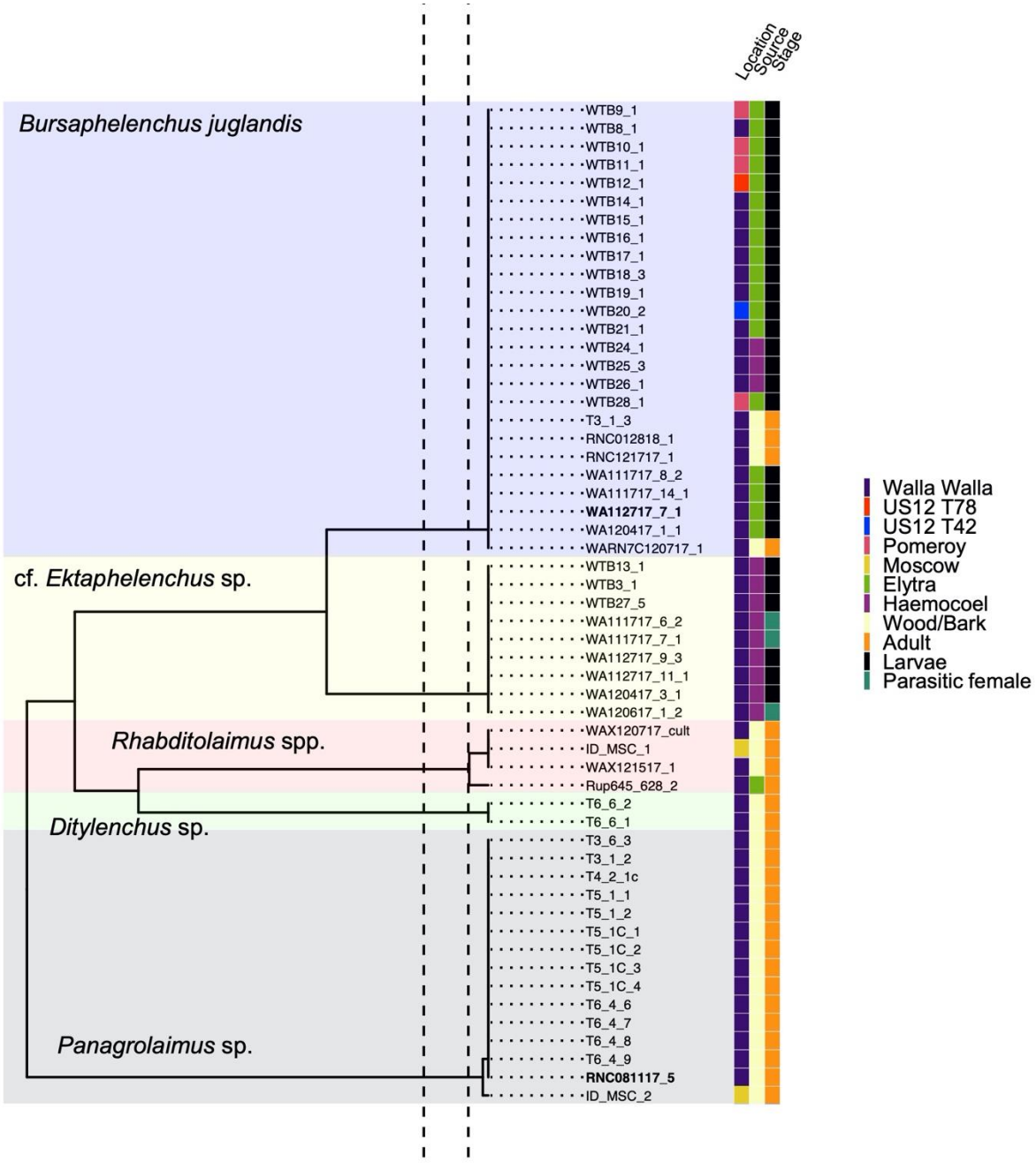

Figure 5.1. 18S UPGMA cluster analysis of pairwise nucleotide distances to distinguish operational taxonomic units by location, host tissue (source), and life stage. Polytomy indicates samples with identical sequences. Vertical dashed lines represent 97 and 99% sequence similarity cutoffs (from left to right). Annotated taxonomic assignments are based on morphological characters and phylogenetic inferences from trees built with voucher sequences from GenBank. Isolates that were cultured and used in inoculation experiments are given in bold.

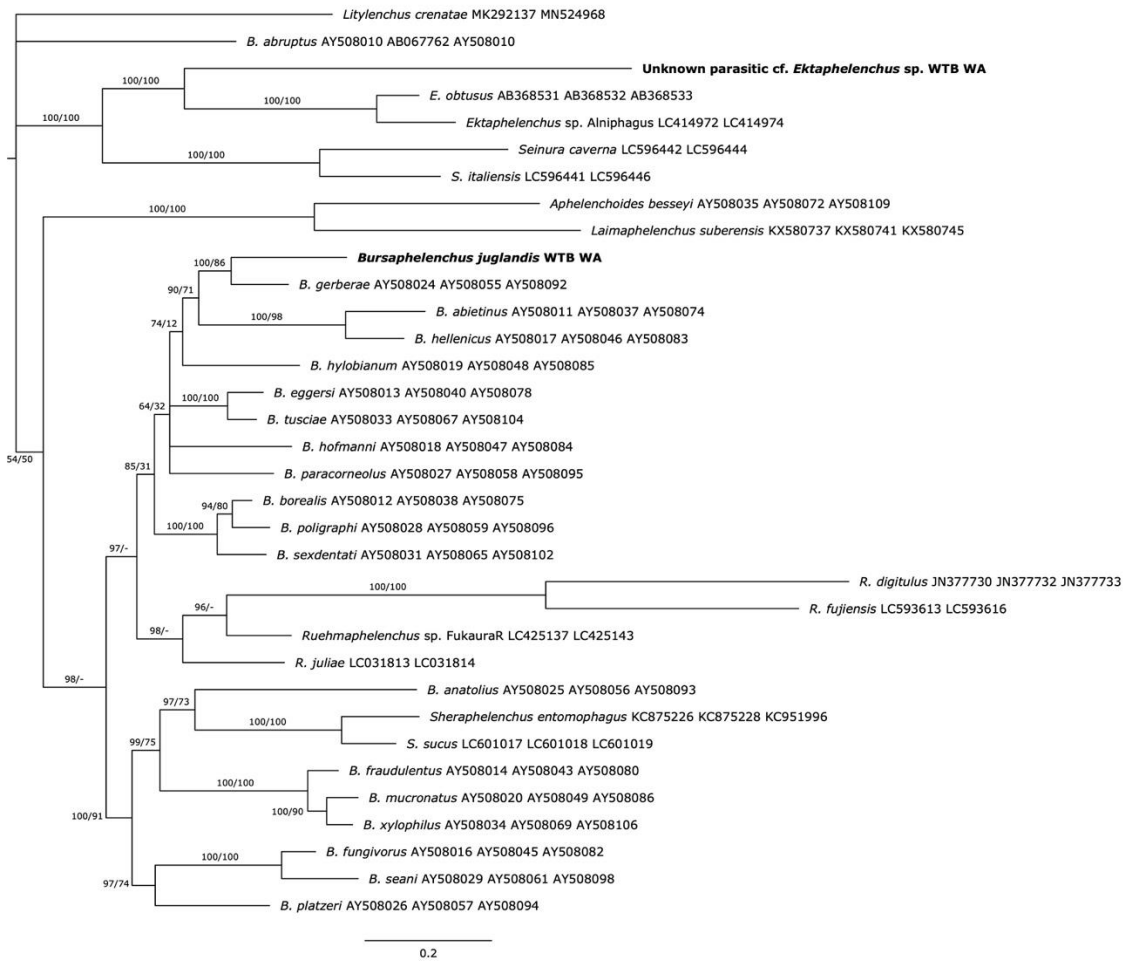

Figure 5.2. 18S+28S+COI consensus tree for Aphelenchoididae. Independent GTR+I+G models among loci. Sequences from this study in bold. Order of GenBank accession numbers: rDNA, mtDNA. Topology, branch lengths, and posteriors calculated in MrBayes 3.1.2 (4 chains, 10 million generations diagnosed once per thousand, 25% burn-in). Node values give Bayesian posterior probability followed by ML bootstrap support (10,000 replicates in RAxML). Nodes without ML bootstrap values indicate nodes that were not recovered in the ML topology.

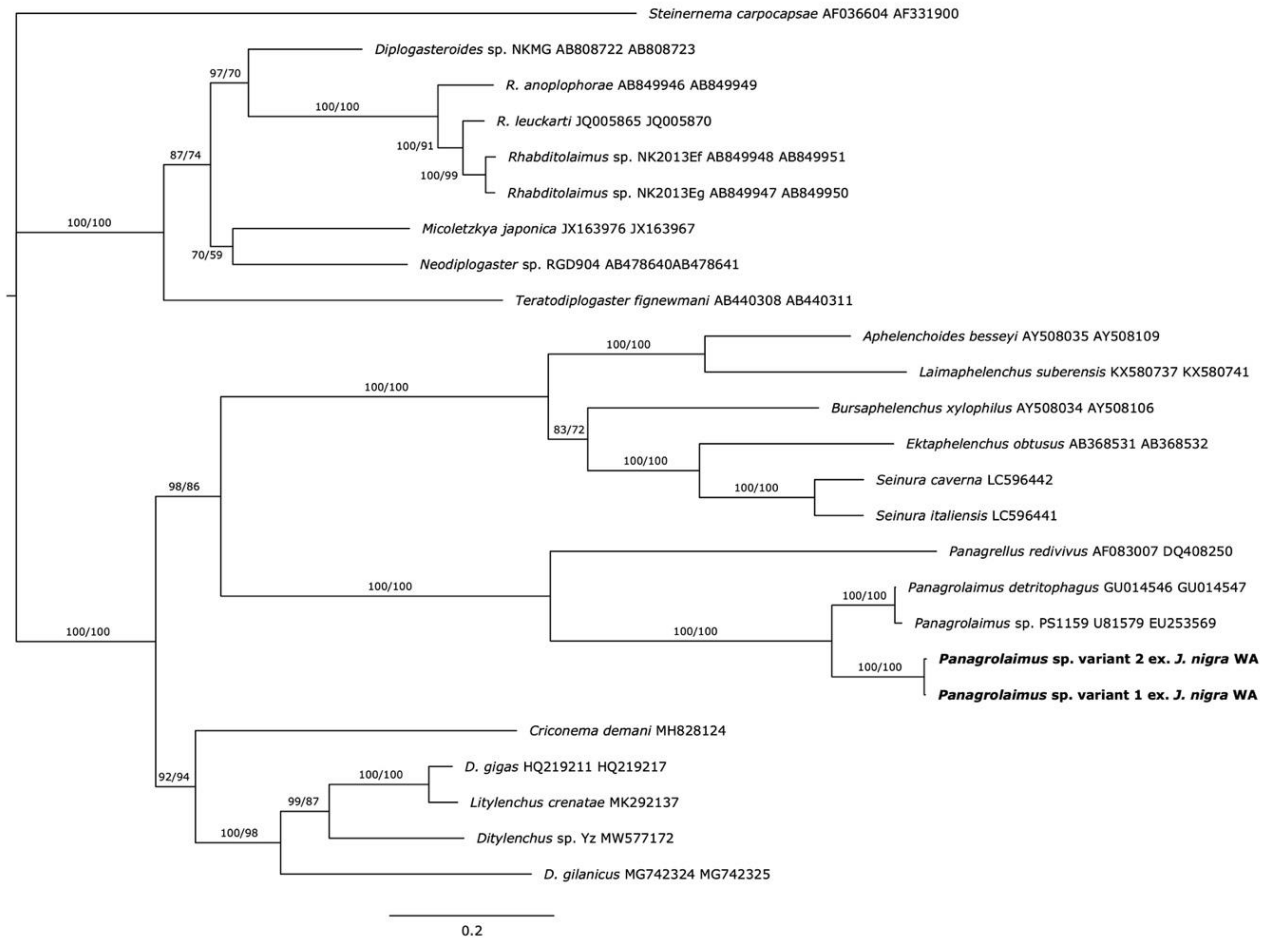

Figure 5.3. 18S+28S consensus tree for Rhabditida. Independent GTR+I+G models among partitions. Sequences from this study in bold. GenBank accessions for 18S are followed by those for 28S sequences. Topology, branch lengths, and posteriors calculated in MrBayes 3.1.2 (4 chains, 10 million generations diagnosed once per thousand, 25% burn-in). Node values give Bayesian posterior probability followed by ML bootstrap support (10,000 replicates in RAxML).

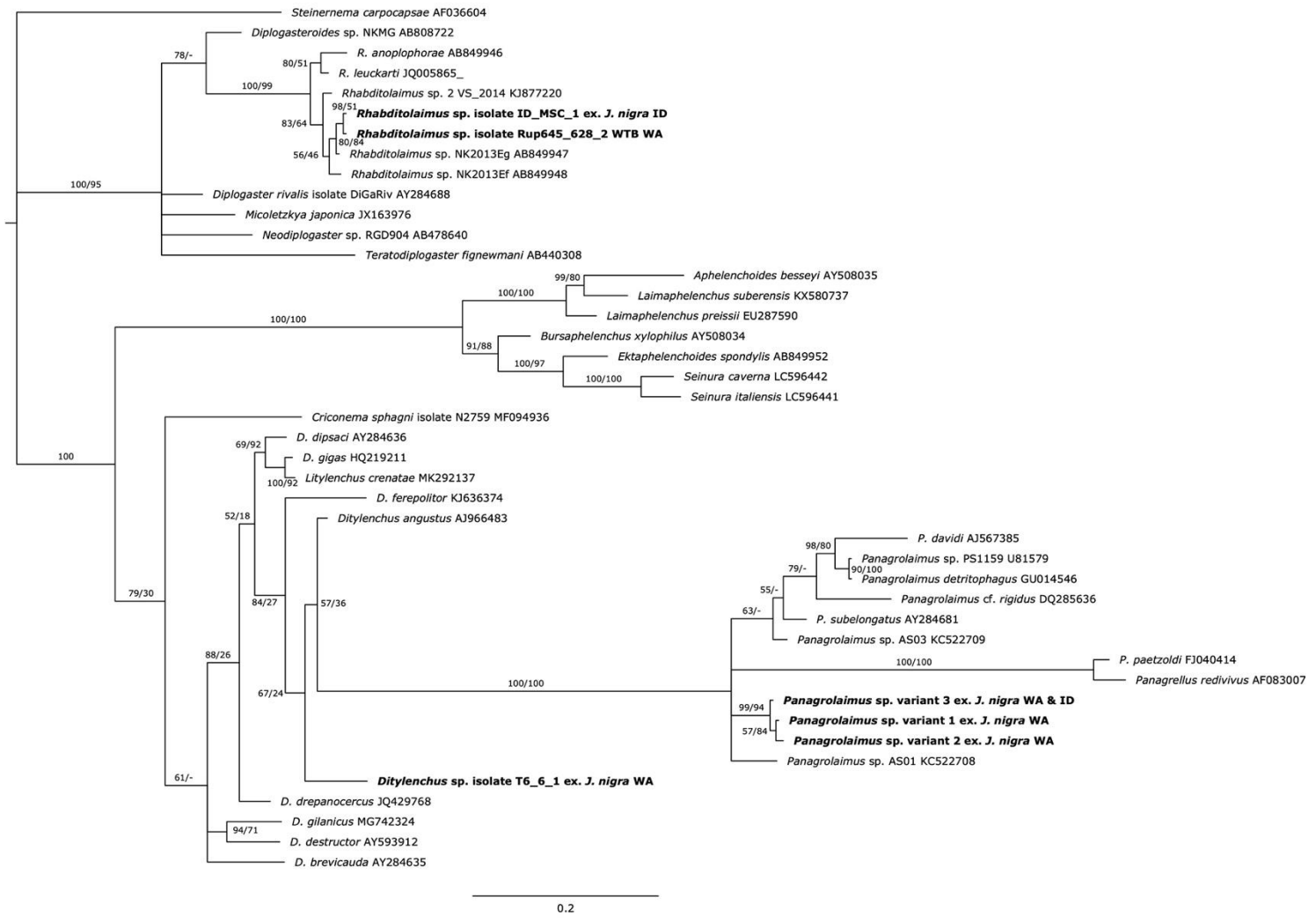

Figure 5.4. 18S consensus tree for Rhabditida. GTR+I+G model. Sequences from this study in bold. Topology, branch lengths, and posteriors calculated in MrBayes 3.1.2 (4 chains, 10 million generations diagnosed once per thousand, 25% burn-in). Node values give Bayesian posterior probability followed by ML bootstrap support (10,000 replicates in RAxML). Nodes without bootstrap were not recovered in ML topology.

Table 5.2. Frequency of nematodes from *P. juglandis* (WTB) in 2017 from Walla Walla, WA.

Class	WTB (*n* = 110)		Nematodes / WTB*
	No.	Rate	(Mean ± SD)
Elytra	24	21.8%	22.5 ± 13.2
Haemocoel	12	10.9%	***Larvae*** 108.5 ± 117.1
			Eggs 86.6 ± 106.1
Overall	35	31.8%	56.1 ± 83.2

** Reflects distribution from nematode-positive WTB only*

Table 5.3. Isolation rate of nematodes from *P. juglandis* (WTB) emerged from *J. nigra* from WA in 2018 and 2019 (only includes locations from which WTB was successfully reared).

Location	Lat	Lon	Trees WTB+* / Sampled	WTB dissected	Infection Rate	
Walla Walla, WA					***Elytra***	***Haem.***
Cottonwood Cr.	46°00'56"N	118°17'44"W	1 / 2	19	0	5%
Russel Cr.	46°02'42"N	118°14'01"W	1 / 3	64	3%	6%
Yellow Hawk Cr.	46°01'51"N	118°21'24"W	2 / 4	125	5%	9%
Foster Rd.	46°01'54"N	118°13'27"W	1 / 1	1	0	100%
US Hwy. 12						
L. Snake Wind Farm	46°32'21.0"N	117°51'18.3"W	1 / 1	3	33%	0
Dayton, WA	46°18'57.2"N	117°59'18.2"W	2 / 2	3	33%	0
Pomeroy, WA	46°28'23.7"N	117°36'06.7"W	1 / 1	6†	67%	0
Total			**9 / 14**	**221**	**6%**	**8%**

** WTB-positive trees = the number of trees with at least one emerged beetle † Includes both P. juglandis (WTB) and A. dispar*

Table 5.4. Abundance of WTB-associated nematodes from *J. nigra* in WA, 2018-19 (all locations).

Branches collected from…	No. of trees	Infected WTB Emergence Rate*	
		Elytra	***Haemocoel***
Trees with > 1 WTB	12	58%	42%
All trees in study	25	28%	20%

** Number of trees with at least one nematode-infected beetle*

Rhabditolaimus, *Panagrolaimus*, *B. juglandis*, and cf. *Ektaphelenchus* sp. were widespread and recovered from many of the locations and populations of *J. nigra* and *P. juglandis* that were sampled. In total 331 WTB were dissected and screened. Rates of parasitism and phorecy on WTB and recovery of nematodes from wood incubations varied between 2017 and 2019 and among locations (Tables 5.2 & 5.3). In 2019, 12 of 25 trees had WTB (Table 5.4), and WTB-positive trees were distributed across eight locations between Walla Walla and Pomeroy, WA. In 2019 at plantation locations in Walla Walla, WA (Cottonwood, Russel, and Yellow Hawk Creek), rates of phorecy and parasitism increased with host population size when the size of WTB populations from reared material was greater 10 individuals. Material collected from the other locations sampled in 2019 had fewer WTB (< 10) and no parasites, but higher rates of phorecy. *Panagrolaimus* sp. and *B. juglandis* were able to be maintained for many generations by serial transfer to fresh cultures of *G. morbida*, which was rapidly consumed by the nematodes (>10 transfers or ~ 200 days). Entomoparasites (cf. *Ektaphelenchus* sp.) could not be cultured.

5.3.2 Functional Roles of Nematodes

Panagrolaimus sp.

The *Panagrolaimus* sp. that we studied is an antagonist of *G. morbida* that has the potential to decrease severity of TCD. In transfers from cultures of *Panagrolaimus* spp., growth of *G. morbida* was inhibited by nematode-associated secretions and/or bacteria. *G. morbida* could not be viably subcultured after *Panagrolaimus* spp. reproduced. Instead, nematodes left trails of bacteria when transferred to sterile agar, and the bacteria appeared to inhibit fungal growth. Of the other fungi tested, *E. nigrum* and *G. fujikori* species complex sp. from walnut supported reproduction of *P. multidentatus*, but not *Trichoderma* sp. However, *E. nigrum* from *Solidago* did not support reproduction of the *Panagrolaimus* sp. isolated in 2017-2018, suggesting that not all *E. nigrum* populations are equal with regard to their suitability as food sources for *Panagrolaimus* spp. from walnut trees.

Remarkably, *P. multidentatus* could be recovered from five-month-old, air-dried wood with very low moisture content. Two 18S alleles of *Panagrolaimus* sp. were recovered in 2017-2019 that only differed at a two-nucleotide polymorphism at alignment positions 445 and 452 on either end of sequence TGAAAA (Fig. B.2). The two alleles were carried by homo or heterozygous

individuals that coexisted in the same locations, trees, and incubated branch cross-sections. They were recovered in both states (WA and ID) including from the same branch of the same tree in Moscow, ID as *P. multidentatus* used in the 2016 branch inoculation experiment, from which we did not obtain sequence data. Cytochrome sequences varied only slightly among the nematodes identified as *Panagrolaimus* sp. that were isolated in our experiment (Figure B.1). Notably, a *P. juglandis* 18S sequence was recovered from one *Panagrolaimus* individual.

Panagrolaimus sp. decreased necrotic area when paired with *G. morbida* in both 2016 and 2018 experiments. In 2016, co-inoculation with *P. multidentatus* MSC-A and *G. morbida* Gm-A resulted in a 24 ± 5% reduction in necrotic area compared to *G. morbida* Gm-A-only controls (Figs. 5.5 & 5.6; $R^2_{fix} = 0.05$; $R^2_{fix+rand} = 0.63$). There was a large amount variation attributable to tree random effect on necrotic area across treatments ($R^2_{rand} = 0.58$; Fig. 5.6B). Neither of the control treatments (nematode-only or sterile PDA) treatments produced measurable necrosis except for in four trees which were nonetheless extreme outliers. There was no significant effect of branch diameter on necrotic area ($p = 0.33$).

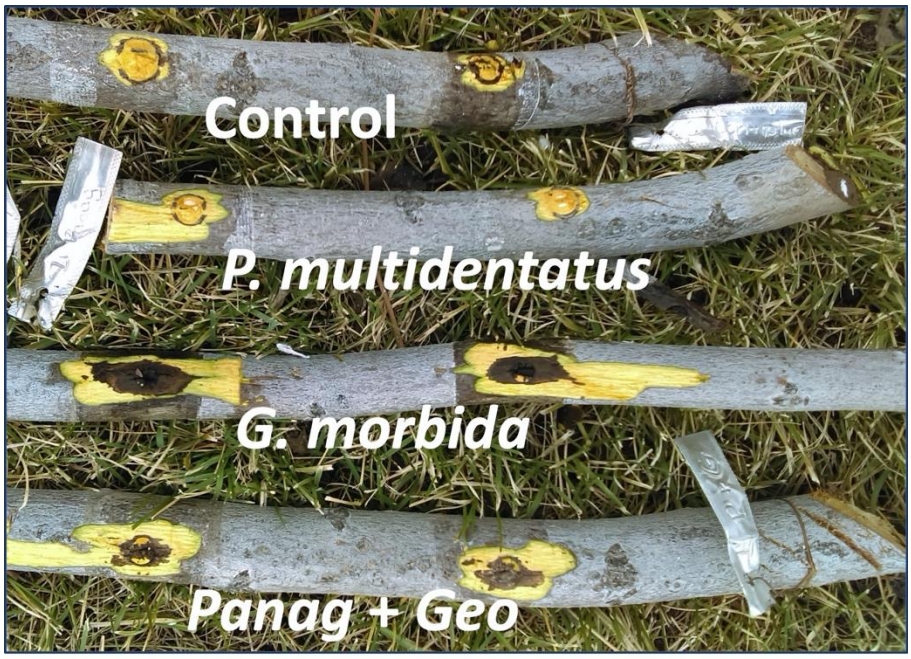

Figure 5.5. A replicate of *Juglans* inoculated with *Panagrolaimus multidentatus*, *Geosmithia morbida*, or both (bottom) depicting reduction in necrotic by *P. multidentatus* and absence of necrosis in agar-only (control) and *P. multidentatus*-only treatments.

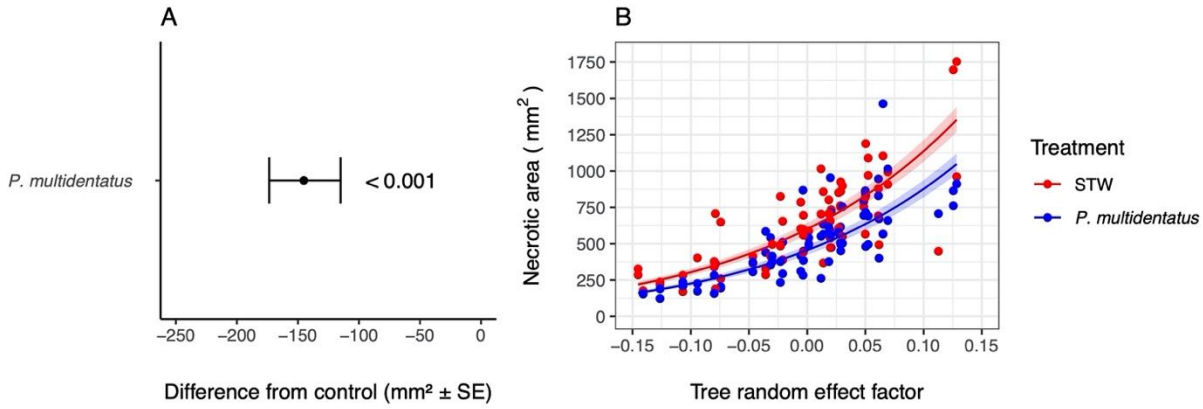

Figure 5.6. Necrotic area in co-inoculations of attached *J. nigra* branches with *G. morbida* isolate Gm-A and *Panagrolaimus multidentatus*, and Gm-A + sterile tap water (STW). (A) Mean ± SE within-tree difference to the TW + *G. morbida* treatment on the same tree and results from Tukey post-hoc test. (B) Predicted (lines) ± SE (shaded area) and observed (points) necrotic area by treatment.

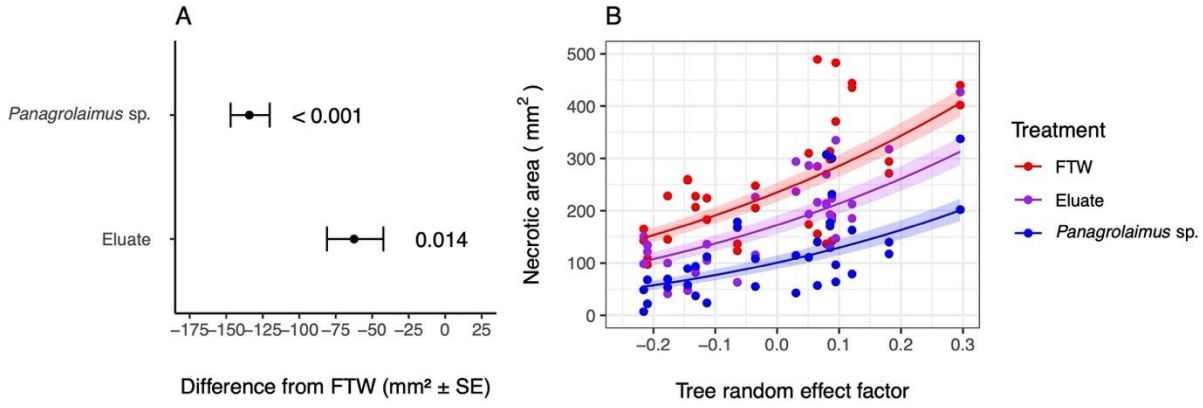

Figure 5.7. Necrotic area in co-inoculations of attached *J. nigra* branches with *G. morbida* isolate RN-2 and *Panagrolaimus* sp. isolate RNC081117, eluate from funnel extractions of nematodes from cultures, and filtered tap water (FTW). (A) Mean ± SE within-tree differences to the FTW + *G. morbida* treatment on the same tree and results from Tukey post-hoc test. (B) Predicted (lines) ± SE (shaded area) and observed (points) necrotic area by treatment.

Only 39 of the original 64 inoculated trees were included in the analysis. On 15 smooth-barked trees that were likely to be *J. nigra* x *J. regia* hybrids, neither *G. morbida* isolate Gm-A alone nor co-inoculation with Gm-A and *P. multidentatus* isolate MSC-A resulted in necrosis that was quantifiable beyond the inoculation wound (Fig. 5.5). Necrosis was inconclusive on one tree

due to the loss of duct tape, parafilm, and agar from the wound. On five additional trees, inoculations with Gm-A or co-inoculation resulted in total mortality of the branch, so necrosis could not be measured. Cankers on 4 more trees were more than 100 cm long, and therefore excluded as extreme outliers.

In 2018 experiments with *Panagrolaimus* sp. in attached tree branches, nematode eluate had a negative effect on necrosis, suggesting nematode secretions or associated microorganisms antagonize the growth of *G. morbida* and its effect on the host *in situ*. Inoculations of nematode eluate and Gm-RN2 resulted in a 27 ± 4% decrease in necrotic area compared to controls containing Gm-RN2 and filtered tap water (Fig. 5.7). Inoculation treatment significantly influenced necrotic area (Fig. 5.5; $p < 0.001$; $R^2_{fix} = 0.25$; $R^2_{fix+rand} = 0.53$). Co-inoculation with Gm-RN2 and *Panagrolaimus* sp. isolate RNC081117 resulted in a 57 ± 8% decrease in necrotic area compared to Gm-RN2 and filtered tap water (Fig. 5.7; $R^2_{rand} = 0.28$). As in the 2016 experiment, there was a large amount variation attributable to tree random effect on necrotic area across treatments, demonstrating substantial variation in host resistance or environmental factors that differed among individual trees (Fig. 5.7B). Five outlier points were removed including cankers from one tree in RN2-only controls that were seven times larger in total area than the next largest canker in the dataset.

Bursaphelenchus juglandis

B. juglandis fed on *G. morbida*, but secretions did not inhibit growth of *G. morbida* in culture. Like *Panagrolaimus* spp., *B. juglandis* could be maintained on *G. morbida*, but unlike *Panagrolaimus* spp., viable colonies of *G. morbida* grew from excised agar from cultures of *G. morbida* RN2 with *B. juglandis*. PCR products for *B. juglands*-specific primers produced a positive band of ~170bp on an agarose gel and the ~1.2kb overlapping rDNA region of *Bursaphelenchus* sp. was 100% similar to *B. juglandis* from CA. Placement of *B. juglandis* in reference to other groups with 18S, 28S, and COI, including the closest relative in our phylogeny, *B. gerberae*, was in accordance with the 18S-based inferences of Ryss et al., (2020). Nematodes with identical 18S barcode sequences to *B. juglandis* were recovered from five distinct populations of *P. juglandis* in WA, incubated wood, and seven different trees (Fig. 5.1). Mitochondrial cytochrome sequences varied substantially among isolates of *B. juglandis* and were distributed among two UPGMA

clusters at 99% sequence similarity, and three smaller clusters at a finer scale (Fig. B.1). *B. juglandis* was also found in the haemocoel of three adult *P. juglandis*, including one individual that also carried *B. juglandis* under its elytra. *B. juglandis* were also encountered as dauerlarvae on the underside of the elytra of *Anisandrus dispar* Fab., the invasive European shot-hole borer, in Pomeroy, WA.

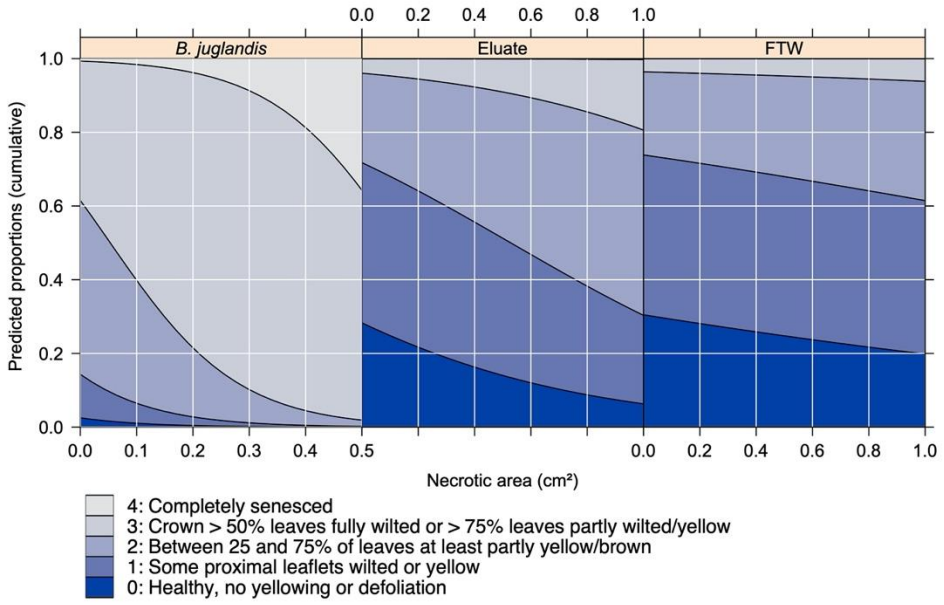

Figure 5.8. Stacked effects plot depicting predicted probabilities of observing crown ratings in seedlings as a function of canker area caused by *G. morbida* isolate RN2 when coinoculated with *Bursaphelenchus juglandis* isolate WA112717, eluate from *B. juglandis* funnel extractions, or filtered tap water (FTW) from a proportional-odds logistic (ordinal) regression.

In 2018 experiments with *B. juglandis* in seedlings, the nematodes synergized with *G. morbida* to cause deterioration in crown condition in trees under shade conditions although they also decreased necrotic area (Figs. 5.8 & 5.9B). Unlike in *Panagrolaimus* eluate inoculations of branches, seedlings receiving the *B. juglandis* eluate treatment did not have significantly different necrotic area ($p = 0.85$), nor did that have different crown condition ratings ($p = 0.23$) compared to RN2-only control. In the *B. juglandis* nematode treatment, crown deterioration was more advanced overall ($p < 0.001$) and positively correlated to necrotic area caused by *G. morbida* (Fig. 5.8) when considered in a stand-alone analysis ($p = 0.03$; Pseudo-$R^2 = 0.14$; AUC = 0.77). However, overall crown rating was not correlated with necrotic area ($p = 0.12$) after accounting

for inoculation treatment ($p < 0.001$) and necrotic-area-by-inoculation-treatment interaction ($p = 0.20$). Seedlings that received the *B. juglandis* treatment had 85 (95% CI: [10, 745]) times higher odds of being in a worse (higher) crown rating category compared to controls containing Gm-RN2 and filtered tap water, and 38 (95% CI: [5, 320]) times higher odds of being in a higher category than the eluate treatment ($p < 0.001$). Inoculation treatments significantly influenced necrotic area (Fig. 5.9A; $p < 0.001$; $R^2 = 0.52$) and crown symptoms (Fig. 5.9B; $p = 0.001$; $R^2 = 0.16$). In co-inoculations of seedlings with *G. morbida* isolate RN2 and *B. juglandis* isolate WA112717-7, nematodes reduced necrotic area by 74 ± 1% ($p < 0.001$) compared to RN2-only controls.

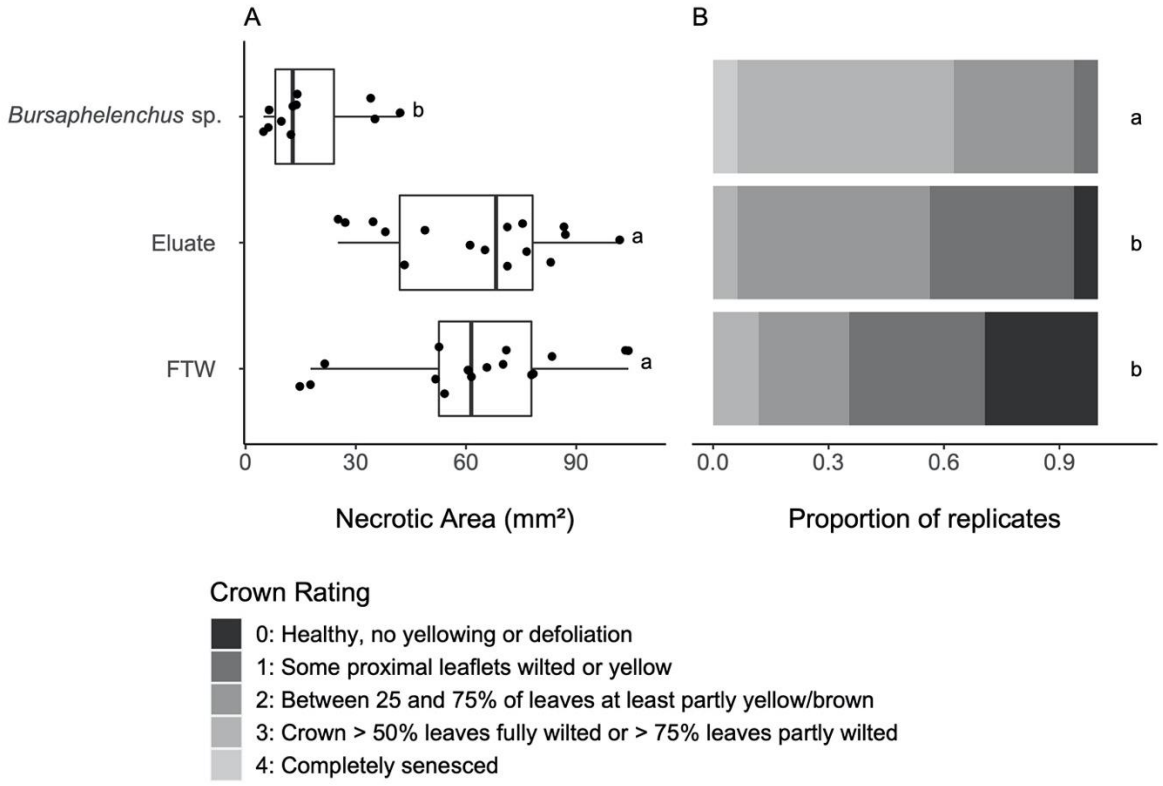

Figure 5.9. Necrotic area (A) and crown condition (B) of *J. nigra* seedlings grown in 50% shade and co-inoculated with *G. morbida* RN-2 and *Bursaphelenchus juglandis* isolate WA112717, eluate from funnel extractions of nematodes from cultures, and filtered tap water (FTW). (A) Mean and distribution of necrotic area. (B) Crown condition of seedlings by treatment, where 0 = healthy and 4 = all leaves completely senesced. Letters denote significant differences from a Tukey post-hoc test (A) or significant contrasts from proportional-odds logistic regression (B).

Other Nematodes

Parasites with identical sequences to cf. *Ektaphelenchus* sp. were found in beetles from three trees across three locations in Walla Walla, WA. The endoparasite was found exclusively in the haemocoel, and females gave birth oviparously to eggs that hatched inside the hemocoel (Fig. 5.10). Typically, one to three enlarged adult parasitic females accompanied the eggs and one hundred or more J1 larval progeny inside an individual beetle. Parasitic cf. *Ektaphelenchus* sp. could not be placed to genus with certainty due to long branches in the three-gene topology (Fig. 5.2) and difficulty acquiring a quality slide mount of the parasitic females.

Nematodes representing one of the two distinct 18S lineages of *Rhabditolaimus* were isolated from both branches and beetles and found in three different locations. One lineage of *Rhabditolaimus* was found in both WA and Moscow, ID (Fig. 5.1). *Ditylenchus* were recovered from moist-incubated branches from WA. All nematode sequences obtained in this study were recovered in WA.

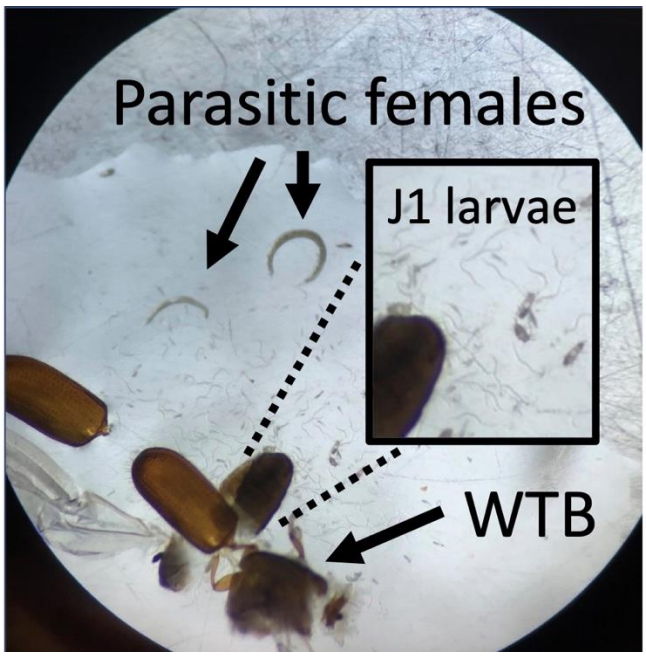

Figure 5.10. Life-stages of the endoparasitic nematode found associated with WTB in Walla Walla, WA. Stereoscope image showing a dissected *P. juglandis* (bottommost arrow) adult harboring phoretic mites and hundreds of J1 nematode larvae (inset), eggs, and two enlarged endoparasitic females (two top arrows) of an unknown endoparasitic Aphelenchoididae cf. *Ektaphelenchus* sp.

5.4 Discussion

5.4.1 Nematode Diversity

We uncovered a diversity of taxonomic and functional groups of nematodes in healthy and TCD-symptomatic *J. nigra* across a large geographical area in southwest Washington and northern Idaho over the course of five years of study. The community of nematodes associated with *J. nigra* bark in WA and ID differed from that described in the native range of black walnut (Eisenback & Paes-Takahashi, 2015). Our study also recovered the same nematode genera found by Massey (1974) associated with *Pityophthorus* spp. in AZ, NM, WV, and CT: *Bursaphelenchus*, *Neoditylenchus* (=*Ditylenchus*), and *Parasitylenchus* (=*Ektaphelenchus*).

Prior to this study *B. juglandis* had not been documented from *J. nigra* (Ryss et al., 2020). This study of *J. nigra* in WA extends the known host and geographic range of *B. juglandis* beyond *J. major* in NM and AZ and native *J. hindsii* and commercial plantings of *J. regia* in California. Prior to this study *B. juglandis* was not known to occupy the hemocoel of *P. juglandis* or the alternative vector *A. dispar*. Nevertheless, several *Bursaphelenchus* spp. are known to transition to an endophoretic habit and be endoparasites of Coleopteran hosts/vectors, (Aikawa, 2008; Crook, 2014, Kanzaki et al., 2009, 2013, Tomalak & Malewski, 2014). We also found *Panagrolaimus* over a large geographic range (both ID and WA). These species appear to be fungal feeders, unlike most of their known relatives (Shannon, 2005). We also found free-living *Ditylenchus* and *Rhabditolaimus,* which add to the diversity of nematodes found in *J. nigra* wood in the Inland Northwest.

The 18S barcode (Kanzaki et al., 2012) distinguished between cf. *Ektaphelenchus*, *Bursaphelenchus*, *Panagrolaimus*, *Ditylenchus*, and *Rhabditolaimus*. However, UPGMA clustering of mtDNA revealed the presence of potentially cryptic species, subspecies or populations within *B. juglandis*. Our placement of *B. juglandis* largely agreed with the placement by Ryss et al., (2020), including with closest neighbor *B. gerberae* and with the *abietinus* group within a larger *sexdantati* superclade. However, inner branches were better resolved and branch lengths much more variable with the inclusion of both mtDNA and multiple nuclear rDNA markers in a multigene phylogeny. If more COI, 18S and 28S sequences for related nematodes had been publicly available or had we employed different or longer markers, we could have made more

robust inferences, especially for *Panagrolaimus* and *Ektaphelenchus*. These key shortcomings of data availability and our reverse taxonomy approach highlight the need for more sequencing efforts, publicly-available molecular data on scolytine-associated nematodes, and agreement on standard loci and primers to be used for assisting in such efforts.

5.4.2 Nematode Functional Roles

Based on the negative relationship between number of *P. juglandis* that emerged from bolts and rates of infection and phorecy, both parasitic and phoretic nematodes appeared to become more abundant with increasing population density of *P. juglandis* in plantation sites in Walla Walla, WA. However, unmanaged trees in later stages of TCD along US-12 and in Walla Walla, WA had much lower *P. juglandis* population density and higher rates of phorecy and parasitism. These findings suggest that abundance of parasites follows a "boom-and-bust" population cycle that coincides with host/vector populations and progression of TCD symptoms. This pattern is consistent with the hypothesis that parasites regulate endemic-stage bark beetle populations (Furniss, 1967, Hofstetter et al., 2007, Klepzig et al., 2001; Massey, 1966, McCambridge & Knight, 1972, Raffa et al., 2015; Thorne, 1935, Weed et al., 2015). As *B. juglandis* populations increase after *P. juglandis* populations decline in mature trees, they are more likely to be acquired and transmitted by beetles that visit trees in later stages of decline, in parallel to the ecology of other *Bursaphelencus* spp. including important destructive phytopathogens (Kanzaki & Giblin-Davis, 2018, L. Zhao et al., 2014).

The two most commonly encountered nematodes, *B. juglandis* and *Panagrolaimus* sp. could reproduce and multiply on cultures of *G. morbida*, but have contrasting hypothesized impacts on tree health and roles in TCD. Although nematodes had a significant effect on host symptoms, a large amount of residual variation in canker size could be attributed to host genetics and/or additional environmental variation, as has been found in previous work (McKenna et al., 2020, Williams and Ginzel, *in review*).

Panagrolaimus spp.

Panagrolaimus spp. found in healthy and diseased trees could be important antagonists of *G. morbida* or even the *G. morbida-P. juglandis* symbiosis. Feeding activity, and possibly microbial

associates of *Panagrolaimus* spp., reduced the amount of necrosis around inoculation points in attached branches on mature trees in two experiments after accounting for individual tree. This result has important implications for tree-improvement research as it corroborates previous work demonstrating that environment and host genetics account for a large amount of variation in the severity of TCD (McKenna et al., 2020, Utley et al., 2013, Williams and Ginzel, *in review*). *Panagrolaimus* spp. were found in both TCD epicenters and in Moscow, ID, a nearby location where signs and symptoms of TCD have yet to be detected, suggesting it may play a role in protecting walnut trees from TCD. However, climatic differences between southwest WA and northern ID could also account for differences in nematode communities as well as the severity of TCD and its impact on *J. nigra* (Williams and Ginzel, *in review*)

Our findings indicate that direct feeding on *G. morbida* and digestion by endogenously or symbiotically produced metabolites account for reduction in canker area by the nematodes, and could reduce the severity of TCD. Eluate that did not contain *Panagrolaimus* spp. but can be presumed to have contained associated microbes, chemical exudates and/or wastes also significantly reduced canker size, unlike what was found for *B. juglandis*. The effect of the eluate is consistent with the observation that co-culture with *Panagrolaimus* spp. eliminates the viability of *G. morbida* following rapid nematode reproduction. *Panagrolaimus* spp. could also limit both the spread of the fungus to other trees and the reproductive success of *P. juglandis*. Furthermore, *Panagrolaimus* spp. may also compete with *G. morbida* for available nitrogen, as the latter is unable to utilize the mineralized forms of N that are left over by beetle and nematode feeding (Chen & Ferris, 1999, Kolařík et al., 2011).

Some members of the genus *Panagrolaimus* are well known for their capacity for extended anhyrobiosis and freeze-tolerance, surviving up to 8.7 years in dormancy (Aroian et al., 1993). A similar ability of *Panagrolaimus* sp. in our study could explain its distribution in colder climates (*i.e.*, Moscow, ID) than *B. juglandis* and its ability to persist in bark which regularly dries and rehydrates with meteorological events. *Panagrolaimus* sp. may withstand dry periods that favor *G. morbida* growth and competition with other fungi in wood but resume activity and antagonize *G. morbida* in humid conditions along with fungal antagonists such as *Trichoderma* spp. whose competitive advantage over *G. morbida* would be further promoted by the nematode feeding preferences that we observed. Anhydrobiosis would also make this nematode amenable for

development into a commercial dehydrated product that could be mixed with tap water and sprayed onto the bark of trees to manage TCD.

Important questions remain regarding the ecology of *Panagrolaimus* sp. associated with walnut trees. Like *B. juglandis*, we were unable to reisolate *Panagrolaimus* from inoculated branch material, raising the question of its fate in trees. It may disperse after feeding on *G. morbida*, evading detection from host material, which was sampled in proximity to the inoculation points. We also do not know if this *Panagrolaimus* sp. inhabits soils or other host tree species. The route of introduction of *Panagrolaimus* spp. to aboveground organs of mature *J. nigra* trees by Coleopteran vectors including Xyleborini (Scolytinae) or Cerambycidae remains unknown. Finally, based on our detection of one *P. juglandis* 18S sequence from *Panagrolaimus* in wood incubations from infested trees and the presence of denticles in their buccal cavities, it is possible *Panagrolaimus* spp. are predators of *P. juglandis* eggs as documented for gallery-associated, omnivorous freeliving species such as *Micoletzkya* (Massey, 1974). However, additional sampling and experiments would need to be conducted to confirm this.

Bursaphelenchus juglandis

B. juglandis is a common partner of *P. juglandis* and *G. morbida*. Although a reduction in canker size in the presence of *B. juglandis* relative to *G. morbida*-only controls was observed, it does not appear that other microbial associates or secretions of *B. juglandis* contributed to reductions in necrosis. Rather, our results suggest that *B. juglandis* acts together with *G. morbida* to cause foliar symptoms of TCD. Decreased necrotic area in the presence of *B. juglandis* compared to other treatments was accompanied by a significant increase in foliar symptoms. When *B. juglandis* was present, crown loss correlated positively with canker size, whereas variation in necrotic area did not correspond to variation in crown condition within the eluate or control treatments. Crown loss and early senescence could have been caused by host physiological responses such as terpene production, cavitation, and/or irreversible xylem disfunction (Fukuda, 1997; Kuroda, 1991, Yazaki et al., 2017), or even tyloses which are known to occur in *J. regia* with apoplexy disorder (McElrone et al., 2010). It is also possible that more of the nematode inoculum made it into the xylem in seedlings with the most severe crown loss, leading to hydraulic stress, less direct feeding

on the *G. morbida* inoculum, and thus a comparatively larger amount of necrotic area in trees that presented more advanced crown decline.

It is difficult to predict the extent to which our findings in seedlings might translate to mature trees. *B. juglandis* is certainly an important component of the subcortical community of late-stage TCD-symptomatic trees in WA; it was isolated from branches of declining trees, from a high proportion of the few remaining *P. juglandis* in late-stage TCD-symptomatic trees, and even from an ambrosia beetle that had colonized a late-stage TCD tree. However, the fate of these nematodes in walnut seedlings in our experiment and *in situ* remains unknown. Comprehensive attempts to re-isolate *B. juglandis* from inoculated seedlings at the conclusion of our experiment were unsuccessful. Additional work to further investigate the role of *B. juglandis* in TCD is needed, including extraction and/or detection from host tissues. These efforts could be aided by the specific primers of Ryss et al., (2020) could be used in a qPCR or other rapid detection method (*e.g.*, Carta et al., 2020). The nematodes may reproduce more successfully in thick bark of medium to large-diameter branches on healthy trees, but have limited survival in seedlings due to thin bark and vigorous host growth. Until *B. juglandis* are inoculated into living branches alone and with *G. morbida*, their effect on foliar symptoms in mature trees cannot be determined. Nevertheless, *B. juglandis* were found in incubated wood material from branches of live trees, frequently on WTB across four states in four *Juglans* spp. and hybrids, and on the European shothole borer, *A. dispar*. Together, these findings combined with sufficiently high phoresy rates in outbreak-level (~5%) and post-outbreak (33-67%) vector populations to ensure transmission, suggest that *B. juglandis* may be an important component of the TCD pathosystem.

Rhabditolaimus and *Ditylenchus* spp.

These nematodes may interact with both the vector and other nematode species. Similar to *Panagrolaimus*, *Rhabditolaimus* spp. are bacterial and to a lesser extent, fungal feeders (Kanzaki & Giblin-Davis, 2014, Ryss et al., 2021). *Rhabditolaimus* were found associated with *J. nigra* in both WA and ID suggesting a widespread distribution. Unlike *Panagrolaimus* sp., *Rhabditolaimus* were found as phoretic associates on *P. juglandis*. *Ditylenchus* which we only found in WA can be free-living fungal feeders or facultative, obligate, and even gall-forming plant parasites (Brzeski, 1991). *Ditylenchus* was recovered as a paraphyletic group when analyzed with only the

short 18S gene, but was resolved as monophyletic when 28S was also included. However, this may be misleading due to the fact that few *Ditylenchus* spp. were available on GenBank with both 18S and 28S data for our alignment.

Cf. *Ektaphelenchus* sp.

With the exception of studies of some parasitic Allantonematidae and Aphelenchoididae by Tomalak et al. (1988, 1989), there has been a paucity of research on the endoparasitic nematodes of bark beetles since Massey (1974), Thong (1973) and Thong and Webster (1975) whose work predates modern molecular tools. Larvae of cf. *Ektaphelenchus* were produced oviparously rather than ovoviviparously, and in this regard they are more similar to *Contortylenchus* than to *Parasitylenchus* (=*Ektaphelenchus*) among well-known described genera with parasitic females of similar size and length from the haemocoel of bark beetles (~ 0.8 to 1.5 mm; Massey, 1974). However, 18S barcode sequences were only 87% similar to representative sequences for *Ektaphelenchus* and *Ektaphelenchoides*. Though they grouped with strong support with *Ektaphelenchus*, combined rDNA+mtDNA sequences differed significantly from available sequences, as shown by long branch-lengths, which could indicate that this species belongs to a different genus of parasitic nematodes for which these three barcode sequences are not yet available. The effect of cf. *Ektaphelenchus* sp. from our study, as well as other endoparasitic nematodes implicated in regulating population dynamics of other destructive bark beetles, on the reproduction and development of *P. juglandis* certainly merits future investigation.

5.4.3 Conclusions

P. juglandis fulfills all the requirements to be considered a vector of plant disease (Leach, 1940), but there remains some debate as to the importance of pathogenicity of *G. morbida* in TCD etiology (Juzwik et al., 2020, Kasson et al., 2014). In other destructive species of bark beetles, primary and secondary fungal associates in the Ophiostomatales cause staining in the sapwood, fulfill important nutritional roles and/or weaken the host and thereby facilitate mass attack to overcome host defenses (Raffa et al., 2015). In novel encounters, some virulently pathogenic fungi in the Microascales and the Ophiostomatales that are associated with bark and ambrosia beetles elicit a vascular response in susceptible, naïve hosts that leads to mortality (Ploetz et al., 2013). In

contrast, other beetles like *P. juglandis* associate with comparatively weak pathogens in the Hypocreales (*e.g.*, *Geosmithia* and *Fusarium* spp.).

Current thinking on TCD attributes crown decline to critical damage to the phloem due to attacks and feeding by large vector populations. This damage would presumably interfere with translocation of phyllosphere-generated photosynthate and nitrogen to roots, but not immediate crown dieback. With the functional xylem intact, interference with the supply of water and mineral nutrients to which crown decline (either senescence or wilting) is generally attributed would be delayed due to gradual starvation of the root system. In order for trees to die within three years as observed by Tisserat et al., (2009), *P. juglandis* would need to reach very high population levels very quickly, which is possible but not always observed. A possible alternative explanation is that *G. morbida* also occludes the xylem; gen. *Geosmithia* includes ambrosial fungi that colonize the sapwood (Kolarik & Kirkendall, 2010, Veselská et al., 2019) and in our study *G. morbida* colonized sapwood parenchyma as well as mature xylem.

Another explanation of the inconsistencies between TCD symptomology and vector, pathogen and host biology is that other associates, including fungal and invertebrate antagonists and synergists, could be involved in modulating the severity of disease through interactions with pathogens, host trees, and/or regulation of vector populations. Relative to their diversity and potential importance, there have been few studies of interactions between nematodes and bark beetles. Since the potential of parasites to regulate pest populations was emphasized by Massey (1966) over 50 years ago, our understanding of their biology has advanced very little considering the advent of molecular biology and other techniques. Most studies of bark-beetle associates have focused on *Bursaphelenchus* spp., due to the presence of important plant pathogens in the genus. Recently, the importance of other groups of nematodes as pathogens or potential pathogens in aboveground tissues of trees has been recognized (Carta et al., 2016, 2020). The role of fungal-feeding free-living nematodes such as *Panagrolaimus* in the bark of trees has received even less attention. Our findings support the need for further investigation of the beneficial and detrimental roles of nematodes in the context of insect-fungal disease complexes.

5.5 References

Aikawa, T. (2008). Transmission biology of *Bursaphelenchus xylophilus* in relation to its insect vector. In *Pine wilt disease* (pp. 123–138). Springer.

Altschul, S. (1990). Basic Local Alignment Search Tool. *Journal of Molecular Biology*, 215, 403–410. https://doi.org/10.1006/jmbi.1990.9999

Anderbrant, O. (1990). Gallery construction and oviposition of the bark beetle *Ips typographus* (Coleoptera: Scolytidae) at different breeding densities. *Ecological Entomology*, 15, 1–8.

Aroian, R. V, Carta, L. K., Kaloshian, I., & Sternberg, P. W. (1993). A free-living *Panagrolaimus* sp. from Armenia can survive in anhydrobiosis for 8.7 years. *Journal of Nematology*, 25, 500.

Baynes, M. A., Russell, D. M., Newcombe, G., Carta, L. K., Rossman, A. Y., & Ismaiel, A. (2012). A mutualistic interaction between a fungivorous nematode and a fungus within the endophytic community of *Bromus tectorum*. *Fungal Ecology*, 5, 610–623.

Bettini, P. P., Frascella, A., Kolařík, M., Comparini, C., Pepori, A. L., Santini, A, Scala, F., & Scala, A. (2014). Widespread horizontal transfer of the cerato-ulmin gene between *Ophiostoma novo-ulmi* and *Geosmithia* species. *Fungal Biology*, 118, 663–674. https://doi.org/https://doi.org/10.1016/j.funbio.2014.04.007

Brzeski, M. W. (1991). Review of the genus *Ditylenchus* Filipjev, 1936 (Nematoda: Anguinidae). *Revue de Nématologie*, 14, 9–59.

Carbone, I., White, J. B., Miadlikowska, J., Arnold, A. E., Miller, M. A., Kauff, F., U'Ren, J., May, G, & Lutzoni, F. (2017). T-BAS: Tree-Based Alignment Selector toolkit for phylogenetic-based placement, alignment downloads and metadata visualization: An example with the Pezizomycotina tree of life. *Bioinformatics*. https://doi.org/10.1093/bioinformatics/btw808

Cardoza, Y. J., Moser, J. C., Klepzig, K. D., & Raffa, K. F. (2008). Multipartite symbioses among fungi, mites, nematodes, and the spruce beetle, *Dendroctonus rufipennis*. *Environmental Entomology*, 37, 956–963.

Cardoza, Y. J., Paskewitz, S., & Raffa, K. F. (2006). Travelling through time and space on wings of beetles: a tripartite insect-fungi-nematode association. *Symbiosis*, 41, 71.

Carta, L. K., Bauchan, G., Hsu, C. Y., & Yuceer, C. (2010). Description of *Parasitorhabditis frontali* n. sp.(Nemata: Rhabditida) from *Dendroctonus frontalis* Zimmermann (Coleoptera: Scolytidae). *Journal of Nematology*, 42, 46.

Carta, L. K., Handoo, Z. A., Li, S., Kantor, M., Bauchan, G., McCann, D., Gabriell, C. K., Yu, Q., Reed, S., Koch, J., Martin, D., & Burke, D. J. (2020). Beech leaf disease symptoms caused by newly recognized nematode subspecies *Litylenchus crenatae mccannii* (Anguinata) described from *Fagus grandifolia* in North America. *Forest Pathology*, 50, e12580.

Carta, L. K., & Li, S. (2019). PCR amplification of a long rDNA segment with one primer pair in agriculturally important nematodes. *Journal of Nematology*, 51.

Carta, L. K., Li, S., Skantar, A. M., & Newcombe, G. (2016). Morphological and molecular characterization of two *Aphelenchoides* endophytic in poplar leaves. *Journal of Nematology*, 48, 28.

Čermák, V., Vieira, P., Gaar, V., Čudejková, M., Foit, J., Široká, K., & Mota, M. (2012). *Bursaphelenchus pinophilus* Brzeski & Baujard, 1997 (Nematoda: Parasitaphelenchinae) associated with nematangia on *Pityogenes bidentatus* (Herbst, 1783) (Coleoptera: Scolytinae), from the Czech Republic. *Nematology*, 14, 385–387.

Chen, J., & Ferris, H. (1999). The effects of nematode grazing on nitrogen mineralization during fungal decomposition of organic matter. *Soil Biology and Biochemistry*, 31, 1265–1279.

Crook, M. (2014). The dauer hypothesis and the evolution of parasitism: 20years on and still going strong. *International Journal for Parasitology*, 44, 1–8. https://doi.org/https://doi.org/10.1016/j.ijpara.2013.08.004

Eisenback, J. D., & Paes-Takahashi, V. (2015). Vertical distribution of nematode communities in the bark of a black walnut tree. *Journal of nematology*, 47, 234.

Enright, M. C., & Spratt, B. G. (1999). Multilocus sequence typing. *Trends in Microbiology*, 7, 482–487. https://doi.org/https://doi.org/10.1016/S0966-842X(99)01609-1

Ewing, C. J., Hausman, C. E., Pogacnik, J., Slot, J., & Bonello, P. (2019). Beech leaf disease: An emerging forest epidemic. *Forest Pathology*, 49.

Fukuda, K. (1997). Physiological process of the symptom development and resistance mechanism in pine wilt disease. *Journal of Forest Research*, 2, 171–181. https://doi.org/10.1007/BF02348216

Fukushige, H. (1991). Effects of Fungi Coexisting with *Ceratocystis* sp. on Propagation of *Bursaphelenchus xylophilus* (Nematoda: Aphelenchoididae). *Applied Entomology and Zoology*, 26, 377–380.

Furniss, M. M. (1967). Nematode Parasites of the Douglas-Fir Beetle in Idaho and Utah. *Journal of Economic Entomology*, 60, 1323–1326. https://doi.org/10.1093/jee/60.5.1323

García De la Cruz, R., Knudsen, G. R., Carta, L. K., & Newcombe, G. (2018). Either low inoculum or a multi-trophic interaction can reduce the ability of *Sclerotinia sclerotiorum* to kill an invasive plant. *Rhizosphere*, *5*, 76–80. https://doi.org/https://doi.org/10.1016/j.rhisph.2018.01.002

Griffin, G. J. (2015). Status of thousand cankers disease on eastern black walnut in the eastern United States at two locations over 3 years. *Forest Pathology*, 45, 203–214. https://doi.org/10.1111/efp.12154

Griffin, G. J., Eisenback, J. D., Yancey, M. M., & Templeton, J. (2009). *Aphelenchoides hylurgi* as a carrier of white, hypovirulent *Cryphonectria parasitica* and its possible role in hypovirulence spread on blight-controlled American chestnut trees. *Journal of Nematology*, 41, 267. Retrieved from http://www.ncbi.nlm.nih.gov/pmc/articles/PMC3381461/

Hofstetter, R. W., Dempsey, T., Klepzig, K., & Ayres, M. (2007). Temperature-dependent effects on mutualistic, antagonistic, and commensalistic interactions among insects, fungi and mites. *Community Ecology*, 8, 47–56. https://doi.org/10.1556/comec.8.2007.1.7

Hofstetter, R. W., Dinkins-Bookwalter, J., Davis, T. S., & Klepzig, K. D. (2015). Symbiotic associations of bark beetles. In F. Vega and R. Hofstetter (Eds.), *Bark Beetles: Biology and Ecology of Native and Invasive Species* (pp 209–245). Academic Press.

Hofstetter, R. W., & Moser, J. C. (2014). The Role of Mites in Insect-Fungus Associations. *Annual Review of Entomology*, 59, 537–557. https://doi.org/10.1146/annurev-ento-011613-162039

Juzwik, J., Moore, M., Williams, G., & Ginzel, M. (2020). Assessment and etiology of thousand cankers disease within the native range of black walnut (*Juglans nigra*). In K. M. Potter & B. L. Conkling (Eds.), *Forest health monitoring: national status, trends, and analysis 2019. Gen. Tech. Rep. SRS-250.* (Vol. 2020, pp. 169–178). Asheville, NC: US Department of Agriculture, Forest Service, Southern Research Station.

Kanzaki, N. (2008). Taxonomy and systematics of the nematode genus *Bursaphelenchus* (Nematoda: Parasitaphelenchidae). In B. G. Zhao, K. Futai, J. R. Sutherland, & Y. Takeuchi (Eds.), *Pine Wilt Disease* (pp. 44–66). Springer Japan.

Kanzaki, N., & Giblin-Davis, R. M. (2014). Phylogenetic Status and Morphological Characters of *Rhabditolaimus anoplophorae* (Rhabditida: Diplogastridae). *Journal of Nematology*, 46, 44–49. Retrieved from https://pubmed.ncbi.nlm.nih.gov/24644370

Kanzaki, N., & Giblin-Davis, R. M. (2018). Diversity and plant pathogenicity of *Bursaphelenchus* and related nematodes in relation to their vector bionomics. *Current Forestry Reports*, 4, 85–100. https://doi.org/10.1007/s40725-018-0074-7

Kanzaki, N., Giblin-Davis, R. M., Cardoza, Y. J., Ye, W., Raffa, K. F., & Center, B. J. (2008). *Bursaphelenchus rufipennis* n. sp.(Nematoda: Parasitaphelenchinae) and redescription of *Ektaphelenchus obtusus* (Nematoda: Ektaphelenchinae), associates from nematangia on the hind wings of *Dendroctonus rufipennis* (Coleoptera: Scolytidae). *Nematology*, 10, 925–955.

Kanzaki, N., Giblin-Davis, R. M., Scheffrahn, R. H., Taki, H., Esquivel, A., Davies, K. A., & Herre, E. A. (2012). Reverse Taxonomy for Elucidating Diversity of Insect-Associated Nematodes: A Case Study with Termites. *PLoS ONE*, 7. https://doi.org/10.1371/journal.pone.0043865

Kanzaki, N., Maehara, N., Aikawa, T., Giblin-Davis, R. M., & Center, B. J. (2009). The first report of a putative "entomoparasitic adult form" in *Bursaphelenchus*. *Journal of Parasitology*, 95, 113–119.

Kanzaki, N., Maehara, N., Aikawa, T., & Nakamura, K. (2013). An entomoparasitic adult form in *Bursaphelenchus doui* (Nematoda: Tylenchomorpha) associated with *Acalolepta fraudatrix*. *The Journal of Parasitology*, 99, 803–815.

Kasson, M., Griffin, G., Geiser, D., O'Neal, E., Juzwik, J., Reed, S., Tisserat, N., Turcotte, R., Martin, D., Davis, D., Fenstermacher, K., & O'Donnel, K. 2014. New perspectives on thousand cankers disease of walnut. *Phytopathology* 104 (S11), 148–148.

Klepzig, K. D., Moser, J. C., Lombardero, F. J., Hofstetter, R. W., & Ayres, M. P. (2001). Symbiosis and competition: complex interactions among beetles, fungi, and mites. *Symbiosis*, 30, 83–96.

Kolařík, M., Freeland, E., Utley, C., & Tisserat, N. (2011). *Geosmithia morbida* sp. nov., a new phytopathogenic species living in symbiosis with the walnut twig beetle (*Pityophthorus juglandis*) on *Juglans* in USA. *Mycologia*, 103. https://doi.org/10.3852/10-124

Kolařík, M., & Kirkendall, L. R. (2010). Evidence for a new lineage of primary ambrosia fungi in *Geosmithia* Pitt (Ascomycota: Hypocreales). *Fungal Biology*, 114, 676–689.

Kumar, S., Stecher, G., Li, M., Knyaz, C., & Tamura, K. (2018). MEGA X: molecular evolutionary genetics analysis across computing platforms. *Molecular Biology and Evolution*, 35, 1547–1549.

Kuroda, K. (1991). Mechanism of cavitation development in the pine wilt disease. *European Journal of Forest Pathology*, 21, 82–89.

Lamichhane, J. R., & Venturi, V. (2015). Synergisms between microbial pathogens in plant disease complexes: A growing trend. *Frontiers in Plant Science*, *6*(MAY), 1–12. https://doi.org/10.3389/fpls.2015.00385

Lauritzen, J. E. (2018). Characterization of Black Walnut Genotypes for Resistance to Thousand Cankers Disease, Frost Hardiness and Other Desirable Horticultural Traits. PhD Thesis. Utah State University, Logan, UT. Utah State Universiy.

Leach, J. G. (1940). *Insect transmission of plant diseases. Insect transmission of plant diseases.* New York, NY: McGraw-Hill.

Lieutier, F. (1982). The variations of the weight of the fat-body and the ovaries, and the variations of the length of the ovocytes in *Ips sexdentatus* (Coleoptera, Scolytidae) - relations with the parasitism by the nematodes. *Annales De Parasitologie Humaine Et Comparee*, 57, 407–418.

Macguidwin, A. E., Macguidwin, G. C., Wilkinson, R. C., & Allen, G. E. (1980). Effect of the nematode *Contortylenchus brevicomi* on gallery construction and fecundity of the southern pine beetle. *Journal of Nematology*, 12, 4.

Mai, W. F., Mullin, P. G., Lyon, H. H., & Loeffler, K. (1996). *Plant-parasitic nematodes: a pictorial key to genera*. Ithaca, NY: Cornell University Press.

Massey, C. L. (1966). The influence of nematode parasites and associates on bark beetles in the United States. *Bulletin of the ESA*, 12, 384–386.

Massey, C. L. (1974). Biology and taxonomy of nematode parasites and associates of bark beetles in the United States. *Agricultural Handbook No*. 446. U. S. Department of Agriculture.

Mayfield III, A. E., Fraedrich, S. W., Taylor, A., Merten, P., & Myers, S. W. (2014). Efficacy of heat treatment for the thousand cankers disease vector and pathogen in small black walnut logs. *Journal of Economic Entomology*, 107, 174–184.

McCambridge, W. F., & Knight, F. B. (1972). Factors affecting spruce beetles during a small outbreak. *Ecology*, 53, 5.

McElrone, A. J., Grant, J. A., & Kluepfel, D. A. (2010). The role of tyloses in crown hydraulic failure of mature walnut trees afflicted by apoplexy disorder. *Tree Physiology*, 30, 761–772.

McKenna, J. R., Sitz, R. A., Tisserat, N., Carlson, D., & Bloese, P. (2020). Screening range-wide black walnut seed families for thousand cankers disease (TCD) resistance and measuring the regional adaptability of resistant seed sources. In D. Nelson, J. Koch, & R. A. Sniezko (Eds.), *Proceedings of the Sixth International Workshop on the Genetics of Host-Parasite Interactions in Forestry—Tree Resistance to Insects and Diseases: Putting Promise into Practice.* e-Gen Tech Rep. Asheville, NC: U.S. Department of Agriculture Forest Service, Southern Research Station. 170 p.

Montecchio, L., Fanchin, G., Berton, V., & Scattolin, L. (2015). Vegetative incompatibility and potential involvement of a mycovirus in the Italian population of *Geosmithia morbida*. *Phytopathologia Mediterranea*. https://doi.org/10.14601/Phytopathol_Mediterr-16376

Moser, J. C., Konrad, H., Blomquist, S. R., & Kirisits, T. (2010). Do mites phoretic on elm bark beetles contribute to the transmission of Dutch elm disease? *Naturwissenschaften*, 97, 219–227. https://doi.org/10.1007/s00114-009-0630-x

Newton, L., & Fowler, G. (2009). Pathway Assessment: *Geosmithia* sp. and *Pityophthorus juglandis* Blackman movement from the western into the eastern United States. In K. A. McManus, K. W. Gottschalk (Eds.), *Proceedings of the 21st U.S. Department of Agriculture interagency research forum on invasive species. January 12-15, Annapolis, MD. General Technical Report NRS-P-75.* U. S. Department of Agriculture, Forest Service, Northern Research Station 112. Available online https://www.uaex.edu/environment-nature/ar-invasives/invasive-diseases/docs/Thousand-Cankers Disease.pdf.

Oldham, J. N. (1930). On the infestation of elm bark beetles (Scolytidae) by a nematode, *Parasitylenchus scolyti* n. sp. *Journal of Helminthology*, 8, 239–248.

Onufrak, A. J., Williams, G. M., Klingeman, W. E., Cregger, M. A., Klingeman, D. M., DeBruyn, J. M., Ginzel, M. D., & Hadžiabdić, Đ.. (2020). Regional Differences in the Structure of *Juglans nigra* Phytobiome Reflect Geographical Differences in Thousand Cankers Disease Severity. *Phytobiomes Journal*, 4, 388–404. https://doi.org/10.1094/PBIOMES-05-20-0044-R

Penas, A. C., Bravo, M. A., Naves, P., Bonifácio, L., Sousa, E., & Mota, M. (2006). Species of *Bursaphelenchus* Fuchs, 1937 (Nematoda: Parasitaphelenchidae) and other nematode genera associated with insects from Pinus pinaster in Portugal. *Annals of Applied Biology*, 148, 121–131.

Pepori, A. L., Bettini, P. P., Comparini, C., Sarrocco, S., Bonini, A., Frascella, A., Ghelardini, L, Scala, A., Vannacci, G,. & Santini, A. (2018). *Geosmithia-Ophiostoma*: a New Fungus-Fungus Association. *Microbial Ecology*, 75, 632–646. https://doi.org/10.1007/s00248-017-1062-3

Ploetz, R. C., Hulcr, J., Wingfield, M. J., & de Beer, Z. W. (2013). Destructive Tree Diseases Associated with Ambrosia and Bark Beetles: Black Swan Events in Tree Pathology? *Plant Disease*, 97, 856–872. https://doi.org/10.1094/PDIS-01-13-0056-FE

Prosser, S. W. J., Velarde-Aguilar, M. G., León-Règagnon, V., & Hebert, P. D. N. (2013). Advancing nematode barcoding: A primer cocktail for the cytochrome c oxidase subunit I gene from vertebrate parasitic nematodes. *Molecular Ecology Resources*, 13, 1108–1115. https://doi.org/10.1111/1755-0998.12082

Raffa, K. F., Gregoire, J.-C., & Lindgren, B. S. (2015). Natural history and ecology of bark beetles. *Bark Beetles. Biology and Ecology of Native and Invasive Species*, 1–40.

Reid, R. W. (1958). Nematodes associated with the mountain pine beetle. *Canadian Dept Ag Sci Serv Forest Biol Div Bi-Monthly Prog Rep*.

Ronquist, F., & Huelsenbeck, J. P. (2003). MrBayes 3: Bayesian phylogenetic inference under mixed models. *Bioinformatics*, 19, 1572–1574.

Ryss, A. Y., Parker, C., Álvarez-Ortega, S., Nadler, S. A., & Subbotin, S. A. (2020). *Bursaphelenchus juglandis* n. sp.(Nematoda: Aphelenchoididae), an associate of walnut twig beetle, Pityophthorus juglandis, the vector of thousand cankers disease. *Nematology*, *1*(aop), 1–30.

Ryss, A. Y., Polyanina, K. S., Álvarez-Ortega, S., & Subbotin, S. A. (2021). Morphology, development stages, and phylogeny of the *Rhabditolaimus ulmi* (Nematoda: Diplogastridae), a phoront of the bark beetle *Scolytus multistriatus* from the elm *Ulmus glabra* Huds. in Northwest Russia. *Journal of Nematology*, *53*, e2021-25. https://doi.org/10.21307/jofnem-2021-025

Ryss, A. Y., Polyanina, K. S., Popovichev, B. G., & Subbotin, S. A. (2015). Description of *Bursaphelenchus ulmophilus* sp. n. (Nematoda: Parasitaphelenchinae) associated with Dutch elm disease of *Ulmus glabra* Huds. in the Russian North West. *Nematology*, 17, 685–703. https://doi.org/10.1163/15685411-00002902

Schloss, P. D., Westcott, S. L., Ryabin, T., Hall, J. R., Hartmann, M., Hollister, E. B., Lesniewski, R. A., Oakley, B. B., Parks, D. H., Robinson, C. J., Sahl, J. W., Stres, B., Thallinger, G. G., Horn, D. J. V., & Weber, C. F. (2009). Introducing mothur: Open-source, platform-independent, community-supported software for describing and comparing microbial communities. *Applied and Environmental Microbiology*, 75. https://doi.org/10.1128/AEM.01541-09

Self, L. H., & Bernard, E. C. (1994). Association of Nematodes and Dogwood Cankers. *Journal of Nematology*, 26.

Seybold, S. J., Klingeman III, W. E., Hishinuma, S. M., Coleman, T. W., & Graves, A. D. (2019). Status and Impact of Walnut Twig Beetle in Urban Forest, Orchard, and Native Forest Ecosystems. *Journal of Forestry*, 117, 152–163. https://doi.org/10.1093/jofore/fvy081

Shannon, A. J. (2005). The anhydrobiotic potential and molecular phylogenetics of species and strains of *Panagrolaimus* (Nematoda, Panagrolaimidae). *Journal of Experimental Biology*, 208. https://doi.org/10.1242/jeb.01629

Shimizu, A., Tanaka, R., Akiba, M., Masuya, H., Iwata, R., Fukuda, K., & Kanzaki, N. (2013). Nematodes Associated With *Dryocoetes uniseriatus* (Coleoptera: Scolytidae). *Environmental Entomology*, 42, 79–88.

Sitz, R. A., Luna, E., Ibarra Caballero, J., Tisserat, N., Cranshaw, W. S., McKenna, J. R., Stoltz, J., & Stewart, J. (2021). Eastern black walnut (*Juglans nigra* L.) originating from native range varies in their response to inoculation with *Geosmithia morbida*. *Frontiers in Forests and Global Change* 4:12. doi.org/10.3389/ffgc.2021.627911.

Six, D. L. (2013). The Bark Beetle Holobiont: Why Microbes Matter. *Journal of Chemical Ecology*, 39. https://doi.org/10.1007/s10886-013-0318-8

Stamatakis, A. (2014). RAxML version 8: a tool for phylogenetic analysis and post-analysis of large phylogenies. *Bioinformatics*, 30, 1312–1313. https://doi.org/10.1093/bioinformatics/btu033

Thong, C. H. S. (1973). Bark beetle nematodes in British Columbia with emphasis on the biology and host-parasite relationship of Contortylenchus reversus. Simon Fraser University: Dissertation.

Thong, C. H. S., & Webster, J. M. (1975a). Effects of bark beetle nematode, contortylenchus-reversus, on gallery construction, fecundity, and egg viability of douglas-fir beetle, *Dendroctonus pseudotsugae* (Coleoptera: Scolytidae). *Journal of Invertebrate Pathology*, 26, 235–238.

Thong, C. H. S., & Webster, J. M. (1975b). Effects of *Contortylenchus reversus* (Nematoda: Sphaerulariidae) on hemolymph composition and oocyte development in beetle *Dendroctonus pseudotsugae* (Coleopteran: Scolytidae). *Journal of Invertebrate Pathology*, 26, 91–98.

Thorne, G. (1935). Nemic parasites and associates of the mountain pine beetle (Dendroctonus monticolae) in Utah. *Journal of Agricultural Research*, 51, 131–144.

Tisserat, N., Cranshaw, W., Leatherman, D., Utley, C., & Alexander, K. (2009). Black walnut mortality in Colorado caused by the walnut twig beetle and thousand cankers disease. *Plant Health Progress* 11, 10. doi:10.1094/php-2009-0811-01-rs.

Tisserat, N., Cranshaw, W., Putnam, M. L., Pscheidt, J., Leslie, C. A., Murray, M., Hoffman, J., Barkley, Y., Alexander, K., & Seybold, S. J. (2011). Thousand Cankers Disease is Widespread in Black Walnut in the Western United States. *Plant Health Progress* 12, 35. doi:10.1094/PHP-2011-0630-01-BR.

Tomalak, M., & Filipiak, A. (2011). *Bursaphelenchus trypophloei* sp. n. (Nematoda: Parasitaphelenchinae)--an associate of the bark beetle, *Trypophloeus asperatus* (Gyll.)(Coleoptera: Curculionidae, Scolytinae). *In Aspen, Populus Tremula L. Nematology*, 13, 619–636.

Tomalak, M., & Filipiak, A. (2014). *Bursaphelenchus fagi* sp. n.(Nematoda: Parasitaphelenchidae), an insect-pathogenic nematode in the Malpighian tubules of the bark beetle, *Taphrorychus bicolor* (Herbst.)(Coleoptera: Curculionidae, Scolytinae) in European beech, *Fagus silvatica* L. *Nematology*, 16, 591–606.

Tomalak, M., & Filipiak, A. (2018). *Bursaphelenchus michalskii* sp. n.(Nematoda: Aphelenchoididae), a nematode associate of the large elm bark beetle, *Scolytus scolytus* Fabr.(Coleoptera: Curculionidae), in Dutch elm disease-affected elm, *Ulmus laevis* Pall. *Nematology*, *1*(aop), 1–18.

Tomalak, M., & Malewski, T. (2014). *Bursaphelenchus tiliae* sp. n. (Nematoda: Parasitaphelenchidae), a nematode associate of the bark beetle *Ernoporus tiliae* (Panz.)(Coleoptera: Curculionidae, Scolytinae) in small-leaved lime, *Tilia cordata* Mill. *Nematology*, 16, 1181–1196.

Tomalak, M., Malewski, T., Gu, J., & Fa-Qiang, Z. (2017). Description of *Bursaphelenchus taphrorychi* sp. n. (Nematoda: Parasitaphelenchidae), the second *Bursaphelenchus* species from larval galleries of the beech bark beetle, *Taphrorychus bicolor* (Herbst.) (Coleoptera. *Nematology*, 19, 1217–1235. https://doi.org/10.1163/15685411-00003121

Tomalak, M., Welch, H. E., & Galloway, T. D. (1988). Interaction of parasitic nematode *Parasitaphelenchus oldhami* (Nematoda: Aphelenchoididae) and a bacterium in Dutch elm disease vector *Hylurgopinus rufipes* (Coleoptera: Scolytidae). *Journal of Invertebrate Pathology*, 52, 301–308.

Tomalak, M., Welch, H. E., & Galloway, T. D. (1989). Nematode parasites of bark beetles (Scolytidae) in southern Manitoba, with descriptions of three new species of *Sulphuretylenchus* Rühm (Nematoda: Allantonematidae). *Canadian Journal of Zoology*, 67, 2497–2505.

Tomalak, M., Worrall, J., & Filipiak, A. (2013). *Bursaphelenchus masseyi* sp. n. (Nematoda: Parasitaphelenchinae)--a nematode associate of the bark beetle, *Trypophloeus populi* Hopkins (Coleoptera: Curculionidae: Scolytinae) in aspen, *Populus tremuloides* Michx. affected by sudden aspen decline in Colorado. *Nematology*, 15, 907–921.

Tomalak, M., Worrall, J., Filipiak, A., & Worrall, J. (2013). *Bursaphelenchus masseyi* sp. n. (Nematoda: Parasitaphelenchinae)--a nematode associate of the bark beetle, *Trypophloeus populi* Hopkins (Coleoptera: Curculionidae: Scolytinae) in aspen, *Populus tremuloides* Michx. affected by sudden aspen decline in Colorado. *Nematology*, 15, 907–921. https://doi.org/10.1163/15685411-00002729

Tóth, T., Lakatos, T., & Koltay, A. (2013). *Lonsdalea quercina* subsp. *populi* subsp. nov., isolated from bark canker of poplar trees. *International Journal of Systematic and Evolutionary Microbiology*, *63*(PART6), 2309–2313. https://doi.org/10.1099/ijs.0.042911-0

U'Ren, J. M., Dalling, J. W., Gallery, R. E., Maddison, D. R., Davis, E. C., Gibson, C. M., & Arnold, A. E. (2009). Diversity and evolutionary origins of fungi associated with seeds of a neotropical pioneer tree: a case study for analysing fungal environmental samples. *Mycological Research*, 113, 432–449. https://doi.org/https://doi.org/10.1016/j.mycres.2008.11.015

Utley, C., Nguyen, T., Roubtsova, T., Coggeshall, M., Ford, T. M., Grauke, L. J., Graves, A D., Leslie, C. A., McKenna, J., Woeste, K., Yaghmour, M A., Cranshaw, W., Seybold, S. J., Bostock, R. M., & Tisserat, M. (2013). Susceptibility of Walnut and Hickory Species to *Geosmithia morbida*. *Plant Disease* 97, 601–607. doi:10.1094/PDIS-07-12-0636-RE.

Van Bezooijen, J. (2006). *Methods and techniques for nematology*. Wageningen University Wageningen.

Veselská, T., Skelton, J., Kostovčík, M., Hulcr, J., Baldrian, P., Chudíčková, M., Cajthaml, T., Vojtová, T., Garcia-Fraile, P., & Kolařík, M. (2019). Adaptive traits of bark and ambrosia beetle-associated fungi. *Fungal Ecology*, *41*, 165–176.

Weed, A. S., Ayres, M. P., & Bentz, B. J. (2015). Population Dynamics of bark beetles. In F. Vega & R. W. Hofstetter (Eds.), *Bark beetles: biology and ecology of native and invasive species. Elsevier Inc, CA* (pp. 209–245). San Diego: Academic Press. https://doi.org/10.1016/B978-0-12-417156-5.00004-6

Yazaki, K., Takanashi, T., Kanzaki, N., Komatsu, M., Levia, D. F., Kabeya, D., Tobita, H., Kitao, M., & Ishida, A. (2017). Pine wilt disease causes cavitation around the resin canals and irrecoverable xylem conduit dysfunction. *Journal of Experimental Botany*, 69, 589–602. https://doi.org/10.1093/jxb/erx417

Zalamea, P.-C., Sarmiento, C., Arnold, A. E., Davis, A. S., Ferrer, A., & Dalling, J. W. (2021). Closely related tree species support distinct communities of seed-associated fungi in a lowland tropical forest. *Journal of Ecology*, 109, 1858–1872. https://doi.org/https://doi.org/10.1111/1365-2745.13611

Zhao, L., Mota, M., Vieira, P., Butcher, R. A., & Sun, J. (2014). Interspecific communication between pinewood nematode, its insect vector, and associated microbes. *Trends in Parasitology*, 30, 299–308. https://doi.org/10.1016/j.pt.2014.04.007

Zhao, L., Wei, W., Kang, L., & Sun, J. H. (2007). Chemotaxis of the pinewood nematode, *Bursaphelenchus xylophilus*, to volatiles associated with host pine, *Pinus massoniana*, and its vector *Monochamus alternatus*. *Journal of Chemical Ecology*, 33, 1207–1216.

CHAPTER 6. THE CULTURABLE ROOT AND STEM ENDOSPHERE OF *JUGLANS NIGRA* DIFFERS BETWEEN TRAP SEEDLINGS GROWN IN THE NATIVE AND NON-NATIVE RANGE

6.1 Introduction

The phytobiome plays an important role in mediating resistance and susceptibility of host plants to disease (Rodriguez et al., 2009, Porras-Alfaro & Bayman, 2011, Busby et al., 2016b, 2017, Pineda et al., 2017, Schlatter et al., 2017) and in mediating the severity of diseases of trees in natural and managed forest ecosystems (Newcombe, 2011, Witzell et al., 2014, Witzell & Martín, 2018). In particular, the host microbiome influences the etiology of thousand canker disease (TCD) (Chapter 3), a bark beetle-fungal disease complex that causes decline and mortality in hosts in the genus *Juglans* and *Pterocarya* spp. (Fagales, Juglandaceae) in North America and Europe (Tisserat et al., 2009, Montecchio et al., 2016, Seybold et al., 2019, Moricca et al., 2020). Among the Juglandaceae, *J. nigra* L. is the most susceptible host for the fungal pathogen component of TCD, *Geosmithia morbida* Kol. Free. Ut. & Tiss. (Utley et al., 2012). *J. nigra* is also an ecologically and economically valuable species native to the Central Hardwood Forest Region, Appalachian Mountains, and southeastern U.S. (Newton & Fowler, 2009). There is a need for a better understanding of specific factors that may predispose *J. nigra* to TCD.

TCD has a severe and detrimental impact on the health and productivity of *J. nigra* planted in the western U.S., but has not caused significant mortality where it has been detected within the native range of *J. nigra*. Previous studies found that *Trichoderma* spp. may control *G. morbida* in the native range and that low moisture and high temperature conditions favor the competitive success of *G. morbida* when it interacts with *Trichoderma* spp. and other fungi in walnut wood (Gazis et al., 2018, Chapter 4). Thus, climate and the phytobiome in the western U.S. are likely to be more conducive to the survival and sporulation of *G. morbida* in galleries and therefore, its transmission by its vector in the western U.S. There are distinct microbial assemblages associated with aboveground tissues and soils below trees infected with *G. morbida* in comparison with healthy trees (Onufrak et al., 2020). *G. morbida* infection also induces shifts in the composition of fungal communities in the root and shoot endospheres that may contribute to the development of disease (Onufrak et al., 2020, Chapter 3).

Previous studies relied on collecting branches or bulk soil beneath walnut trees (Onufrak et al. 202) or amending intensively produced nursery stock with forest soil in the greenhouse (Chapter 3). The community of microfungi colonizing the root endosphere of *J. nigra* in the field, the extent to which these colonizers persist and influence microbiome assembly, and consequences for plant disease have not been characterized or compared between the native and introduced range of *J. nigra*.

Moreover, little is known about the fungal and bacterial microbiome associated directly with black walnut roots under field conditions, with the exception of a small number of studies on mycorrhizae and bacteria. Black walnut associates with a wide range of arbuscular mycorrhizal (AM) fungi, but is not known to associate with ectomycorrhizal (ECM) fungi (Kormanik et al., 1982; Dixon, 1988, Ponder et al., 1990, Wang & Qiu, 2006). Arbuscular mycorrhizal fungi increase growth and nutrient uptake, but these benefits and colonization of seedlings differ across fungal species and soils (Kormanik et al., 1982; Ponder, 1983, 1986, Ponder Jr. 1984; Kormanik, 1985, Melichar et al., 1986; Dixon, 1988). Current knowledge of mycorrhizal associations of *J. nigra* and related species have been geographically limited and potential associations with lesser-known functional groups of symbiotic fungi such as dark septate endophytes (DSE) and ericoid or orchid mycorrhizae have not been further investigated (Jummponen & Trappe, 1998, Yukawa et al., 2009, Oberwinkler et al., 2013, Tedersoo et al., 2020).

We hypothesized that fungal root endosphere communities derived from different locations in the native and introduced range would differ a) in taxonomic composition; b) in their response to host stress caused by aboveground infection with the pathogen *G. morbida*; and c) in their effect on host resistance or susceptibility to *G. morbida*. To test our hypotheses, we cultured fungi that colonized *J. nigra* "trap seedlings" that germinated in plots in Indiana (IN; native range of *J. nigra*) and Washington (WA; non-native range). We compared community composition among plots and States as well as the amount of phloem necrosis caused by inoculation with *G. morbida*. Additional objectives were to obtain baseline data and a physical collection of the fungi that colonized roots of *J. nigra* in its native and introduced range. Additionally, we investigated specific mechanisms of disease modification attributed to the microbiome by identifying taxa that were positively or negatively associated with one another and with larger- or smaller-sized cankers.

6.2 Methods

6.2.1 Planting Trap Seedlings in the Field in IN and WA

Trap seedlings were grown from seeds sown and germinated in the field to "trap" fungi that colonized their roots in different locations. A total of 225 seeds were collected in 2018 from improved *J. nigra* genotypes at the Hardwood Tree Improvement and Regeneration Center (HTIRC) at Martell Forest (West Lafayette, IN; 40°25'60.0"N, 87°02'07.3"W). Seeds were cleaned thoroughly and cold-stratified according to HTIRC protocols (J. McKenna, *unpublished protocols*). In May 2019, seeds were planted in walnut plantations at Martell Forest and on a landowner's property in Walla Walla, WA. Prior to planting the soil was turned by a gas-powered rototiller. In both IN and WA, individual seeds were planted at approximately 50-cm spacing in three plots (n = 25 seeds per plot) to provide variation in the microbiome within each site. In IN, one plot was located in a seed orchard and the other two in plantations aged approximately 25 and 50 years. WA plots were located at the margins of a 25-year-old plantation. Each seed was protected from squirrels aboveground with chicken-wire and belowground to a depth of approximately 7.5 cm with a tube of lightweight corrugated plastic. Each plot was surrounded by a 2-m-tall plastic-mesh deer exclosure to discourage herbivory (Redick & Jacobs, 2020). In WA, plots were placed on supplemental biweekly irrigation to account for the relatively dry growing season. Prior weed management had eliminated most competing vegetation in WA, but in IN weeds were treated with glyphosate prior to turning the soil and again midseason.

6.2.2 Transplanting, inoculation in the greenhouse and measurement of necrotic area

In February 2020, the dormant one-year-old trap seedlings colonized by fungi in the field were excavated using a shovel, wrapped in peat moss that had been autoclaved three times for 40 minutes at 15 PSI and 121°C with 24-hour cooling periods between cycles, and then stored at 4°C until transplanting. To maintain rhizosphere microbiota from the soil in which they had germinated and grown in the field, the roots of the trap seedlings were not washed. Instead of washing roots, soil was gently shaken from the roots. Seedlings were transplanted March 20-21, 2020 at the Environmental Entomology Lab (EEL, Purdue University, West Lafayette, IN) to 9.6 L TP818 Treepots (Stuewe and Sons, Corvallis, OR) filled with Metro-Mix 560SC potting media that had

been heat-pasteurized in a 54 Soil Steamer (Hummert International, Topeka, KS) twice for 5-6 hours at 30 PSIG and 274°C with a 24-hour cooling period. The 560SC potting mix was not amended but supplemental fertilizer was applied to the leaves per label instructions when they showed signs of nutrient deficiency.

Approximately 90 days after transplanting (June 22, 2020), each seedling was inoculated at 5 and 10 cm above the root collar with a spore suspension of *G. morbida* isolate IN-66 (100,000 uL^{-1} in 1:10K Tween 20 and sterile distilled H_2O) or control (1:10K Tween 20 and sterile distilled H_2O) as described previously (Chapter 3). In 2019, germination was lower in IN than WA, so the experimental design was revised to allow for both a roughly balanced comparision of inoculated seedlings between States and comparison of *G. morbida*-inoculated and control-inoculated seedlings from WA only. In IN, a total of 25 seedlings across Plot 1 (n = 14) and Plot 2 (n = 12) were inoculated with *G. morbida*; no seedlings germinated in IN Plot 3; and no seedlings from IN received control inoculations. In WA, a total of 27 seedlings across Plot 1 (n = 8), Plot 2 (n = 10), and Plot 3 (n = 9) were inoculated with *G. morbida*; and a total of 21 seedlings across Plot 1 (n = 7), Plot 2 (n = 10), and Plot 3 (n = 4) received control inoculations. Seedlings were harvested 77 days post-inoculation (September 8, 2020). Total area of necrosis was measured as described in Chapter 3. As potential covariates with necrosis, stem caliper at 2.5 cm above the root collar and root volume displacement were measured at the time of harvesting.

All statistical analyses were performed in R 3.6.0 (R Core Team, 2019). Necrosis was analyzed among *G. morbida*-inoculated seedlings using Box-Cox-adjusted mixed effects models. Cankers with area > 200 mm^2 were considered outliers and excluded from the analysis. Root volume, shoot caliper, and the ratio of root volume to shoot caliper (root:shoot ratio) were tested for significance as covariates in regressions comparing necrotic area among States and plots within States. The effect of the State where the seedling was grown on necrotic area was analyzed with analysis of deviance Wald χ^2 test using a nested model with random effects for plot within State and plant within plot. Pairwise differences between plots were also tested with linear contrasts from a model without a State main effect, fixed effects for individual plot, and random effects for plant within plot.

6.2.3 Characterization and Analysis of the Root and Canker Microbiome

Roots were collected and surface-sterilized, and fungi were isolated from them following the methods of Chapter 3 with modification to the types of selective media employed. Briefly, a total of 3,650 lateral roots (~2 cm) were plated (n = 50 per plant) onto five types of growth media (n = 10 root pieces per media per plant): 1/2-strength PDA + 50 g/L chloramphenicol and streptomycin (1/2PDA++); *Fusarium* selective agar (SFA; Leslie & Summerell, 2008); 3% malt agar (Elías-Román et al., 2018) for *Armillaria* spp. + 50 g/L chloramphenicol and streptomycin; glucose-yeast extract-rose Bengal agar (GYRBA; Newhouse & Hunter, 1983) for the selective isolation of *Trichoderma*; and 5 ppm juglone (added as 10 mM acetone stock) mineral salts agar (MSJ) for enrichment of juglone-metabolizing microorganisms (Schmidt, 1988). To validate surface sterilization, a total of 400 randomly selected roots were briefly imprinted onto a total of 40 plates (n = 8 plates per media type). We also isolated fungi from *G. morbida*- and control-inoculated stem tissue. After scanning necrotic tissue for area measurement, it was cut into 2 mm^2 pieces (n = 1 to 5 per plant depending on the amount of necrotic area available). Sections of necrotic area were then surface-sterilized as described in Chapter 3 and plated onto 1/2PDA++.

Root cultures were inspected weekly for fungal growth for 42 days. Canker cultures were checked after 7 to 14 days. All fungi that grew from roots and onto the media were subcultured and maintained on 1/4-strength PDA. Fungi on canker tissue plates were first classified into morphotypes and counted on each plate before voucher specimens were subcultured and maintained on 1/4-strength PDA. Morphotyping was performed on subcultures of the same age. For each batch of isolates subcultured from roots and cankers from a given day (~100-200 per day), the fungi were allowed to grow for 15-30 days, the isolates were then classified into morphotypes under low and high magnification, and two to five isolates were selected as vouchers from each morphospecies from that day. DNA was extracted from the selected vouchers in buffer containing sodium dodecyl sulfate (SDS) and betamercaptoethanol and purified with the phenol-chloroform method described by Lee and Taylor (1990). After 2-4 weeks of growth, apparently pure cultures of fungi were stored at 4°C.

After obtaining DNA barcodes and placing them into molecular operational taxonomic units (MOTUs) as described below, all batches of fungal isolates were sorted together to verify morphotype designations. Voucher cultures for nonsingleton OTUs are deposited at the USDA Agricultural Research Service Culture Collection (NRRL) and the Arthur Fungarium (PUR;

Purdue University, West Lafayette, IN). All representative voucher isolates for OTUs were also photographed without magnification growing on 1/4-strength PDA and stored in the Purdue Forestry and Natural Resources Genetics Lab, to be made available upon request.

Polymerase chain reactions (PCR) were performed to obtain sequence data for the internal transcribed spacer (ITS) and 28S large subunit (LSU) regions of the ribosome (rDNA) from voucher cultures with primers SR6R and LR3 (Vilgalys, 1992). Individual 25uL PCR mixtures contained forward and reverse primers and dNTPs (0.2 mM each), $MgCl_2$ (1.5 mM), Platinum Taq Buffer (1X), and 0.1 uL Platinum Taq Polymerase (Invitrogen Corp.). A touchdown thermal cycle profile was employed with a hot start and initial denaturing at 94°C (4 min); 10 cycles of 94°C (45 sec), 1° decrease/cycle from 58 to 49°C (45 sec), 72°C (1 min); 25 cycles of 94°C (45 sec), 48°C (45 sec), 72°C (1 min); and a final extension at 72°C (10 min). DNA was sequenced with the same primers that were used for PCR at GeneWiz Corp. (South Plainfield, NJ). Sequences from voucher isolates are deposited in GenBank under Accession Nos. MZ423537-MZ423823.

Bases were called and forward- and reverse-reads were assembled and trimmed in Mesquite with the Chromaseq package (Maddison and Maddison 2019a, 2019b). ITS and LSU sequences were extracted with ITSX (Bengtsson-Palme et al., 2013), clustered at 99% sequence similarity and given taxonomic assignments based on multilocus partitioned phylogenetic placement among reference taxa within well-supported trees using the online tool T-BAS (Tree-Based Assignment Selector, Miller et al., 2015, Carbone et al., 2019) on DeCIFR public high-performance computing clusters (Center for Integrated Fungal Research, North Carolina State University; https://decifr.hpc.ncsu.edu). Isolates belonging to Leotiomycetes were aligned to a Leotiomycetes tree and all other Ascomycetes were aligned to the tree Pezizomyctonia 2.1. Basidiomycetes were placed on trees for Sebacinales or *Rhizoctonia*. Isolates not classified to the aforementioned taxa were placed on the tree for all fungi. OTUs were split apart when they contained isolates whose sequences were resolved with different clades on T-BAS trees. For isolates of interest, NCBI-BLAST (http://blast.ncbi.nih.gov) and *Fusarium* MLST (http://fusarium.mycobank.org) searches were also conducted to find the closest available sequence. Synonymy to other described species was checked on Species Fungorum (http://www.speciesfungorum.org).

All downstream community analyses were performed in R 3.6.0 (R Core Team, 2019) with functions from the packages *ape* and *vegan* (Oksanen et al., 2018, Paradis & Schliep, 2019). OTU

abundances were tabulated by combining morphospecies whose voucher sequences clustered to the same OTU and splitting morphospecies whose vouchers were placed in different OTUs after reexamining cultures. For each tissue type (roots and cankers), overall relative abundance of fungal orders was summarized and Shannon diversity of OTUs was compared with ANOVA between States (IN and WA). Relative abundance of fungi were also compared among each State-plot-inoculation combination at the level of family for roots and at the level of genus for cankers.

To analyze beta-diversity among treatments, a community matrix of Jaccard distances was calculated for sites and OTUs containing at least two isolates. Permutational multivariate analyses of community composition (ADONIS) were performed with 9,999 permutations. In separate ADONIS analyses of fungal communities from *G. morbida*-inoculated seedlings: a one-way analysis was performed to compare community composition between States; and a two-way analysis was performed with a factor for State and another factor for plot. In separate ADONIS analyses of fungal communities from WA: separate one-way analyses were performed for plot and for inoculation (*G. morbida vs*. control); a two-way analysis was performed with both plot and inoculation; and an interactive analysis was also conducted. For the visual presentation of differences in community composition among State, block, and inoculation treatment, non-metric multidimensional scaling (NMDS) was employed to reduce dimensionality of a standardized distance matrix to three axes.

To explore relationships between potential disease synergists and antagonists in the root and canker endosphere, we analyzed correlation among fungal taxa and average necrotic area of *G. morbida*-inoculated plants. Spearman rank correlations were calculated among relative abundances of fungal families from roots of seedlings and average necrotic area. Abundance of fungi from cankers were reasonably dispersed, and permitted the use of Pearson correlations of log-transformed relative abundances of fungal genera from cankers and average necrotic area. For visualization of the relative abundance of fungal families from roots according to disease severity, *G. morbida*-inoculated plants from both States were ranked into eight equally proportioned bins by average necrotic area.

6.3 Results

6.3.1 Necrosis in WA vs. IN Seedlings

There was no discernable difference in necrotic area between seedlings from WA and those from IN ($p = 0.58$). However, there were significant differences ($p = 0.01$) in necrosis and variation among individual plots. Necrotic area was lowest overall in IN Plot 1 and generally higher in the three WA plots, while IN Plot 2 had the highest median canker size overall (Fig. 6.1). Necrotic cankers around inoculation points on seedlings that germinated and grew for one year in IN Plot 1 were 25 ± 9 (1 SE) mm^2 smaller than those on seedlings from IN Plot 2 ($p < 0.01$), 29 ± 11 mm^2 smaller than those from WA Plot 1 ($p < 0.01$) and 19 ± 10 mm^2 smaller than those from WA Plot 2 ($p < 0.05$). Necrosis on seedlings from IN Plot 2 and plots in WA were not significantly different from one another ($p > 0.1$). Three cankers in seedlings from WA plots exceeded 200 mm^2 and were excluded as extreme outliers. As a negative covariate in both analyses, root:shoot ratio only marginally accounted for observed variation in necrotic area of inoculated seedlings ($p = 0.11$).

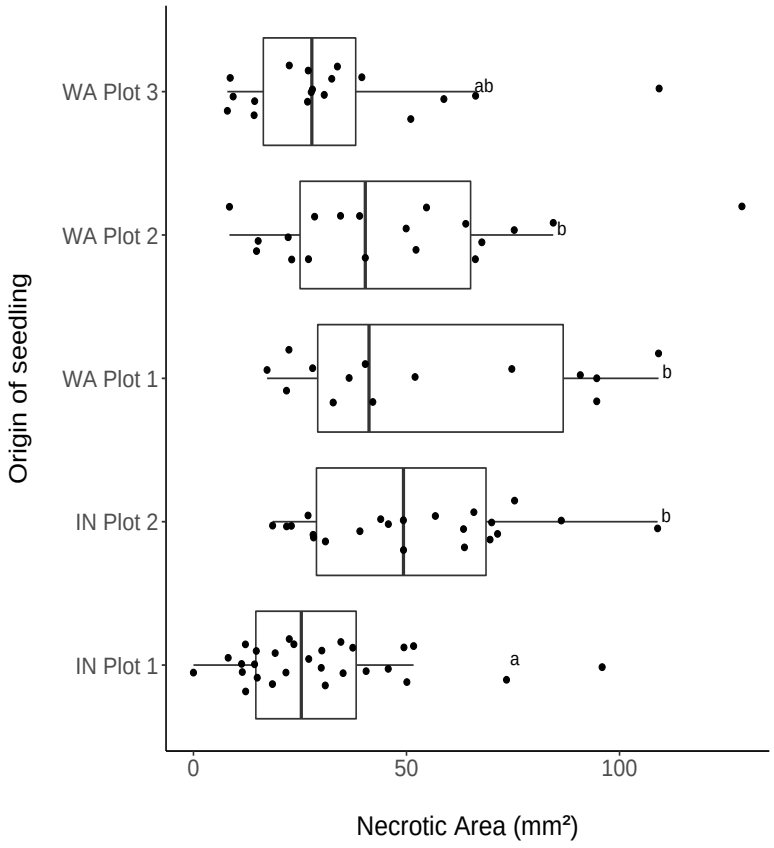

Figure 6.1. Necrotic area of seedlings grown in two plots in West Lafayette IN and three plots in Walla Walla WA and then inoculated with the pathogen *Geosmithia morbida* isolate IN-66 in the greenhouse. Groups with different letters were found to be significantly different in a Box-Cox transformed linear mixed effect model that included a covariate for the ratio of root volume displacement and stem caliper diameter above the root collar.

6.3.2 Fungal Alpha Diversity of the Root and Canker Endospheres

The use of trap seedlings and culture-based sequence typing uncovered a diverse community of fungi in the endosphere of stems and roots of *J. nigra* in its native (IN) and introduced range (WA). Clustering sequences at 99% similarity led to the classification of the isolated fungi into a total of 68 operational taxonomic units (OTUs) in roots (n = 56 OTUs) and cankers (n = 17 OTUs) spanning 46 genera, 32 families, 15 orders and 6 classes of fungi (Fig. 6.2). Diversity of fungi from roots was higher in seedlings germinated in the native range of *J. nigra* in IN than WA, but diversity of fungi from cankers did not differ between States (Fig. 6.3A).

A total of 769 fungal isolates were obtained over the course of the study; 154 from cankers and 615 from roots. Fungi isolated from cankers represented 375 colonies that grew onto the plates. Quality sequences were obtained from 267 vouchers that represented 554 isolates from root plates and 99 isolates from canker tissue representing 220 observed colonies on canker plates. The fungi that were left unsequenced were mostly rare morphospecies. Some OTUs in Dothidiomycetes (OTU18), Leotiomycetes (OTU22), and Sordariomycetes (OTU23, OTU25 and OTU34) contained vouchers assigned to multiple clades of known reference taxa by T-BAS (Fig. 6.2), and were therefore split according to their classification.

6.3.3 Community Composition of the Root Endosphere and Relationship with Necrotic Area

The State (IN or WA) where seeds were planted, germinated, and grown in the first year strongly influenced the diversity and composition of fungal communities from roots of seedlings. State and plot within State had a stronger influence than *G. morbida* inoculation on fungal community composition in roots (Fig. 6.4A). In ADONIS, the composition of the fungal community from roots of *G. morbida*-inoculated seedlings differed between States ($p < 0.01$) and marginally among plots after accounting for the State that the plot was in ($p = 0.06$). The composition of the fungal community in the roots of seedlings from WA differed between plots ($p = 0.04$) but not between *G. morbida*-inoculated and control-inoculated seedlings ($p = 0.73$). In roots, Sordariales (Sordariomycetes), Pleosporales (Dothidiomyecetes) and Cantherellales (Agaricomycetes) had higher relative abundance in IN compared to WA, and Glomerellales and Hypocreales

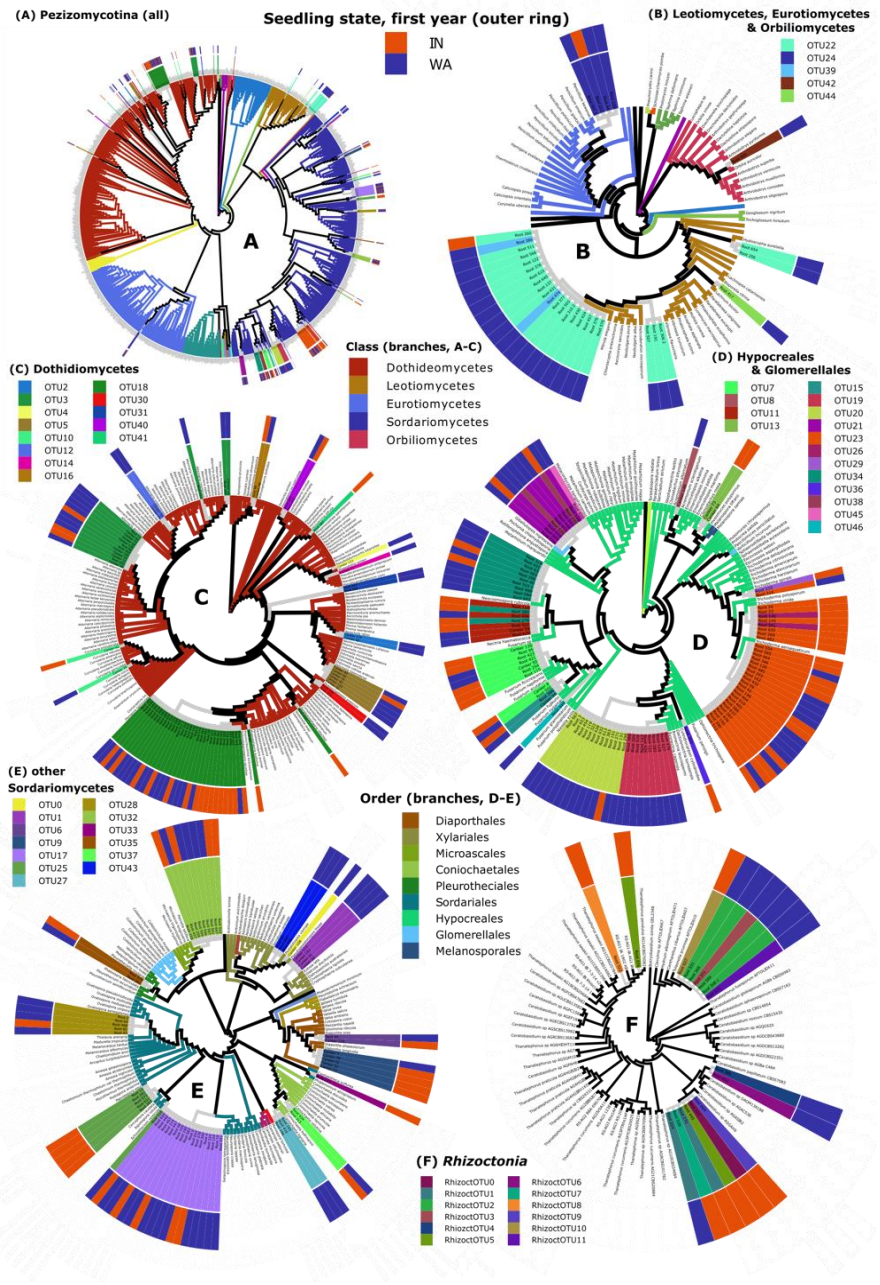

Figure 6.2. Tree-based multi-locus phylogenetic placement (T-BAS) of internal transcribed spacer and large subunit ribosomal DNA from voucher sequences from study of fungi from roots and necrotized stem tissues of *Juglans nigra* seedlings: (A) all Pezizomycotina; (B) Leotiomycetes and less abundant classes; (C) Dothidiomycetes; (D & E) Sordariomycetes; and (F) Agaricomycetes. On each tree, branches are colored by lower-level taxonomic placement, leaves are colored by operational taxonomic unit at 99% sequence similarity listed under the letter heading for each tree (B-F), and outer ring color indicates the state where seedlings that vouchers were isolated from came from. A large-size image is available for viewing and zooming in at https://readingradio.github.io/Dissertation/Composite_tree_all_final.pdf.

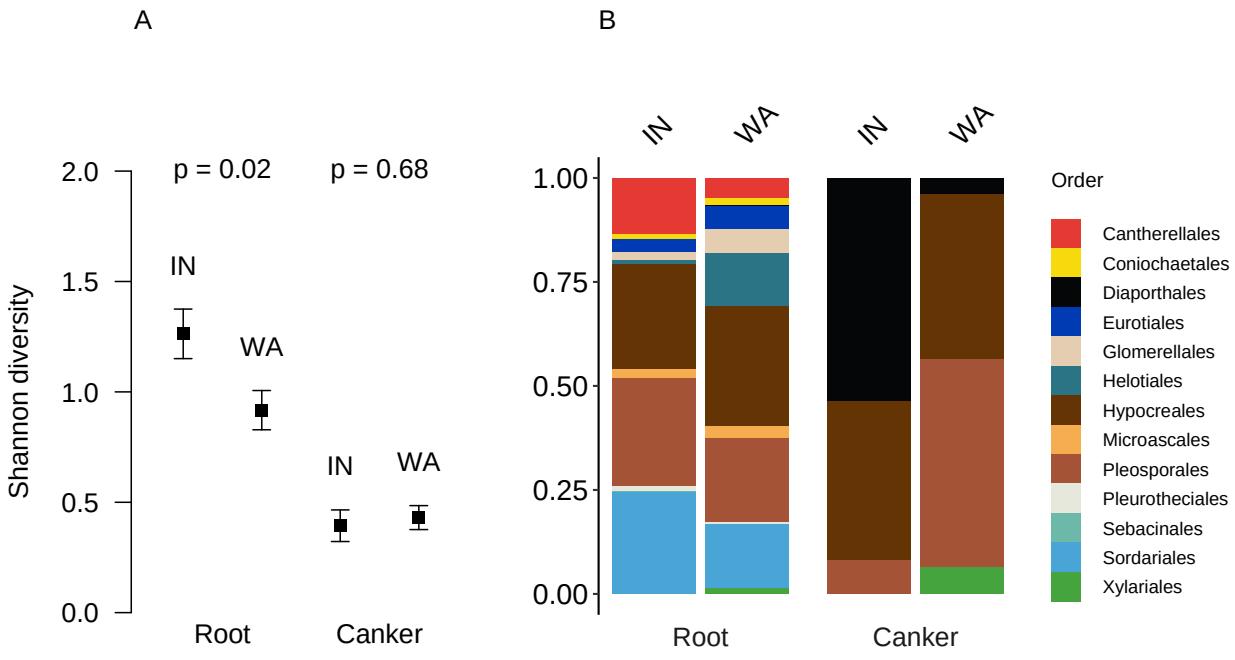

Figure 6.3. Shannon diversity of operational taxonomic units based on clustering of ITS and LSU sequences at 99% similarity (A) and composition by fungal order (B) of fungi isolated from roots and cankers of seedlings that germinated and grew for one year in the field in the native range (IN) or outside the native range (WA) and then for a second year in the greenhouse.

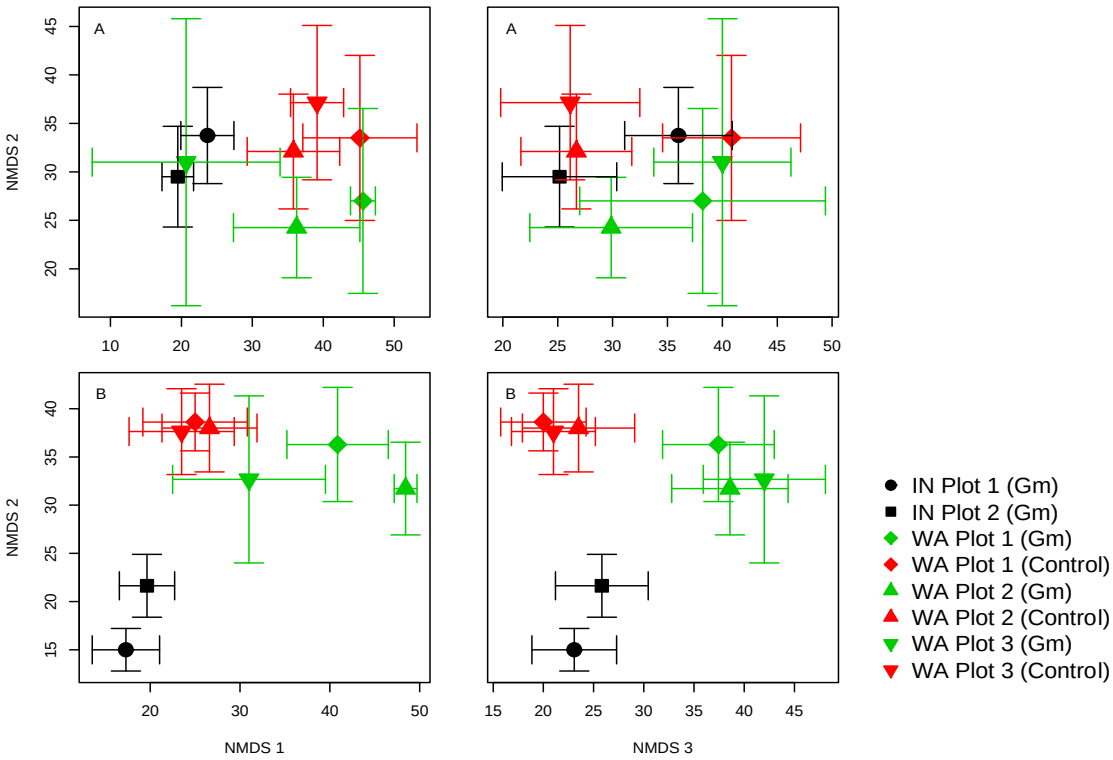

Figure 6.4. Non-metric multidimensional scaling (NMDS) of fungi from roots (A, top) and cankers (B, bottom) of *J. nigra* seedlings germinated and grown for the first year in different plots in the native (IN) and non-native range (WA) and inoculated with *G. morbida* (Gm) or a control treatment (Control). Points and error bars denote the mean ± 1SE position in ordination space for plants from a given State, plot, and inoculation treatment.

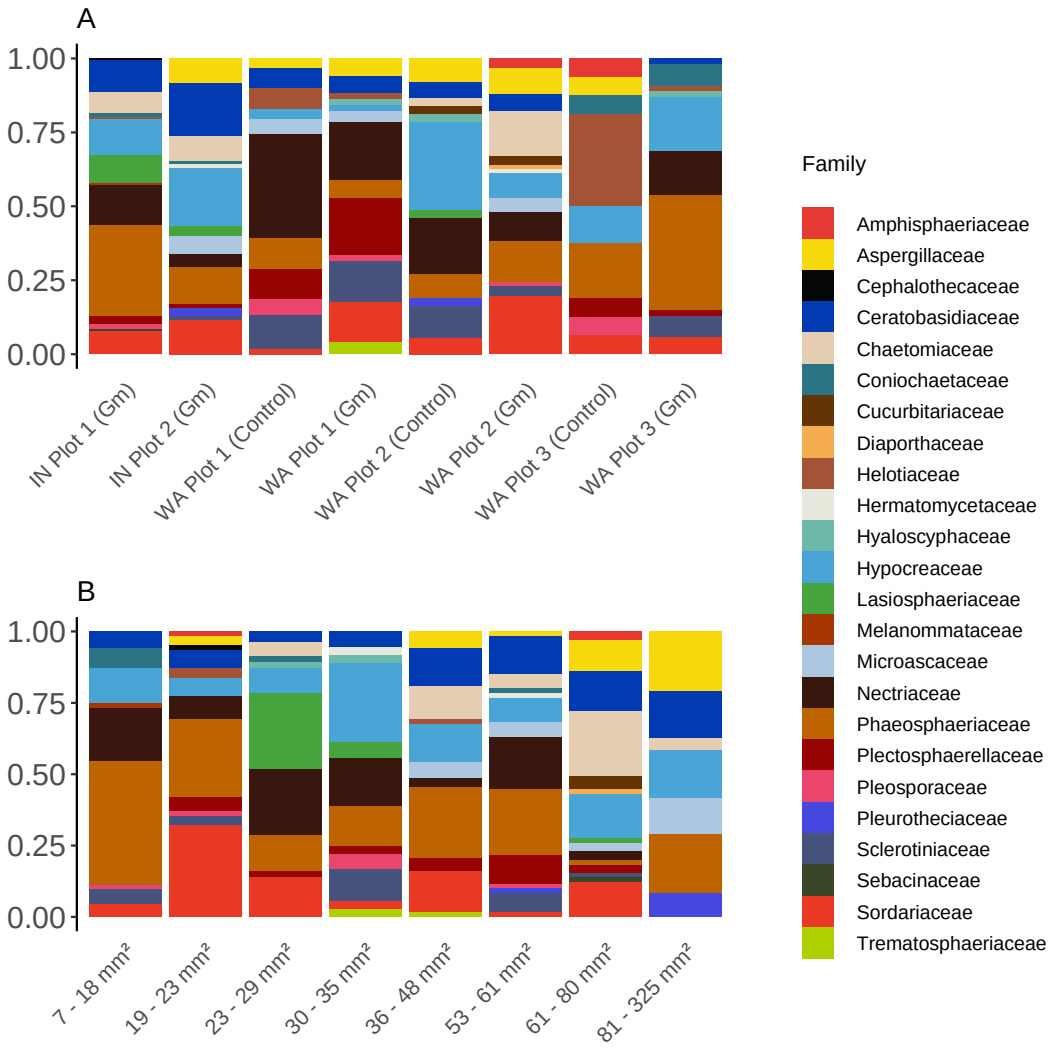

Figure 6.5. Relative abundance of fungal families from roots of *J. nigra* seedlings: (A) by State where they germinated and grew in the first year (IN & WA), plot within State, and inoculation with *Geosmithia morbida* (Gm) or water (Control); (B) by average necrotic area around inoculation points for seedlings inoculated with *G. morbida*.

(Sordariomycetes) were more abundant in WA (Fig. 6.5A). In particular, several taxa were found nearly exclusively in WA-grown seedlings, including the pathogenic genera *Ilyonectria*, *Dactylionectria*, and *Cylindrocarpon* spp. (Hypocreales: Nectricaceae) and *Gibellulopsis* sp. (Hypocreales: Plectosphaeriaceae) as well as fungi in the taxa *Chaetomium* (Chaetomiaceae), Xylariales and Helotiales spp., and a clade of *Rhizoctonia-Ceratobasidium* sp. mostly specific to WA (Figs. 6.2, 6.3B & 6.5A). Taxa only found in the roots of IN-grown seedlings (Figs. 6.2 & 6.5A) included *Trichoderma viridis* (Hypocreales: Hypocreaceae) and *Zopfiella* sp. (Lasiosphaeriaceae).

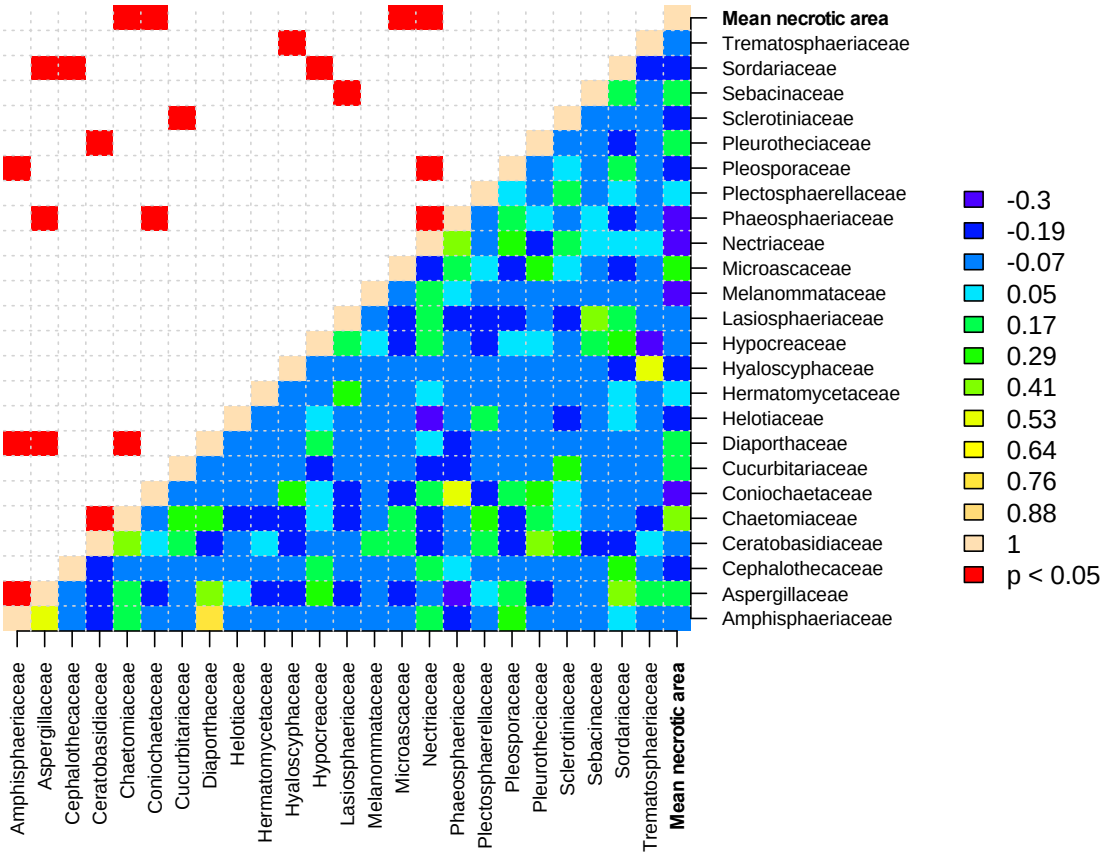

Figure 6.6. Co-occurrence among fungal taxa in walnut roots and relationships with necrotic area caused by *G. morbida*. Significance at $p < 0.05$ (upper triangle) of Spearman rank-correlation coefficients (bottom triangle) among fungal families from roots and average necrotic area of *J. nigra* seedlings inoculated with *G. morbida*.

Several fungal families from roots were associated with seedlings with greater necrotic area (Figs. 6.5B & 6.6). In particular, Microascaceae and Chaetomiaceae sp. were more abundant in seedling with larger cankers (Fig. 6.5B) and their abundance correlated with necrotic area (Fig. 6.6). Chaetomiaceae were also positively correlated with Diaporthaceae in roots. Fungal families that were negatively associated with necrotic area and more abundantly represented in seedlings with smaller cankers included Coniochaetaceae, Nectriaceae (Figs. 6.5B & 6.6), and Sordariaceae (Fig. 6.5B). A number of other fungal families preferentially co-occurred with one another in roots (Fig. 6.6).

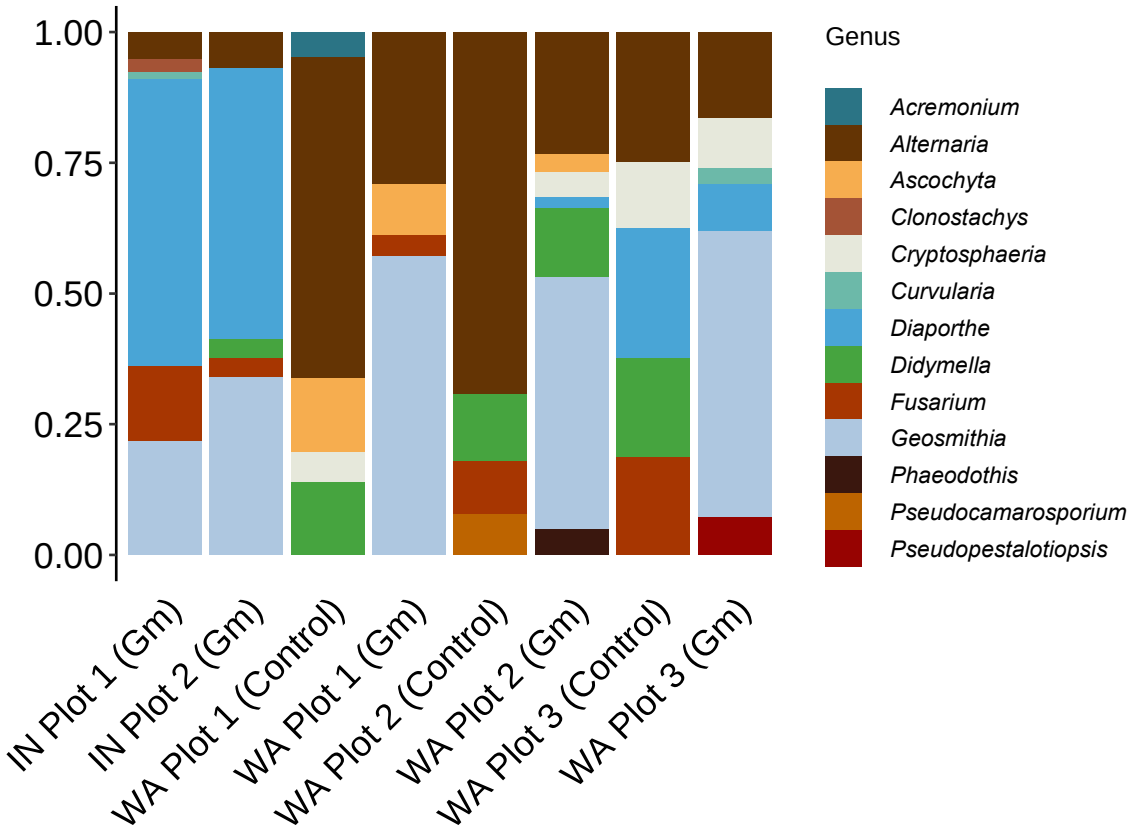

Figure 6.7. Relative abundance of fungal genera from cankers of *J. nigra* seedlings by State where they were grown in the first year (IN & WA), plot within State, and whether they were inoculated with the fungal pathogen *Geosmithia morbida* (Gm) or a control.

6.3.4 Community Composition of Fungi from Cankers and Relationship with Necrotic Area

The State where seeds were planted, germinated, and grown in the first year strongly influenced the fungi reisolated from cankers. State and *G. morbida* inoculation had a significant influence on fungal community composition in cankers (Fig. 6.4B). In ADONIS, the composition of the fungal community from cankers of *G. morbida*-inoculated seedlings differed between the States where they were grown ($p = 0.001$) but not among plots after accounting for State ($p = 0.95$). The composition of the fungal community in cankers of seedlings from WA differed between *G. morbida*-inoculated and control seedlings ($p = 0.001$) but not State or block ($p > 0.2$). *Diaporthe* sp. (Diaporthales) had higher relative abundance in cankers from IN compared to WA (Fig. 6.7). Upon careful examination of cultures, it was noted that 53% (28 out of n = 53) of isolates of *Diaporthe* from IN (n = 52) and WA (n = 1) were visibly parasitized by *Clonostachys rosea* (Hypocreales: Bionectriaceae). The fungus *Diaporthe* sp. from cankers was associated with smaller necrotic area and *G. morbida* was associated with larger cankers (Fig. 6.8).

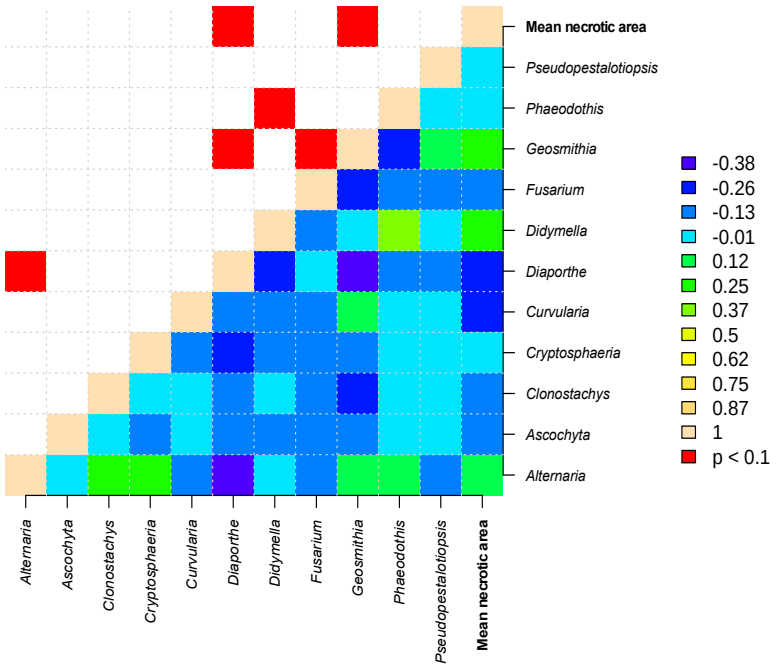

Figure 6.8. Co-occurrence among fungal taxa in walnut stems and relationships with necrotic area caused by *G. morbida*. Significance at $p < 0.1$ (upper triangle) and Pearson correlation coefficients (bottom triangle) among log-transformed abundances of fungal genera from roots and log-transformed average necrotic area of *J. nigra* seedlings inoculated with *G. morbida*.

Cankers in WA-grown seedlings were dominated by a potentially novel community of fungi. Taxa found exclusively or more abundantly in WA-grown seedlings included *Didymella* sp. (Pleosporales: Didymellaceae), *Acremonium* sp. (Hypocreales: Hypocreaceae), and Xylariales spp. *Alternaria* sp. (Pleosporales: Pleosporaceae) was much more abundant in canker tissues of WA than IN-grown seedlings (Figs. 6.2 & 6.7).

As in roots, Nectriaceae in cankers exhibited a significant detectable relationship with *G. morbida*. *Fusarium* spp. in cankers were negatively correlated with *G. morbida* across inoculated seedlings from both States (Fig. 6.8). *Fusarium* spp. were more abundant in WA-grown control-inoculated seedlings but mostly absent from WA-grown *G. morbida*-inoculated seedlings. *Fusarium* spp. were common in inoculated seedlings from IN (Fig. 6.7). Lineages of *Fusarium* spp. that were isolated from cankers were distinct between WA- and IN-grown seedlings (Fig 6.2).

6.4 Discussion

Together, host genotype, the environment and local microbial communities drive the assembly of the host microbiome, and by extension, plant health (Busby et al., 2016b, Obadia et al., 2017, Bahram et al., 2018, Leopold & Busby, 2020, Trivedi et al., 2020). The use of trap seedlings provided us with a first look at the colonization of walnut seeds and seedlings by fungi in the field in the native and non-native range of *J. nigra*. The seeds that we planted in the field can be thought of as a bottleneck in plant microbiome community assembly (Newcombe et al., 2018). Therefore, in addition to their demonstrated impact on seedling recruitment (Spear & Broders, 2020, Zalamea et al., 2021), first colonizers could be expected to exert founder effects that could push the microbiome of seedlings into alternative stable states from an early stage (Leopold & Busby, 2020). These founder effects act in concert with filtering environmental factors (Miller et al., 2018) and to drive differentiation of microbiomes across multiple scales (Tedersoo et al., 2014, Glassman et al., 2017, Bahram et al., 2018, Onufrak et al., 2020, Chapter 4), with potential downstream consequences for susceptibility to disease.

In support of this founder effect hypothesis for phytobiome community assembly, the endosphere differed between trap seedlings planted in IN and WA even after several months of growth in the greenhouse. The taxonomic composition of fungi that colonized trap seedlings in walnut plantations differed from what was previously found in seedlings from fumigated nursery

beds (Chapter 3). In a previous study, soil amendments from forests and plantations did not lead to significant, detectable differentiation in community composition in nursery-grown seedlings (Chapter 3). By contrast, initial colonizers of trap seedlings had a strong influence on community assembly in the roots of seedlings (*this study*—Chapter 6), providing additional support for the existence of alternative stable states in the plant microbiome that are derived from founder effects or the influence of "hub taxa" that structure the rest of the community in forests and plantations (Agler et al., 2016, Leopold & Busby, 2020, Onufrak et al., 2020). In contrast to the perturbing effect of *G. morbida* on the microbiome reported for nursery-grown seedlings (Chapter 3) and mature trees (Onufrak et al., 2020) in previous studies, the fungal community of trap seedlings did not respond to *G. morbida*, even with a more comprehensive sapling effort than Chapter 3. This suggests that, like amendments of forest soil (Chapter 3), the microbiome of seedlings germinated in the field imparts a greater level of resilience to perturbation by invading pathogens (Amor et al., 2020). However, more sampling and a study directly comparing nursery-grown seedlings to field-grown trap seedlings would be needed to confirm this.

In stems and soils beneath mature *J. nigra* trees and in other host systems, the fungi that colonize the roots and shoots of seedlings differ between the native and introduced ranges of the host (Gundale et al., 2016, Lu-Irving et al., 2019, Onufrak et al., 2020). The microbiome of plants growing at the edge or outside of their home range typically differ from those at the core of the native range, particularly when accompanying plant communities are also more dissimilar (Lankau & Keymer, 2016, Ramirez et al., 2019, Collins et al., 2020, Malacrinò et al., 2020). Unlike IN where *J. nigra* is native, there were no close plant relatives (i.e., fam. Juglandaceae) in WA. The nearest naturally-forested areas to our study site in WA are dominated by mixed conifer forest. Vinyards of *Vitis vinifera* and exotic fruit, nut, and shade trees, including urban *J. nigra*, are common in the vicinity of the plantings. These exotic plants may have provided a reservoir for the endophytes we encountered in *J. nigra* in WA. The fungi found in association with black walnut in WA should therefore be expected to be heavily predominated by novel associations, and this is what we observed.

In support of the expectation of novel microbiomes in WA trap seedlings, we found taxa that are reported from *V. vinifera* and *Prunus* spp. as novel associates from the non-native range of *J. nigra*. In particular, members of the Nectriaceae, *Ilyonectria*, *Dactylionectria*, *Fusarium solani* species complex (FSSC; =*Neocosmospora* sp.) and members of the Helotiales, *Cadophora*

luteo-olivaceae, *C. malorum* and *Mollisia* are known to contain important pathogens of woody orchard crops and *V. vinifera* (Cabral et al., 2012, Travadon et al., 2015, Manici et al., 2018). *Cadophora* and *Gibellulopsis*, which we found in roots of WA-grown seedlings, were also indicators of the WA soil microbiome for *J. nigra* (Onufrak et al., 2020). These taxa may have filled the unoccupied niche in the *J. nigra* phytobiome of latent or opportunistic pathogens from the native range (Weber, 1980; Kessler, 1983, Mielke et al., 2004, Lombard et al., 2015). In our study, abundance of these novel associations exhibited mutual interference with *G. morbida*, compared to FSSC sp. isolate Rh-217 from IN that synergized with *G. morbida* causing larger necrotic area (Chapter 3).

Fungi that were antagonistic to canker growth in this study have also shown similar properties in other systems, including *Coniochaeta* spp. (Damm et al., 2010, Kokaew et al., 2011, Xie et al., 2015), and *Diaporthe* (= *Phomopsis*) spp. which could be a pathogen or endophyte of *Juglans* spp. (Thomidis & Michailides, 2009, Gomes et al., 2013, Tanney et al., 2016, López-Moral et al., 2019, Mihaescu et al., 2021). *Clonostachys rosea*, which was found parasitizing *Diaporthe*, is also an indicator of TCD-negative trees in the soils below *J. nigra*. (Onufrak et al., 2020). *C. rosea* is favored by prevailing environmental conditions in the native range of *J. nigra* where it may function as an antagonist of insect-fungal diseases of trees (Chapter 4, Morrison et al., 2021).

Taxa with widespread distribution in both IN- and WA-grown trap seedlings synergized with disease. *Chaetomium* (=*Trichocladium*, Chaetomiaceae) and *Scedosporium* (Microascaceae) spp. were associated with roots of seedlings with larger cankers and were present in seedlings from both States. These fungi could have spread among seedlings from different States or originated within the greenhouse environment as observed for disease synergists in a previous study (Chapter 3), or they could have had a cosmopolitan distribution.

Within the community, direct and indirect interference among fungi could have altered disease progression (Busby et al., 2019). As found in nursery-grown seedlings (Chapter 3), the abundance of fungi in the families Nectriaceae and Ceratobasidiaceae in the roots of trap seedlings from IN and WA plantations showed an antagonistic relationship with one another. However, Nectriaceae were negatively correlated with necrotic area and the resisolation of *G. morbida* from necrotized tissue of trap seedlings from both IN and WA. Infection with avirulent but related pathogens can increase defenses by stimulating relevant defense pathways without causing disease

(Rodriguez et al., 2009, Aimé et al., 2013, Freeman & Rodriguez, 2018). Thus *Fusarium* sp. and *G. morbida* (both Hypocreales) may antagonize one another through the priming of defenses or direct competition for the same host resources.

In the Juglandaceae, most host other lineages form ectomycorrhizal associations, but *J. nigra* and other *Juglans* spp. in *Juglans* sect. *Rhysocaryon* are not known to do so (Wang & Qiu, 2006, Corrales et al., 2016b, 2016a, 2020, 2021). Considerable diversity of Ceratobasidiaceae, Sebacinales, and *Cadophora* spp. (Leotiomycetes) were recovered as endophytes in the roots of *J. nigra* seedlings in the present study. These taxa are commonly encountered in the roots of trees but are rich in ericoid and orchid mycorrhizae and dark septate endophytes whose role in plant performance and resistance and resilience to biotic and abiotic stress are recognized but still poorly understood (Mandyam & Jumpponen, 2005, Selosse et al., 2007, Oberwinkler et al., 2013; Ruotsalainen, 2018, Tedersoo et al., 2020).

This study has provided additional evidence that aboveground-belowground interactions between fungi and host plants have an influence on the trajectory of disease (Chapter 3). Furthermore, our results suggest that the influence of such interactions on tree and forest health depend on interactions within the microbiome as well as the context of native vs. non-native host ranges. Additional study will provide fundamental insights into plant evolution and biogeography and powerful tools for conserving and protecting the ecological and economic services forests and woody plants provide (Newcombe, 2011, Hale et al., 2014, Witzell & Martín, 2018).

6.5 References

Agler, M. T., Ruhe, J., Kroll, S., Morhenn, C., Kim, S. T., Weigel, D., & Kemen, E. M. (2016). Microbial Hub Taxa Link Host and Abiotic Factors to Plant Microbiome Variation. *PLoS Biology*, 14.

Aimé S., Alabouvette, C., Steinberg, C., & Olivain, C. 2013. The Endophytic Strain *Fusarium* oxysporum Fo47: A Good Candidate for Priming the Defense Responses in Tomato Roots. *Molecular Plant-Microbe Interactions*, 26: 918–926.

Amor, D. R., Ratzke, C., & Gore, J. 2020. Transient invaders can induce shifts between alternative stable states of microbial communities. *Science Advances*, 6.

Arnold, A. E., Mejia, L. C., Kyllo, D., Rojas, E. I., Maynard, Z., Robbins, N., & Herre, E. A. 2003. Fungal endophytes limit pathogen damage in a tropical tree. *PNAS*, 100.

Bahram, M., Hildebrand, F., Forslund S. K., Anderson J. L., Soudzilovskaia N. A., Bodegom, P. M., Bengtsson-Palme, J., Anslan, S., Coelho, L. P., Harend, H., Huerta-Cepas, J., Medema, M. H., Maltz, M. R., Mundra, S., Olsson, P. A., Pent, M., Põlme, S., Sunagawa, S., Ryberg, M., Tedersoo, L., & & Bork, P. (2018). Structure and function of the global topsoil microbiome. *Nature,* 560: 233–237.

Baynes, M., Newcombe, G., Dixon, L., Castlebury, L., & O'& Donnell, K. (2012). A novel plant-fungal mutualism associated with fire. *Fungal Biology,* 116: 133–144.

Bengtsson-Palme, J., Ryberg, M., Hartmann, M., Branco, S., Wang, Z., Godhe, A., De Wit, P., Sánchez-García, M., Ebersberger, I., de Sousa, F., Amend, A., Jumpponen, A., Unterseher, M., Kristiansson, E., Abarenkov, K., Bertrand YJK, Sanli, K., Eriksson, K. M., Vik, U., Veldre, V., & Nilsson, R. H. (2013). Improved software detection and extraction of ITS1 and ITS2 from ribosomal ITS sequences of fungi and other eukaryotes for analysis of environmental sequencing data. *Methods in Ecology and Evolution,* 4: 914–919.

Blumenthal, D., Mitchell, C. E., Pyšek, P., Jarošík V. (2009). Synergy between pathogen release and resource availability in plant invasion. Pro*ceedings of the National Academy of Sciences,* 106: 7899–7904.

Busby, P. E., Crutsinger, G., Barbour, M., & Newcombe, G. (2019). Contingency rules for pathogen competition and antagonism in a genetically based, plant defense hierarchy. *Ecology and Evolution,* 9, 6860–6868. doi:https://doi.org/10.1002/ece3.5253.

Busby, P. E., Peay, K. G., Newcombe G. (2016a). Common foliar fungi of Populus trichocarpa modify Melampsora rust disease severity. *New Phytologist,* 209: 1681–1692.

Busby, P. E., Ridout, M., Newcombe G. (2016b). Fungal endophytes: modifiers of plant disease. *Plant Molecular Biology,* 90.

Busby, P. E., Soman, C., Wagner, M. R., Friesen, M. L., Kremer, J., Bennett, A., Morsy, M., Eisen, J. A., Leach, J. E., & Dangl, J. L. (2017). Research priorities for harnessing plant microbiomes in sustainable agriculture. *PLoS Biology,* 15.

Busby, P. E., Zimmerman, N., Weston, D. J., Jawdy, S. S., Houbraken, J., & Newcombe, G. (2013). Leaf endophytes and Populus genotype affect severity of damage from the necrotrophic leaf pathogen, Drepanopeziza populi. *Ecosphere,* 4: art125.

Cabral, A., Rego, C., Nascimento, T., Oliveira, H., Groenewald, J. Z., & Crous, P. W. (2012). Multi-gene analysis and morphology reveal novel Ilyonectria species associated with black foot disease of grapevines. *Fungal Biology,* 116: 62–80.

Carbone, I., White, J. B., Miadlikowska, J., Arnold, A. E., Miller, M. A., Magain, N., U'Ren, Jana M., & Lutzoni, F. (2019). T-BAS version 2.1: Tree-Based Alignment Selector toolkit for evolutionary placement of DNA sequences and viewing alignments and specimen metadata on curated and custom trees. *Microbiology Resource Announcements,* 8.

Collins, C. G., Spasojevic, M. J., Alados, C. L., Aronson, E. L., Benavides, J. C., Cannone, N., Caviezel, C., Grau, O., Guo, H., Kudo, G., Kuhn, N. J., Müllerová, J., Phillips, M. L., Pombubpa, N., Reverchon, F., Shulman, H. B., Stajich, J. E., Stokes, A., Weber, S. E., & Diez, J. M. (2020). Belowground impacts of alpine woody encroachment are determined by plant traits, local climate, and soil conditions. *Global Change Biology*, 26: 7112–7127.

Corrales, A., Arnold, A. E., Ferrer, A., Turner, B. L., Dalling JW. (2016a). Variation in ectomycorrhizal fungal communities associated with *Oreomunnea mexicana* (Juglandaceae) in a Neotropical montane forest. *Mycorrhiza*, 26: 1–17.

Corrales, A., Mangan, S. A., Turner, B. L., Dalling JW. (2016b). An ectomycorrhizal nitrogen economy facilitates monodominance in a neotropical forest. *Ecology Letters*, 19: 383–392.

Corrales, A., Wilson, A. W., Mueller, G. M., & Ovrebo, C. (2020). Novel *Laccaria* Species From Juglandaceae Forest in Panama With Notes on Their Ecology. *Frontiers in Microbiology*, 11: 1597.

Corrales, A., Xu, H., Garibay-Orijel, R., Alfonso-Corrado, C., Williams-Linera, G., Chu, C., Truong, C., Jusino, M. A., Clark-Tapia, R., Dalling, J. W., Liu, Y., & Smith, M. E. (2021). Fungal communities associated with roots of two closely related Juglandaceae species with a disjunct distribution in the tropics. *Fungal Ecology*, 50: 101023.

Damm, U., Fourie, P. H., & Crous, P. W. (2010). *Coniochaeta* (Lecythophora), *Collophora* gen. nov. and Phaeomoniella species associated with wood necroses of Prunus trees. *Persoonia*, 24: 60–80.

Dixon, R. K. (1988). Seed source and vesicular-arbuscular mycorrhizal symbiont affects growth of *Juglans nigra* seedlings. *New Forests*, 2: 203–211.

Elías-Román, R. D., Medel-Ortiz, R., Alvarado-Rosales, D., Hanna, J. W., Ross-Davis, A. L., Kim M-S, & Klopfenstein, N. B. (2018). *Armillaria mexicana*, a newly described species from Mexico. *Mycologia*, 110: 347–360.

Freeman, S., & Rodriguez, R. J. (2018). Genetic Conversion of a Fungal Plant Pathogen to a Nonpathogenic , Endophytic Mutualist. *Science*, 260: 75–78.

Glassman, S. I., Wang, I. J., & Bruns, T. D. (2017). Environmental filtering by pH and soil nutrients drives community assembly in fungi at fine spatial scales. *Molecular Ecolo*,*y* 26: 6960–6973.

Gomes, R. R., Glienke, C., Videira SIR, Lombard, L., Groenewald, J. Z., & Crous, P. W. (2013). *Diaporthe*: a genus of endophytic, saprobic and plant pathogenic fungi. *Persoonia*, 31: 1–41.

Gundale, M. J., Almeida, J. P., Wallander, H., Wardle, D. A., Kardol, P., Nilsson, M. C., Fajardo, A., Pauchard, A., Peltzer, D. A., Ruotsalainen, S., Mason, B., Rosenstock N. (2016). Differences in endophyte communities of introduced trees depend on the phylogenetic relatedness of the receiving forest. *Journal of Ecology*, 104: 1219–1232.

Hale, I. L., Broders, K., & Iriarte, G. (2014). A Vavilovian approach to discovering crop-associated microbes with potential to enhance plant immunity. *Frontiers in Plant Science,* 5: 492.

Heger, T., & Jeschke, J. M. (2014). The enemy release hypothesis as a hierarchy of hypotheses. *Oikos,* 123: 741–750.

Jummponen ARI, & Trappe, J. M. (1998). Dark septate endophytes: a review of facultative biotrophic root-colonizing fungi. *New Phytologist,* 140: 295–310.

Kaplan, I., Pineda, A., & Bezemer, M. (2018). Application and Theory of Plant--Soil Feedbacks on Aboveground Herbivores. Pages 319–343 in Ohgushi, T., Wurst, S., & Johnson, S. N., eds. Aboveground--Belowground Community Ecology. Springer International Publishing.

Kessler, K. J. (1983). Control of black walnut root rot diseases in nurseries. United States Department of Agriculture, Forest Service, North Central Forest Experiment Station.

Klironomos, J. N. (2002). Feedback with soil biota contributes to plant rarity and invasiveness in communities. *Nature*, 417: 1096–1099.

Kokaew, J., Manoch, L., Worapong, J., Chamswarng, C., Singburaudom, N., Visarathanonth, N., Piasai, O., & Strobel, G. 2011. *Coniochaeta ligniaria* an endophytic fungus from Baeckea frutescens and its antagonistic effects against plant pathogenic fungi. *Thai Journal of Agricultural Science,* 44: 123–131.

Kormanik, P. P. (1985). Effects of phosphorous and vesicular-arbuscular mycorrhizae on growth and leaf retention of black walnut seedlings. *Canadian Journal of Forestry*, 15.

Kormanik, P. P., Schultz, R. C., & Bryan, W. C. (1982). The influence of vesicular-arbuscular mycorrhizae on the growth and development of eight hardwood tree species. *Forest Science,* 28: 531–539.

Lankau, R. A., & Keymer, D. P. (2016). Ectomycorrhizal fungal richness declines towards the host species' range edge. *Molecular ecology*, 25: 3224–3241.

Leopold, D. R., & Busby, P. E. (2020). Host Genotype and Colonist Arrival Order Jointly Govern Plant Microbiome Composition and Function. *Current Biology,* 30: 3260-3266.e5.

Leslie, J. F., & Summerell, B. A. (2008). *The Fusarium laboratory manual*. John Wiley & Sons.

Liebhold, A. M., Brockerhoff, E. G., Kalisz, S., Nuñez, M. A., Wardle, D. A., & Wingfield, M. J. (2017). Biological invasions in forest ecosystems. *Biological Invasions,* 19: 3437–3458.

Lombard, L., van der Merwe, N. A., Groenewald, J. Z., & Crous, P. W. (2015). Generic concepts in Nectriaceae. *Studies in Mycology,* 80: 189–245.

López-Moral, A., Lovera, M., Raya M del C, Cortés-Cosano, N., Arquero, O., Trapero, A., Agustí- & Brisach, C. (2019). Etiology of Branch Dieback and Shoot Blight of English Walnut Caused by Botryosphaeriaceae and *Diaporthe* Species in Southern Spain. *Plant Disease,* 104: 533–550.

Lu-Irving, P., Harenčár, J. G., Sounart, H., Welles, S. R., Swope, S. M., Baltrus, D. A., & Dlugosch, K. M. (2019). Native and invading yellow starthistle (*Centaurea solstitialis*) microbiomes differ in composition and diversity of bacteria. *Msphere,* 4: e00088--19.

Maddison, D. R., Maddison W. P. (2019a). Chromaseq: a Mesquite package for analyzing sequence chromatograms. Version 1.51 [WWW document] URL http://mesquiteproject.org/http://mesquiteproject.org/packages/chromaseq/. [accessed 29 November 2020]. (29 November 2020; http://mesquiteproject.org/packages/chromaseq/).

Maddison, W. P., Maddison D. R. (2019b). Mesquite: a modular system for evolutionary analysis. Version 3.61 [WWW document] URL http://mesquiteproject.org. [accessed 29 November 2020]. (29 November 2020; http://mesquiteproject.org).

Malacrinò, A., Sadowski, V. A., Martin, T. K., de Oliveira, N., Brackett, I. J., Feller, J. D., Harris, K. J., Combita Heredia, O., Vescio, R., & Bennett, A. E. (2020). Biological invasions alter environmental microbiomes: a meta-analysis. *PloS one,* 15: e0240996.

Mandyam, K., & Jumpponen, A. (2005). Seeking the elusive function of the root-colonising dark septate endophytic fungi. *Studies in Mycology,* 53: 173–189.

Manici, L. M., Kelderer, M., Caputo, F., Saccà, M. L., Nicoletti, F., Topp, A. R., & Mazzola, M. (2018). Involvement of *Dactylonectria* and *Ilyonectria* spp. in tree decline affecting multi-generation apple orchards. *Plant and Soil,* 425: 217–230.

Melichar, M. W., Garrett, H. E., & Cox, G. S. (1986). Mycorrhizae Benefit Growth and Development of Eastern Black Walnut Seedlings. *Northern Journal of Applied Forestry,* 3: 151–153.

Michler, C. H., Pijut, P. M., Van Sambeek, J. W., Coggeshell, M. V., Seifert, J., Woeste, K., Overton, R., & Ponder, F. J. (2004). Diseases of Intensively Managed Eastern Black Walnut. In C. H. Michler, P. M. Pijut, J. W. Van Sambeek, M. V. Coggeshall, J. Seifert, K. Woeste, R. Overton, & F. J. Ponder (Eds.), *Black Walnut in a New Century, Proceedings of the 6th Walnut Council Research Symposium*. St. Paul, MN: U.S. Department of Agriculture, Forest Service, North Central Research Station, 110–113.

Mihaescu, C., Dunea, D., Bășa, A. G., & Frasin, L. N. (2021). Characteristics of *Phomopsis juglandina* (Sacc.) Hohn. Associated with Dieback of Walnut in the Climatic Conditions of Southern Romania. *Agronomy,* 11.

Miller, E. T., Svanbäck, R., Bohannan B. J. M. (2018). Microbiomes as Metacommunities: Understanding Host-Associated Microbes through Metacommunity Ecology. *Trends in Ecology & Evolution*, 33: 926–935.

Miller, M. A., Schwartz, T., Pickett, B. E., He, S., Klem, E. B., Scheuermann, R. H., Passarotti, M., Kaufman, S., O'& Leary, M. A. (2015). A RESTful API for Access to Phylogenetic Tools via the CIPRES Science Gateway. *Evolutionary bioinformatics online,* 11: 43–48.

Mircetich, S. M., & Matheron, M. E. (1983). Phytophthora root and crown rot of walnut trees. *Phytopathology,* 73: 1481–1488.

Mitchell, C. E., Agrawal, A. A., Bever, J. D., Gilbert, G. S., Hufbauer, R. A., Klironomos, J. N., Maron, J. L., Morris, W. F., Parker, I. M., Power, A. G., Seabloom, E. W., Torchin, M. E., & Vázquez, D. P. (2006). Biotic interactions and plant invasions. *Ecology Letters*, 9: 726–740.

Montecchio, L., Vettorazzo, M., & Faccoli, M. (2016). Thousand cankers disease in Europe: an overview. *EPPO Bulletin*, 46: 335–340.

Moricca, S., Bracalini, M., Benigno, A., Ghelardini, L., Furtado, E. L., Marino, C. L., & Panzavolta, T. (2020). Observations on the non-native thousand cankers disease of walnut in Europe's southernmost outbreak. *Global Ecology and Conservation*, 23: e01159.

Morrison, E. W., Kasson, M. T., Heath, J. J., & Garnas, J. R. (2021). Pathogen and Endophyte Assemblages Co-vary With Beech Bark Disease Progression, Tree Decline, and Regional Climate. *Frontiers in Forests and Global Change*, 4: 43.

Newcombe, G. (2011). Endophytes in forest management: four challenges. In A. M. Pirttilä, A. C. Frank (Eds.), *Endophytes of Forest Trees* (pp. 251–262). Springer.

Newcombe, G., Harding, A., Ridout, M., & Busby, P. E. (2018). A Hypothetical Bottleneck in the Plant Microbiome. *Frontiers in Microbiology*, 9: 1–10.

Newhouse, J. R., & Hunter, B. B. (1983). Selective Media for Recovery of Cylindrocladium and Fusarium Species from Roots and Stems of Tree Seedlings. *Mycologia*, 75: 228–233.

Newton, L., & Fowler, G. (2009). Pathway Assessment: *Geosmithia* sp. and *Pityophthorus juglandis* Blackman movement from the western into the eastern United States. In K. A. McManus, K. W. Gottschalk (Eds.), *Proceedings of the 21st U.S. Department of Agriculture interagency research forum on invasive species. January 12-15, Annapolis, MD. General Technical Report NRS-P-75.* U. S. Department of Agriculture, Forest Service, Northern Research Station 112. Available online https://www.uaex.edu/environment-nature/ar-invasives/invasive-diseases/docs/Thousand-Cankers Disease.pdf.

Obadia, B., Güvener, Z. T., Zhang, V., Ceja-Navarro, J. A., Brodie, E. L., Ja, W. W., & Ludington, W. B. (2017). Probabilistic Invasion Underlies Natural Gut Microbiome Stability. C*urrent Biology*, 27: 1999-2006.e8.

Oberwinkler, F., Riess, K., Bauer, R., Kirschner, R., & Garnica, S. (2013). Taxonomic re-evaluation of the Ceratobasidium-Rhizoctonia complex and Rhizoctonia butinii, a new species attacking spruce. *Mycological Progress*, 12: 763–776.

Oksanen, J., Blanchet, F. G., Friendly, M., Kindt, R., Legendre, P., McGlinn, D., Minchin, P. R., O'Hara, R. B., Simpson, G. L., Solymos, P., Stevens MHH, Szoecs, E., & Wagner, H. (2018). vegan: Community Ecology Package.

Onufrak, A. J., Williams, G. M., Klingeman, W. E., Cregger, M. A., Klingeman, D. M., DeBruyn, J. M., Ginzel, M. D., & Hadžiabdić, Đ. (2020). Regional Differences in the Structure of Juglans nigra Phytobiome Reflect Geographical Differences in Thousand Cankers Disease Severity. *Phytobiomes Journal*, 4: 388–404.

Paradis, E., & Schliep, K. (2019). ape 5.0: an environment for modern phylogenetics and evolutionary analyses in R. *Bioinformatics*, 35: 526–528.

Pineda, A., Kaplan, I., & Bezemer, T. M. (2017). Steering Soil Microbiomes to Suppress Aboveground Insect Pests. *Trends in Plant Science*, 22: 770–778.

Ponder, F. (1983). Soil Moisture Levels and Mycorrhizal Infection in Black Walnut Seedlings. *Communications in Soil Science and Plant Analysis*, 14: 507–511.

Ponder, F. (1986). Effect of three weeds on the growth and mycorrhizal infection of black walnut seedlings. *Canadian Journal of Botany*, 64: 1888–1892.

Ponder, F., Fatahe Khore Abad, M., & Shahoe, S. (1990). Soil structure and mycorhizae encourage black walnut growth on old fields. Research Note NC-249. U. S. Department of Agriculture, Forest Service, North Central Forest Experiment Station.

Ponder, F. (1984). Growth and mycorrhizal development of potted white ash and black walnut fertilized by two methods. *Canadian Journal of Botany*, 62: 509–512.

Porras-Alfaro, A., & Bayman, P. (2011). Hidden Fungi, Emergent Properties: Endophytes and Microbiomes. *Annual Review of Phytopathology*, 49: 291–315.

R Core Team. (2019). R: A Language and Environment for Statistical Computing.

Ramirez, K. S., Snoek, L. B., Koorem, K., Geisen, S., Bloem, L. J., ten Hooven, F., Kostenko, O., Krigas, N., Manrubia, M., Caković, D., van Raaij, D., Tsiafouli, M. A., Vreš, B., Čelik, T., Weser, C., Wilschut, R. A., van der & Putten, W. H. (2019). Range-expansion effects on the belowground plant microbiome. *Nature Ecology and Evolution*, 3: 604–611.

Redick, C. H., & Jacobs, D. F. (2020). Mitigation of deer herbivory in temperate hardwood forest regeneration: A meta-analysis of research literature. *Forests*, 11: 1–16.

Ridout, M., & Newcombe, G. (2015). The frequency of modification of Dothistroma pine needle blight severity by fungi within the native range. *Forest Ecology and Management*, 337: 153–160.

Rodriguez, R. J., White, J. F., Arnold, A. E., & Redman, R. S. (2009). Fungal endophytes: Diversity and functional roles: Tansley review. *New Phytologist*, 182.

Ruotsalainen, A. L. (2018). Dark Septate Endophytes (DSE) in Boreal and Subarctic Forests BT - Endophytes of Forest Trees: Biology and Applications. Pages 105–117 in Pirttilä AM and Frank, A. C., eds. Springer International Publishing.

Schlatter, D., Kinkel, L., Thomashow, L., Weller, D., & Paulitz, T. (2017). Disease Suppressive Soils: New Insights from the Soil Microbiome. *Phytopathology*, 107.

Selosse M-A, Setaro, S., Glatard, F., Richard, F., Urcelay, C., & Weiß, M. (2007). Sebacinales are common mycorrhizal associates of Ericaceae. *New Phytologist*, 174: 864–878.

Seybold, S. J., Klingeman III WE, Hishinuma, S. M., Coleman, T. W., & Graves, A. D. (2019). Status and Impact of Walnut Twig Beetle in Urban Forest, Orchard, and Native Forest Ecosystems. *Journal of Forestry*, 117: 152–163.

Spear, E. R., & Broders, K. (2020). Host-generalist fungal pathogens of seedlings may maintain forest diversity via host-specific impacts and differential susceptibility among tree species. *bioRxiv*.

Stamp, N. (2003). Out of the quagmire of plant defense hypotheses. *The Quarterly Review of Biology*, 78: 23–55.

Tanney, J. B., McMullin, D. R., Green, B. D., Miller, J. D., & Seifert, K. A. (2016). Production of antifungal and antiinsectan metabolites by the *Picea* endophyte *Diaporthe maritima* sp. nov. *Fungal Biology,* 120: 1448–1457.

Tedersoo, L., Bahram, M., & Zobel, M. (2020). How mycorrhizal associations drive plant population and community biology. *Science,* 367.

Tedersoo, L., Wardle, D. A., Lindahl, B. D., Bahram, M., Põlme, S., Kõljalg, U., Yorou, N. S., Wijesundera, R., Ruiz, L. V., Vasco-Palacios, A. M., Thu, P. Q., Suija, A., Smith, M. E., Sharp, C., Saluveer, E., Saitta, A., Rosas, M., Riit, T., Ratkowsky, D., Pritsch, K., Põldmaa, K., Piepenbring, M., Phosri, C., Peterson, M., Parts, K., Pärtel, K., Otsing, E., Nouhra, E., Njouonkou, A. L., Nilsson, R. H., Morgado, L. N., Mayor, J., May, T. W., Majuakim, L., Lodge, D. J., Lee, S. S., Larsson K-H, Kohout, P., Hosaka, K., Hiiesalu, I., Henkel, T. W., Harend, H., Guo, L., Greslebin, A., Grelet, G., Geml, J., Gates, G., Dunstan, W., Dunk, C., Drenkhan, R., Dearnaley, J., De Kesel, A., Dang, T., Chen, X., Buegger, F., Brearley, F. Q., Bonito, G., Anslan, S., Abell, S., & Abarenkov, K. (2014). Global diversity and geography of soil fungi. *Science,* 28.

Thomidis, T., & Michailides, T. J. (2009). Studies on Diaporthe eres as a New Pathogen of Peach Trees in Greece. *Plant Disease*, 93: 1293–1297.

Tisserat, N., Cranshaw, W., Leatherman, D., Utley, C., & Alexander, K. (2009). Black walnut mortality in Colorado caused by the walnut twig beetle and thousand cankers disease. *Plant Health Progres,s* 11, 10. doi:10.1094/php-2009-0811-01-rs.

Travadon, R., Lawrence, D. P., Rooney-Latham, S., Gubler, W. D., Wilcox, W. F., Rolshausen, P. E., & Baumgartner, K. (2015). Cadophora species associated with wood-decay of grapevine in North America. *Fungal Biology,* 119: 53–66.

Trivedi, P., Leach, J. E., Tringe, S. G., Sa, T., & Singh, B. K. (2020). Plant–microbiome interactions: from community assembly to plant health. *Nature Reviews Microbiology,* 18: 607–621.

Utley, C., Nguyen, T., Roubtsova, T., Coggeshall, M., Ford, T. M., Grauke, L. J., Graves, A D., Leslie, C. A., McKenna, J., Woeste, K., Yaghmour, M A., Cranshaw, W., Seybold, S. J., Bostock, R. M., & Tisserat, M. (2013). Susceptibility of Walnut and Hickory Species to *Geosmithia morbida*. *Plant Disease,* 97, 601–607. doi:10.1094/PDIS-07-12-0636-RE.

Vilgalys, R. (1992). Conserved primer sequences for PCR amplification and sequencing from nuclear ribosomal RNA. Duke University, USA. (https://sites.duke.edu/vilgalyslab/files/2017/08/rDNA-primers-for-fungi.pdf).

Wang, B., Qiu Y-L. (2006). Phylogenetic distribution and evolution of mycorrhizas in land plants. *Mycorrhiza,* 16: 299–363.

Weber, B. C. (1980). How to diagnose black walnut damage. General Technical Report NC-57. U. S. Department of Agriculture, Forest Service, North Central Forest Experiment Station.

Williams, R. D. (1990). Juglans nigra L., black walnut. *Silvics of North America Vol. 2*: 391–399. U. S. Department of Agriculture, Forest Service.

Witzell, J., & Martín, J. A. (2018). Endophytes and forest health. Pages 261–282 in. Endophytes of forest trees. Springer.

Witzell, J., Martín, J. A., & Blumenstein, K. (2014). Ecological Aspects of Endophyte-Based Biocontrol of Forest Diseases BT - Advances in Endophytic Research. Pages 321–333 in Verma VC and Gange, A. C., eds. Springer India.

Xie, J., Strobel, G. A., Feng, T., Ren, H., Mends, M. T., Zhou, Z., & Geary, B. (2015). An endophytic *Coniochaeta velutina* producing broad spectrum antimycotics. Journal of Microbiology 53: 390–397.

Yukawa, T., Ogura-Tsujita, Y., Shefferson, R. P., & Yokoyama, J. (2009). Mycorrhizal diversity in *Apostasia* (Orchidaceae) indicates the origin and evolution of orchid mycorrhiza. *American Journal of Botany* 96: 1997–2009.

Zalamea P-C, Sarmiento, C., Arnold, A. E., Davis, A. S., Ferrer, A., & Dalling, J. W. (2021). Closely related tree species support distinct communities of seed-associated fungi in a lowland tropical forest. *Journal of Ecology* 109: 1858–1872.

APPENDIX A. SUPPLEMENTAL MATERIAL FOR CHAPTER 2

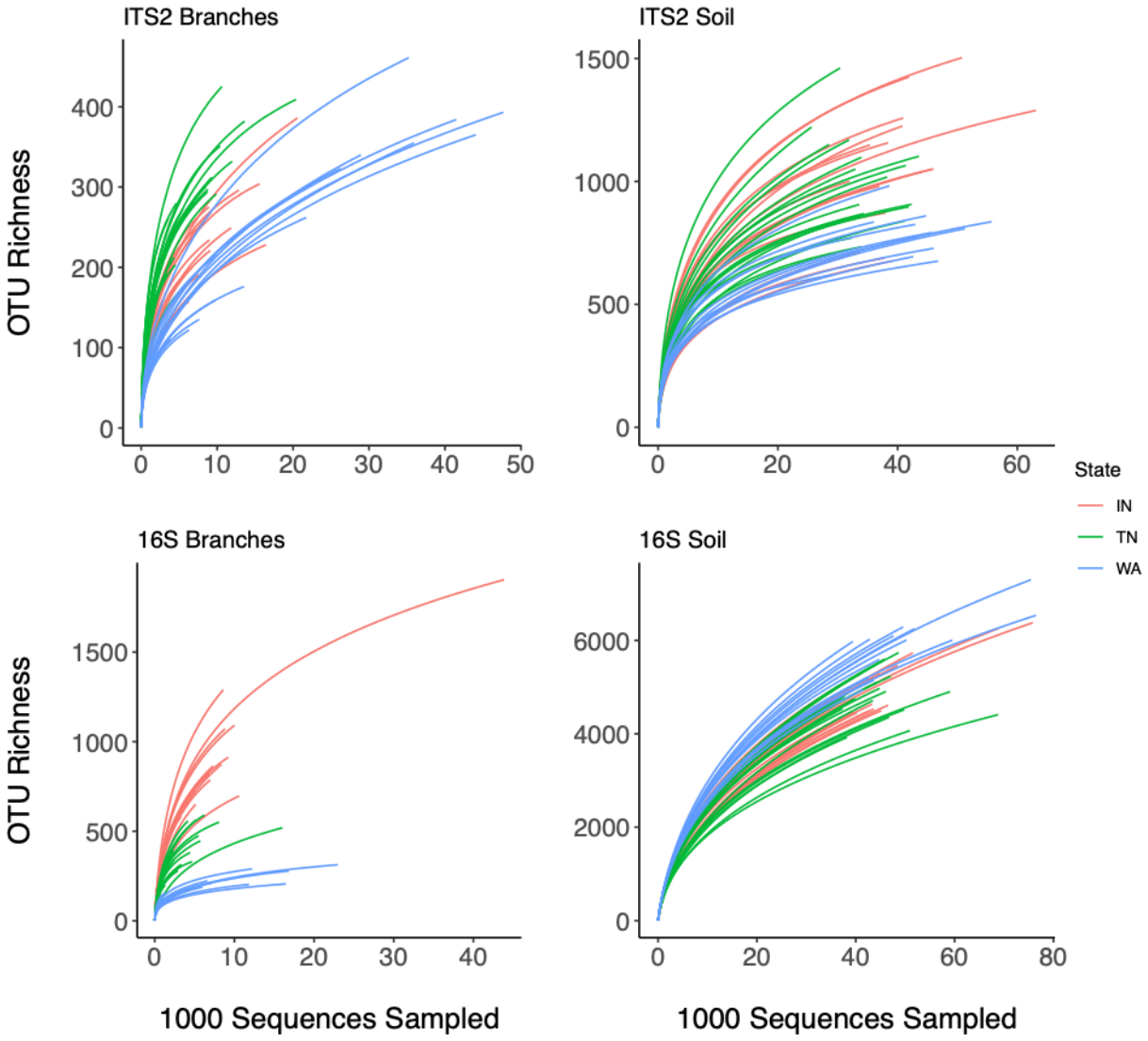

Figure A.1. Rarefaction curves for branches (caulosphere) and soils of *Juglans nigra* fungal (ITS2) and bacterial (16S) communities from Indiana (IN), Tennessee (TN), and Washington (WA).

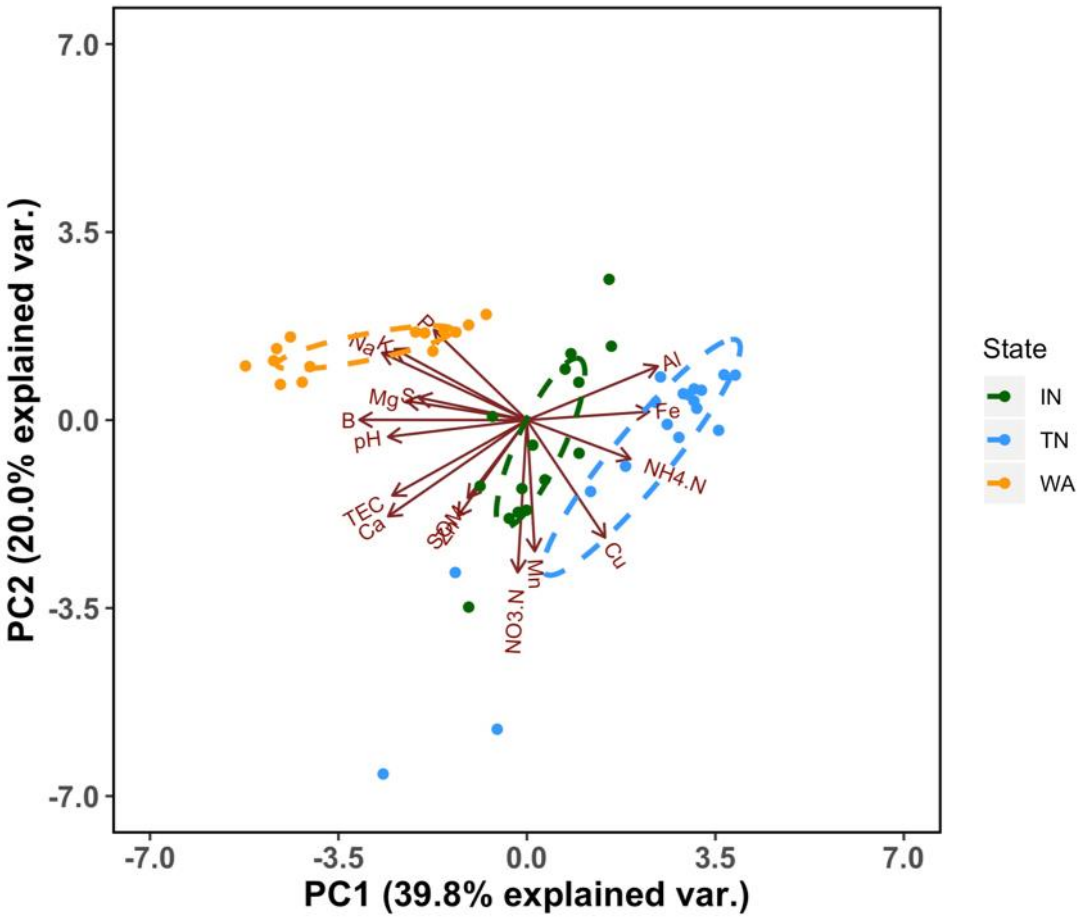

Figure A.2. Principal component analysis of soil physicochemical properties of bulk soils collected from 47 *Juglans nigra* trees in Indiana (IN), Tennessee (TN), and Washington (WA). PC1 correlates with B, Na, pH, Ca, TEC, K, Al, Fe, and Mg. PC2 correlates with NO_3.N, Mn, Cu, Ca, Zn, and P. Soil physicochemical properties significantly differed by state (Figure 1; Pseudo-$F_{2,44} = 7.0$, $P < 0.001$, $R^2 = 0.24$). Points and ellipses are colored by state, and ellipses represent standard deviation of axis scores from the group centroids. Length of arrows indicate magnitude of the association.

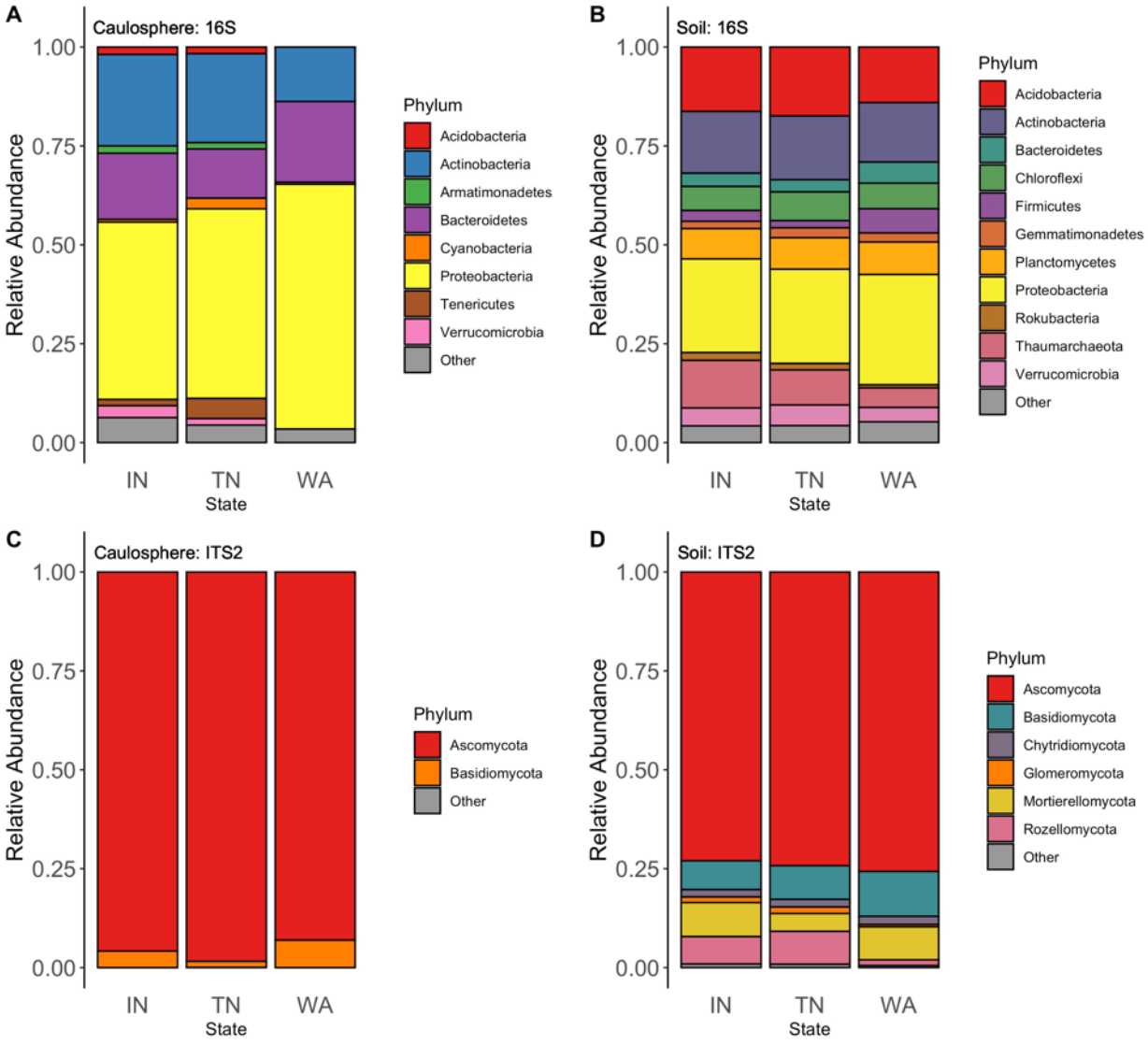

Figure A.3. Relative abundance of caulosphere (A, C) and soil (B, D) bacterial and archaeal (A, B) and fungal (C, D) phyla from *Juglans nigra* trees in Indiana (IN), Tennessee (TN), and Washington (WA). Other represents phyla that comprised less than 1% of all bacterial and archaeal sequences or fungal sequences in the study.

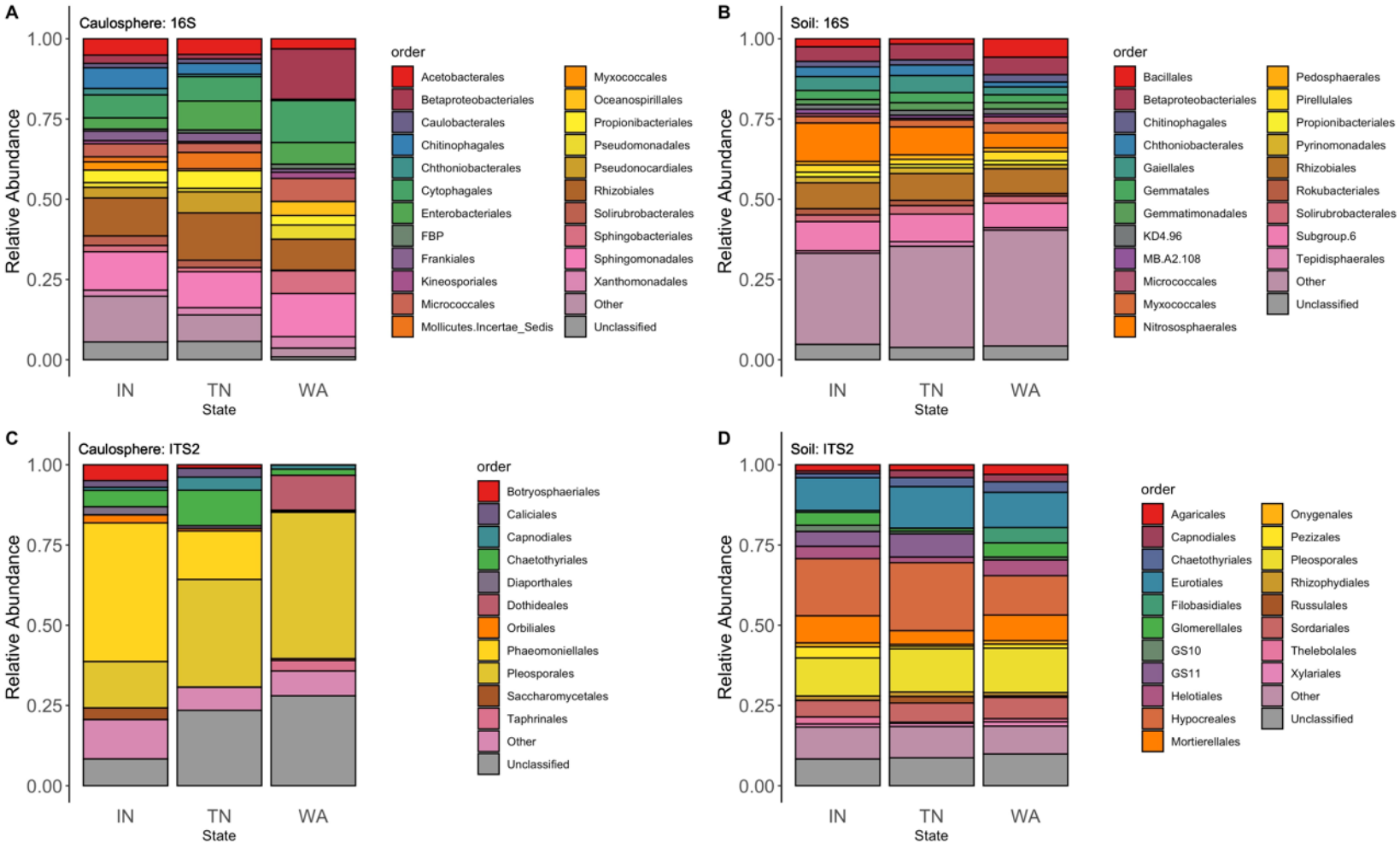

Figure A.4. Relative abundance of caulosphere (A, C) and soil (B, D) bacterial and archaeal (A, B) and fungal (C, D) orders from *Juglans nigra* trees in Indiana (IN), Tennessee (TN), and Washington (WA). Other represents orders that comprised less than 1% of all bacterial and archaeal sequences or fungal sequences in the study. Unclassified represent OTUs classified at the phylum or class level but not at the order level.

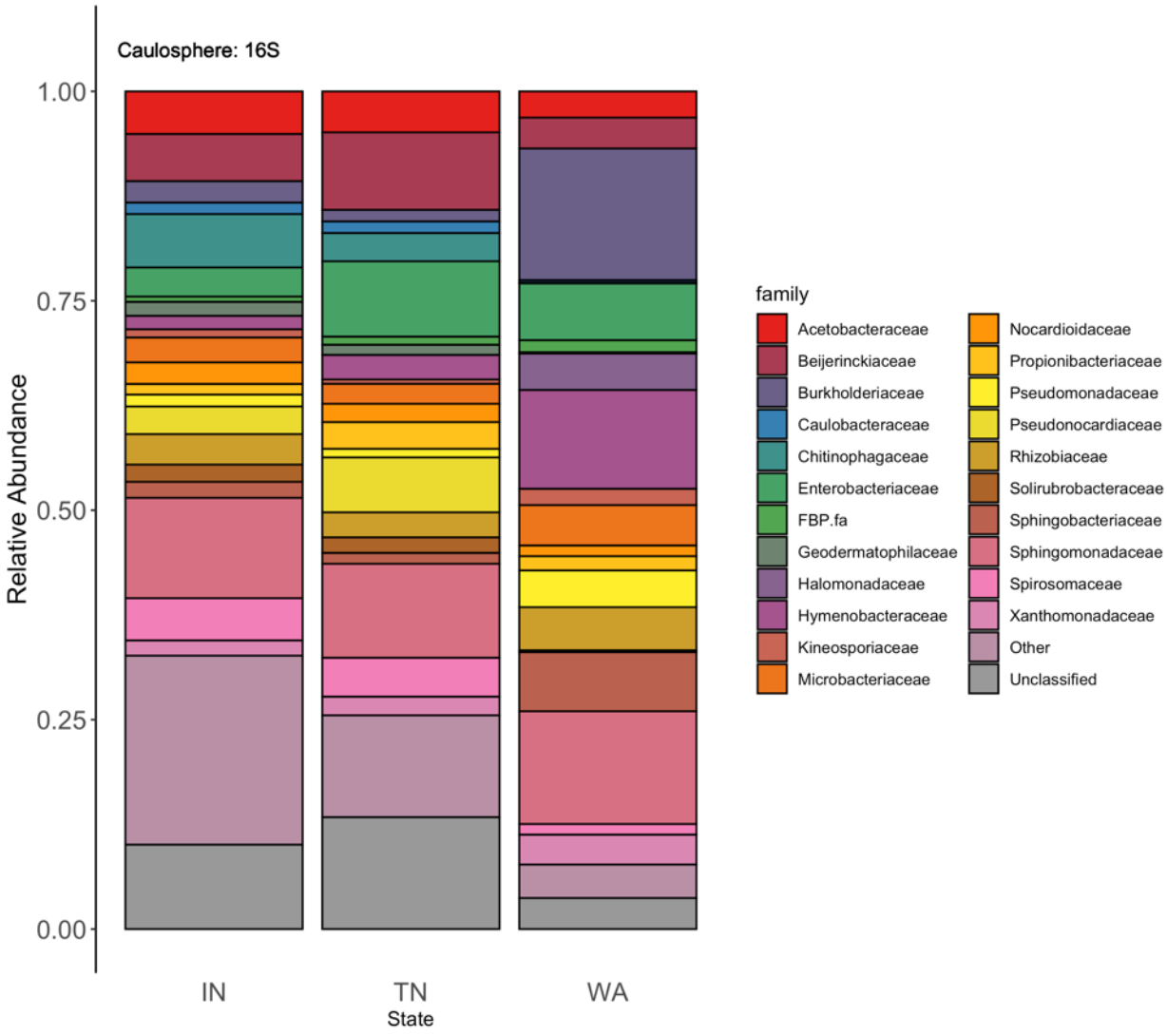

Figure A.5. Relative abundance of caulosphere bacterial families from *Juglans nigra* trees in Indiana (IN), Tennessee (TN), and Washington (WA). Other represents families that comprised less than 1% of all bacterial and archaeal sequences or fungal sequences in the study. Unclassified represent OTUs classified at the phylum or class level but not at the order level.

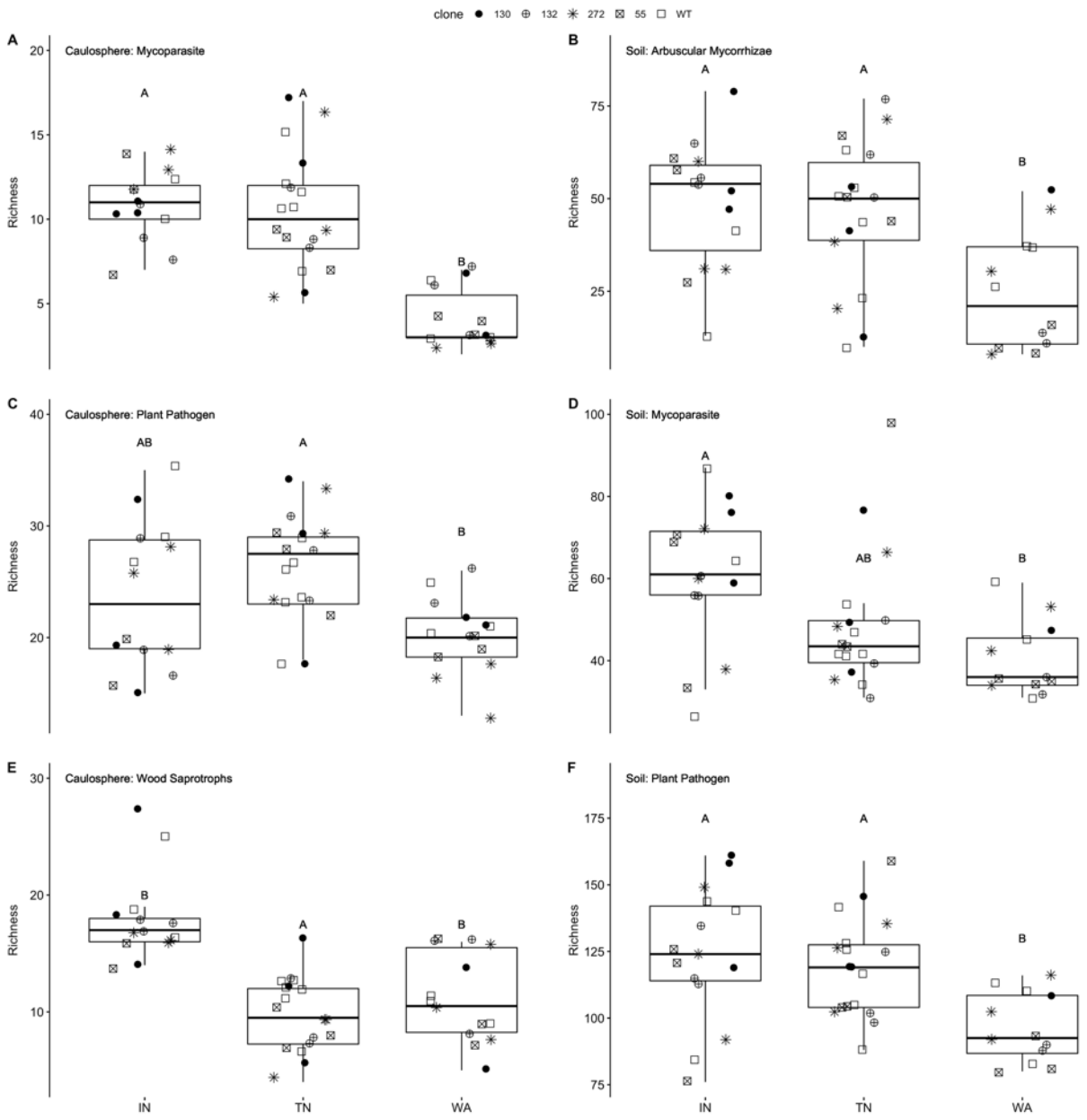

Figure A.6. Richness of *Juglans nigra* caulosphere mycoparasite (A), plant pathogen (C), and wood saprotrophs (E) and the richness of soil arbuscular mycorrhizae (B), mycoparasite (D), and plant pathogens (F) for Indiana (IN), Tennessee (TN), and Washington (WA).

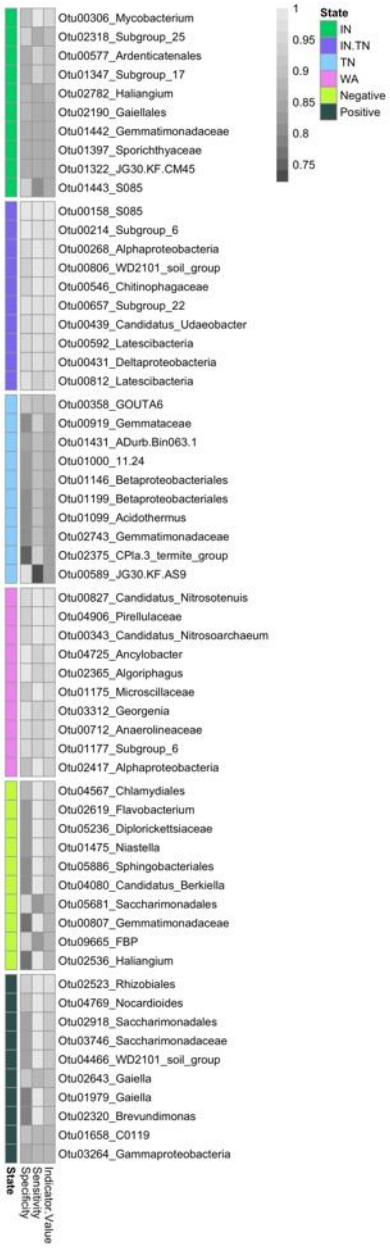

Figure A.7. Sensitivity, specificity, and indicator values for top 10 bacterial indicator OTUS for soil of *Juglans nigra* in Indiana (IN), Tennessee (TN), Washington (WA), IN+TN, and TCD positive trees and TCD negative trees in WA and associated specificity, sensitivity, and indicator values. Only top 10 OTUs classified to at least the class level for each group are depicted. Full list of indicator species can be found in supplementary materials (see Table A.6).

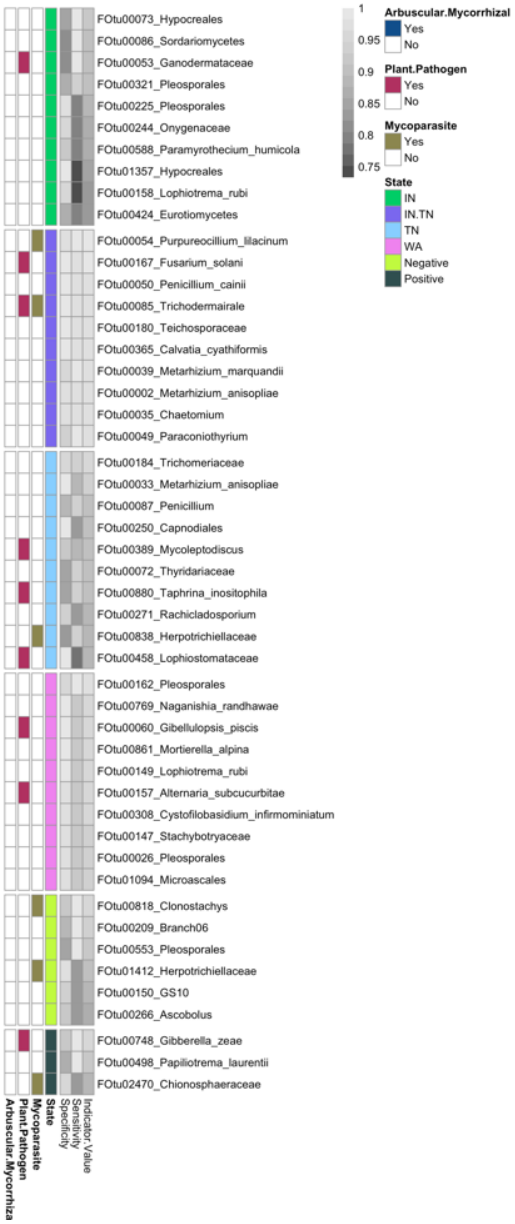

Figure A.8. Sensitivity, specificity, and indicator values for top 10 fungal indicator OTUs for soil of *Juglans nigra* in Indiana (IN), Tennessee (TN), Washington (WA), IN+TN, and TCD positive trees and TCD negative trees in WA and associated specificity, sensitivity, and indicator values. Only top 10 OTUs classified to at least the class level for each group are depicted. Full list of indicator species can be found in supplementary materials (see Table A.8). Left three columns indicate whether the OTU was assigned to the saprotroph, plant pathogen, or mycoparasite functional guilds in FUNGuild database (accessed 26 November, 2019).

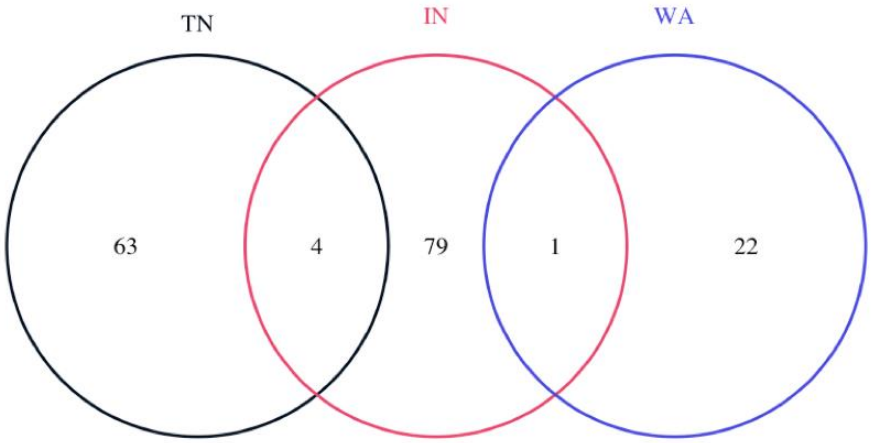

Figure A.9. Overlap in hub taxa of caulosphere phytobiome of *Juglans nigra* between Indiana (IN), Tennessee (TN), and Washington (WA).

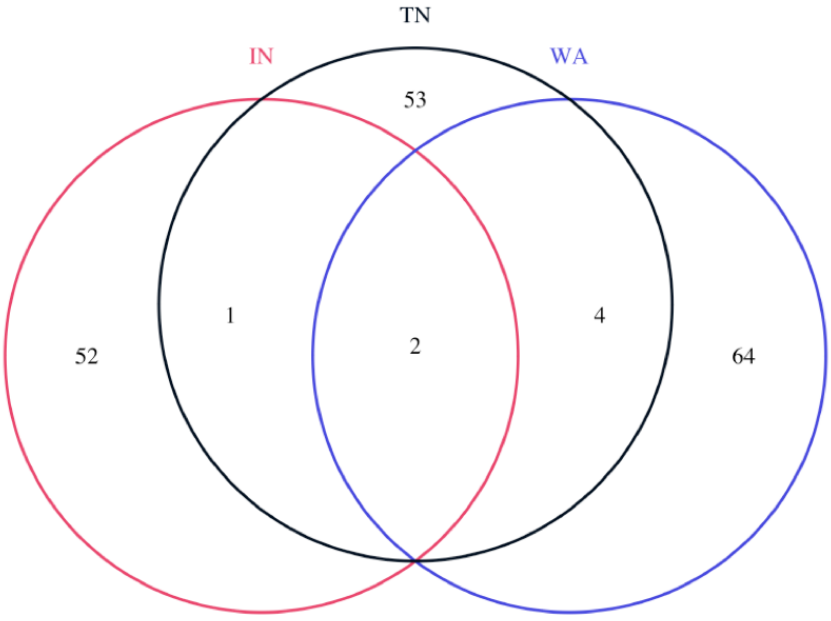

Figure A.10. Overlap in hub taxa of soil microbiome of *Juglans nigra* between Indiana (IN), Tennessee (TN), and Washington (WA).

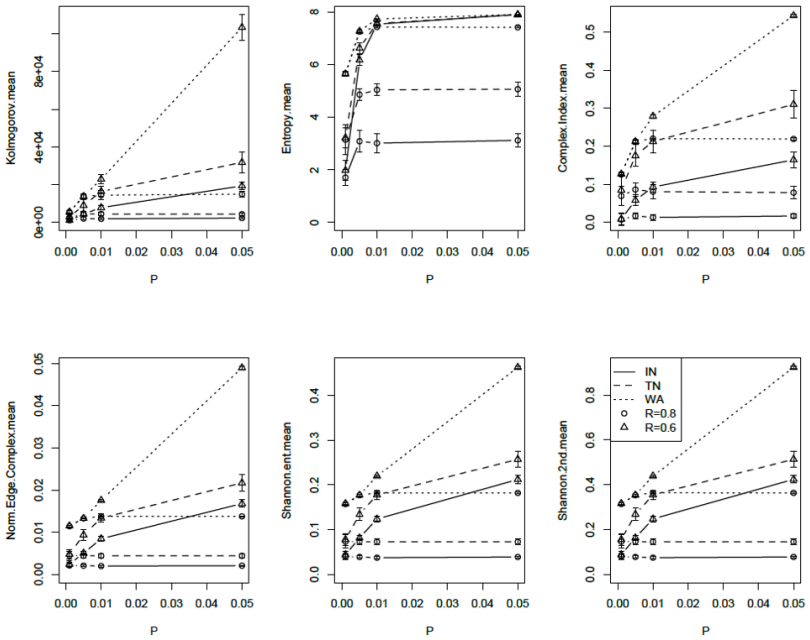

Figure A.11. Network complexity of caulosphere microbiomes *Juglans nigra* for Indiana (IN), Tennessee (TN), and Washington (WA) across all *R* and *P* cutoffs tested.

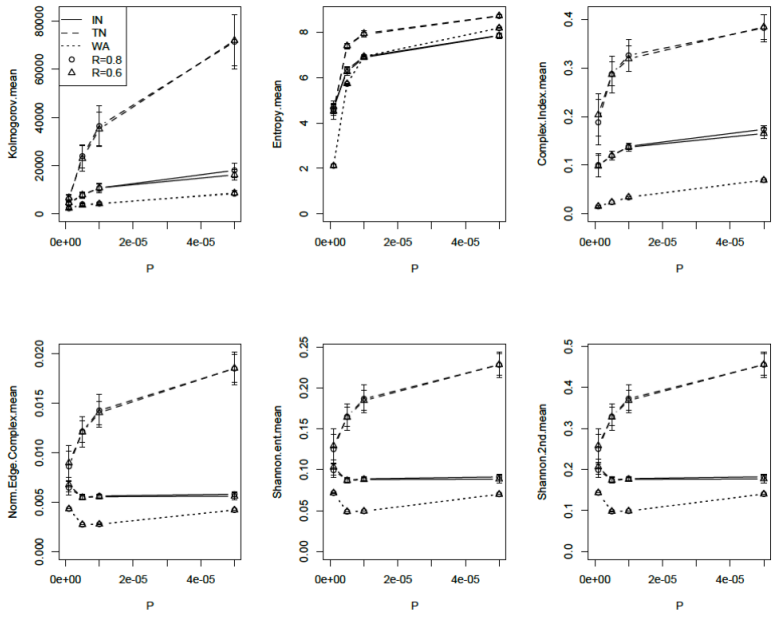

Figure A.12. Network complexity of soil microbiomes *Juglans nigra* for Indiana (IN), Tennessee (TN), and Washington (WA) across all *R* and *P* cutoffs tested.

Table A.1. Goods coverage for *Juglans nigra* caulosphere bacterial communities in Indiana (IN), Tennessee (TN), and Washington (WA).

Sample ID	Number of Sequences	Goods (%)	Amplicon	Habitat
IN_MCB10_272	2000	88.1	16S	Caulosphere
IN_MCB11_272	2000	88.7	16S	Caulosphere
IN_MCB16_132	2000	90.0	16S	Caulosphere
IN_MCB17_132	2000	91.3	16S	Caulosphere
IN_MCB2_130	2000	85.8	16S	Caulosphere
IN_MCB24_272	2000	85.0	16S	Caulosphere
IN_MCB26_130	2000	90.3	16S	Caulosphere
IN_MCB27_132	2000	90.7	16S	Caulosphere
IN_MCB28_WT	2000	88.3	16S	Caulosphere
IN_MCB6_55	2000	87.2	16S	Caulosphere
IN_MCB7_55	2000	88.3	16S	Caulosphere
IN_MCB8_55	2000	88.8	16S	Caulosphere
IN_MCB9_130	2000	82.0	16S	Caulosphere
IN_MCB29_WT	2000	86.1	16S	Caulosphere
IN_MCB33_WT	2000	89.0	16S	Caulosphere
TN_130B	2000	93.4	16S	Caulosphere
TN_130C	2000	93.1	16S	Caulosphere
TN_132A	2000	94.5	16S	Caulosphere
TN_132B	2000	94.3	16S	Caulosphere
TN_272A	2000	96.0	16S	Caulosphere
TN_272C	2000	95.8	16S	Caulosphere
TN_55A	2000	95.8	16S	Caulosphere
TN_55B	2000	95.3	16S	Caulosphere
TN_55C	2000	95.7	16S	Caulosphere
TN_LS1_WT	2000	91.0	16S	Caulosphere
TN_LS2_WT	2000	91.4	16S	Caulosphere
TN_LS3_WT	2000	94.7	16S	Caulosphere
TN_MB19_WT	2000	92.9	16S	Caulosphere
TN_MB20_WT	2000	90.9	16S	Caulosphere
TN_MB21_WT	2000	94.0	16S	Caulosphere
WA_BNL18_272	2000	97.7	16S	Caulosphere
WA_BNL19_55	2000	97.4	16S	Caulosphere
WA_BNL21_WT	2000	97.7	16S	Caulosphere
WA_BNL22_WT	2000	98.3	16S	Caulosphere
WA_BNL23_WT	2000	98.0	16S	Caulosphere
WA_RN1_55	2000	97.1	16S	Caulosphere
WA_RN4_130	2000	96.9	16S	Caulosphere
WA_RN7_132	2000	97.7	16S	Caulosphere
WA_RN8_132	2000	97.4	16S	Caulosphere
WA_RN9_132	2000	97.4	16S	Caulosphere

Table A.2. Goods coverage for *Juglans nigra* soil bacterial communities in Indiana (IN), Tennessee (TN), and Washington (WA).

Sample ID	Number of Sequences	Goods (%)	Amplicon	Habitat
IN_MCB26_130	37329	94.7	16S	Soil
IN_MCB2_130	37329	94.5	16S	Soil
IN_MCB9_130	37329	93.7	16S	Soil
IN_MCB16_132	37329	93.4	16S	Soil
IN_MCB17_132	37329	93.5	16S	Soil
IN_MCB27_132	37329	94.1	16S	Soil
IN_MCB10_272	37329	94.6	16S	Soil
IN_MCB11_272	37329	94.8	16S	Soil
IN_MCB24_272	37329	94.1	16S	Soil
IN_MCB6_55	37329	93.9	16S	Soil
IN_MCB7_55	37329	94.7	16S	Soil
IN_MCB8_55	37329	93.3	16S	Soil
IN_MCB28_WT	37329	94.3	16S	Soil
INMCB29_WT	37329	94.7	16S	Soil
IN_MCB33_WT	37329	93.7	16S	Soil
TN_130A	37329	94.2	16S	Soil
TN_130B	37329	94.3	16S	Soil
TN_130C	37329	95.1	16S	Soil
TN_132A	37329	94.2	16S	Soil
TN_132B	37329	93.4	16S	Soil
TN_132C	37329	95.6	16S	Soil
TN_272A	37329	94.3	16S	Soil
TN_272B	37329	95.0	16S	Soil
TN_272C	37329	94.1	16S	Soil
TN_55A	37329	93.5	16S	Soil
TN_55B	37329	95.2	16S	Soil
TN_55C	37329	94.1	16S	Soil
TN_LS1_WT	37329	93.2	16S	Soil
TN_LS2_WT	37329	94.1	16S	Soil
TN_LS3_WT	37329	94.5	16S	Soil
TN_MB19_WT	37329	94.0	16S	Soil
TN_MB20_WT	37329	95.1	16S	Soil
TN_MB21_WT	37329	96.1	16S	Soil
WA_BNL20_130	37329	92.8	16S	Soil
WA_RN4_130	37329	94.5	16S	Soil
WA_RN7_130	37329	94.4	16S	Soil
WA_RN8_132	37329	94.1	16S	Soil
WA_RN9_132	37329	93.2	16S	Soil
WA_BNL17_272	37329	93.2	16S	Soil
WA_BNL18_272	37329	94.2	16S	Soil
WA_RN10_272	37329	92.9	16S	Soil
WA_BNL19_55	37329	93.9	16S	Soil
WA_RN1_55	37329	94.3	16S	Soil
WA_RN2_55	37329	94.2	16S	Soil
WA_BNL21_WT	37329	93.4	16S	Soil
WA_BNL22_WT	37329	93.6	16S	Soil
WA_BNL23_WT	37329	93.2	16S	Soil

Table A.3. Goods coverage for *Juglans nigra* caulosphere fungal communities in Indiana (IN), Tennessee (TN), and Washington (WA).

Sample ID	Number of Sequences	Goods (%)	Amplicon	Habitat
IN_MCB10_272	3400	98.1	ITS	Caulosphere
IN_MCB11_272	3400	97.4	ITS	Caulosphere
IN_MCB16_132s	3400	98.6	ITS	Caulosphere
IN_MCB17_132	3400	98.4	ITS	Caulosphere
IN_MCB24_272	3400	97.8	ITS	Caulosphere
IN_MCB26_130	3400	98.5	ITS	Caulosphere
IN_MCB27_132	3400	98.0	ITS	Caulosphere
IN_MCB28_WT	3400	97.9	ITS	Caulosphere
IN_MCB2_130	3400	97.8	ITS	Caulosphere
IN_MCB6_55	3400	98.1	ITS	Caulosphere
IN_MCB7_55	3400	98.5	ITS	Caulosphere
IN_MCB9_130	3400	98.3	ITS	Caulosphere
IN_MCB29_WT	3400	97.9	ITS	Caulosphere
IN_MCB33_WT	3400	98.2	ITS	Caulosphere
TN_130A	3400	98.2	ITS	Caulosphere
TN_130B	3400	97.2	ITS	Caulosphere
TN_130C	3400	96.9	ITS	Caulosphere
TN_132A	3400	97.1	ITS	Caulosphere
TN_132B	3400	97.6	ITS	Caulosphere
TN_132C	3400	97.6	ITS	Caulosphere
TN_272A	3400	96.6	ITS	Caulosphere
TN_272B	3400	97.9	ITS	Caulosphere
TN_272C	3400	97.8	ITS	Caulosphere
TN_55A	3400	97.7	ITS	Caulosphere
TN_55B	3400	97.9	ITS	Caulosphere
TN_55C	3400	97.4	ITS	Caulosphere
TN_LS1_WT	3400	98.3	ITS	Caulosphere
TN_LS2_WT	3400	97.5	ITS	Caulosphere
TN_LS3_WT	3400	97.6	ITS	Caulosphere
TN_MB19_WT	3400	98.6	ITS	Caulosphere
TN_MB20_WT	3400	97.4	ITS	Caulosphere
TN_MB21_WT	3400	98.6	ITS	Caulosphere
WA_BNL17_272	3400	98.6	ITS	Caulosphere
WA_BNL18_272	3400	98.4	ITS	Caulosphere
WA_BNL19_55	3400	98.7	ITS	Caulosphere
WA_BNL20_130	3400	98.8	ITS	Caulosphere
WA_BNL21_WT	3400	98.4	ITS	Caulosphere
WA_BNL22_WT	3400	98.1	ITS	Caulosphere
WA_BNL23_WT	3400	98.6	ITS	Caulosphere
WA_RN10_272	3400	99.1	ITS	Caulosphere
WA_RN1_55	3400	98.5	ITS	Caulosphere
WA_RN2_55	3400	98.8	ITS	Caulosphere
WA_RN4_130	3400	98.3	ITS	Caulosphere
WA_RN7_132	3400	98.0	ITS	Caulosphere
WA_RN8_132	3400	98.5	ITS	Caulosphere
WA_RN9_132	3400	98.4	ITS	Caulosphere

Table A.4. Goods coverage for *Juglans nigra* soil fungal communities in Indiana (IN), Tennessee (TN), and Washington (WA).

Sample ID	Number of Sequences	Goods (%)	Amplicon	Habitat
IN_MCB26_130	25000	98.508	ITS	Soil
IN_MCB2_130	25000	98.512	ITS	Soil
IN_MCB9_130	25000	99.056	ITS	Soil
IN_MCB16_132	25000	98.988	ITS	Soil
IN_MCB17_132	25000	98.948	ITS	Soil
IN_MCB27_132	25000	99.316	ITS	Soil
IN_MCB10_272	25000	98.524	ITS	Soil
IN_MCB11_272	25000	99.244	ITS	Soil
IN_MCB24_272	25000	98.784	ITS	Soil
IN_MCB6_55	25000	99.268	ITS	Soil
IN_MCB7_55	25000	98.912	ITS	Soil
IN_MCB8_55	25000	98.952	ITS	Soil
IN_MCB28_WT	25000	98.8	ITS	Soil
IN_MCB29_WT	25000	99.324	ITS	Soil
IN_MCB33_WT	25000	98.68	ITS	Soil
TN_130A	25000	98.188	ITS	Soil
TN_130B	25000	98.868	ITS	Soil
TN_130C	25000	99.148	ITS	Soil
TN_132A	25000	99.204	ITS	Soil
TN_132B	25000	99.392	ITS	Soil
TN_132C	25000	98.768	ITS	Soil
TN_272A	25000	99.304	ITS	Soil
TN_272B	25000	98.42	ITS	Soil
TN_272C	25000	98.852	ITS	Soil
TN_55A	25000	98.932	ITS	Soil
TN_55B	25000	98.252	ITS	Soil
TN_55C	25000	99.164	ITS	Soil
TN_LS1_WT	25000	99.088	ITS	Soil
TN_LS2_WT	25000	99.084	ITS	Soil
TN_LS3_WT	25000	99.04	ITS	Soil
TN_MB19_WT	25000	98.684	ITS	Soil
TN_MB20_WT	25000	99.256	ITS	Soil
TN_MB21_WT	25000	98.472	ITS	Soil
WA_BNL20_130	25000	99.204	ITS	Soil
WA_RN7_132	25000	99.372	ITS	Soil
WA_RN8_132	25000	99.2	ITS	Soil
WA_BNL17_272	25000	99.208	ITS	Soil
WA_BNL18_272	25000	99.272	ITS	Soil
WA_RN10_272	25000	99.204	ITS	Soil
WA_BNL19_55	25000	99.52	ITS	Soil
WA_RN1_55	25000	99.252	ITS	Soil
WA_RN2_55	25000	99.176	ITS	Soil
WA_BNL21_WT	25000	99.288	ITS	Soil
WA_BNL22_WT	25000	99.156	ITS	Soil
WA_BNL23_WT	25000	98.816	ITS	Soil

Table A.5. Sensitivity, specificity, and indicator values for bacterial indicator OTUs for caulosphere of *Juglans nigra* in Indiana (IN), Tennessee (TN), Washington (WA), IN+TN, and TCD positive trees and TCD negative trees in WA.

OTU	Specificity	Sensitivity	Indicator Valu	P-Value	Group	Habitat
BOtu0121_Terrimonas	0.9823	1	0.991	1.00E-04	IN	Caulosphere
BOtu0145_Microscillaceae	0.967	1	0.983	1.00E-04	IN	Caulosphere
BOtu0136_Flavisolibacter	0.963	1	0.981	1.00E-04	IN	Caulosphere
BOtu0212_Spirosoma	1	0.9333	0.966	1.00E-04	IN	Caulosphere
BOtu0187_Roseiflexaceae	0.9265	1	0.963	1.00E-04	IN	Caulosphere
BOtu0252_Armatimonadales	0.9615	0.9333	0.947	1.00E-04	IN	Caulosphere
BOtu0209_Spirosoma	0.9524	0.9333	0.943	1.00E-04	IN	Caulosphere
BOtu0162_Subgroup_6	0.9242	0.9333	0.929	1.00E-04	IN	Caulosphere
BOtu0172_Spirosomaceae	0.9211	0.9333	0.927	1.00E-04	IN	Caulosphere
BOtu0109_Spirosoma	0.8293	1	0.911	1.00E-04	IN	Caulosphere
BOtu0144_67.14	0.9545	0.8667	0.91	1.00E-04	IN	Caulosphere
BOtu0064_Ferruginibacter	0.8232	1	0.907	1.00E-04	IN	Caulosphere
BOtu0034_Pseudonocardia	0.9379	0.8667	0.902	0.0003	IN	Caulosphere
BOtu0411_Rhizobiaceae	0.9333	0.8667	0.899	1.00E-04	IN	Caulosphere
BOtu0117_Cryptosporangium	0.9304	0.8667	0.898	1.00E-04	IN	Caulosphere
BOtu0167_Spirosomaceae	0.8587	0.9333	0.895	1.00E-04	IN	Caulosphere
BOtu0272_Beijerinckiaceae	1	0.8	0.894	1.00E-04	IN	Caulosphere
BOtu0238_Chthoniobacter	0.7846	1	0.886	1.00E-04	IN	Caulosphere
BOtu0258_Acetobacteraceae	0.84	0.9333	0.885	1.00E-04	IN	Caulosphere
BOtu0108_Chitinophagaceae	0.7787	1	0.882	1.00E-04	IN	Caulosphere
BOtu0054_Geodermatophilus	0.7749	1	0.88	1.00E-04	IN	Caulosphere
BOtu0281_Hymenobacter	0.8837	0.8667	0.875	1.00E-04	IN	Caulosphere
BOtu0113_Kineosporia	0.8166	0.9333	0.873	1.00E-04	IN	Caulosphere
BOtu0299_R7C24	0.9412	0.8	0.868	1.00E-04	IN	Caulosphere
BOtu0203_Devosia	0.806	0.9333	0.867	1.00E-04	IN	Caulosphere
BOtu0312_Caulobacter	0.9268	0.8	0.861	1.00E-04	IN	Caulosphere
BOtu0152_Spirosoma	0.9245	0.8	0.86	0.0002	IN	Caulosphere
BOtu0129_Spirosomaceae	0.9859	0.7333	0.85	1.00E-04	IN	Caulosphere
BOtu0171_Sphingomonas	0.8342	0.8667	0.85	0.0003	IN	Caulosphere
BOtu0232_Chthoniobacter	0.8958	0.8	0.847	0.0002	IN	Caulosphere
BOtu0135_JG30.KF.CM45	0.8197	0.8667	0.843	1.00E-04	IN	Caulosphere
BOtu0374_Flavobacterium	0.9643	0.7333	0.841	1.00E-04	IN	Caulosphere
BOtu0179_Sphingomonadaceae	0.75	0.9333	0.837	0.0002	IN	Caulosphere
BOtu0176_Methylobacterium	0.873	0.8	0.836	1.00E-04	IN	Caulosphere
BOtu0410_Acetobacteraceae	0.9524	0.7333	0.836	1.00E-04	IN	Caulosphere
BOtu0352_Chthoniobacter	0.8718	0.8	0.835	1.00E-04	IN	Caulosphere
BOtu0243_Chthoniobacter	0.7925	0.8667	0.829	0.0004	IN	Caulosphere
BOtu0277_Spirosoma	0.9219	0.7333	0.822	1.00E-04	IN	Caulosphere
BOtu0296_Fimbriiglobus	0.7234	0.9333	0.822	1.00E-04	IN	Caulosphere
BOtu0354_Chthoniobacter	0.8438	0.8	0.822	1.00E-04	IN	Caulosphere
BOtu0301_Xanthobacteraceae	1	0.6667	0.816	1.00E-04	IN	Caulosphere
BOtu0303_Spirosoma	1	0.6667	0.816	1.00E-04	IN	Caulosphere
BOtu0441_Mucilaginibacter	1	0.6667	0.816	0.0002	IN	Caulosphere
BOtu0681_Phenylobacterium	1	0.6667	0.816	0.0004	IN	Caulosphere
BOtu0223_Haliangium	0.8909	0.7333	0.808	0.0004	IN	Caulosphere
BOtu0262_Spirosoma	0.9714	0.6667	0.805	0.0002	IN	Caulosphere
BOtu0235_Blastocatella	0.88	0.7333	0.803	0.0006	IN	Caulosphere
BOtu0008_Actinomycetospora	1	1	1	1.00E-04	IN.TN	Caulosphere
BOtu0063_Labrys	1	1	1	1.00E-04	IN.TN	Caulosphere
BOtu0066_Verrucomicrobiae	1	1	1	1.00E-04	IN.TN	Caulosphere
BOtu0033_Micromonosporaceae	0.9956	1	0.998	1.00E-04	IN.TN	Caulosphere
BOtu0035_Methylobacterium	0.9953	1	0.998	1.00E-04	IN.TN	Caulosphere
BOtu0080_Solirubrobacter	0.9934	1	0.997	1.00E-04	IN.TN	Caulosphere
BOtu0060_Sphingomonadaceae	0.9916	1	0.996	1.00E-04	IN.TN	Caulosphere
BOtu0026_Psychroglaciecola	0.9907	1	0.995	1.00E-04	IN.TN	Caulosphere
BOtu0029_Actinomycetospora	1	0.9667	0.983	1.00E-04	IN.TN	Caulosphere
BOtu0040_Solirubrobacteraceae	1	0.9667	0.983	1.00E-04	IN.TN	Caulosphere
BOtu0050_Blastocatella	1	0.9667	0.983	1.00E-04	IN.TN	Caulosphere
BOtu0051_Chitinophagaceae	1	0.9667	0.983	1.00E-04	IN.TN	Caulosphere
BOtu0059_Acidiphilium	1	0.9667	0.983	1.00E-04	IN.TN	Caulosphere
BOtu0132_Beijerinckiaceae	1	0.9667	0.983	1.00E-04	IN.TN	Caulosphere
BOtu0073_Caulobacteraceae	0.9839	0.9667	0.975	1.00E-04	IN.TN	Caulosphere
BOtu0032_Amnibacterium	0.9476	1	0.973	1.00E-04	IN.TN	Caulosphere
BOtu0118_Marmoricola	0.9684	0.9667	0.968	1.00E-04	IN.TN	Caulosphere
BOtu0012_Candidatus_Phytoplasma	1	0.9333	0.966	1.00E-04	IN.TN	Caulosphere
BOtu0101_Sphingomonadaceae	1	0.9333	0.966	1.00E-04	IN.TN	Caulosphere
BOtu0123_Fimbriimonadaceae	1	0.9333	0.966	1.00E-04	IN.TN	Caulosphere
BOtu0112_Belnapia	0.991	0.9333	0.962	1.00E-04	IN.TN	Caulosphere
BOtu0070_Sphingomonadaceae	0.951	0.9667	0.959	1.00E-04	IN.TN	Caulosphere
BOtu0137_Beijerinckiaceae	0.9792	0.9333	0.956	1.00E-04	IN.TN	Caulosphere
BOtu0023_Actinobacteria	1	0.9	0.949	1.00E-04	IN.TN	Caulosphere
BOtu0072_Craurococcus	1	0.9	0.949	1.00E-04	IN.TN	Caulosphere
BOtu0120_Chitinophagaceae	1	0.9	0.949	1.00E-04	IN.TN	Caulosphere
BOtu0131_Alphaproteobacteria	1	0.9	0.949	1.00E-04	IN.TN	Caulosphere
BOtu0191_Armatimonadales	1	0.9	0.949	1.00E-04	IN.TN	Caulosphere
BOtu0283_Armatimonadales	1	0.9	0.949	1.00E-04	IN.TN	Caulosphere
BOtu0065_Sphingomonadaceae	0.995	0.9	0.946	1.00E-04	IN.TN	Caulosphere
BOtu0077_Methylobacterium	0.9507	0.9333	0.942	1.00E-04	IN.TN	Caulosphere
BOtu0093_Chitinophagaceae	0.9858	0.9	0.942	1.00E-04	IN.TN	Caulosphere
BOtu0175_Solirubrobacteraceae	0.9487	0.9333	0.941	1.00E-04	IN.TN	Caulosphere
BOtu0071_Spirosoma	1	0.8667	0.931	1.00E-04	IN.TN	Caulosphere
BOtu0084_67.14	1	0.8667	0.931	1.00E-04	IN.TN	Caulosphere
BOtu0090_1174.901.12	1	0.8667	0.931	1.00E-04	IN.TN	Caulosphere
BOtu0095_Solirubrobacter	1	0.8667	0.931	1.00E-04	IN.TN	Caulosphere
BOtu0163_Sphingomonadaceae	1	0.8667	0.931	1.00E-04	IN.TN	Caulosphere
BOtu0164_Spirosoma	1	0.8667	0.931	1.00E-04	IN.TN	Caulosphere
BOtu0166_Acetobacteraceae	1	0.8667	0.931	1.00E-04	IN.TN	Caulosphere
BOtu0199_Methylobacterium	1	0.8667	0.931	1.00E-04	IN.TN	Caulosphere
BOtu0216_Quadrisphaera	1	0.8667	0.931	1.00E-04	IN.TN	Caulosphere
BOtu0231_Frankiales	1	0.8667	0.931	1.00E-04	IN.TN	Caulosphere
BOtu0074_Sphingomonadaceae	0.9901	0.8667	0.926	1.00E-04	IN.TN	Caulosphere
BOtu0110_Burkholderiaceae	0.989	0.8667	0.926	0.0002	IN.TN	Caulosphere
BOtu0138_Sphingomonadaceae	0.9779	0.8667	0.921	0.0002	IN.TN	Caulosphere
BOtu0124_Geodermatophilus	0.9263	0.9	0.913	0.0014	IN.TN	Caulosphere
BOtu0097_Actinobacteria	1	0.8333	0.913	0.0002	IN.TN	Caulosphere
BOtu0105_Spirosoma	1	0.8333	0.913	0.0002	IN.TN	Caulosphere
BOtu0146_Geodermatophilaceae	1	0.8333	0.913	1.00E-04	IN.TN	Caulosphere
BOtu0150_Nocardioides	1	0.8333	0.913	1.00E-04	IN.TN	Caulosphere
BOtu0158_Fimbriimonadaceae	1	0.8333	0.913	1.00E-04	IN.TN	Caulosphere
BOtu0197_Methylobacterium	1	0.8333	0.913	1.00E-04	IN.TN	Caulosphere
BOtu0225_Fimbriimonadales	1	0.8333	0.913	1.00E-04	IN.TN	Caulosphere
BOtu0269_Caulobacteraceae	1	0.8333	0.913	1.00E-04	IN.TN	Caulosphere
BOtu0134_Terriglobus	0.958	0.8667	0.911	1.00E-04	IN.TN	Caulosphere
BOtu0147_FBP	0.913	0.9	0.906	0.0003	IN.TN	Caulosphere
BOtu0104_Microlunatus	1	0.8	0.894	1.00E-04	IN.TN	Caulosphere
BOtu0181_Sphingomonadaceae	1	0.8	0.894	1.00E-04	IN.TN	Caulosphere
BOtu0224_Fimbriimonadaceae	1	0.8	0.894	0.0002	IN.TN	Caulosphere
BOtu0233_Methylobacterium	1	0.8	0.894	1.00E-04	IN.TN	Caulosphere
BOtu0294_Burkholderiaceae	1	0.8	0.894	1.00E-04	IN.TN	Caulosphere
BOtu0126_Devosiaceae	0.9492	0.8333	0.889	0.0006	IN.TN	Caulosphere
BOtu0127_Sphingomonadaceae	0.9822	0.8	0.886	0.0006	IN.TN	Caulosphere
BOtu0041_Aureimonas	0.8398	0.9333	0.885	0.0014	IN.TN	Caulosphere
BOtu0130_Spirosomaceae	1	0.7667	0.876	1.00E-04	IN.TN	Caulosphere
BOtu0133_Aureimonas	1	0.7667	0.876	0.0002	IN.TN	Caulosphere
BOtu0143_Beijerinckiaceae	1	0.7667	0.876	1.00E-04	IN.TN	Caulosphere
BOtu0214_Chloroflexi	1	0.7667	0.876	0.0002	IN.TN	Caulosphere
BOtu0237_Chthoniobacterales	1	0.7667	0.876	0.0002	IN.TN	Caulosphere
BOtu0103_Frankiales	0.9643	0.7667	0.86	0.0021	IN.TN	Caulosphere
BOtu0125_Chitinophagaceae	1	0.7333	0.856	0.0002	IN.TN	Caulosphere
BOtu0195_Acetobacteraceae	1	0.7333	0.856	0.0002	IN.TN	Caulosphere
BOtu0200_Ellin6055	1	0.7333	0.856	0.0004	IN.TN	Caulosphere
BOtu0286_Ellin6055	1	0.7333	0.856	0.0003	IN.TN	Caulosphere
BOtu0376_Jatrophihabitans	1	0.7333	0.856	0.0002	IN.TN	Caulosphere
BOtu0141_1174.901.12	0.9449	0.7667	0.851	0.007	IN.TN	Caulosphere
BOtu0259_Nocardioides	0.9725	0.7333	0.844	0.0006	IN.TN	Caulosphere
BOtu0122_Janibacter	1	0.7	0.837	0.0002	IN.TN	Caulosphere
BOtu0190_Chitinophagaceae	1	0.7	0.837	0.0002	IN.TN	Caulosphere
BOtu0205_Jatrophihabitans	1	0.7	0.837	0.0003	IN.TN	Caulosphere
BOtu0341_Sphingomonas	1	0.7	0.837	0.0007	IN.TN	Caulosphere
BOtu0419_Beijerinckiaceae	1	0.7	0.837	1.00E-04	IN.TN	Caulosphere
BOtu0083_Micromonosporaceae	0.9928	0.7	0.834	0.0021	IN.TN	Caulosphere
BOtu0248_Bradyrhizobium	0.9684	0.7	0.823	0.001	IN.TN	Caulosphere
BOtu0217_Flavitalea	1	0.6667	0.816	0.0004	IN.TN	Caulosphere
BOtu0245_Phaselicystis	1	0.6667	0.816	0.0009	IN.TN	Caulosphere
BOtu0270_Chthoniobacter	1	0.6667	0.816	0.0008	IN.TN	Caulosphere
BOtu0229_Hymenobacter	0.9171	0.7	0.801	0.0099	IN.TN	Caulosphere
BOtu0796_Hymenobacter	1	1	1	0.0081	Negative	Caulosphere
BOtu0475_Hymenobacter	0.9681	1	0.984	0.0081	Negative	Caulosphere
BOtu0193_Spirosoma	0.9211	1	0.96	0.0237	Negative	Caulosphere
BOtu0111_Modestobacter	0.9172	1	0.958	0.0332	Negative	Caulosphere
BOtu0194_Pseudomonas	0.875	1	0.935	0.0235	Negative	Caulosphere
BOtu0574_FBP	0.8448	1	0.919	0.0398	Negative	Caulosphere
BOtu0139_Devosiaceae	0.8151	1	0.903	0.0253	Negative	Caulosphere
BOtu0009_Halotalea	1	1	1	0.0081	Positive	Caulosphere
BOtu0067_Aeromicrobium	1	1	1	0.0081	Positive	Caulosphere
BOtu0087_Pedobacter	1	1	1	0.0081	Positive	Caulosphere
BOtu0309_Sphingomonas	1	1	1	0.0081	Positive	Caulosphere
BOtu0057_Azotobacter	0.9798	1	0.99	0.0081	Positive	Caulosphere
BOtu0107_Dyadobacter	0.9677	1	0.984	0.0081	Positive	Caulosphere
BOtu0011_Microbacteriaceae	0.9424	1	0.971	0.0081	Positive	Caulosphere
BOtu0016_Micrococcales	1	0.8571	0.926	0.0442	Positive	Caulosphere
BOtu0007_Xanthomonadaceae	0.9948	0.8571	0.923	0.0371	Positive	Caulosphere
BOtu0027_Rhizobiaceae	0.852	1	0.923	0.033	Positive	Caulosphere
BOtu0055_Pedobacter	0.9435	0.8571	0.899	0.0405	Positive	Caulosphere
BOtu0100_Oxyphotobacteria	0.9698	0.9333	0.951	1.00E-04	TN	Caulosphere
BOtu0142_Spirosoma	0.958	0.9333	0.946	1.00E-04	TN	Caulosphere
BOtu0094_1174.901.12	0.9967	0.8667	0.929	1.00E-04	TN	Caulosphere
BOtu0305_Microlunatus	0.8548	0.9333	0.893	1.00E-04	TN	Caulosphere
BOtu0246_Psychroglaciecola	0.828	0.9333	0.879	1.00E-04	TN	Caulosphere
BOtu0219_Acetobacteraceae	0.9364	0.8	0.866	1.00E-04	TN	Caulosphere
BOtu0148_Hymenobacter	1	0.7333	0.856	1.00E-04	TN	Caulosphere
BOtu0454_Oxyphotobacteria	0.8421	0.8667	0.854	1.00E-04	TN	Caulosphere
BOtu0276_Beijerinckiaceae	0.8375	0.8667	0.852	1.00E-04	TN	Caulosphere
BOtu0347_Acetobacteraceae	0.8772	0.8	0.838	1.00E-04	TN	Caulosphere
BOtu0384_Acetobacteraceae	0.8704	0.8	0.834	0.0002	TN	Caulosphere
BOtu0210_1174.901.12	0.9356	0.7333	0.828	1.00E-04	TN	Caulosphere
BOtu0282_1174.901.12	0.9136	0.7333	0.819	0.0002	TN	Caulosphere
BOtu0550_Acetobacteraceae	0.9655	0.6667	0.802	1.00E-04	TN	Caulosphere
BOtu0292_FBP	0.8	0.8	0.8	0.0016	TN	Caulosphere
BOtu0332_Acetobacteraceae	0.8	0.8	0.8	0.0002	TN	Caulosphere
BOtu0003_Sphingomonas	0.9911	1	0.996	1.00E-04	WA	Caulosphere
BOtu0024_Hymenobacter	0.9888	1	0.994	1.00E-04	WA	Caulosphere
BOtu0028_Hymenobacter	0.984	1	0.992	1.00E-04	WA	Caulosphere
BOtu0069_Acidiphilium	0.9817	1	0.991	1.00E-04	WA	Caulosphere
BOtu0004_Burkholderiaceae	0.9796	1	0.99	1.00E-04	WA	Caulosphere
BOtu0078_Massilia	0.9753	1	0.988	1.00E-04	WA	Caulosphere
BOtu0025_Methylobacterium	0.9677	1	0.984	1.00E-04	WA	Caulosphere
BOtu0058_Deinococcus	0.9537	1	0.977	1.00E-04	WA	Caulosphere
BOtu0089_FBP	0.9284	1	0.964	1.00E-04	WA	Caulosphere
BOtu0043_Microbacteriaceae	0.9028	1	0.95	1.00E-04	WA	Caulosphere
BOtu0017_Pseudomonas	0.9018	1	0.95	1.00E-04	WA	Caulosphere
BOtu0085_Spirosomaceae	1	0.9	0.949	1.00E-04	WA	Caulosphere
BOtu0177_Acetobacteraceae	1	0.9	0.949	1.00E-04	WA	Caulosphere
BOtu0196_Hymenobacter	1	0.9	0.949	1.00E-04	WA	Caulosphere
BOtu0046_Kineococcus	0.8906	1	0.944	1.00E-04	WA	Caulosphere
BOtu0151_Sphingomonadaceae	0.9759	0.9	0.937	1.00E-04	WA	Caulosphere
BOtu0092_Nakamurella	0.8425	1	0.918	0.0002	WA	Caulosphere
BOtu0304_Hymenobacter	0.9669	0.8	0.88	1.00E-04	WA	Caulosphere
BOtu0319_Burkholderiaceae	0.9623	0.8	0.877	1.00E-04	WA	Caulosphere
BOtu0009_Halotalea	1	0.7	0.837	1.00E-04	WA	Caulosphere
BOtu0535_Hymenobacter	1	0.7	0.837	1.00E-04	WA	Caulosphere
BOtu0309_Sphingomonas	0.9706	0.7	0.824	1.00E-04	WA	Caulosphere
BOtu0107_Dyadobacter	0.8486	0.8	0.824	1.00E-04	WA	Caulosphere

Table A.6 (Page 1 of 3). Sensitivity, specificity, and indicator values for bacterial indicator OTUs for soils of Juglans nigra in Indiana (IN), Tennessee (TN), Washington (WA), IN+TN, and TCD positive trees and TCD negative trees in WA.

OTU	Specificity	Sensitivity	Indicator Value	P-Value	Group	Habitat
Otu00306_Mycobacterium	0.8997	1	0.949	1.00E-04	IN	Soil
Otu02318_Subgroup_25	0.9344	0.8667	0.9	1.00E-04	IN	Soil
Otu00577_Ardenticatenales	0.8598	0.9333	0.896	0.0003	IN	Soil
Otu01347_Subgroup_17	0.8583	0.9333	0.895	1.00E-04	IN	Soil
Otu02782_Haliangium	0.8773	0.8667	0.872	1.00E-04	IN	Soil
Otu02190_Gaiellales	0.8737	0.8667	0.87	1.00E-04	IN	Soil
Otu01442_Gemmatimonadaceae	0.8677	0.8667	0.867	0.0002	IN	Soil
Otu01397_Sporichthyaceae	0.8632	0.8667	0.865	1.00E-04	IN	Soil
Otu01322_JG30.KF.CM45	0.8587	0.8667	0.863	1.00E-04	IN	Soil
Otu01443_S085	0.9269	0.8	0.861	1.00E-04	IN	Soil
Otu00262_Deltaproteobacteria	0.9184	0.8	0.857	0.0004	IN	Soil
Otu05672_SBR1031	1	0.7333	0.856	1.00E-04	IN	Soil
Otu00640_Subgroup_11	0.8426	0.8667	0.855	1.00E-04	IN	Soil
Otu02434_Gemmataceae	0.8356	0.8667	0.851	1.00E-04	IN	Soil
Otu02563_Gemmataceae	0.8328	0.8667	0.85	1.00E-04	IN	Soil
Otu00667_Nitrospira	0.8989	0.8	0.848	1.00E-04	IN	Soil
Otu02421_mle1.8	0.7184	1	0.848	0.0017	IN	Soil
Otu00945_mle1.7	0.828	0.8667	0.847	1.00E-04	IN	Soil
Otu00240_Subgroup_6	0.8941	0.8	0.846	1.00E-04	IN	Soil
Otu01792_Myxococcales	0.8246	0.8667	0.845	1.00E-04	IN	Soil
Otu00910_Subgroup_6	0.8892	0.8	0.843	0.0004	IN	Soil
Otu01763_Gammaproteobacteria	0.8891	0.8	0.843	1.00E-04	IN	Soil
Otu01163_mle1.7	0.7597	0.9333	0.842	0.0005	IN	Soil
Otu02134_Gemmataceae	0.8171	0.8667	0.842	1.00E-04	IN	Soil
Otu02148_Actinobacteria	0.9656	0.7333	0.841	1.00E-04	IN	Soil
Otu02485_Subgroup_18	0.8843	0.8	0.841	1.00E-04	IN	Soil
Otu02422_Entotheonellaceae	0.8826	0.8	0.84	1.00E-04	IN	Soil
Otu02235_Subgroup_25	0.8796	0.8	0.839	0.0002	IN	Soil
Otu01572_MB.A2.108	0.8776	0.8	0.838	1.00E-04	IN	Soil
Otu00242_Geminicoccaceae	0.8095	0.8667	0.838	0.0002	IN	Soil
Otu01816_Gemmataceae	0.7452	0.9333	0.834	0.0002	IN	Soil
Otu02011_Deltaproteobacteria	0.7916	0.8667	0.828	1.00E-04	IN	Soil
Otu03661_Subgroup_6	0.9351	0.7333	0.828	1.00E-04	IN	Soil
Otu02589_Acidobacteriales	0.8566	0.8	0.828	1.00E-04	IN	Soil
Otu02487_Anaerolineae	0.8564	0.8	0.828	1.00E-04	IN	Soil
Otu02677_Gaiella	0.853	0.8	0.826	1.00E-04	IN	Soil
Otu01506_Pedosphaeraceae	0.787	0.8667	0.826	1.00E-04	IN	Soil
Otu02921_Subgroup_25	0.9248	0.7333	0.824	1.00E-04	IN	Soil
Otu03140_OM190	0.8458	0.8	0.823	1.00E-04	IN	Soil
Otu00957_RBG.13.54.9	0.7235	0.9333	0.822	0.0007	IN	Soil
Otu05198_RB41	0.7792	0.8667	0.822	1.00E-04	IN	Soil
Otu02707_Gemmataceae	0.8424	0.8	0.821	1.00E-04	IN	Soil
Otu00207_B1.7BS	0.8417	0.8	0.821	1.00E-04	IN	Soil
Otu01176_Chitinophagales	0.7204	0.9333	0.82	0.0013	IN	Soil
Otu00538_RCP2.54	0.775	0.8667	0.82	1.00E-04	IN	Soil
Otu02733_Pedosphaeraceae	0.7744	0.8667	0.819	0.0002	IN	Soil
Otu01346_Anaerolineae	0.9147	0.7333	0.819	1.00E-04	IN	Soil
Otu03953_NB1.j	1	0.6667	0.816	1.00E-04	IN	Soil
Otu04460_Ardenticatenales	1	0.6667	0.816	1.00E-04	IN	Soil
Otu02399_Ilumatobacteraceae	0.7632	0.8667	0.813	1.00E-04	IN	Soil
Otu02156_Gaiellales	0.9918	0.6667	0.813	1.00E-04	IN	Soil
Otu02720_Pla3_lineage	0.8262	0.8	0.813	1.00E-04	IN	Soil
Otu00964_wb1.P19	0.8205	0.8	0.81	1.00E-04	IN	Soil
Otu02096_Caldilineaceae	0.7541	0.8667	0.808	0.0002	IN	Soil
Otu04187_Lineage_IV	0.8904	0.7333	0.808	1.00E-04	IN	Soil
Otu01804_JG30.KF.CM66	0.7511	0.8667	0.807	0.0092	IN	Soil
Otu04300_Pedosphaeraceae	0.8869	0.7333	0.806	1.00E-04	IN	Soil
Otu00699_Pirellulaceae	0.695	0.9333	0.805	0.004	IN	Soil
Otu02773_Ardenticatenales	0.8091	0.8	0.805	1.00E-04	IN	Soil
Otu02949_Latescibacteria	0.7468	0.8667	0.805	0.0003	IN	Soil
Otu06443_Myxococcales	0.8819	0.7333	0.804	1.00E-04	IN	Soil
Otu01446_Latescibacteria	0.7383	0.8667	0.8	1.00E-04	IN	Soil
Otu00158_S085	0.9885	1	0.994	1.00E-04	IN.TN	Soil
Otu00214_Subgroup_6	0.9855	0.9697	0.978	1.00E-04	IN.TN	Soil
Otu00268_Alphaproteobacteria	0.9483	1	0.974	1.00E-04	IN.TN	Soil
Otu00806_WD2101_soil_group	0.9399	1	0.969	1.00E-04	IN.TN	Soil
Otu00546_Chitinophagaceae	0.9381	1	0.969	1.00E-04	IN.TN	Soil
Otu00657_Subgroup_22	0.9656	0.9697	0.968	1.00E-04	IN.TN	Soil
Otu00439_Candidatus_Udaeobacter	0.9603	0.9697	0.965	1.00E-04	IN.TN	Soil
Otu00592_Latescibacteria	0.9533	0.9697	0.961	1.00E-04	IN.TN	Soil
Otu00431_Deltaproteobacteria	0.9459	0.9697	0.958	1.00E-04	IN.TN	Soil
Otu00812_Latescibacteria	0.9679	0.9394	0.954	1.00E-04	IN.TN	Soil
Otu01502_Gemmatimonadaceae	0.9622	0.9394	0.951	1.00E-04	IN.TN	Soil
Otu00467_WD2101_soil_group	0.9021	1	0.95	0.0002	IN.TN	Soil
Otu01122_Gemmataceae	0.9302	0.9697	0.95	1.00E-04	IN.TN	Soil
Otu01795_Pedosphaeraceae	0.99	0.9091	0.949	1.00E-04	IN.TN	Soil
Otu00837_Gaiellales	0.9865	0.9091	0.947	1.00E-04	IN.TN	Soil
Otu01342_Steroidobacteraceae	0.9684	0.9091	0.938	1.00E-04	IN.TN	Soil
Otu01264_Chloroflexales	1	0.8788	0.937	1.00E-04	IN.TN	Soil
Otu00009_Candidatus_Udaeobacter	0.9013	0.9697	0.935	1.00E-04	IN.TN	Soil
Otu00245_Latescibacteria	0.8735	1	0.935	1.00E-04	IN.TN	Soil
Otu00432_Beijerinckiaceae	0.9497	0.9091	0.929	1.00E-04	IN.TN	Soil
Otu01603_Myxococcales	0.8901	0.9697	0.929	1.00E-04	IN.TN	Soil

OTU	Specificity	Sensitivity	Indicator Value	P-Value	Group	Habitat
Otu00735_MB.A2.108	0.9473	0.9091	0.928	0.0002	IN.TN	Soil
Otu00873_Pedosphaeraceae	0.9443	0.9091	0.927	1.00E-04	IN.TN	Soil
Otu01051_WD2101_soil_group	0.9079	0.9394	0.923	1.00E-04	IN.TN	Soil
Otu00944_Gaiellales	1	0.8485	0.921	1.00E-04	IN.TN	Soil
Otu01379_Gemmataceae	0.9293	0.9091	0.919	1.00E-04	IN.TN	Soil
Otu00741_Latescibacteria	0.952	0.8788	0.915	1.00E-04	IN.TN	Soil
Otu00713_Burkholderiaceae	0.9852	0.8485	0.914	1.00E-04	IN.TN	Soil
Otu01392_Gemmataceae	0.919	0.9091	0.914	0.0002	IN.TN	Soil
Otu00752_Frankiales	0.9474	0.8788	0.912	0.0006	IN.TN	Soil
Otu01473_Gemmataceae	0.9787	0.8485	0.911	1.00E-04	IN.TN	Soil
Otu01209_Roseiflexaceae	0.9738	0.8485	0.909	1.00E-04	IN.TN	Soil
Otu01480_MB.A2.108	0.9402	0.8788	0.909	1.00E-04	IN.TN	Soil
Otu01684_Terrabacter	0.9735	0.8485	0.909	1.00E-04	IN.TN	Soil
Otu01303_Geminicoccaceae	0.9082	0.9091	0.909	0.0008	IN.TN	Soil
Otu00274_Gaiellales	0.9876	0.8182	0.899	0.0007	IN.TN	Soil
Otu01101_Chitinophagaceae	0.9484	0.8485	0.897	0.0002	IN.TN	Soil
Otu01087_MB.A2.108	0.8847	0.9091	0.897	0.0016	IN.TN	Soil
Otu01104_Rokubacteriales	0.8468	0.9394	0.892	0.0015	IN.TN	Soil
Otu00291_Terrimonas	0.933	0.8485	0.89	0.0029	IN.TN	Soil
Otu00968_Nitrospira	1	0.7879	0.888	1.00E-04	IN.TN	Soil
Otu01311_Subgroup_6	0.9267	0.8485	0.887	0.0015	IN.TN	Soil
Otu01412_Subgroup_22	0.9602	0.8182	0.886	1.00E-04	IN.TN	Soil
Otu00995_Rokubacteriales	0.9923	0.7879	0.884	0.0002	IN.TN	Soil
Otu00127_Gaiellales	0.9206	0.8485	0.884	0.0012	IN.TN	Soil
Otu01207_Gemmatimonadaceae	0.9894	0.7879	0.883	1.00E-04	IN.TN	Soil
Otu01023_Subgroup_25	0.9513	0.8182	0.882	0.0003	IN.TN	Soil
Otu00492_GOUTA6	0.9497	0.8182	0.882	0.0014	IN.TN	Soil
Otu00641_IMCC26256	0.9438	0.8182	0.879	0.0008	IN.TN	Soil
Otu00540_Geobacter	0.9751	0.7879	0.877	0.001	IN.TN	Soil
Otu00410_A21b	0.8736	0.8788	0.876	0.0038	IN.TN	Soil
Otu01081_Roseiflexaceae	0.9364	0.8182	0.875	0.0034	IN.TN	Soil
Otu01639_Desulfarculaceae	0.9339	0.8182	0.874	1.00E-04	IN.TN	Soil
Otu01371_NB1.j	0.93	0.8182	0.872	0.0014	IN.TN	Soil
Otu02384_OM190	0.93	0.8182	0.872	0.0002	IN.TN	Soil
Otu01893_Actinobacteria	0.8955	0.8485	0.872	0.0014	IN.TN	Soil
Otu00320_Streptomyces	0.9633	0.7879	0.871	0.0061	IN.TN	Soil
Otu00352_C0119	0.9259	0.8182	0.87	0.0084	IN.TN	Soil
Otu00915_Latescibacteria	1	0.7576	0.87	1.00E-04	IN.TN	Soil
Otu00553_Subgroup_6	0.9581	0.7879	0.869	0.0391	IN.TN	Soil
Otu01766_Rokubacteriales	0.9907	0.7576	0.866	1.00E-04	IN.TN	Soil
Otu00975_MB.A2.108	0.9136	0.8182	0.865	0.0032	IN.TN	Soil
Otu01867_Roseiflexaceae	0.9051	0.8182	0.861	0.0015	IN.TN	Soil
Otu02284_Microtrichales	0.8964	0.8182	0.856	0.0012	IN.TN	Soil
Otu01218_WD2101_soil_group	0.9303	0.7879	0.856	0.0023	IN.TN	Soil
Otu00519_Acidothermus	0.9302	0.7879	0.856	0.0002	IN.TN	Soil
Otu00265_Subgroup_6	0.9257	0.7879	0.854	0.0067	IN.TN	Soil
Otu00728_JG30.KF.CM45	0.954	0.7576	0.85	1.00E-04	IN.TN	Soil
Otu00297_Gaiella	0.9901	0.7273	0.849	1.00E-04	IN.TN	Soil
Otu02813_Micromonosporaceae	0.9134	0.7879	0.848	0.0014	IN.TN	Soil
Otu00983_Isosphaeraceae	0.9111	0.7879	0.847	0.0078	IN.TN	Soil
Otu01879_Geobacter	0.9447	0.7576	0.846	0.0006	IN.TN	Soil
Otu02121_Chloroflexi	0.9054	0.7879	0.845	0.002	IN.TN	Soil
Otu00959_Rhodomicrobium	0.9047	0.7879	0.844	0.0071	IN.TN	Soil
Otu03168_Sandaracinaceae	0.9789	0.7273	0.844	1.00E-04	IN.TN	Soil
Otu00950_Subgroup_11	0.9373	0.7576	0.843	0.0016	IN.TN	Soil
Otu02186_Pedosphaeraceae	0.8678	0.8182	0.843	0.0036	IN.TN	Soil
Otu02528_SC.I.84	0.9697	0.7273	0.84	0.0002	IN.TN	Soil
Otu02326_Armatimonadetes	0.93	0.7576	0.839	0.0009	IN.TN	Soil
Otu02805_mle1.8	0.9678	0.7273	0.839	1.00E-04	IN.TN	Soil
Otu01477_Gemmatimonas	0.9639	0.7273	0.837	0.0003	IN.TN	Soil
Otu03209_Pajaroellobacter	0.9247	0.7576	0.837	0.0006	IN.TN	Soil
Otu00634_Pirellula	0.9626	0.7273	0.837	0.0044	IN.TN	Soil
Otu01581_SC.I.84	1	0.697	0.835	1.00E-04	IN.TN	Soil
Otu02652_Clostridium_sensu_stricto_12	1	0.697	0.835	1.00E-04	IN.TN	Soil
Otu03552_Gemmataceae	1	0.697	0.835	1.00E-04	IN.TN	Soil
Otu00862_Subgroup_6	0.9962	0.697	0.833	1.00E-04	IN.TN	Soil
Otu01485_Subgroup_6	0.9519	0.7273	0.832	0.0006	IN.TN	Soil
Otu02164_Xanthobacteraceae	0.9873	0.697	0.83	0.0002	IN.TN	Soil
Otu02079_Micromonosporaceae	0.8728	0.7879	0.829	0.009	IN.TN	Soil
Otu01012_Roseiflexaceae	0.9423	0.7273	0.828	0.0024	IN.TN	Soil
Otu01782_Roseiflexaceae	0.8345	0.8182	0.826	0.0079	IN.TN	Soil
Otu02063_Gemmatimonas	0.9774	0.697	0.825	0.0002	IN.TN	Soil
Otu01812_Haliangium	0.86	0.7879	0.823	0.0057	IN.TN	Soil
Otu02556_Haliangium	0.9707	0.697	0.823	0.0004	IN.TN	Soil
Otu01526_Armatimonadetes	0.9279	0.7273	0.822	0.0143	IN.TN	Soil
Otu02560_Rhodococcus	0.8907	0.7576	0.821	0.0099	IN.TN	Soil
Otu00486_Oryzihumus	0.8897	0.7576	0.821	0.001	IN.TN	Soil
Otu00246_Acidothermus	0.9259	0.7273	0.821	0.0005	IN.TN	Soil
Otu02091_Subgroup_22	0.9244	0.7273	0.82	0.0014	IN.TN	Soil
Otu02857_Frankiales	0.8523	0.7879	0.819	0.0068	IN.TN	Soil
Otu02354_Gemmataceae	0.9618	0.697	0.819	0.0004	IN.TN	Soil
Otu01800_Latescibacteria	0.9612	0.697	0.818	0.0011	IN.TN	Soil
Otu01746_Vermiphilaceae	0.8495	0.7879	0.818	0.0077	IN.TN	Soil

Table A.6. Continued (Page 2 of 3)

OTU	Specificity	Sensitivity	Indicator Value	P-Value	Group	Habitat
Otu01681_Subgroup_6	1	0.6667	0.816	1.00E-04	IN.TN	Soil
Otu02470_Gammaproteobacteria	1	0.6667	0.816	0.0002	IN.TN	Soil
Otu00938_Gemmatimonadaceae	0.8791	0.7576	0.816	0.0109	IN.TN	Soil
Otu02173_Subgroup_5	0.9154	0.7273	0.816	0.0163	IN.TN	Soil
Otu00851_Entotheonellaceae	0.996	0.6667	0.815	0.0004	IN.TN	Soil
Otu01841_Burkholderiaceae	0.991	0.6667	0.813	0.0006	IN.TN	Soil
Otu00148_Subgroup_2	0.9047	0.7273	0.811	0.0048	IN.TN	Soil
Otu01773_Subgroup_7	0.9824	0.6667	0.809	0.0002	IN.TN	Soil
Otu01679_Latescibacteria	0.8942	0.7273	0.806	0.0016	IN.TN	Soil
Otu01928_Flavobacterium	0.8525	0.7576	0.804	0.0213	IN.TN	Soil
Otu02443_Chitinophagaceae	0.8843	0.7273	0.802	0.0086	IN.TN	Soil
Otu02171_Beijerinckiaceae	0.9212	0.697	0.801	0.0017	IN.TN	Soil
Otu04567_Chlamydiales	0.88	1	0.938	0.0036	Negative	Soil
Otu02619_Flavobacterium	0.8333	1	0.913	0.0143	Negative	Soil
Otu05236_Diplorickettsiaceae	0.8302	1	0.911	0.0099	Negative	Soil
Otu01475_Niastella	0.8276	1	0.91	0.0072	Negative	Soil
Otu05886_Sphingobacteriales	0.8101	1	0.9	0.0146	Negative	Soil
Otu04080_Candidatus_Berkiella	0.8	1	0.894	0.0062	Negative	Soil
Otu05681_Saccharimonadales	0.9455	0.8333	0.888	0.0067	Negative	Soil
Otu00807_Gemmatimonadaceae	0.7761	1	0.881	0.0128	Negative	Soil
Otu09665_FBP	0.9302	0.8333	0.88	0.0124	Negative	Soil
Otu02536_Haliangium	0.7742	1	0.88	0.0372	Negative	Soil
Otu07401_Saccharimonadaceae	0.9032	0.8333	0.868	0.0142	Negative	Soil
Otu08160_Tepidisphaeraceae	0.9032	0.8333	0.868	0.0122	Negative	Soil
Otu04860_Myxococcales	0.75	1	0.866	0.037	Negative	Soil
Otu02452_Micromonosporaceae	0.747	1	0.864	0.0477	Negative	Soil
Otu07722_Haliangium	0.8889	0.8333	0.861	0.0205	Negative	Soil
Otu07399_Pirellulaceae	0.88	0.8333	0.856	0.0117	Negative	Soil
Otu07273_Bacteroidia	0.7273	1	0.853	0.0203	Negative	Soil
Otu05923_Omnitrophicaeota	0.8571	0.8333	0.845	0.0393	Negative	Soil
Otu05368_Gracilibacteria	0.7033	1	0.839	0.036	Negative	Soil
Otu04296_Diplorickettsiaceae	0.8302	0.8333	0.832	0.0416	Negative	Soil
Otu05843_Verruc.01	0.8302	0.8333	0.832	0.0377	Negative	Soil
Otu04481_Aquicella	0.8235	0.8333	0.828	0.0415	Negative	Soil
Otu06300_WD2101_soil_group	0.8235	0.8333	0.828	0.0299	Negative	Soil
Otu06858_Babeliales	0.8235	0.8333	0.828	0.0432	Negative	Soil
Otu08045_UBA12409	0.8235	0.8333	0.828	0.0429	Negative	Soil
Otu02421_mle1.8	0.8	0.8333	0.816	0.0407	Negative	Soil
Otu04809_Alphaproteobacteria	0.8	0.8333	0.816	0.0453	Negative	Soil
Otu04911_SAR324_clade	0.8	0.8333	0.816	0.0465	Negative	Soil
Otu05284_Gemmataceae	0.8	0.8333	0.816	0.041	Negative	Soil
Otu05643_Silvanigrella	0.6667	1	0.816	0.0446	Negative	Soil
Otu06004_WD2101_soil_group	0.8	0.8333	0.816	0.0419	Negative	Soil
Otu07431_Pirellula	1	0.6667	0.816	0.0157	Negative	Soil
Otu08244_Hydrogenedensaceae	1	0.6667	0.816	0.0156	Negative	Soil
Otu08859_Chlamydiales	1	0.6667	0.816	0.016	Negative	Soil
Otu10779_possiblenus_04	1	0.6667	0.816	0.0145	Negative	Soil
Otu11357_Chthoniobacter	1	0.6667	0.816	0.0161	Negative	Soil
Otu15420_0319.6G20	1	0.6667	0.816	0.0161	Negative	Soil
Otu02523_Rhizobiales	0.9292	1	0.964	0.0056	Positive	Soil
Otu04769_Nocardioides	0.8919	1	0.944	0.0023	Positive	Soil
Otu02918_Saccharimonadales	0.8491	1	0.921	0.0418	Positive	Soil
Otu03746_Saccharimonadaceae	0.8462	1	0.92	0.0043	Positive	Soil
Otu04466_WD2101_soil_group	0.84	1	0.917	0.0078	Positive	Soil
Otu02643_Gaiella	0.913	0.875	0.894	0.0158	Positive	Soil
Otu01979_Gaiella	0.7959	1	0.892	0.0071	Positive	Soil
Otu02320_Brevundimonas	0.7941	1	0.891	0.0197	Positive	Soil
Otu01658_C0119	0.9	0.875	0.887	0.019	Positive	Soil
Otu03264_Gammaproteobacteria	0.8684	0.875	0.872	0.0414	Positive	Soil
Otu03028_Candidatus_Paracaedibacter	0.75	1	0.866	0.036	Positive	Soil
Otu04654_Rhizobiaceae	1	0.75	0.866	0.0104	Positive	Soil
Otu05973_Cryptosporangium	0.8571	0.875	0.866	0.0214	Positive	Soil
Otu07218_Pirellulaceae	1	0.75	0.866	0.0226	Positive	Soil
Otu07246_KD3.93	1	0.75	0.866	0.0217	Positive	Soil
Otu04820_Bacteroidia	0.8298	0.875	0.852	0.0382	Positive	Soil
Otu05664_Diplorickettsiaceae	0.8182	0.875	0.846	0.0252	Positive	Soil
Otu02298_Thermoplasmata	0.8095	0.875	0.842	0.0457	Positive	Soil
Otu04997_Aquicella	0.8049	0.875	0.839	0.0443	Positive	Soil
Otu02510_JG30.KF.CM66	0.9273	0.75	0.834	0.0415	Positive	Soil
Otu03667_Chthonomonas	0.9231	0.75	0.832	0.0324	Positive	Soil
Otu04228_WCHB1.41	0.8919	0.75	0.818	0.0496	Positive	Soil
Otu07800_MB.A2.108	0.7333	0.875	0.801	0.0342	Positive	Soil
Otu00358_GOUTA6	0.9089	0.8889	0.899	1.00E-04	TN	Soil
Otu00919_Gemmataceae	0.7988	0.9444	0.869	1.00E-04	TN	Soil
Otu01431_ADurb.Bin063.1	0.8347	0.8889	0.861	1.00E-04	TN	Soil
Otu01000_11.24	0.8248	0.8889	0.856	1.00E-04	TN	Soil
Otu01146_Betaproteobacteriales	0.8214	0.8889	0.855	0.0002	TN	Soil
Otu01199_Betaproteobacteriales	0.8127	0.8889	0.85	1.00E-04	TN	Soil
Otu01099_Acidothermus	0.8099	0.8889	0.848	0.0004	TN	Soil
Otu02743_Gemmatimonadaceae	0.7988	0.8889	0.843	1.00E-04	TN	Soil
Otu02375_CPla.3_termite_group	0.7466	0.9444	0.84	0.0002	TN	Soil
Otu00589_JG30.KF.AS9	0.9649	0.7222	0.835	1.00E-04	TN	Soil
Otu02010_Frankiales	0.8361	0.8333	0.835	1.00E-04	TN	Soil

OTU	Specificity	Sensitivity	Indicator Value	P-Value	Group	Habitat
Otu01054_Acidothermus	0.7835	0.8889	0.835	0.0021	TN	Soil
Otu01811_Gemmataceae	0.8925	0.7778	0.833	1.00E-04	TN	Soil
Otu00739_Gemmatimonas	0.7774	0.8889	0.831	0.011	TN	Soil
Otu00374_Solirubrobacterales	0.887	0.7778	0.831	0.0009	TN	Soil
Otu00388_Acidimicrobiaceae	0.7729	0.8889	0.829	0.0144	TN	Soil
Otu00637_JG30.KF.AS9	0.9504	0.7222	0.828	1.00E-04	TN	Soil
Otu00309_Nitrososphaeraceae	0.877	0.7778	0.826	0.0263	TN	Soil
Otu01057_Nitrososphaeraceae	0.7639	0.8889	0.824	1.00E-04	TN	Soil
Otu01417_Elsterales	0.9353	0.7222	0.822	1.00E-04	TN	Soil
Otu00436_Gaiellales	0.8652	0.7778	0.82	0.009	TN	Soil
Otu01236_Pirellulaceae	0.807	0.8333	0.82	1.00E-04	TN	Soil
Otu02758_Gemmataceae	0.8645	0.7778	0.82	0.0002	TN	Soil
Otu04568_Ktedonobacteraceae	0.9302	0.7222	0.82	1.00E-04	TN	Soil
Otu00459_JG30.KF.AS9	0.8633	0.7778	0.819	0.0007	TN	Soil
Otu00835_Candidatus_Nitrosotalea	0.9296	0.7222	0.819	1.00E-04	TN	Soil
Otu00517_Sphingomonas	0.8047	0.8333	0.819	0.0008	TN	Soil
Otu01309_Acidobacteriaceae	0.8615	0.7778	0.819	0.0009	TN	Soil
Otu01098_Gaiellales	0.8613	0.7778	0.818	1.00E-04	TN	Soil
Otu02383_Streptomyces	0.9259	0.7222	0.818	1.00E-04	TN	Soil
Otu00927_Myxococcales	0.7512	0.8889	0.817	0.0028	TN	Soil
Otu04510_Methylobacterium	1	0.6667	0.816	1.00E-04	TN	Soil
Otu01203_Gemmataceae	0.8556	0.7778	0.816	0.0048	TN	Soil
Otu03776_Gemmataceae	0.9193	0.7222	0.815	1.00E-04	TN	Soil
Otu01058_SC.I.84	0.8523	0.7778	0.814	1.00E-04	TN	Soil
Otu01435_Gemmataceae	0.8514	0.7778	0.814	0.0012	TN	Soil
Otu01637_Gemmatimonas	0.8509	0.7778	0.814	1.00E-04	TN	Soil
Otu01810_TK10	0.8505	0.7778	0.813	1.00E-04	TN	Soil
Otu00759_Subgroup_2	0.8492	0.7778	0.813	1.00E-04	TN	Soil
Otu00489_JG30.KF.AS9	0.9881	0.6667	0.812	1.00E-04	TN	Soil
Otu01373_Planctomycetes	0.7901	0.8333	0.811	0.0055	TN	Soil
Otu03038_Polycyclovorans	0.9077	0.7222	0.81	1.00E-04	TN	Soil
Otu02052_SC.I.84	0.8429	0.7778	0.81	1.00E-04	TN	Soil
Otu00828_Thermoleophilia	0.786	0.8333	0.809	0.0079	TN	Soil
Otu02051_Elsterales	0.7367	0.8889	0.809	0.0013	TN	Soil
Otu00442_Gaiellales	0.8415	0.7778	0.809	0.0022	TN	Soil
Otu00494_Gaiellales	0.7837	0.8333	0.808	0.0172	TN	Soil
Otu01274_Geminicoccaceae	0.8397	0.7778	0.808	1.00E-04	TN	Soil
Otu01034_Acidothermus	0.9038	0.7222	0.808	1.00E-04	TN	Soil
Otu03643_WD2101_soil_group	0.9036	0.7222	0.808	1.00E-04	TN	Soil
Otu00247_Gemmatimonadaceae	0.8364	0.7778	0.807	0.0024	TN	Soil
Otu02116_Alphaproteobacteria	0.8323	0.7778	0.805	0.0002	TN	Soil
Otu01195_MB.A2.108	0.9705	0.6667	0.804	1.00E-04	TN	Soil
Otu01891_WD2101_soil_group	0.8954	0.7222	0.804	1.00E-04	TN	Soil
Otu00259_Acidobacteriales	0.8314	0.7778	0.804	0.0043	TN	Soil
Otu01542_IMCC26256	0.8311	0.7778	0.804	0.0003	TN	Soil
Otu03592_Reyranella	0.7723	0.8333	0.802	1.00E-04	TN	Soil
Otu01148_Pseudolabrys	0.8265	0.7778	0.802	0.005	TN	Soil
Otu02378_Bryobacter	0.7699	0.8333	0.801	0.0015	TN	Soil
Otu01076_Acidobacteriales	0.8857	0.7222	0.8	1.00E-04	TN	Soil
Otu00827_Candidatus_Nitrosotenuis	0.9585	1	0.979	1.00E-04	WA	Soil
Otu04906_Pirellulaceae	0.9353	1	0.967	1.00E-04	WA	Soil
Otu00343_Candidatus_Nitrosoarchaeum	0.9292	1	0.964	1.00E-04	WA	Soil
Otu04725_Ancylobacter	1	0.9286	0.964	1.00E-04	WA	Soil
Otu02365_Algoriphagus	0.9894	0.9286	0.958	1.00E-04	WA	Soil
Otu01175_Microscillaceae	0.9158	1	0.957	1.00E-04	WA	Soil
Otu03312_Georgenia	0.9677	0.9286	0.948	1.00E-04	WA	Soil
Otu00712_Anaerolineaceae	0.9626	0.9286	0.945	1.00E-04	WA	Soil
Otu01177_Subgroup_6	0.9626	0.9286	0.945	1.00E-04	WA	Soil
Otu02417_Alphaproteobacteria	0.8908	1	0.944	1.00E-04	WA	Soil
Otu03543_Gammaproteobacteria	0.9565	0.9286	0.942	1.00E-04	WA	Soil
Otu01758_Pirellulaceae	0.8878	1	0.942	1.00E-04	WA	Soil
Otu00184_Williamsia	0.8873	1	0.942	1.00E-04	WA	Soil
Otu01018_Solirubrobacteraceae	0.8861	1	0.941	1.00E-04	WA	Soil
Otu04021_Vermiphilaceae	0.9507	0.9286	0.94	1.00E-04	WA	Soil
Otu03058_Bacteriovoracaceae	0.8827	1	0.94	1.00E-04	WA	Soil
Otu01192_Gammaproteobacteria	0.9451	0.9286	0.937	1.00E-04	WA	Soil
Otu02875_Phycisphaeraceae	0.8774	1	0.937	1.00E-04	WA	Soil
Otu02642_PeM15	0.9386	0.9286	0.934	1.00E-04	WA	Soil
Otu01680_Microtrichales	0.9278	0.9286	0.928	1.00E-04	WA	Soil
Otu00561_Rhodobacteraceae	0.861	1	0.928	0.0003	WA	Soil
Otu00772_Geodermatophilus	0.9267	0.9286	0.928	1.00E-04	WA	Soil
Otu00338_SJA.28	0.8599	1	0.927	0.0002	WA	Soil
Otu01314_S0134_terrestrial_group	0.9238	0.9286	0.926	1.00E-04	WA	Soil
Otu03614_OLB12	1	0.8571	0.926	1.00E-04	WA	Soil
Otu00996_Candidatus_Udaeobacter	0.8518	1	0.923	0.0002	WA	Soil
Otu00917_Saccharimonadaceae	0.8508	1	0.922	1.00E-04	WA	Soil
Otu00883_Propionibacteriaceae	0.8455	1	0.919	1.00E-04	WA	Soil
Otu02655_Alphaproteobacteria	0.9088	0.9286	0.919	1.00E-04	WA	Soil
Otu00765_IMCC26207	0.8435	1	0.918	1.00E-04	WA	Soil
Otu01858_Saccharimonadales	0.8435	1	0.918	1.00E-04	WA	Soil
Otu01584_Reyranellaceae	0.9033	0.9286	0.916	1.00E-04	WA	Soil
Otu01736_Actinobacteria	0.9003	0.9286	0.914	1.00E-04	WA	Soil
Otu01074_Euryarchaeota	0.898	0.9286	0.913	1.00E-04	WA	Soil

Table A.6. Continued (Page 3 of 3)

OTU	Specificity	Sensitivity	Indicator Value	P-Value	Group	Habitat
Otu02247_Subgroup_6	0.9688	0.8571	0.911	1.00E-04	WA	Soil
Otu01798_Paracoccus	0.829	1	0.91	1.00E-04	WA	Soil
Otu02407_Gemmatimonadaceae	0.8926	0.9286	0.91	1.00E-04	WA	Soil
Otu02267_Saccharimonadales	0.9666	0.8571	0.91	1.00E-04	WA	Soil
Otu00834_JG30.KF.CM45	0.8276	1	0.91	1.00E-04	WA	Soil
Otu02109_Myxococcales	0.8251	1	0.908	1.00E-04	WA	Soil
Otu05278_Gammaproteobacteria	0.961	0.8571	0.908	1.00E-04	WA	Soil
Otu01285_Demequinaceae	0.8228	1	0.907	1.00E-04	WA	Soil
Otu04067_Vampirovibrionales	0.8859	0.9286	0.907	1.00E-04	WA	Soil
Otu02283_MB.A2.108	0.8855	0.9286	0.907	1.00E-04	WA	Soil
Otu00816_Gammaproteobacteria	0.8208	1	0.906	1.00E-04	WA	Soil
Otu01610_Rhodococcus	0.8199	1	0.905	1.00E-04	WA	Soil
Otu01053_Chitinophagaceae	0.8186	1	0.905	1.00E-04	WA	Soil
Otu01194_MB.A2.108	0.8181	1	0.904	1.00E-04	WA	Soil
Otu01794_Gemmataceae	0.8173	1	0.904	1.00E-04	WA	Soil
Otu01079_Actinobacteria	0.8167	1	0.904	0.0003	WA	Soil
Otu01296_Sanguibacter	0.8789	0.9286	0.903	1.00E-04	WA	Soil
Otu01580_Bauldia	0.8776	0.9286	0.903	1.00E-04	WA	Soil
Otu02070_Unknown_Family	0.8141	1	0.902	1.00E-04	WA	Soil
Otu03110_Gaiellales	0.8724	0.9286	0.9	1.00E-04	WA	Soil
Otu03439_S0134_terrestrial_group	0.9449	0.8571	0.9	1.00E-04	WA	Soil
Otu00933_Mycobacterium	0.8085	1	0.899	1.00E-04	WA	Soil
Otu02575_Fodinicurvataceae	0.8693	0.9286	0.898	1.00E-04	WA	Soil
Otu01872_Amb.16S.1323	0.8688	0.9286	0.898	1.00E-04	WA	Soil
Otu03584_cvE6	0.9402	0.8571	0.898	1.00E-04	WA	Soil
Otu01464_MB.A2.108	0.8638	0.9286	0.896	1.00E-04	WA	Soil
Otu02271_Chthonobacter	0.8637	0.9286	0.896	1.00E-04	WA	Soil
Otu01825_Alphaproteobacteria	0.8618	0.9286	0.895	1.00E-04	WA	Soil
Otu02963_TRA3.20	0.8607	0.9286	0.894	1.00E-04	WA	Soil
Otu02700_Gemmataceae	0.7934	1	0.891	1.00E-04	WA	Soil
Otu01719_OM190	0.7922	1	0.89	0.0004	WA	Soil
Otu02667_MBNT15	0.8526	0.9286	0.89	1.00E-04	WA	Soil
Otu01254_Betaproteobacteriales	0.8497	0.9286	0.888	1.00E-04	WA	Soil
Otu02293_Rhodobacteraceae	0.8495	0.9286	0.888	1.00E-04	WA	Soil
Otu03605_JTB23	0.8478	0.9286	0.887	1.00E-04	WA	Soil
Otu01836_Bryobacter	0.7866	1	0.887	0.0002	WA	Soil
Otu02261_Nocardioidaceae	0.8469	0.9286	0.887	1.00E-04	WA	Soil
Otu06193_Gemmatimonadaceae	1	0.7857	0.886	1.00E-04	WA	Soil
Otu00831_Candidatus_Nitrososphaera	0.8457	0.9286	0.886	1.00E-04	WA	Soil
Otu01980_MB.A2.108	0.916	0.8571	0.886	1.00E-04	WA	Soil
Otu01939_Rhodobacteraceae	0.9146	0.8571	0.885	1.00E-04	WA	Soil
Otu02659_Microscillaceae	0.9122	0.8571	0.884	1.00E-04	WA	Soil
Otu02016_Alphaproteobacteria	0.781	1	0.884	1.00E-04	WA	Soil
Otu03709_Planctomycetales	0.8379	0.9286	0.882	1.00E-04	WA	Soil
Otu02557_PB19	0.8355	0.9286	0.881	1.00E-04	WA	Soil
Otu01941_Pirellula	0.833	0.9286	0.879	1.00E-04	WA	Soil
Otu01752_Acidimicrobiia	0.8327	0.9286	0.879	1.00E-04	WA	Soil
Otu03868_Gammaproteobacteria	0.8981	0.8571	0.877	1.00E-04	WA	Soil
Otu01724_Gemmataceae	0.7687	1	0.877	0.0013	WA	Soil
Otu05556_cvE6	0.894	0.8571	0.875	1.00E-04	WA	Soil
Otu01704_Gemmataceae	0.7656	1	0.875	0.0002	WA	Soil
Otu04083_Planctomycetales	0.974	0.7857	0.875	1.00E-04	WA	Soil
Otu03230_Actinobacteria	0.822	0.9286	0.874	1.00E-04	WA	Soil
Otu02290_Pirellulaceae	0.7627	1	0.873	1.00E-04	WA	Soil
Otu02498_Verrucomicrobiaceae	0.7627	1	0.873	1.00E-04	WA	Soil
Otu03374_Deltaproteobacteria	0.7627	1	0.873	1.00E-04	WA	Soil
Otu04838_AKIW781	0.9698	0.7857	0.873	1.00E-04	WA	Soil
Otu03147_SAR324_clade	0.7603	1	0.872	1.00E-04	WA	Soil
Otu01095_Anaerolineaceae	0.8153	0.9286	0.87	1.00E-04	WA	Soil
Otu03675_Gemmatimonadaceae	0.755	1	0.869	1.00E-04	WA	Soil
Otu01173_Lautropia	0.7516	1	0.867	0.0005	WA	Soil
Otu02256_Pirellula	0.7498	1	0.866	1.00E-04	WA	Soil
Otu04048_Roseimicrobium	0.8727	0.8571	0.865	1.00E-04	WA	Soil
Otu04523_Blfdi19	0.8042	0.9286	0.864	1.00E-04	WA	Soil
Otu01540_Acidobacteriales	0.8032	0.9286	0.864	1.00E-04	WA	Soil
Otu01860_Parachlamydiaceae	0.8699	0.8571	0.863	0.0002	WA	Soil
Otu03596_Microtrichales	0.8685	0.8571	0.863	1.00E-04	WA	Soil
Otu02427_Candidatus_Alysiosphaera	0.7438	1	0.862	1.00E-04	WA	Soil
Otu03929_Babeliales	0.7994	0.9286	0.862	1.00E-04	WA	Soil
Otu03531_Alphaproteobacteria	0.8654	0.8571	0.861	1.00E-04	WA	Soil
Otu04646_Pirellulaceae	0.9414	0.7857	0.86	1.00E-04	WA	Soil
Otu01871_MB.A2.108	0.8628	0.8571	0.86	1.00E-04	WA	Soil
Otu01344_Rhodanobacteraceae	0.8593	0.8571	0.858	1.00E-04	WA	Soil
Otu01688_Micropruina	0.7363	1	0.858	0.0036	WA	Soil
Otu03501_Pirellula	0.9346	0.7857	0.857	1.00E-04	WA	Soil
Otu04603_mle1.27	0.8526	0.8571	0.855	1.00E-04	WA	Soil
Otu03996_Anaerolineae	0.9296	0.7857	0.855	1.00E-04	WA	Soil
Otu02649_Subgroup_7	0.7839	0.9286	0.853	1.00E-04	WA	Soil
Otu02591_Gemmataceae	0.7838	0.9286	0.853	1.00E-04	WA	Soil
Otu03222_0319.6G20	0.7836	0.9286	0.853	1.00E-04	WA	Soil
Otu01988_SWB02	0.8487	0.8571	0.853	1.00E-04	WA	Soil
Otu02890_Bauldia	0.7226	1	0.85	1.00E-04	WA	Soil
Otu02363_Pirellulaceae	0.8427	0.8571	0.85	1.00E-04	WA	Soil
Otu04876_Coxiella	0.8408	0.8571	0.849	1.00E-04	WA	Soil
Otu01368_MB.A2.108	0.9162	0.7857	0.848	1.00E-04	WA	Soil
Otu04874_Vampirovibrionales	0.9126	0.7857	0.847	1.00E-04	WA	Soil
Otu02858_IMCC26256	1	0.7143	0.845	1.00E-04	WA	Soil
Otu05332_Cellvibrionaceae	1	0.7143	0.845	1.00E-04	WA	Soil
Otu02784_Opitutaceae	0.8328	0.8571	0.845	1.00E-04	WA	Soil
Otu02927_Planctomycetales	0.8318	0.8571	0.844	1.00E-04	WA	Soil
Otu01096_MND1	0.7643	0.9286	0.842	1.00E-04	WA	Soil
Otu00914_Rhizobiales	0.825	0.8571	0.841	1.00E-04	WA	Soil
Otu01806_0319.6G20	0.7068	1	0.841	0.002	WA	Soil
Otu04816_Blrii41	0.8993	0.7857	0.841	1.00E-04	WA	Soil
Otu02352_BD2.11_terrestrial_group	0.7598	0.9286	0.84	1.00E-04	WA	Soil
Otu01447_Paenibacillaceae	0.9835	0.7143	0.838	1.00E-04	WA	Soil
Otu03866_Parachlamydiaceae	0.8186	0.8571	0.838	1.00E-04	WA	Soil
Otu03519_0319.6G20	0.8921	0.7857	0.837	1.00E-04	WA	Soil
Otu03835_EF100.94H03	0.8852	0.7857	0.834	1.00E-04	WA	Soil
Otu01452_JG30.KF.CM45	0.8113	0.8571	0.834	1.00E-04	WA	Soil
Otu01410_MB.A2.108	0.8108	0.8571	0.834	1.00E-04	WA	Soil
Otu02022_CL500.29_marine_group	0.8108	0.8571	0.834	1.00E-04	WA	Soil
Otu02842_Terribacillus	0.8842	0.7857	0.833	1.00E-04	WA	Soil
Otu04049_Blfdi19	0.9708	0.7143	0.833	1.00E-04	WA	Soil
Otu04470_CL500.3	0.8824	0.7857	0.833	1.00E-04	WA	Soil
Otu02081_0319.7L14	0.9678	0.7143	0.831	1.00E-04	WA	Soil
Otu02349_Caldilineaceae	0.805	0.8571	0.831	1.00E-04	WA	Soil
Otu01892_Verrucomicrobium	0.7428	0.9286	0.83	1.00E-04	WA	Soil
Otu03710_Pedosphaeraceae	0.804	0.8571	0.83	1.00E-04	WA	Soil
Otu02599_Diplorickettsiaceae	0.8769	0.7857	0.83	1.00E-04	WA	Soil
Otu03034_Saprospiraceae	0.7416	0.9286	0.83	1.00E-04	WA	Soil
Otu03458_WD2101_soil_group	0.7414	0.9286	0.83	1.00E-04	WA	Soil
Otu01289_Subgroup_6	0.8742	0.7857	0.829	0.0084	WA	Soil
Otu04960_Burkholderiaceae	0.961	0.7143	0.829	1.00E-04	WA	Soil
Otu04551_Fimbriimonadaceae	0.8735	0.7857	0.828	1.00E-04	WA	Soil
Otu02432_OLB14	0.7385	0.9286	0.828	1.00E-04	WA	Soil
Otu01575_Stenotrophobacter	0.7385	0.9286	0.828	1.00E-04	WA	Soil
Otu05559_Saccharimonadales	0.9593	0.7143	0.828	1.00E-04	WA	Soil
Otu03994_Saccharimonadales	0.8721	0.7857	0.828	1.00E-04	WA	Soil
Otu02982_Steroidobacteraceae	0.7988	0.8571	0.827	1.00E-04	WA	Soil
Otu03432_Paenibacillaceae	0.7965	0.8571	0.826	0.0002	WA	Soil
Otu03804_Pirellula	0.7347	0.9286	0.826	1.00E-04	WA	Soil
Otu03186_KF.JG30.C25	0.8676	0.7857	0.826	1.00E-04	WA	Soil
Otu02899_Pla4_lineage	0.7321	0.9286	0.824	0.0007	WA	Soil
Otu02665_Vermiphilaceae	0.793	0.8571	0.824	1.00E-04	WA	Soil
Otu01244_Angustibacter	0.7918	0.8571	0.824	0.0155	WA	Soil
Otu01527_Pedosphaeraceae	0.7916	0.8571	0.824	0.0004	WA	Soil
Otu01960_Chitinophagaceae	0.7911	0.8571	0.823	1.00E-04	WA	Soil
Otu06834_Gaiellales	0.948	0.7143	0.823	1.00E-04	WA	Soil
Otu01900_Latescibacteria	0.7898	0.8571	0.823	0.0273	WA	Soil
Otu03091_Pedosphaeraceae	0.7898	0.8571	0.823	1.00E-04	WA	Soil
Otu02810_Nannocystis	0.8612	0.7857	0.823	0.0002	WA	Soil
Otu04832_Saccharimonadales	0.8549	0.7857	0.82	1.00E-04	WA	Soil
Otu05650_Opitutaceae	0.8539	0.7857	0.819	1.00E-04	WA	Soil
Otu08224_Nannocystis	0.9391	0.7143	0.819	1.00E-04	WA	Soil
Otu03233_Zavarzinella	0.721	0.9286	0.818	1.00E-04	WA	Soil
Otu00427_Anaerolineaceae	0.9372	0.7143	0.818	0.0002	WA	Soil
Otu04634_MB.A2.108	0.9353	0.7143	0.817	1.00E-04	WA	Soil
Otu05393_Subgroup_5	0.779	0.8571	0.817	1.00E-04	WA	Soil
Otu02100_Rubinisphaeraceae	0.7779	0.8571	0.817	0.0002	WA	Soil
Otu01973_Chlamydiales	0.6665	1	0.816	0.005	WA	Soil
Otu06414_Gemmataceae	0.933	0.7143	0.816	1.00E-04	WA	Soil
Otu03392_OM190	0.8433	0.7857	0.814	1.00E-04	WA	Soil
Otu03658_Simkaniaceae	0.8427	0.7857	0.814	1.00E-04	WA	Soil
Otu04629_Anaeromyxobacter	0.8408	0.7857	0.813	1.00E-04	WA	Soil
Otu04559_Saccharimonadales	0.8402	0.7857	0.813	1.00E-04	WA	Soil
Otu01223_SC.I.84	0.6582	1	0.811	0.021	WA	Soil
Otu03354_SBR1031	0.7076	0.9286	0.811	0.0002	WA	Soil
Otu02532_Gemmata	0.8355	0.7857	0.81	0.0002	WA	Soil
Otu02527_Pedosphaeraceae	0.6559	1	0.81	0.0061	WA	Soil
Otu02924_Rubinisphaeraceae	0.8344	0.7857	0.81	1.00E-04	WA	Soil
Otu03595_Haliangium	0.8321	0.7857	0.809	1.00E-04	WA	Soil
Otu03660_Polycyclovorans	0.7627	0.8571	0.809	1.00E-04	WA	Soil
Otu04046_Sandaracinaceae	0.9123	0.7143	0.807	1.00E-04	WA	Soil
Otu04370_Gemmataceae	0.9119	0.7143	0.807	1.00E-04	WA	Soil
Otu00731_PeM15	0.8267	0.7857	0.806	0.0007	WA	Soil
Otu02730_Rhodobacteraceae	0.7575	0.8571	0.806	1.00E-04	WA	Soil
Otu04079_Thermoplasmata	0.8259	0.7857	0.806	1.00E-04	WA	Soil
Otu02748_Amb.16S.1323	0.8258	0.7857	0.806	1.00E-04	WA	Soil
Otu05114_Saccharimonadales	0.8212	0.7857	0.803	1.00E-04	WA	Soil
Otu02994_UBA12409	0.7521	0.8571	0.803	0.0002	WA	Soil
Otu04032_Haliangium	0.7504	0.8571	0.802	0.0002	WA	Soil
Otu05886_Sphingobacteriales	1	0.6429	0.802	1.00E-04	WA	Soil
Otu07591_Pirellulaceae	1	0.6429	0.802	1.00E-04	WA	Soil
Otu07608_Bryobacter	1	0.6429	0.802	1.00E-04	WA	Soil
Otu04582_Acidipila	0.9	0.7143	0.802	1.00E-04	WA	Soil
Otu03769_Gemmatimonadaceae	0.8169	0.7857	0.801	1.00E-04	WA	Soil
Otu03641_Sandaracinaceae	0.8981	0.7143	0.801	1.00E-04	WA	Soil
Otu06957_Deltaproteobacteria	0.8976	0.7143	0.801	1.00E-04	WA	Soil
Otu02302_Sandaracinaceae	0.6903	0.9286	0.801	0.0105	WA	Soil
Otu02650_Blrii41	0.8155	0.7857	0.8	1.00E-04	WA	Soil
Otu02957_Pirellulaceae	0.747	0.8571	0.8	0.0002	WA	Soil
Otu00224_Azotobacter	0.9958	0.6429	0.8	1.00E-04	WA	Soil
Otu05081_Stella	0.8955	0.7143	0.8	1.00E-04	WA	Soil
Otu03575_Sandaracinus	0.8138	0.7857	0.8	0.0002	WA	Soil
Otu02948_Tepidisphaerales	0.8138	0.7857	0.8	0.0002	WA	Soil

Table A.7 Sensitivity, specificity, and indicator values for fungal indicator OTUs for caulosphere of Juglans nigra in Indiana (IN), Tennessee (TN), Washington (WA), IN+TN, and TCD positive trees and TCD negative trees in WA..

OTU	Specificity	Sensitivity	Indicator Value	P-Value	Group	Habitat
FOtu0050_Rhinocladiella	0.9968	1	0.998	1.00E-04	IN	Caulosphere
FOtu0070_Ascomycota	0.9958	1	0.998	1.00E-04	IN	Caulosphere
FOtu0023_Diplodia	0.951	1	0.975	1.00E-04	IN	Caulosphere
FOtu0075_Orbilia	1	0.9286	0.964	1.00E-04	IN	Caulosphere
FOtu0206_Pleosporales	1	0.9286	0.964	1.00E-04	IN	Caulosphere
FOtu0257_Rhinocladiella	0.9349	0.9286	0.932	1.00E-04	IN	Caulosphere
FOtu0071_Pleosporales	1	0.8571	0.926	1.00E-04	IN	Caulosphere
FOtu0086_Ascomycota	0.9767	0.8571	0.915	1.00E-04	IN	Caulosphere
FOtu0080_Ascomycota	0.9661	0.8571	0.91	1.00E-04	IN	Caulosphere
FOtu0121_Candelariaceae	0.9602	0.8571	0.907	1.00E-04	IN	Caulosphere
FOtu0435_Ascomycota	0.972	0.7857	0.874	1.00E-04	IN	Caulosphere
FOtu0018_Phaeomoniellales	0.8162	0.9286	0.871	1.00E-04	IN	Caulosphere
FOtu0031_Pleosporales	0.8704	0.8571	0.864	1.00E-04	IN	Caulosphere
FOtu0317_Basidiomycota	1	0.7143	0.845	1.00E-04	IN	Caulosphere
FOtu0233_Candelaria.fibrosa	0.9054	0.7857	0.843	1.00E-04	IN	Caulosphere
FOtu0029_Phaeoacremonium	0.9746	0.7143	0.834	0.0002	IN	Caulosphere
FOtu0200_Phaeomoniellales	0.8596	0.7857	0.822	1.00E-04	IN	Caulosphere
FOtu0393_Rhinocladiella	0.93	0.7143	0.815	1.00E-04	IN	Caulosphere
FOtu0169_Physcia.millegrana	0.9149	0.7143	0.808	1.00E-04	IN	Caulosphere
FOtu0003_Phaeomoniellales	1	1	1	1.00E-04	IN+TN	Caulosphere
FOtu0022_Helminthosporium.asterinum	1	1	1	1.00E-04	IN+TN	Caulosphere
FOtu0027_Trichomeriaceae	1	1	1	1.00E-04	IN+TN	Caulosphere
FOtu0040_Helminthosporium	1	0.9688	0.984	1.00E-04	IN+TN	Caulosphere
FOtu0005_Phaeomoniellales	1	0.9375	0.968	1.00E-04	IN+TN	Caulosphere
FOtu0069_Didymosphaeriaceae	1	0.9375	0.968	1.00E-04	IN+TN	Caulosphere
FOtu0030_Trichomeriaceae	0.9991	0.9375	0.968	1.00E-04	IN+TN	Caulosphere
FOtu0103_Trichomeriaceae	1	0.8438	0.919	1.00E-04	IN+TN	Caulosphere
FOtu0064_Arthrocatena.tenebrio	0.9966	0.8438	0.917	0.0002	IN+TN	Caulosphere
FOtu0063_Pleosporales	1	0.7812	0.884	1.00E-04	IN+TN	Caulosphere
FOtu0082_Physcia	1	0.7812	0.884	0.0002	IN+TN	Caulosphere
FOtu0135_Ascomycota	1	0.75	0.866	1.00E-04	IN+TN	Caulosphere
FOtu0061_Ascomycota	0.998	0.75	0.865	1.00E-04	IN+TN	Caulosphere
FOtu0066_Rhinocladiella	0.9979	0.75	0.865	1.00E-04	IN+TN	Caulosphere
FOtu0130_Rhinocladiella	1	0.7188	0.848	1.00E-04	IN+TN	Caulosphere
FOtu0128_Ascomycota	1	0.6875	0.829	1.00E-04	IN+TN	Caulosphere
FOtu0230_Capnodiales	1	0.6562	0.81	0.0002	IN+TN	Caulosphere
FOtu0093_Phaeophyscia	0.9792	0.6562	0.802	0.0011	IN+TN	Caulosphere
FOtu0014_Paraconiothyrium	0.977	1	0.988	1.00E-04	TN	Caulosphere
FOtu0081_Lecanorales	1	0.9444	0.972	1.00E-04	TN	Caulosphere
FOtu0177_Capnodiales	1	0.9444	0.972	1.00E-04	TN	Caulosphere
FOtu0058_Ascomycota	0.9963	0.9444	0.97	1.00E-04	TN	Caulosphere
FOtu0124_Trichomeriaceae	0.9639	0.9444	0.954	1.00E-04	TN	Caulosphere
FOtu0068_Ascomycota	1	0.8889	0.943	1.00E-04	TN	Caulosphere
FOtu0104_Ascomycota	1	0.8889	0.943	1.00E-04	TN	Caulosphere
FOtu0252_Capnodiales	1	0.8889	0.943	1.00E-04	TN	Caulosphere
FOtu0019_Ascomycota	0.9935	0.8889	0.94	1.00E-04	TN	Caulosphere
FOtu0017_Pleosporales	0.9886	0.8889	0.937	1.00E-04	TN	Caulosphere
FOtu0077_Pleosporales	0.9874	0.8889	0.937	1.00E-04	TN	Caulosphere
FOtu0049_Leotiomycetes	0.9836	0.8889	0.935	1.00E-04	TN	Caulosphere
FOtu0176_Lecanoromycetes	1	0.8333	0.913	1.00E-04	TN	Caulosphere
FOtu0219_Myriangium.citri	1	0.8333	0.913	1.00E-04	TN	Caulosphere
FOtu0015_Ascomycota	0.9995	0.8333	0.913	1.00E-04	TN	Caulosphere
FOtu0167_Ascomycota	0.9946	0.8333	0.91	1.00E-04	TN	Caulosphere
FOtu0163_Endosporium	0.9852	0.8333	0.906	1.00E-04	TN	Caulosphere
FOtu0105_Rachicladosporium	1	0.7778	0.882	1.00E-04	TN	Caulosphere
FOtu0117_Pleosporales	1	0.7778	0.882	1.00E-04	TN	Caulosphere
FOtu0154_Trichomeriaceae	1	0.7778	0.882	1.00E-04	TN	Caulosphere
FOtu0173_Trichomeriaceae	1	0.7778	0.882	1.00E-04	TN	Caulosphere
FOtu0204_Lecanorales	1	0.7778	0.882	1.00E-04	TN	Caulosphere
FOtu0347_Capnodiales	1	0.7778	0.882	1.00E-04	TN	Caulosphere
FOtu0136_Endosporium.aviarium	0.9939	0.7778	0.879	1.00E-04	TN	Caulosphere
FOtu0091_Lecanoromycetes	0.9932	0.7778	0.879	1.00E-04	TN	Caulosphere
FOtu0251_Ascomycota	0.984	0.7778	0.875	1.00E-04	TN	Caulosphere
FOtu0048_Pleosporales	0.8768	0.8333	0.855	0.0011	TN	Caulosphere
FOtu0088_Pleosporales	1	0.7222	0.85	1.00E-04	TN	Caulosphere
FOtu0098_Trichomeriaceae	1	0.7222	0.85	1.00E-04	TN	Caulosphere
FOtu0126_Trichomeriaceae	1	0.7222	0.85	1.00E-04	TN	Caulosphere
FOtu0175_Ascomycota	1	0.7222	0.85	1.00E-04	TN	Caulosphere
FOtu0190_Trichomeriaceae	1	0.7222	0.85	1.00E-04	TN	Caulosphere
FOtu0232_Lecanoromycetes	1	0.7222	0.85	1.00E-04	TN	Caulosphere
FOtu0056_Hyperphyscia.adglutinata	0.9954	0.7222	0.848	1.00E-04	TN	Caulosphere
FOtu0270_Strelitziana.africana	0.9868	0.7222	0.844	1.00E-04	TN	Caulosphere
FOtu0195_Capnodiales	0.9694	0.7222	0.837	1.00E-04	TN	Caulosphere

OTU	Specificity	Sensitivity	Indicator Value	P-Value	Group	Habitat
FOtu0215_Lecanoromycetes	1	0.6667	0.816	1.00E-04	TN	Caulosphere
FOtu0236_Lecanoromycetes	1	0.6667	0.816	0.0002	TN	Caulosphere
FOtu0303_Chaetothyriales	1	0.6667	0.816	1.00E-04	TN	Caulosphere
FOtu0305_Orbiliales	1	0.6667	0.816	1.00E-04	TN	Caulosphere
FOtu0101_Lophiostoma.fuckelii	0.9934	0.6667	0.814	1.00E-04	TN	Caulosphere
FOtu0269_Ascomycota	0.9901	0.6667	0.812	1.00E-04	TN	Caulosphere
FOtu0238_Capnodiales	0.9901	0.6667	0.812	1.00E-04	TN	Caulosphere
FOtu0007_Pleosporales.fam_Incertae_sedis	1	1	1	1.00E-04	WA	Caulosphere
FOtu0008_Melanommataceae	1	1	1	1.00E-04	WA	Caulosphere
FOtu0013_Taphrinales	1	1	1	1.00E-04	WA	Caulosphere
FOtu0026_Ascomycota	1	1	1	1.00E-04	WA	Caulosphere
FOtu0033_Ascomycota	1	1	1	1.00E-04	WA	Caulosphere
FOtu0034_Phaeococcomyces	1	1	1	1.00E-04	WA	Caulosphere
FOtu0036_Coniothyriaceae	1	1	1	1.00E-04	WA	Caulosphere
FOtu0041_Dothideales	1	1	1	1.00E-04	WA	Caulosphere
FOtu0057_Aureobasidium.pullulans	1	1	1	1.00E-04	WA	Caulosphere
FOtu0059_Filobasidium.wieringae	1	1	1	1.00E-04	WA	Caulosphere
FOtu0078_Dothideales	1	1	1	1.00E-04	WA	Caulosphere
FOtu0002_Ascomycota	0.9996	1	1	1.00E-04	WA	Caulosphere
FOtu0021_Ascomycota	0.9989	1	0.999	1.00E-04	WA	Caulosphere
FOtu0039_Buckleyzyma.aurantiaca	0.9985	1	0.999	1.00E-04	WA	Caulosphere
FOtu0006_Aureobasidium.pullulans	0.9975	1	0.999	1.00E-04	WA	Caulosphere
FOtu0010_Endoconidioma.populi	0.9714	1	0.986	1.00E-04	WA	Caulosphere
FOtu0001_Didymellaceae	0.9647	1	0.982	1.00E-04	WA	Caulosphere
FOtu0044_Ascomycota	1	0.9286	0.964	1.00E-04	WA	Caulosphere
FOtu0095_Filobasidiales	1	0.9286	0.964	1.00E-04	WA	Caulosphere
FOtu0131_Taphrina	1	0.9286	0.964	1.00E-04	WA	Caulosphere
FOtu0326_Taphrinales	1	0.9286	0.964	1.00E-04	WA	Caulosphere
FOtu0009_Alternaria.alternata	0.9126	1	0.955	0.0002	WA	Caulosphere
FOtu0194_Sydowia.polyspora	0.9496	0.9286	0.939	1.00E-04	WA	Caulosphere
FOtu0004_Melanommataceae	1	0.8571	0.926	1.00E-04	WA	Caulosphere
FOtu0028_Cryptococcus.cuniculi	1	0.8571	0.926	1.00E-04	WA	Caulosphere
FOtu0054_Microbotryomycetes	1	0.8571	0.926	1.00E-04	WA	Caulosphere
FOtu0074_Kondoa	1	0.8571	0.926	1.00E-04	WA	Caulosphere
FOtu0110_Vishniacozyma.dimennae	1	0.8571	0.926	1.00E-04	WA	Caulosphere
FOtu0118_Knufia	1	0.8571	0.926	1.00E-04	WA	Caulosphere
FOtu0146_Gelidatrema	1	0.8571	0.926	1.00E-04	WA	Caulosphere
FOtu0157_Dothideales	1	0.8571	0.926	1.00E-04	WA	Caulosphere
FOtu0198_Phaeococcomyces	1	0.8571	0.926	1.00E-04	WA	Caulosphere
FOtu0329_Ascomycota	1	0.8571	0.926	1.00E-04	WA	Caulosphere
FOtu0032_Phaeosphaeriaceae	0.998	0.8571	0.925	1.00E-04	WA	Caulosphere
FOtu0112_Filobasidium.magnum	0.9424	0.8571	0.899	1.00E-04	WA	Caulosphere
FOtu0094_Alternaria.metachromatica	1	0.7857	0.886	1.00E-04	WA	Caulosphere
FOtu0108_Orbilia	1	0.7857	0.886	1.00E-04	WA	Caulosphere
FOtu0138_Dothideomycetes	1	0.7857	0.886	1.00E-04	WA	Caulosphere
FOtu0162_Cystobasidiomycetes	1	0.7857	0.886	1.00E-04	WA	Caulosphere
FOtu0205_Ascomycota	1	0.7857	0.886	1.00E-04	WA	Caulosphere
FOtu0332_Genolevuria	1	0.7857	0.886	1.00E-04	WA	Caulosphere
FOtu0076_Endoconidioma.populi	0.9944	0.7857	0.884	1.00E-04	WA	Caulosphere
FOtu0264_Didymellaceae	0.9118	0.7857	0.846	1.00E-04	WA	Caulosphere
FOtu0120_Leucosporidiales	1	0.7143	0.845	1.00E-04	WA	Caulosphere
FOtu0140_Camarosporidiella	1	0.7143	0.845	1.00E-04	WA	Caulosphere
FOtu0170_Cryptococcus.cuniculi	1	0.7143	0.845	1.00E-04	WA	Caulosphere
FOtu0182_Taphrina.carpini	1	0.7143	0.845	1.00E-04	WA	Caulosphere
FOtu0289_Ascomycota	0.9643	0.7143	0.83	1.00E-04	WA	Caulosphere
FOtu0035_Microbotryomycetes	1	0.6429	0.802	1.00E-04	WA	Caulosphere
FOtu0097_Phaeosphaeriaceae	1	0.6429	0.802	1.00E-04	WA	Caulosphere
FOtu0149_Phaeomoniellales	1	0.6429	0.802	1.00E-04	WA	Caulosphere
FOtu0185_Cystobasidiomycetes	1	0.6429	0.802	1.00E-04	WA	Caulosphere
FOtu0250_Chionosphaeraceae	1	0.6429	0.802	1.00E-04	WA	Caulosphere
FOtu0282_Ascomycota	1	0.6429	0.802	0.0002	WA	Caulosphere
FOtu0286_Ramimonilia.apicalis	1	0.6429	0.802	1.00E-04	WA	Caulosphere
Otu0349_Ascomycota	0.9256	1	0.962	0.0023	Negative	Caulosphere
Otu0184_Corticifraga.peltigerae	0.9941	0.8333	0.91	0.0073	Negative	Caulosphere
Otu0108_Orbilia	0.8101	1	0.9	0.0273	Negative	Caulosphere
Otu0182_Taphrina.carpini	0.7864	1	0.887	0.0334	Negative	Caulosphere
Otu0151_Chaetosphaeronema	1	0.6667	0.816	0.0149	Negative	Caulosphere
Otu0359_Orbiliaceae	0.973	0.6667	0.805	0.0258	Negative	Caulosphere
Otu0035_Microbotryomycetes	0.972	1	0.986	0.0013	Positive	Caulosphere
Otu0185_Cystobasidiomycetes	0.9692	1	0.984	0.0014	Positive	Caulosphere
Otu0074_Kondoa	0.9261	1	0.962	0.0022	Positive	Caulosphere
Otu0047_Wickerhamomyces.hampshirensis	1	0.875	0.935	0.0043	Positive	Caulosphere
Otu0115_Geosmithia	1	0.875	0.935	0.0043	Positive	Caulosphere
Otu0094_Alternaria.metachromatica	0.8467	1	0.92	0.0113	Positive	Caulosphere
Otu0192_Leptosphaeriaceae	1	0.75	0.866	0.0183	Positive	Caulosphere
Otu0256_Microbotryomycetes	1	0.75	0.866	0.0206	Positive	Caulosphere
Otu0474_Pleosporales	1	0.75	0.866	0.0102	Positive	Caulosphere

Table A.8. Sensitivity, specificity, and indicator values for fungall indicator OTUs for soil of Juglans nigra in Indiana (IN), Tennessee (TN), Washington (WA), IN+TN, and TCD positive trees and TCD negative trees in WA.

OTU	Specificity	Sensitivity	Indicator Val	P-Value	Group	Habitat
FOtu00073_Hypocreales	0.8446	1	0.919	0.0015	IN	Soil
FOtu00086_Sordariomycetes	0.8163	1	0.903	0.0049	IN	Soil
FOtu00053_Ganodermataceae	0.8142	1	0.902	0.0107	IN	Soil
FOtu00321_Pleosporales	0.8659	0.9333	0.899	1.00E-04	IN	Soil
FOtu00225_Pleosporales_sp	0.9765	0.8	0.884	1.00E-04	IN	Soil
FOtu00244_Onygenaceae_sp	0.9486	0.8	0.871	1.00E-04	IN	Soil
FOtu00588_Paramyrothecium_humicola	0.9267	0.8	0.861	0.0002	IN	Soil
FOtu01357_Hypocreales	1	0.7333	0.856	1.00E-04	IN	Soil
FOtu00158_Lophiotrema_rubi	0.9602	0.7333	0.839	1.00E-04	IN	Soil
FOtu00424_Eurotiomycetes	0.8663	0.8	0.833	0.0002	IN	Soil
FOtu01270_Cystobasidiomycetes	0.8552	0.8	0.827	0.0002	IN	Soil
FOtu00314_Plectosphaerellaceae	0.843	0.8	0.821	0.002	IN	Soil
FOtu00168_Talaromyces	0.8308	0.8	0.815	0.0006	IN	Soil
FOtu00712_Pyrenochaetopsis_pratorum	0.8168	0.8	0.808	0.0002	IN	Soil
FOtu00062_Plectosphaerella	0.8841	0.7333	0.805	0.0014	IN	Soil
FOtu00743_Pleosporales	0.8045	0.8	0.802	0.0002	IN	Soil
FOtu00968_Septoglomus_viscosum	0.8759	0.7333	0.801	1.00E-04	IN	Soil
FOtu00054_Purpureocillium_lilacinum	0.9775	1	0.989	1.00E-04	IN.TN	Soil
FOtu00167_Fusarium_solani	0.9976	0.9697	0.984	1.00E-04	IN.TN	Soil
FOtu00050_Penicillium_cainii	0.9919	0.9697	0.981	1.00E-04	IN.TN	Soil
FOtu00085_Trichoderma_spirale	0.9912	0.9697	0.98	1.00E-04	IN.TN	Soil
FOtu00180_Teichosporaceae_sp	0.9866	0.9697	0.978	1.00E-04	IN.TN	Soil
FOtu00365_Calvatia_cyathiformis	0.9859	0.9697	0.978	1.00E-04	IN.TN	Soil
FOtu00039_Metarhizium_marquandii	0.9553	1	0.977	1.00E-04	IN.TN	Soil
FOtu00002_Metarhizium_anisopliae	0.9732	0.9697	0.971	1.00E-04	IN.TN	Soil
FOtu00035_Chaetomium_sp	0.9721	0.9697	0.971	1.00E-04	IN.TN	Soil
FOtu00049_Paraconiothyrium	0.9424	1	0.971	1.00E-04	IN.TN	Soil
FOtu00007_Chaetomiaceae	0.9947	0.9394	0.967	1.00E-04	IN.TN	Soil
FOtu00540_Lycoperdon_pyriforme	0.976	0.9394	0.958	1.00E-04	IN.TN	Soil
FOtu00070_Didymellaceae	0.9718	0.9394	0.955	1.00E-04	IN.TN	Soil
FOtu00096_Penicillium_brasilianum	0.9715	0.9394	0.955	1.00E-04	IN.TN	Soil
FOtu00123_Fusicolla_aquaeductuum	0.9698	0.9394	0.954	1.00E-04	IN.TN	Soil
FOtu00311_Periconia_macrospinosa	1	0.9091	0.953	1.00E-04	IN.TN	Soil
FOtu00317_Halosphaeriaceae_sp	0.9975	0.9091	0.952	1.00E-04	IN.TN	Soil
FOtu00021_Penicillium_thiersii	0.9321	0.9697	0.951	1.00E-04	IN.TN	Soil
FOtu00689_Ganoderma_adspersum	0.9929	0.9091	0.95	1.00E-04	IN.TN	Soil
FOtu00098_Rhizophydiales_sp	0.9437	0.9394	0.942	1.00E-04	IN.TN	Soil
FOtu00175_Penicillium	0.9701	0.9091	0.939	0.0002	IN.TN	Soil
FOtu00249_Pyronemataceae_sp	1	0.8788	0.937	1.00E-04	IN.TN	Soil
FOtu00442_Pestalotiopsis	0.9347	0.9394	0.937	1.00E-04	IN.TN	Soil
FOtu00125_Pleosporales	0.9991	0.8788	0.937	1.00E-04	IN.TN	Soil
FOtu00119_Idriella	0.8858	0.9697	0.927	1.00E-04	IN.TN	Soil
FOtu00133_Lophiotrema_rubi	0.9335	0.9091	0.921	0.0013	IN.TN	Soil
FOtu00289_Pleosporales	0.9569	0.8788	0.917	1.00E-04	IN.TN	Soil
FOtu00710_Neopestalotiopsis_foedans	0.9868	0.8485	0.915	1.00E-04	IN.TN	Soil
FOtu00185_Talaromyces_trachyspermus	0.9752	0.8485	0.91	0.0002	IN.TN	Soil
FOtu00372_Paraphoma	0.9717	0.8485	0.908	1.00E-04	IN.TN	Soil
FOtu00479_Glomeraceae	0.9334	0.8788	0.906	0.0004	IN.TN	Soil
FOtu00515_Glomeromycota_sp	0.9771	0.8182	0.894	1.00E-04	IN.TN	Soil
FOtu00704_Pleosporales_sp	0.9929	0.7879	0.884	1.00E-04	IN.TN	Soil
FOtu01028_Pleosporales	0.988	0.7879	0.882	1.00E-04	IN.TN	Soil
FOtu00388_Penicillium_sumatraense	0.968	0.7879	0.873	0.0006	IN.TN	Soil
FOtu00623_Veronaea_japonica	0.9614	0.7879	0.87	0.001	IN.TN	Soil
FOtu01019_Herpotrichiellaceae	0.961	0.7879	0.87	1.00E-04	IN.TN	Soil
FOtu00198_Ceratobasidiaceae	0.993	0.7576	0.867	1.00E-04	IN.TN	Soil
FOtu00558_Minutisphaera_aspera	0.9547	0.7879	0.867	0.0005	IN.TN	Soil
FOtu00504_Phaeoacremonium	0.9911	0.7576	0.866	0.0004	IN.TN	Soil
FOtu00067_Mortierella	0.952	0.7879	0.866	0.0068	IN.TN	Soil
FOtu00598_Pleosporales	0.9896	0.7576	0.866	1.00E-04	IN.TN	Soil
FOtu00243_Roussoella_solani	1	0.7273	0.853	1.00E-04	IN.TN	Soil
FOtu01402_Hypoxylon	1	0.7273	0.853	1.00E-04	IN.TN	Soil
FOtu00480_Chaetothyriaceae_sp	0.9918	0.7273	0.849	0.0002	IN.TN	Soil
FOtu00585_Cucurbitariaceae	0.9777	0.7273	0.843	0.0012	IN.TN	Soil
FOtu00501_Clonostachys_rosea	1	0.697	0.835	1.00E-04	IN.TN	Soil
FOtu00683_Chaetothyriales	1	0.697	0.835	1.00E-04	IN.TN	Soil
FOtu01144_Phialemoniopsis_ocularis	1	0.697	0.835	0.0002	IN.TN	Soil
FOtu00298_Chaetomiaceae	0.9575	0.7273	0.834	0.0011	IN.TN	Soil
FOtu00805_Helotiales	0.9914	0.697	0.831	0.0005	IN.TN	Soil
FOtu00604_Hypocreales_sp	0.9898	0.697	0.831	0.0019	IN.TN	Soil
FOtu00722_Pseudeurotium_hygrophilum	1	0.6667	0.816	0.0008	IN.TN	Soil
FOtu00305_Cucurbitariaceae	0.9954	0.6667	0.815	0.0008	IN.TN	Soil
FOtu00352_Pleosporales	0.9916	0.6667	0.813	0.0015	IN.TN	Soil
FOtu00316_Lophiostomataceae_sp	0.9825	0.6667	0.809	0.0011	IN.TN	Soil
FOtu00276_Mucor_moelleri	0.8995	0.7273	0.809	0.0056	IN.TN	Soil
FOtu00474_Pleosporales	0.9804	0.6667	0.808	0.0006	IN.TN	Soil
FOtu00931_Phaeoacremonium_scolyti	0.9763	0.6667	0.807	0.0026	IN.TN	Soil
FOtu00818_Clonostachys	0.9185	1	0.958	0.0144	Negative	Soil
FOtu00209_Branch06_sp	0.8783	1	0.937	0.0225	Negative	Soil
FOtu00553_Pleosporales	0.8448	1	0.919	0.0229	Negative	Soil
FOtu01412_Herpotrichiellaceae	0.9667	0.8333	0.898	0.022	Negative	Soil
FOtu00150_GS10_sp	0.9408	0.8333	0.885	0.0435	Negative	Soil
FOtu00266_Ascobolus	0.9159	0.8333	0.874	0.0404	Negative	Soil
FOtu00748_Gibberella_zeae	0.9176	1	0.958	0.0425	Positive	Soil
FOtu00498_Papiliotrema_laurentii	0.8596	1	0.927	0.0372	Positive	Soil
FOtu02470_Chionosphaeraceae_sp	0.9474	0.8333	0.889	0.0331	Positive	Soil
FOtu00184_Trichomeriaceae_sp	0.9555	0.9444	0.95	1.00E-04	TN	Soil
FOtu00033_Metarhizium_anisopliae	0.9897	0.8889	0.938	0.0014	TN	Soil
FOtu00087_Penicillium	0.8771	0.9444	0.91	1.00E-04	TN	Soil
FOtu00250_Capnodiales	0.9912	0.8333	0.909	1.00E-04	TN	Soil
FOtu00389_Mycoleptodiscus_sp	0.9254	0.8889	0.907	1.00E-04	TN	Soil
FOtu00072_Thyridariaceae	0.8538	0.9444	0.898	0.0002	TN	Soil
FOtu00880_Taphrina_inositophila	0.8454	0.9444	0.894	1.00E-04	TN	Soil
FOtu00271_Rachicladosporium	0.9402	0.8333	0.885	1.00E-04	TN	Soil
FOtu00838_Herpotrichiellaceae	0.8266	0.9444	0.884	0.0002	TN	Soil
FOtu00458_Lophiostomataceae	0.9972	0.7778	0.881	1.00E-04	TN	Soil
FOtu01052_Sphaceloma	0.9881	0.7778	0.877	1.00E-04	TN	Soil
FOtu00237_Trichomeriaceae	0.9867	0.7778	0.876	1.00E-04	TN	Soil
FOtu00508_Ascobolus_sp	0.9162	0.8333	0.874	1.00E-04	TN	Soil
FOtu00519_Sympoventuriaceae_sp	0.9147	0.8333	0.873	0.0005	TN	Soil
FOtu00485_Pleosporales	0.913	0.8333	0.872	1.00E-04	TN	Soil
FOtu01082_Pleosporales	0.9774	0.7778	0.872	1.00E-04	TN	Soil
FOtu00417_Thyridariaceae	0.8535	0.8889	0.871	1.00E-04	TN	Soil
FOtu00095_Pleosporales	0.9409	0.7778	0.855	1.00E-04	TN	Soil
FOtu00385_Mortierellomycota_sp	0.8701	0.8333	0.852	0.0003	TN	Soil
FOtu00350_Ascomycota	1	0.7222	0.85	1.00E-04	TN	Soil

OTU	Specificity	Sensitivity	Indicator Val	P-Value	Group	Habitat
FOtu00719_Capnodiales	1	0.7222	0.85	1.00E-04	TN	Soil
FOtu00881_Helminthosporium_asterinur	1	0.7222	0.85	1.00E-04	TN	Soil
FOtu00899_Diaporthe	0.8617	0.8333	0.847	0.0002	TN	Soil
FOtu00327_Articulospora_sp	0.9869	0.7222	0.844	1.00E-04	TN	Soil
FOtu00606_Phaeosphaeriaceae	0.9162	0.7778	0.844	0.0015	TN	Soil
FOtu00040_Lophiostomataceae	0.7975	0.8889	0.842	1.00E-04	TN	Soil
FOtu00290_Exophiala	0.8442	0.8333	0.839	1.00E-04	TN	Soil
FOtu00397_Subulicystidium_perlongispo	0.967	0.7222	0.836	0.0002	TN	Soil
FOtu00565_Pleosporales	0.8815	0.7778	0.828	1.00E-04	TN	Soil
FOtu00637_Pleosporales	0.9434	0.7222	0.825	1.00E-04	TN	Soil
FOtu00058_Lophiostomataceae	0.8163	0.8333	0.825	1.00E-04	TN	Soil
FOtu00626_Articulospora_sp	0.8042	0.8333	0.819	0.0016	TN	Soil
FOtu00089_Ascomycota	0.8591	0.7778	0.817	1.00E-04	TN	Soil
FOtu00867_Ascomycota	1	0.6667	0.816	1.00E-04	TN	Soil
FOtu00215_Basidiomycota_sp	0.9972	0.6667	0.815	1.00E-04	TN	Soil
FOtu00144_Ascomycota	0.9944	0.6667	0.814	1.00E-04	TN	Soil
FOtu00706_Strelitziana_africana	0.9879	0.6667	0.812	1.00E-04	TN	Soil
FOtu00727_Thelephoraceae	0.8442	0.7778	0.81	0.0003	TN	Soil
FOtu00329_Cladophialophora	0.9773	0.6667	0.807	1.00E-04	TN	Soil
FOtu00476_Lophiostomataceae	0.8943	0.7222	0.804	0.0002	TN	Soil
FOtu01058_Sporobolomyces	0.8929	0.7222	0.803	0.0002	TN	Soil
FOtu01360_Valsonectria_pulchella	0.9609	0.6667	0.8	1.00E-04	TN	Soil
FOtu00162_Pleosporales	0.9609	1	0.98	1.00E-04	WA	Soil
FOtu00364_Ascomycota	0.9961	0.9167	0.956	1.00E-04	WA	Soil
FOtu00769_Naganishia_randhawae	0.9951	0.9167	0.955	1.00E-04	WA	Soil
FOtu00060_Gibellulopsis_piscis	0.9914	0.9167	0.953	1.00E-04	WA	Soil
FOtu00861_Mortierella_alpina	0.988	0.9167	0.952	1.00E-04	WA	Soil
FOtu00149_Lophiotrema_rubi	0.9858	0.9167	0.951	1.00E-04	WA	Soil
FOtu00157_Alternaria_subcucurbitae	0.9807	0.9167	0.948	1.00E-04	WA	Soil
FOtu00308_Cystofilobasidium_infirmomi	0.9791	0.9167	0.947	1.00E-04	WA	Soil
FOtu00147_Stachybotryaceae	0.9732	0.9167	0.945	1.00E-04	WA	Soil
FOtu00026_Pleosporales	0.973	0.9167	0.944	1.00E-04	WA	Soil
FOtu01094_Microascales	0.966	0.9167	0.941	1.00E-04	WA	Soil
FOtu00413_Fusarium_redolens	0.9568	0.9167	0.936	1.00E-04	WA	Soil
FOtu00016_Penicillium_neocrassum	0.9522	0.9167	0.934	0.0165	WA	Soil
FOtu01358_Mortierella	0.9502	0.9167	0.933	1.00E-04	WA	Soil
FOtu00664_Oidiodendron_truncatum	0.9416	0.9167	0.929	1.00E-04	WA	Soil
FOtu00758_Holtermanniella_takashimae	0.8608	1	0.928	1.00E-04	WA	Soil
FOtu00332_Tetracladium	0.9369	0.9167	0.927	1.00E-04	WA	Soil
FOtu01276_Syncephalis_sp	0.9344	0.9167	0.926	1.00E-04	WA	Soil
FOtu00713_Alternaria_metachromatica	0.9222	0.9167	0.919	1.00E-04	WA	Soil
FOtu00023_Mortierella_alpina	0.9219	0.9167	0.919	0.0008	WA	Soil
FOtu00048_Xylariales	0.9148	0.9167	0.916	1.00E-04	WA	Soil
FOtu00787_Naganishia_albida	0.9137	0.9167	0.915	1.00E-04	WA	Soil
FOtu00698_Dendryphion	0.9082	0.9167	0.912	1.00E-04	WA	Soil
FOtu00163_Ascomycota	0.9937	0.8333	0.91	1.00E-04	WA	Soil
FOtu00038_Penicillium_bialowiezense	0.9935	0.8333	0.91	1.00E-04	WA	Soil
FOtu00822_Gymnoascus_reessii	0.8984	0.9167	0.907	1.00E-04	WA	Soil
FOtu00342_Sordariomycetes	0.9882	0.8333	0.907	1.00E-04	WA	Soil
FOtu00430_Chytridiomycota_sp	0.8977	0.9167	0.907	1.00E-04	WA	Soil
FOtu00527_Chrysosporium_pseudomerda	0.9809	0.8333	0.904	1.00E-04	WA	Soil
FOtu00526_Nectriaceae	0.9787	0.8333	0.903	1.00E-04	WA	Soil
FOtu00071_Penicillium_polonicum	0.8102	1	0.9	0.0055	WA	Soil
FOtu00367_Chaetosphaeria_sp	0.802	1	0.896	0.0009	WA	Soil
FOtu00738_Ustilago_hordei	0.8747	0.9167	0.895	1.00E-04	WA	Soil
FOtu00164_Cystofilobasidium_capitatum	0.8705	0.9167	0.893	1.00E-04	WA	Soil
FOtu00849_Sarocladium_kiliense	0.9526	0.8333	0.891	1.00E-04	WA	Soil
FOtu00356_Chytridiomycota_sp	0.9526	0.8333	0.891	1.00E-04	WA	Soil
FOtu01033_Pseudeurotiaceae	0.9476	0.8333	0.889	1.00E-04	WA	Soil
FOtu00518_Filobasidiales	0.8614	0.9167	0.889	1.00E-04	WA	Soil
FOtu00210_Melanommataceae	0.8534	0.9167	0.884	1.00E-04	WA	Soil
FOtu00354_Cephalotrichum_asperulum	0.938	0.8333	0.884	1.00E-04	WA	Soil
FOtu00759_Pleosporales	0.9256	0.8333	0.878	1.00E-04	WA	Soil
FOtu00446_Acrostalagmus_luteoalbus	0.9152	0.8333	0.873	1.00E-04	WA	Soil
FOtu00665_Pleurotheciella_sp	0.8291	0.9167	0.872	0.0002	WA	Soil
FOtu0148S_Thelonectria	0.8201	0.9167	0.867	1.00E-04	WA	Soil
FOtu00546_Peziza_buxea	1	0.75	0.866	1.00E-04	WA	Soil
FOtu01000_Sordariomycetes	1	0.75	0.866	1.00E-04	WA	Soil
FOtu00340_Paurocotylis	0.9966	0.75	0.865	1.00E-04	WA	Soil
FOtu00393_Trichoderma	0.815	0.9167	0.864	1.00E-04	WA	Soil
FOtu00693_Rozellomycota_sp	0.9954	0.75	0.864	1.00E-04	WA	Soil
FOtu00921_Mortierella_alpina	0.9946	0.75	0.864	1.00E-04	WA	Soil
FOtu00120_Apodus_deciduus	0.8923	0.8333	0.862	0.0002	WA	Soil
FOtu00456_Metarhizium_marquandii	0.8064	0.9167	0.86	1.00E-04	WA	Soil
FOtu01070_Cephalotrichum	0.9843	0.75	0.859	1.00E-04	WA	Soil
FOtu00371_Chrysosporium_lobatum	0.9706	0.75	0.853	1.00E-04	WA	Soil
FOtu01016_Helotiales	0.969	0.75	0.852	1.00E-04	WA	Soil
FOtu00212_Ascomycota	0.9679	0.75	0.852	0.0003	WA	Soil
FOtu00172_Chrysosporium_pseudomerda	0.8642	0.8333	0.849	0.0104	WA	Soil
FOtu00505_Tetracladium	0.7855	0.9167	0.849	0.0002	WA	Soil
FOtu00525_Chaetothyriales	0.9578	0.75	0.848	1.00E-04	WA	Soil
FOtu00452_Ascomycota	0.7795	0.9167	0.845	0.0002	WA	Soil
FOtu01020_Tranzscheliella_yupeitaniae	0.9504	0.75	0.844	1.00E-04	WA	Soil
FOtu00548_Hypocreales	0.8533	0.8333	0.843	1.00E-04	WA	Soil
FOtu01216_Stachybotrys_chartarum	0.9432	0.75	0.841	1.00E-04	WA	Soil
FOtu00139_Operculomyces_laminatus	0.8447	0.8333	0.839	0.0002	WA	Soil
FOtu00523_Coniochaeta	0.7634	0.9167	0.837	0.0002	WA	Soil
FOtu00130_Pyrenochaeta	0.7624	0.9167	0.836	1.00E-04	WA	Soil
FOtu00415_Leohumicola	0.9269	0.75	0.834	0.0003	WA	Soil
FOtu00541_Chaetomiaceae	0.9261	0.75	0.833	1.00E-04	WA	Soil
FOtu00295_Plectosphaerellaceae	0.8278	0.8333	0.831	0.0003	WA	Soil
FOtu01140_Phaeosphaeriaceae	0.8974	0.75	0.82	1.00E-04	WA	Soil
FOtu01781_Tranzscheliella	0.8947	0.75	0.819	1.00E-04	WA	Soil
FOtu00818_Clonostachys	1	0.6667	0.816	1.00E-04	WA	Soil
FOtu01582_Fusarium_solani	1	0.6667	0.816	1.00E-04	WA	Soil
FOtu02327_Onygenales	1	0.6667	0.816	1.00E-04	WA	Soil
FOtu00559_Ascomycota	0.9975	0.6667	0.815	1.00E-04	WA	Soil
FOtu00705_Chaetothyriales	0.9956	0.6667	0.815	1.00E-04	WA	Soil
FOtu00451_Ascomycota	0.8844	0.75	0.814	1.00E-04	WA	Soil
FOtu00629_Mortierellomycota	0.9919	0.6667	0.813	1.00E-04	WA	Soil
FOtu00514_Pyrenochaeta	0.9859	0.6667	0.811	1.00E-04	WA	Soil
FOtu01234_Arachnomyces_sp	0.7878	0.8333	0.81	1.00E-04	WA	Soil

Table A.9 (Page 1 of 2). Hub caulsophere OTUs across all R and P values tested for Juglans nigra trees in Indiana (IN), Tennessee (TN), and Washington (WA).

	Kingdom	Phylum	Class	Order	Family	Genus	Species	State	p0.05.r0.6	p0.01.r0.6	p0.005.r0.6	p0.001.r0.6	p0.05.r0.8	p0.01.r0.8	p0.005.r0.8	p0.001.r0.8
FOtu0183	k__Fungi	p__Ascomycota	c__Eurotiomycetes	o__Phaeomoniellales	o__Phaeomoniellales_unclassified	o__Phaeomoniellales_unclassified	o__Phaeomoniellales_unclassified	IN	1	1	1	0	0	0	0	0
Botu0066	Bacteria	Verrucomicrobia	Verrucomicrobiae	Verrucomicrobiae_unclassified	Verrucomicrobiae_unclassified	Verrucomicrobiae_unclassified	NA	IN	1	1	1	0	1	1	1	0
Botu0074	Bacteria	Proteobacteria	Alphaproteobacteria	Sphingomonadales	Sphingomonadaceae	Sphingomonadaceae_unclassified	NA	IN	1	0	0	0	0	0	0	0
Botu0090	Bacteria	Proteobacteria	Alphaproteobacteria	Rhizobiales	Beijerinckiaceae	1174-901-12	NA	IN	1	1	1	0	0	0	0	0
Botu0113	Bacteria	Actinobacteria	Actinobacteria	Kineosporiales	Kineosporiaceae	Kineosporia	NA	IN	1	1	1	0	0	0	0	0
Botu0167	Bacteria	Bacteroidetes	Bacteroidia	Cytophagales	Spirosomaceae	Spirosomaceae_unclassified	NA	IN	1	1	1	0	0	0	0	0
Botu0187	Bacteria	Chloroflexi	Chloroflexia	Chloroflexales	Roseiflexaceae	uncultured	NA	IN	1	1	1	0	0	0	0	0
Botu0302	Bacteria	Bacteroidetes	Bacteroidia	Chitinophagales	Chitinophagaceae	Chitinophagaceae_unclassified	NA	IN	1	0	0	0	0	0	0	0
Botu0325	Bacteria	Proteobacteria	Alphaproteobacteria	Sphingomonadales	Sphingomonadaceae	Sphingomonadaceae_unclassified	NA	IN	1	0	1	0	0	0	0	0
Botu0455	Bacteria	Bacteroidetes	Bacteroidia	Chitinophagales	Chitinophagaceae	Ferruginibacter	NA	IN	1	1	1	0	0	0	0	0
Botu0277	Bacteria	Bacteroidetes	Bacteroidia	Cytophagales	Spirosomaceae	Spirosoma	NA	IN	1	1	1	0	0	0	0	0
Botu0395	Bacteria	Proteobacteria	Alphaproteobacteria	Tistrellales	Geminicoccaceae	Candidatus_Alysiosphaera	NA	IN	1	1	1	0	1	1	1	0
Botu0537	Bacteria	Bacteroidetes	Bacteroidia	Chitinophagales	Chitinophagaceae	Segetibacter	NA	IN	1	1	0	0	1	1	1	0
Botu0587	Bacteria	Actinobacteria	Thermoleophilia	Solirubrobacterales	67-14	67-14_ge	NA	IN	1	0	1	0	0	0	0	0
Botu0402	Bacteria	Actinobacteria	Actinobacteria	Propionibacteriales	Nocardioidaceae	Nocardioides	NA	IN	1	0	1	0	0	0	0	0
Botu0239	Bacteria	Proteobacteria	Deltaproteobacteria	Myxococcales	Archangiaceae	Archangiaceae_unclassified	NA	IN	1	0	1	0	0	0	0	0
Botu0174	Bacteria	Proteobacteria	Deltaproteobacteria	Myxococcales	Polyangiaceae	Polyangium	NA	IN	1	1	0	0	1	1	1	0
Botu0575	Bacteria	Gemmatimonadetes	Gemmatimonadetes	Gemmatimonadales	Gemmatimonadaceae	Gemmatirosa	NA	IN	1	0	1	0	0	0	0	0
Botu0101	Bacteria	Proteobacteria	Alphaproteobacteria	Sphingomonadales	Sphingomonadaceae	Sphingomonadaceae_unclassified	NA	IN	1	0	0	0	0	0	0	0
Botu0568	Bacteria	Proteobacteria	Alphaproteobacteria	Caulobacterales	Caulobacteraceae	uncultured	NA	IN	0	0	0	0	1	1	1	0
Botu0204	Bacteria	Proteobacteria	Alphaproteobacteria	Rhizobiales	Beijerinckiaceae	Microvirga	NA	IN	0	0	0	0	1	1	1	0
Botu0049	Bacteria	Actinobacteria	Actinobacteria	Micrococcales	Microbacteriaceae	Microbacterium	NA	IN	0	1	1	0	1	1	1	0
FOtu0299	k__Fungi	p__Ascomycota	c__Dothideomycetes	o__Capnodiales	f__Teratosphaeriaceae	g__Devriesia	s__Devriesia_pseudoamericana	IN	0	1	1	0	1	1	1	0
Botu0616	Bacteria	Cyanobacteria	Melainabacteria	Vampirovibrionales	Vampirovibrionales_fa	Vampirovibrionales_ge	NA	IN	0	0	0	0	1	1	1	0
Botu0617	Bacteria	Proteobacteria	Alphaproteobacteria	Rhizobiales	Beijerinckiaceae	1174-901-12	NA	IN	0	0	0	0	1	1	1	0
Botu0641	Bacteria	Acidobacteria	Acidobacteriia	Acidobacteriales	Acidobacteriaceae_(Subgroup_1)	Acidobacteriaceae_(Subgroup_1)_unclassified	NA	IN	0	1	1	0	1	1	1	0
Botu0695	Bacteria	Proteobacteria	Gammaproteobacteria	Betaproteobacteriales	Burkholderiaceae	Burkholderiaceae_unclassified	NA	IN	0	0	0	0	1	1	1	0
Botu0168	Bacteria	Proteobacteria	Alphaproteobacteria	Acetobacterales	Acetobacteraceae	Roseomonas	NA	IN	0	0	0	0	1	1	1	0
Botu0495	Bacteria	Cyanobacteria	Oxyphotobacteria	Nostocales	Nostocaceae	Nostoc_PCC-73102	NA	IN	0	0	0	0	1	1	1	0
Botu0268	Bacteria	Proteobacteria	Alphaproteobacteria	Rhizobiales	Beijerinckiaceae	1174-901-12	NA	IN	0	0	1	0	1	1	1	0
Botu0427	Bacteria	Actinobacteria	Thermoleophilia	Solirubrobacterales	Solirubrobacterales_unclassified	Solirubrobacterales_unclassified	NA	IN	0	0	1	0	1	1	1	0
Botu0373	Bacteria	Bacteroidetes	Bacteroidia	Chitinophagales	Chitinophagaceae	Chitinophagaceae_unclassified	NA	IN	0	0	0	0	1	1	1	0
Botu0289	Bacteria	Proteobacteria	Deltaproteobacteria	Myxococcales	Sandaracinaceae	uncultured	NA	IN	0	1	1	0	1	1	1	0
Botu0645	Bacteria	Proteobacteria	Alphaproteobacteria	Acetobacterales	Acetobacteraceae	Roseococcus	NA	IN	0	0	0	0	1	1	1	0
Botu0703	Bacteria	Bacteroidetes	Bacteroidia	Bacteroidia_unclassified	Bacteroidia_unclassified	Bacteroidia_unclassified	NA	IN	0	0	0	0	1	1	1	0
Botu0966	Bacteria	Proteobacteria	Alphaproteobacteria	Acetobacterales	Acetobacteraceae	Acetobacteraceae_unclassified	NA	IN	0	0	0	0	1	1	1	0
Botu0473	Bacteria	Proteobacteria	Alphaproteobacteria	Rhizobiales	Xanthobacteraceae	Ancylobacter	NA	IN	0	0	0	0	1	1	1	0
Botu0531	Bacteria	Proteobacteria	Alphaproteobacteria	Alphaproteobacteria_unclassified	Alphaproteobacteria_unclassified	Alphaproteobacteria_unclassified	NA	IN	0	0	0	0	1	1	1	0
Botu0763	Bacteria	Actinobacteria	Actinobacteria	Kineosporiales	Kineosporiaceae	Kineosporiaceae_unclassified	NA	IN	0	0	0	0	1	1	1	0
FOtu0029	k__Fungi	p__Ascomycota	c__Sordariomycetes	o__Togniniales	f__Togniniaceae	g__Phaeoacremonium	g__Phaeoacremonium_unclassified	IN	0	1	1	0	1	1	1	0
FOtu0083	k__Fungi	p__Ascomycota	p__Ascomycota_unclassif	p__Ascomycota_unclassified	p__Ascomycota_unclassified	p__Ascomycota_unclassified	p__Ascomycota_unclassified	IN	0	0	0	0	1	1	1	0
FOtu0230	k__Fungi	p__Ascomycota	c__Dothideomycetes	o__Capnodiales	o__Capnodiales_unclassified	o__Capnodiales_unclassified	o__Capnodiales_unclassified	IN	0	0	1	0	1	1	1	0
FOtu0280	k__Fungi	p__Ascomycota	p__Ascomycota_unclassif	p__Ascomycota_unclassified	p__Ascomycota_unclassified	p__Ascomycota_unclassified	p__Ascomycota_unclassified	IN	0	0	0	0	1	1	1	0
FOtu0298	k__Fungi	p__Ascomycota	c__Sordariomycetes	c__Sordariomycetes_unclassified	c__Sordariomycetes_unclassified	c__Sordariomycetes_unclassified	c__Sordariomycetes_unclassified	IN	0	0	0	0	1	1	1	0
FOtu0486	k__Fungi	p__Ascomycota	c__Dothideomycetes	o__Pleosporales	o__Pleosporales_unclassified	o__Pleosporales_unclassified	o__Pleosporales_unclassified	IN	0	0	0	0	1	1	1	0
Botu0023	Bacteria	Actinobacteria	Actinobacteria	Actinobacteria_unclassified	Actinobacteria_unclassified	Actinobacteria_unclassified	NA	IN	0	1	0	0	0	0	0	0
Botu0681	Bacteria	Proteobacteria	Alphaproteobacteria	Caulobacterales	Caulobacteraceae	Phenylobacterium	NA	IN	0	1	1	0	0	0	0	0
FOtu0038	k__Fungi	p__Ascomycota	c__Orbiliomycetes	o__Orbiliales	f__Orbiliaceae	g__Orbilia	g__Orbilia_unclassified	IN	0	1	0	0	0	0	0	0
Botu0081	Bacteria	Proteobacteria	Gammaproteobacteria	Enterobacteriales	Enterobacteriaceae	Sodalis	NA	IN	0	1	1	0	0	0	0	0
FOtu0064	k__Fungi	p__Ascomycota	c__Dothideomycetes	o__Capnodiales	f__Capnodiales_fam_Incertae_sedis	g__Arthrocatena	s__Arthrocatena_tenebrio	IN	0	1	0	0	0	0	0	0
FOtu0314	k__Fungi	p__Ascomycota	p__Ascomycota_unclassif	p__Ascomycota_unclassified	p__Ascomycota_unclassified	p__Ascomycota_unclassified	p__Ascomycota_unclassified	IN	0	1	0	0	0	0	0	0
Botu0073	Bacteria	Proteobacteria	Alphaproteobacteria	Caulobacterales	Caulobacteraceae	Caulobacteraceae_unclassified	NA	IN	0	1	0	0	0	0	0	0
Botu0433	Bacteria	Proteobacteria	Alphaproteobacteria	Rhizobiales	uncultured	uncultured_ge	NA	IN	0	1	1	0	0	0	0	0
Botu0898	Bacteria	Planctomycetes	Planctomycetacia	Isosphaerales	Isosphaeraceae	Isosphaeraceae_unclassified	NA	IN	0	1	0	0	0	0	0	0
FOtu0171	k__Fungi	p__Ascomycota	c__Eurotiomycetes	o__Chaetothyriales	o__Chaetothyriales_unclassified	o__Chaetothyriales_unclassified	o__Chaetothyriales_unclassified	IN	0	1	1	0	0	0	0	0
Botu0388	Bacteria	Proteobacteria	Alphaproteobacteria	Rhizobiales	Beijerinckiaceae	Beijerinckiaceae_unclassified	NA	IN	0	1	1	0	0	0	0	0
Botu0540	Bacteria	Proteobacteria	Gammaproteobacteria	Betaproteobacteriales	Burkholderiaceae	Burkholderiaceae_unclassified	NA	IN	0	1	1	0	0	0	0	0
Botu0218	Bacteria	Actinobacteria	Actinobacteria	Propionibacteriales	Nocardioidaceae	Nocardioides	NA	IN	0	1	0	0	0	0	0	0
FOtu0003	k__Fungi	p__Ascomycota	c__Eurotiomycetes	o__Phaeomoniellales	o__Phaeomoniellales_unclassified	o__Phaeomoniellales_unclassified	o__Phaeomoniellales_unclassified	IN	0	1	1	0	0	0	0	0
FOtu0043	k__Fungi	p__Basidiomycota	c__Agaricomycetes	o__Agaricales	f__Tricholomataceae	g__Mycena	g__Mycena_unclassified	IN	0	1	0	0	0	0	0	0
Botu0051	Bacteria	Bacteroidetes	Bacteroidia	Chitinophagales	Chitinophagaceae	uncultured	NA	IN	0	0	1	0	0	0	0	0
Botu0192	Bacteria	Proteobacteria	Alphaproteobacteria	Rhizobiales	Rhizobiaceae	Rhizobiaceae_unclassified	NA	IN	0	0	1	0	0	0	0	0
Botu0281	Bacteria	Bacteroidetes	Bacteroidia	Cytophagales	Hymenobacteraceae	Hymenobacter	NA	IN	0	0	1	0	0	0	0	0
Botu0957	Bacteria	Bacteroidetes	Bacteroidia	Sphingobacteriales	Sphingobacteriaceae	Mucilaginibacter	NA	IN	0	0	1	0	0	0	0	0
Botu0313	Bacteria	Chloroflexi	Chloroflexia	Chloroflexales	Chloroflexales_unclassified	Chloroflexales_unclassified	NA	IN	0	0	1	0	0	0	0	0
Botu0336	Bacteria	Bacteroidetes	Bacteroidia	Chitinophagales	Chitinophagaceae	Chitinophagaceae_unclassified	NA	IN	0	0	1	0	0	0	0	0
Botu0733	Bacteria	Chloroflexi	Chloroflexia	Kallotenuales	AKIW781	AKIW781_ge	NA	IN	0	0	1	0	0	0	0	0
Botu0005	Bacteria	Bacteroidetes	Bacteroidia	Sphingobacteriales	Sphingobacteriaceae	Sphingobacteriaceae_unclassified	NA	IN	0	0	1	0	0	0	0	0
FOtu0587	k__Fungi	p__Ascomycota	c__Sordariomycetes	o__Hypocreales	f__Nectriaceae	f__Nectriaceae_unclassified	f__Nectriaceae_unclassified	IN	0	0	1	0	0	0	0	0
Botu0125	Bacteria	Bacteroidetes	Bacteroidia	Chitinophagales	Chitinophagaceae	Chitinophagaceae_unclassified	NA	IN	0	0	1	0	0	0	0	0
Botu0199	Bacteria	Proteobacteria	Alphaproteobacteria	Rhizobiales	Beijerinckiaceae	Methylobacterium	NA	IN	0	0	1	0	0	0	0	0
Botu0271	Bacteria	Actinobacteria	Actinobacteria	Propionibacteriales	Nocardioidaceae	Nocardioides	NA	IN	0	0	1	0	0	0	0	0
Botu1403	Bacteria	Bacteroidetes	Bacteroidia	Chitinophagales	Chitinophagaceae	Chitinophagaceae_unclassified	NA	IN	0	0	1	0	0	0	0	0
Botu0246	Bacteria	Proteobacteria	Alphaproteobacteria	Rhizobiales	Beijerinckiaceae	Psychroglaciecola	NA	IN	0	0	0	0	0	0	0	0

Table A.9. Continued (Page 2 of 2).

	Kingdom	Phylum	Class	Order	Family	Genus	Species	State	p0.05.r0.6	p0.01.r0.6	p0.005.r0.6	p0.001.r0.6	p0.05.r0.8	p0.01.r0.8	p0.005.r0.8	p0.001.r0.8
Botu0055	Bacteria	Bacteroidetes	Bacteroidia	Sphingobacteriales	Sphingobacteriaceae	Pedobacter	NA	IN	0	0	0	0	0	0	0	0
Botu0400	Bacteria	Actinobacteria	Actinobacteria	Micromonosporales	Micromonosporaceae	Actinoplanes	NA	IN	0	0	0	0	0	0	0	0
FOtu0527	k__Fungi	p__Ascomycota	c__Dothideomycetes	o__Pleosporales	o__Pleosporales_unclassified	o__Pleosporales_unclassified	o__Pleosporales_unclassified	IN	0	0	0	0	0	0	0	0
Botu0071	Bacteria	Bacteroidetes	Bacteroidia	Cytophagales	Spirosomaceae	Spirosoma	NA	IN	0	0	0	0	0	0	0	0
Botu0541	Bacteria	Proteobacteria	Alphaproteobacteria	Sphingomonadales	Sphingomonadaceae	Sphingomonas	NA	IN	0	0	0	0	0	0	0	0
FOtu0174	k__Fungi	p__Ascomycota	c__Lecanoromycetes	o__Candelariales	f__Candelariaceae	g__Candelariella	g__Candelariella_unclassified	IN	0	0	0	0	0	0	0	0
FOtu0654	k__Fungi	p__Basidiomycota	c__Tremellomycetes	o__Tremellales	f__Cuniculitremaceae	f__Cuniculitremaceae_unclassified	f__Cuniculitremaceae_unclassified	IN	0	0	0	0	0	0	0	0
Botu0463	Bacteria	Proteobacteria	Alphaproteobacteria	Rhodobacterales	Rhodobacteraceae	Rubellimicrobium	NA	IN	0	0	0	0	0	0	0	0
Botu0255	Bacteria	Proteobacteria	Alphaproteobacteria	Micavibrionales	uncultured	uncultured_ge	NA	IN	0	0	0	0	0	0	0	0
FOtu0404	k__Fungi	p__Ascomycota	c__Sordariomycetes	c__Sordariomycetes_unclassified	c__Sordariomycetes_unclassified	c__Sordariomycetes_unclassified	c__Sordariomycetes_unclassified	IN	0	0	0	0	0	0	0	0
FOtu0061	k__Fungi	p__Ascomycota	p__Ascomycota_unclassif	p__Ascomycota_unclassified	p__Ascomycota_unclassified	p__Ascomycota_unclassified	p__Ascomycota_unclassified	TN	1	1	1	0	0	0	0	0
FOtu0089	k__Fungi	p__Ascomycota	c__Lecanoromycetes	o__Caliciales	f__Physciaceae	g__Phaeophyscia	g__Phaeophyscia_unclassified	TN	1	0	1	0	1	1	1	0
FOtu0253	k__Fungi	p__Ascomycota	c__Lecanoromycetes	c__Lecanoromycetes_unclassified	c__Lecanoromycetes_unclassified	c__Lecanoromycetes_unclassified	c__Lecanoromycetes_unclassified	TN	1	1	0	0	1	1	1	0
Botu0034	Bacteria	Actinobacteria	Actinobacteria	Pseudonocardiales	Pseudonocardiaceae	Pseudonocardia	NA	TN	1	0	0	0	0	0	0	0
Botu0082	Bacteria	Actinobacteria	Actinobacteria	Pseudonocardiales	Pseudonocardiaceae	Pseudonocardia	NA	TN	1	0	0	0	0	0	0	0
Botu0093	Bacteria	Bacteroidetes	Bacteroidia	Chitinophagales	Chitinophagaceae	Chitinophagaceae_unclassified	NA	TN	1	0	0	0	0	0	0	0
Botu0119	Bacteria	Bacteroidetes	Bacteroidia	Cytophagales	Spirosomaceae	Spirosoma	NA	TN	1	1	1	0	1	1	1	0
FOtu0005	k__Fungi	p__Ascomycota	c__Eurotiomycetes	o__Phaeomoniellales	o__Phaeomoniellales_unclassified	o__Phaeomoniellales_unclassified	o__Phaeomoniellales_unclassified	TN	1	0	0	0	0	0	0	0
FOtu0037	k__Fungi	p__Ascomycota	c__Eurotiomycetes	o__Coryneliales	f__Coryneliaceae	g__Caliciopsis	s__Caliciopsis_valentina	TN	1	1	1	0	1	1	1	0
FOtu0058	k__Fungi	p__Ascomycota	p__Ascomycota_unclassif	p__Ascomycota_unclassified	p__Ascomycota_unclassified	p__Ascomycota_unclassified	p__Ascomycota_unclassified	TN	1	0	0	0	0	0	0	0
FOtu0062	k__Fungi	p__Ascomycota	c__Dothideomycetes	o__Pleosporales	f__unclassified_Pleosporales	g__unclassified_Pleosporales	s__Pleosporales_sp	TN	1	0	0	0	0	0	0	0
FOtu0091	k__Fungi	p__Ascomycota	c__Lecanoromycetes	c__Lecanoromycetes_unclassified	c__Lecanoromycetes_unclassified	c__Lecanoromycetes_unclassified	c__Lecanoromycetes_unclassified	TN	1	1	0	0	0	0	0	0
FOtu0104	k__Fungi	p__Ascomycota	p__Ascomycota_unclassif	p__Ascomycota_unclassified	p__Ascomycota_unclassified	p__Ascomycota_unclassified	p__Ascomycota_unclassified	TN	1	0	0	0	0	0	0	0
Botu0071	Bacteria	Bacteroidetes	Bacteroidia	Cytophagales	Spirosomaceae	Spirosoma	NA	TN	1	1	1	0	1	1	1	0
Botu0170	Bacteria	Actinobacteria	Actinobacteria	Actinobacteria_unclassified	Actinobacteria_unclassified	Actinobacteria_unclassified	NA	TN	1	0	1	0	1	1	1	0
Botu0219	Bacteria	Proteobacteria	Alphaproteobacteria	Acetobacterales	Acetobacteraceae	Acetobacteraceae_unclassified	NA	TN	1	1	0	0	0	0	0	0
Botu0240	Bacteria	Proteobacteria	Alphaproteobacteria	Rhodobacterales	Rhodobacteraceae	Rubellimicrobium	NA	TN	1	0	0	0	0	0	0	0
Botu0253	Bacteria	Proteobacteria	Alphaproteobacteria	Acetobacterales	Acetobacteraceae	Roseomonas	NA	TN	1	1	1	0	1	1	1	0
Botu0274	Bacteria	Gemmatimonadetes	Gemmatimonadetes	Gemmatimonadales	Gemmatimonadaceae	Gemmatirosa	NA	TN	1	0	1	0	1	1	1	0
Botu0347	Bacteria	Proteobacteria	Alphaproteobacteria	Acetobacterales	Acetobacteraceae	Acetobacteraceae_unclassified	NA	TN	1	1	1	0	0	0	0	0
Botu0077	Bacteria	Proteobacteria	Alphaproteobacteria	Rhizobiales	Beijerinckiaceae	Methylobacterium	NA	TN	1	0	0	0	0	0	0	0
Botu0120	Bacteria	Bacteroidetes	Bacteroidia	Chitinophagales	Chitinophagaceae	Chitinophagaceae_unclassified	NA	TN	1	1	1	0	0	0	0	0
Botu0454	Bacteria	Cyanobacteria	Oxyphotobacteria	Oxyphotobacteria_unclassified	Oxyphotobacteria_unclassified	Oxyphotobacteria_unclassified	Oxyphotobacteria_unclassified	TN	1	1	1	0	0	0	0	0
FOtu0274	k__Fungi	p__Ascomycota	c__Dothideomycetes	o__Pleosporales	o__Pleosporales_unclassified	o__Pleosporales_unclassified	o__Pleosporales_unclassified	TN	1	0	0	0	0	0	0	0
FOtu0019	k__Fungi	p__Ascomycota	p__Ascomycota_unclassif	p__Ascomycota_unclassified	p__Ascomycota_unclassified	p__Ascomycota_unclassified	p__Ascomycota_unclassified	TN	1	1	1	0	1	1	1	0
FOtu0068	k__Fungi	p__Ascomycota	p__Ascomycota_unclassif	p__Ascomycota_unclassified	p__Ascomycota_unclassified	p__Ascomycota_unclassified	p__Ascomycota_unclassified	TN	1	1	0	0	0	0	0	0
FOtu0167	k__Fungi	p__Ascomycota	p__Ascomycota_unclassif	p__Ascomycota_unclassified	p__Ascomycota_unclassified	p__Ascomycota_unclassified	p__Ascomycota_unclassified	TN	1	1	0	0	0	0	0	0
Botu0008	Bacteria	Actinobacteria	Actinobacteria	Pseudonocardiales	Pseudonocardiaceae	Actinomycetospora	NA	TN	1	1	0	0	0	0	0	0
Botu0035	Bacteria	Proteobacteria	Alphaproteobacteria	Rhizobiales	Beijerinckiaceae	Methylobacterium	NA	TN	1	1	1	0	1	1	1	0
Botu0148	Bacteria	Bacteroidetes	Bacteroidia	Cytophagales	Hymenobacteraceae	Hymenobacter	NA	TN	1	1	1	0	1	1	1	0
Botu0214	Bacteria	Chloroflexi	Chloroflexi_unclassified	Chloroflexi_unclassified	Chloroflexi_unclassified	Chloroflexi_unclassified	NA	TN	1	1	1	0	0	0	0	0
FOtu0066	k__Fungi	p__Ascomycota	c__Eurotiomycetes	o__Chaetothyriales	f__Herpotrichiellaceae	g__Rhinocladiella	s__Rhinocladiella_sp	TN	1	1	0	0	0	0	0	0
FOtu0221	k__Fungi	p__Ascomycota	c__Lecanoromycetes	o__Caliciales	f__Physciaceae	g__Physciella	s__Physciella_chloantha	TN	1	0	1	0	0	0	0	0
FOtu0357	k__Fungi	p__Ascomycota	c__Eurotiomycetes	o__Phaeomoniellales	f__Phaeomoniellaceae	f__Phaeomoniellaceae_unclassified	f__Phaeomoniellaceae_unclassified	TN	1	1	1	0	0	0	0	0
Botu0073	Bacteria	Proteobacteria	Alphaproteobacteria	Caulobacterales	Caulobacteraceae	Caulobacteraceae_unclassified	NA	TN	1	1	1	0	0	0	0	0
FOtu0309	k__Fungi	p__Ascomycota	c__Dothideomycetes	o__Myriangiales	f__Elsinoaceae	g__Sphaceloma	g__Sphaceloma_unclassified	TN	0	0	0	0	1	1	1	0
Botu0094	Bacteria	Proteobacteria	Alphaproteobacteria	Rhizobiales	Beijerinckiaceae	1174-901-12	NA	TN	0	0	1	0	1	1	1	0
Botu0388	Bacteria	Proteobacteria	Alphaproteobacteria	Rhizobiales	Beijerinckiaceae	Beijerinckiaceae_unclassified	NA	TN	0	1	0	0	1	1	1	0
FOtu0203	k__Fungi	p__Ascomycota	c__Eurotiomycetes	o__Chaetothyriales	f__Chaetothyriales_fam_Incertae_se	g__Strelitziana	s__Strelitziana_africana	TN	0	0	0	0	1	1	1	0
Botu0592	Bacteria	Verrucomicrobia	Verrucomicrobiae	Chthoniobacterales	Chthoniobacteraceae	Chthoniobacter	NA	TN	0	0	0	0	1	1	1	0
Botu0356	Bacteria	Acidobacteria	Acidobacteriia	Acidobacteriales	Acidobacteriaceae_(Subgroup_1)	Acidobacteriaceae_(Subgroup_1)_unclassified	NA	TN	0	0	0	0	1	1	1	0
FOtu0595	k__Fungi	p__Ascomycota	p__Ascomycota_unclassif	p__Ascomycota_unclassified	p__Ascomycota_unclassified	p__Ascomycota_unclassified	p__Ascomycota_unclassified	TN	0	0	0	0	1	1	1	0
Botu0210	Bacteria	Proteobacteria	Alphaproteobacteria	Rhizobiales	Beijerinckiaceae	1174-901-12	NA	TN	0	0	0	0	1	1	1	0
FOtu0324	k__Fungi	p__Ascomycota	c__Dothideomycetes	o__Pleosporales	f__Phaeosphaeriaceae	g__Paraphoma	s__Paraphoma_sp	TN	0	0	0	0	1	1	1	0
Botu0316	Bacteria	Chloroflexi	Ktedonobacteria	CD119	CD119_fa	CD119_ge	NA	TN	0	0	1	0	1	1	1	0
Botu0074	Bacteria	Proteobacteria	Alphaproteobacteria	Sphingomonadales	Sphingomonadaceae	Sphingomonadaceae_unclassified	NA	TN	0	0	0	0	1	1	1	0
Botu0488	Bacteria	Proteobacteria	Alphaproteobacteria	Rhizobiales	Beijerinckiaceae	1174-901-12	NA	TN	0	0	0	0	1	1	1	0
Botu0053	Bacteria	Proteobacteria	Alphaproteobacteria	Rhizobiales	Beijerinckiaceae	Beijerinckiaceae_unclassified	NA	TN	0	1	1	0	0	0	0	0
FOtu0175	k__Fungi	p__Ascomycota	p__Ascomycota_unclassif	p__Ascomycota_unclassified	p__Ascomycota_unclassified	p__Ascomycota_unclassified	p__Ascomycota_unclassified	TN	0	1	1	0	0	0	0	0
FOtu0238	k__Fungi	p__Ascomycota	c__Dothideomycetes	o__Capnodiales	o__Capnodiales_unclassified	o__Capnodiales_unclassified	o__Capnodiales_unclassified	TN	0	1	0	0	0	0	0	0
Botu0109	Bacteria	Bacteroidetes	Bacteroidia	Cytophagales	Spirosomaceae	Spirosoma	NA	TN	0	1	1	0	0	0	0	0
Botu0044	Bacteria	Proteobacteria	Alphaproteobacteria	Acetobacterales	Acetobacteraceae	Acetobacteraceae_unclassified	NA	TN	0	1	0	0	0	0	0	0
FOtu0098	k__Fungi	p__Ascomycota	c__Eurotiomycetes	o__Chaetothyriales	f__Trichomeriaceae	f__Trichomeriaceae_unclassified	f__Trichomeriaceae_unclassified	TN	0	1	0	0	0	0	0	0
Botu0117	Bacteria	Actinobacteria	Actinobacteria	Frankiales	Cryptosporangiaceae	Cryptosporangium	NA	TN	0	1	1	0	0	0	0	0
FOtu0130	k__Fungi	p__Ascomycota	c__Eurotiomycetes	o__Chaetothyriales	f__Herpotrichiellaceae	g__Rhinocladiella	s__Rhinocladiella_sp	TN	0	1	1	0	0	0	0	0
Botu0097	Bacteria	Actinobacteria	Actinobacteria	Actinobacteria_unclassified	Actinobacteria_unclassified	Actinobacteria_unclassified	NA	TN	0	1	1	0	0	0	0	0
Botu0134	Bacteria	Acidobacteria	Acidobacteriia	Acidobacteriales	Acidobacteriaceae_(Subgroup_1)	Terriglobus	NA	TN	0	0	1	0	0	0	0	0
Botu0648	Bacteria	Acidobacteria	Acidobacteriia	Acidobacteriales	Acidobacteriaceae_(Subgroup_1)	Acidobacteriaceae_(Subgroup_1)_unclassified	NA	TN	0	0	1	0	0	0	0	0
FOtu0018	k__Fungi	p__Ascomycota	c__Eurotiomycetes	o__Phaeomoniellales	o__Phaeomoniellales_unclassified	o__Phaeomoniellales_unclassified	o__Phaeomoniellales_unclassified	TN	0	0	1	0	0	0	0	0
Botu0611	Bacteria	Proteobacteria	Alphaproteobacteria	Acetobacterales	Acetobacteraceae	Acetobacteraceae_unclassified	NA	TN	0	0	1	0	0	0	0	0
FOtu0367	k__Fungi	p__Ascomycota	p__Ascomycota_unclassif	p__Ascomycota_unclassified	p__Ascomycota_unclassified	p__Ascomycota_unclassified	p__Ascomycota_unclassified	TN	0	0	1	0	0	0	0	0
Botu0157	Bacteria	Bacteroidetes	Bacteroidia	Chitinophagales	Chitinophagaceae	Segetibacter	NA	TN	0	0	1	0	0	0	0	0
FOtu0154	k__Fungi	p__Ascomycota	c__Eurotiomycetes	o__Chaetothyriales	f__Trichomeriaceae	f__Trichomeriaceae_unclassified	f__Trichomeriaceae_unclassified	TN	0	0	0	0	0	0	0	0
FOtu0325	k__Fungi	p__Ascomycota	p__Ascomycota_unclassif	p__Ascomycota_unclassified	p__Ascomycota_unclassified	p__Ascomycota_unclassified	p__Ascomycota_unclassified	TN	0	0	0	0	0	0	0	0
FOtu0231	k__Fungi	p__Ascomycota	c__Eurotiomycetes	o__Chaetothyriales	f__Chaetothyriales_fam_Incertae_se	g__Strelitziana	s__Strelitziana_africana	TN	0	0	0	0	0	0	0	0
Botu0976	Bacteria	Proteobacteria	Alphaproteobacteria	Rhizobiales	Beijerinckiaceae	Beijerinckiaceae_unclassified	NA	TN	0	0	0	0	0	0	0	0
FOtu0015	k__Fungi	p__Ascomycota	p__Ascomycota_unclassif	p__Ascomycota_unclassified	p__Ascomycota_unclassified	p__Ascomycota_unclassified	p__Ascomycota_unclassified	TN	0	0	0	0	0	0	0	0
Botu0046	Bacteria	Actinobacteria	Actinobacteria	Kineosporiales	Kineosporiaceae	Kineococcus	NA	WA	1	0	1	0	0	0	1	0
Botu0024	Bacteria	Bacteroidetes	Bacteroidia	Cytophagales	Hymenobacteraceae	Hymenobacter	NA	WA	1	1	0	0	0	0	0	0
Botu0058	Bacteria	Deinococcus-Thermus	Deinococci	Deinococcales	Deinococcaceae	Deinococcus	NA	WA	1	1	1	0	1	1	1	0
Botu0010	Bacteria	Actinobacteria	Actinobacteria	Propionibacteriales	Propionibacteriaceae	Friedmanniella	NA	WA	1	1	1	0	1	1	1	0
Botu0475	Bacteria	Bacteroidetes	Bacteroidia	Cytophagales	Hymenobacteraceae	Hymenobacter	NA	WA	1	1	1	0	1	1	1	0
Botu0031	Bacteria	Bacteroidetes	Bacteroidia	Cytophagales	Hymenobacteraceae	Hymenobacter	NA	WA	0	0	0	0	1	1	0	0
FOtu0032	k__Fungi	p__Ascomycota	c__Dothideomycetes	o__Pleosporales	f__Phaeosphaeriaceae	f__Phaeosphaeriaceae_unclassified	f__Phaeosphaeriaceae_unclassified	WA	0	0	1	0	1	1	1	0
Botu0087	Bacteria	Bacteroidetes	Bacteroidia	Sphingobacteriales	Sphingobacteriaceae	Pedobacter	NA	WA	0	0	1	0	1	1	1	0
Botu0007	Bacteria	Proteobacteria	Gammaproteobacteria	Xanthomonadales	Xanthomonadaceae	Xanthomonadaceae_unclassified	NA	WA	0	1	1	0	1	1	1	0
Botu0014	Bacteria	Proteobacteria	Alphaproteobacteria	Rhizobiales	Rhizobiaceae	Rhizobiaceae_unclassified	NA	WA	0	1	1	0	1	1	1	0
FOtu0115	k__Fungi	p__Ascomycota	c__Sordariomycetes	o__Hypocreales	f__Bionectriaceae	g__Geosmithia	g__Geosmithia_unclassified	WA	0	0	1	0	1	1	1	0
FOtu0118	k__Fungi	p__Ascomycota	c__Eurotiomycetes	o__Chaetothyriales	f__Trichomeriaceae	g__Knufia	g__Knufia_unclassified	WA	0	0	1	0	1	1	1	0
Botu0011	Bacteria	Actinobacteria	Actinobacteria	Micrococcales	Microbacteriaceae	Microbacteriaceae_unclassified	NA	WA	0	1	1	0	1	1	1	0
Botu0047	Bacteria	Proteobacteria	Gammaproteobacteria	Xanthomonadales	Xanthomonadaceae	Luteimonas	NA	WA	0	0	1	0	1	1	1	0
Botu0067	Bacteria	Actinobacteria	Actinobacteria	Propionibacteriales	Nocardioidaceae	Aeromicrobium	NA	WA	0	1	1	0	1	1	1	0
FOtu0021	k__Fungi	p__Ascomycota	p__Ascomycota_unclassif	p__Ascomycota_unclassified	p__Ascomycota_unclassified	p__Ascomycota_unclassified	p__Ascomycota_unclassified	WA	0	1	1	0	0	0	1	0
Botu0290	Bacteria	Proteobacteria	Alphaproteobacteria	Acetobacterales	Acetobacteraceae	Acetobacteraceae_unclassified	NA	WA	0	1	0	0	0	0	0	0
FOtu0319	k__Fungi	p__Ascomycota	p__Ascomycota_unclassif	p__Ascomycota_unclassified	p__Ascomycota_unclassified	p__Ascomycota_unclassified	p__Ascomycota_unclassified	WA	0	1	0	0	0	0	0	0
Botu0055	Bacteria	Bacteroidetes	Bacteroidia	Sphingobacteriales	Sphingobacteriaceae	Pedobacter	NA	WA	0	1	0	0	0	0	0	0
FOtu0278	k__Fungi	p__Basidiomycota	p__Basidiomycota_unclas	p__Basidiomycota_unclassified	p__Basidiomycota_unclassified	p__Basidiomycota_unclassified	p__Basidiomycota_unclassified	WA	0	0	1	0	0	0	1	0
Botu0039	Bacteria	Actinobacteria	Actinobacteria	Propionibacteriales	Nocardioidaceae	Marmoricola	NA	WA	0	0	1	0	0	0	1	0
Botu0069	Bacteria	Proteobacteria	Alphaproteobacteria	Acetobacterales	Acetobacteraceae	Acidiphilium	NA	WA	0	0	1	0	0	0	1	0
Botu0161	Bacteria	Bacteroidetes	Bacteroidia	Sphingobacteriales	Sphingobacteriaceae	Pedobacter	NA	WA	0	0	0	0	0	0	0	0

Table A.10 (Page 1 of 2). Hub soil OTUs across all R and P values tested for Juglans nigra trees in Indiana (IN), Tennessee (TN), and Washington (WA).

	Kingdom	Phylum	Class	Order	Family	Genus	Species	State	p.00005.r0.6	p.00001.r0.6	p.0000005.r0.6	p.0000001.r0.6	p.0000005.r0.8	p.0000001.r0.8	p.0000005.r0.8	p.0000001.r0.8
Botu02964	Bacteria	Planctomycetes	Phycisphaerae	Tepidisphaerales	WD2101_soil_group	WD2101_soil_group_ge	NA	IN	1	1	0	0	1	1	0	0
FOtu00375	k__Fungi	p__Ascomycota	c__Sordariomycetes	o__Hypocreales	f__Hypocreales_fam_Incertae_sedis	g__Acremonium	s__Acremonium_furcatum	IN	1	0	0	0	1	0	0	0
Botu00061	Bacteria	Actinobacteria	Thermoleophilia	Gaiellales	uncultured	uncultured_ge	NA	IN	1	1	1	1	1	1	1	1
Botu00260	Bacteria	Actinobacteria	MB-A2-108	MB-A2-108_or	MB-A2-108_fa	MB-A2-108_ge	NA	IN	1	1	1	1	1	1	1	1
Botu00049	Bacteria	Actinobacteria	MB-A2-108	MB-A2-108_or	MB-A2-108_fa	MB-A2-108_ge	NA	IN	1	0	0	0	1	0	0	0
Botu00068	Bacteria	Chloroflexi	AD3	AD3_or	AD3_fa	AD3_ge	NA	IN	1	0	1	0	1	0	1	0
Botu00148	Bacteria	Acidobacteria	Acidobacteriia	Subgroup_2	Subgroup_2_fa	Subgroup_2_ge	NA	IN	1	1	1	0	1	1	1	0
Botu00265	Bacteria	Acidobacteria	Subgroup_6	Subgroup_6_or	Subgroup_6_fa	Subgroup_6_ge	NA	IN	1	0	0	0	1	0	0	0
Botu00851	Bacteria	Entotheonellaeota	Entotheonellia	Entotheonellales	Entotheonellaceae	Entotheonellaceae_ge	NA	IN	1	0	0	0	1	0	0	0
Botu01240	Bacteria	Chloroflexi	Anaerolineae	RBG-13-54-9	RBG-13-54-9_fa	RBG-13-54-9_ge	NA	IN	1	1	1	1	1	1	1	1
Botu00012	Archaea	Thaumarchaeota	Nitrososphaeria	Nitrososphaerales	Nitrososphaeraceae	Nitrososphaeraceae_ge	NA	IN	1	0	0	0	1	0	0	0
Botu00553	Bacteria	Acidobacteria	Subgroup_6	Subgroup_6_or	Subgroup_6_fa	Subgroup_6_ge	NA	IN	1	1	1	0	1	1	1	0
Botu01067	Bacteria	Proteobacteria	Gammaproteobacteria	Betaproteobacteriales	SC-I-84	SC-I-84_ge	NA	IN	1	0	0	0	1	0	0	0
Botu00615	Bacteria	Actinobacteria	Actinobacteria	Propionibacteriales	Propionibacteriaceae	Propionibacteriaceae_unclassifiec	NA	IN	1	1	1	1	1	1	1	1
Botu00699	Bacteria	Planctomycetes	Planctomycetacia	Pirellulales	Pirellulaceae	uncultured	NA	IN	1	1	1	1	1	1	1	1
Botu01232	Bacteria	Acidobacteria	Subgroup_6	Subgroup_6_or	Subgroup_6_fa	Subgroup_6_ge	NA	IN	1	0	0	0	1	0	0	0
Botu00113	Bacteria	Rokubacteria	NC10	Rokubacteriales	Rokubacteriales_fa	Rokubacteriales_ge	NA	IN	1	0	0	0	1	0	0	0
Botu00026	Bacteria	Proteobacteria	Alphaproteobacteria	Rhizobiales	Xanthobacteraceae	uncultured	NA	IN	1	1	1	0	1	1	1	0
Botu00240	Bacteria	Acidobacteria	Subgroup_6	Subgroup_6_or	Subgroup_6_fa	Subgroup_6_ge	NA	IN	1	1	1	1	1	1	1	1
Botu00131	Bacteria	Proteobacteria	Alphaproteobacteria	Rhizobiales	Xanthobacteraceae	Xanthobacteraceae_unclassified	NA	IN	1	0	0	0	1	0	0	0
Botu00137	Bacteria	Proteobacteria	Gammaproteobacteria	Betaproteobacteriales	Nitrosomonadaceae	mle1-7	NA	IN	1	1	0	0	1	1	0	0
Botu00230	Bacteria	Actinobacteria	Acidimicrobiia	Actinomarinales	uncultured	uncultured_ge	NA	IN	1	1	0	0	1	1	0	0
Botu00048	Bacteria	Verrucomicrobia	Verrucomicrobiae	Chthoniobacterales	Chthoniobacteraceae	Candidatus_Udaeobacter	NA	IN	1	1	1	0	1	1	1	0
Botu00273	Bacteria	Acidobacteria	Acidobacteriia	Acidobacteriales	uncultured	uncultured_ge	NA	IN	1	1	1	1	1	1	1	1
Botu00269	Bacteria	Proteobacteria	Gammaproteobacteria	Betaproteobacteriales	Nitrosomonadaceae	MND1	NA	IN	1	1	1	0	1	1	1	0
Botu01044	Bacteria	Actinobacteria	Acidimicrobiia	Actinomarinales	Actinomarinales_fa	Actinomarinales_ge	NA	IN	1	1	0	0	1	1	0	0
Botu01108	Bacteria	Planctomycetes	Planctomycetacia	Gemmatales	Gemmataceae	uncultured	NA	IN	1	1	0	0	1	1	0	0
Botu00578	Bacteria	Actinobacteria	Thermoleophilia	Solirubrobacterales	Solirubrobacteraceae	Conexibacter	NA	IN	1	0	0	0	1	0	0	0
Botu00833	Bacteria	Actinobacteria	Thermoleophilia	Solirubrobacterales	67-14	67-14_ge	NA	IN	1	0	0	0	1	0	0	0
Botu00023	Bacteria	Proteobacteria	Alphaproteobacteria	Rhizobiales	Xanthobacteraceae	Pseudolabrys	NA	IN	1	0	0	0	1	0	0	0
Botu00207	Bacteria	Proteobacteria	Gammaproteobacteria	Betaproteobacteriales	B1-7BS	B1-7BS_ge	NA	IN	0	1	1	1	0	1	1	1
Botu00815	Bacteria	Rokubacteria	NC10	Rokubacteriales	Rokubacteriales_fa	Rokubacteriales_ge	NA	IN	0	1	1	1	0	1	1	1
Botu00306	Bacteria	Actinobacteria	Actinobacteria	Corynebacteriales	Mycobacteriaceae	Mycobacterium	NA	IN	0	1	0	0	0	1	0	0
Botu00242	Bacteria	Proteobacteria	Alphaproteobacteria	Tistrellales	Geminicoccaceae	uncultured	NA	IN	0	1	1	1	0	1	1	1
FOtu00948	k__Fungi	p__Basidiomycota	c__Tremellomycetes	o__Cystofilobasidiales	f__Cystofilobasidiaceae	g__Cystofilobasidium	s__Cystofilobasidium_macerans	IN	0	1	1	0	0	1	1	0
Botu00076	Bacteria	Actinobacteria	Thermoleophilia	Gaiellales	Gaiellaceae	Gaiella	NA	IN	0	1	0	1	0	1	0	1
Botu00945	Bacteria	Proteobacteria	Gammaproteobacteria	Betaproteobacteriales	Nitrosomonadaceae	mle1-7	NA	IN	0	1	1	0	0	1	1	0
Botu01295	Bacteria	Planctomycetes	Planctomycetacia	Pirellulales	Pirellulaceae	Pirellulaceae_unclassified	NA	IN	0	1	1	0	0	1	1	0
Botu00127	Bacteria	Actinobacteria	Thermoleophilia	Gaiellales	uncultured	uncultured_ge	NA	IN	0	1	1	0	0	1	1	0
Botu00538	Bacteria	Proteobacteria	Deltaproteobacteria	RCP2-54	RCP2-54_fa	RCP2-54_ge	NA	IN	0	1	1	0	0	1	1	0
Botu00640	Bacteria	Acidobacteria	Subgroup_11	Subgroup_11_or	Subgroup_11_fa	Subgroup_11_ge	NA	IN	0	1	1	0	0	1	1	0
Botu00189	Bacteria	Actinobacteria	Thermoleophilia	Gaiellales	uncultured	uncultured_ge	NA	IN	0	1	1	0	0	1	1	0
Botu00341	Bacteria	Gemmatimonadetes	Gemmatimonadetes	Gemmatimonadales	Gemmatimonadaceae	uncultured	NA	IN	0	1	1	0	0	1	1	0
Botu00291	Bacteria	Bacteroidetes	Bacteroidia	Chitinophagales	Chitinophagaceae	Terrimonas	NA	IN	0	1	1	1	0	1	1	1
Botu00652	Bacteria	Proteobacteria	Gammaproteobacteria	Betaproteobacteriales	Burkholderiaceae	uncultured	NA	IN	0	1	1	1	0	1	1	1
Botu00295	Bacteria	Actinobacteria	Acidimicrobiia	IMCC26256	IMCC26256_fa	IMCC26256_ge	NA	IN	0	1	1	0	0	1	1	0
Botu00391	Bacteria	Proteobacteria	Alphaproteobacteria	Rhizobiales	Xanthobacteraceae	uncultured	NA	IN	0	0	1	0	0	0	1	0
Botu00807	Bacteria	Gemmatimonadetes	Gemmatimonadetes	Gemmatimonadales	Gemmatimonadaceae	Gemmatimonadaceae_unclassifie	NA	IN	0	0	1	0	0	0	1	0
Botu00654	Bacteria	Actinobacteria	Acidimicrobiia	Microtrichales	uncultured	uncultured_ge	NA	IN	0	0	1	0	0	0	1	0
Botu01159	Bacteria	Actinobacteria	Thermoleophilia	Solirubrobacterales	67-14	67-14_ge	NA	IN	0	0	1	0	0	0	1	0
Botu01328	Bacteria	Actinobacteria	Acidimicrobiia	Actinomarinales	uncultured	uncultured_ge	NA	IN	0	0	1	0	0	0	1	0
Botu00066	Bacteria	Actinobacteria	Thermoleophilia	Gaiellales	Gaiellales_unclassified	Gaiellales_unclassified	NA	IN	0	0	1	0	0	0	1	0
Botu00369	Bacteria	Acidobacteria	Subgroup_6	Subgroup_6_unclassified	Subgroup_6_unclassified	Subgroup_6_unclassified	NA	IN	0	0	1	1	0	0	1	1
Botu00667	Bacteria	Nitrospirae	Nitrospira	Nitrospirales	Nitrospiraceae	Nitrospira	NA	IN	0	0	1	0	0	0	1	0
Botu00082	Bacteria	Acidobacteria	Subgroup_6	Subgroup_6_or	Subgroup_6_fa	Subgroup_6_ge	NA	IN	0	0	0	1	0	0	0	1
Botu00013	Bacteria	Proteobacteria	Alphaproteobacteria	Rhizobiales	Xanthobacteraceae	Bradyrhizobium	NA	TN	1	0	0	0	1	0	0	0
Botu00288	Bacteria	Actinobacteria	Thermoleophilia	Gaiellales	Gaiellales_unclassified	Gaiellales_unclassified	NA	TN	1	0	1	0	1	0	1	0
Botu01137	Bacteria	Acidobacteria	Acidobacteriia	Acidobacteriales	Koribacteraceae	Candidatus_Koribacter	NA	TN	1	1	1	1	1	1	1	1
Botu01144	Bacteria	Acidobacteria	Acidobacteriia	Subgroup_2	Subgroup_2_fa	Subgroup_2_ge	NA	TN	1	1	1	1	1	1	1	1
Botu01309	Bacteria	Acidobacteria	Acidobacteriia	Acidobacteriales	Acidobacteriaceae_(Subgroup_1)	uncultured	NA	TN	1	0	0	0	1	0	0	0
Botu01811	Bacteria	Planctomycetes	Planctomycetacia	Gemmatales	Gemmataceae	uncultured	NA	TN	1	0	0	0	1	0	0	0
Botu00504	Bacteria	Acidobacteria	Blastocatellia_(Subgroup_4)	Blastocatellales	Blastocatellaceae	uncultured	NA	TN	1	1	1	0	1	1	1	0
Botu01934	Bacteria	Acidobacteria	Subgroup_6	Subgroup_6_or	Subgroup_6_fa	Subgroup_6_ge	NA	TN	1	1	1	1	1	1	1	1
Botu02654	Bacteria	Planctomycetes	Planctomycetacia	Gemmatales	Gemmataceae	uncultured	NA	TN	1	1	0	0	1	1	0	0
FOtu00217	k__Fungi	p__Ascomycota	c__Sordariomycetes	o__Hypocreales	f__Nectriaceae	f__Nectriaceae_unclassified	f__Nectriaceae_unclassified	TN	1	0	0	0	1	0	0	0
Botu00506	Bacteria	Actinobacteria	Acidimicrobiia	Microtrichales	uncultured	uncultured_ge	NA	TN	1	1	0	0	1	1	0	0
Botu00016	Bacteria	Verrucomicrobia	Verrucomicrobiae	Chthoniobacterales	Xiphinematobacteraceae	Candidatus_Xiphinematobacter	NA	TN	1	1	0	0	1	1	0	0
Botu00049	Bacteria	Actinobacteria	MB-A2-108	MB-A2-108_or	MB-A2-108_fa	MB-A2-108_ge	NA	TN	1	1	0	1	1	1	0	1
Botu00054	Bacteria	Actinobacteria	Thermoleophilia	Solirubrobacterales	67-14	67-14_ge	NA	TN	1	1	1	1	1	1	1	1
Botu00072	Bacteria	Proteobacteria	Gammaproteobacteria	Steroidobacterales	Steroidobacteraceae	Steroidobacter	NA	TN	1	1	1	1	1	1	1	1
Botu00107	Bacteria	Proteobacteria	Gammaproteobacteria	Steroidobacterales	Steroidobacteraceae	uncultured	NA	TN	1	1	1	1	1	1	1	1
Botu00173	Bacteria	Acidobacteria	Acidobacteriia	Acidobacteriales	uncultured	uncultured_ge	NA	TN	1	0	0	1	1	0	0	1
Botu00226	Bacteria	Acidobacteria	Subgroup_5	Subgroup_5_or	Subgroup_5_fa	Subgroup_5_ge	NA	TN	1	0	1	1	1	0	1	1
Botu00239	Bacteria	Actinobacteria	Thermoleophilia	Gaiellales	uncultured	uncultured_ge	NA	TN	1	1	0	0	1	1	0	0
Botu00247	Bacteria	Gemmatimonadetes	Gemmatimonadetes	Gemmatimonadales	Gemmatimonadaceae	Gemmatimonadaceae_unclassifie	NA	TN	1	1	1	0	1	1	1	0
Botu00382	Bacteria	Gemmatimonadetes	Gemmatimonadetes	Gemmatimonadales	Gemmatimonadaceae	uncultured	NA	TN	1	0	0	0	1	0	0	0
Botu00455	Bacteria	Acidobacteria	Acidobacteriia	Solibacterales	Solibacteraceae_(Subgroup_3)	Bryobacter	NA	TN	1	1	1	1	1	1	1	1
Botu00459	Bacteria	Chloroflexi	Ktedonobacteria	Ktedonobacterales	JG30-KF-AS9	JG30-KF-AS9_ge	NA	TN	1	0	0	0	1	0	0	0
Botu00508	Bacteria	Actinobacteria	Thermoleophilia	Gaiellales	uncultured	uncultured_ge	NA	TN	1	0	0	1	1	0	0	1
Botu01092	Bacteria	Gemmatimonadetes	Gemmatimonadetes	Gemmatimonadales	Gemmatimonadaceae	Gemmatimonadaceae_unclassifie	NA	TN	1	1	0	0	1	1	0	0
Botu01161	Bacteria	Proteobacteria	Gammaproteobacteria	Xanthomonadales	Rhodanobacteraceae	Dokdonella	NA	TN	1	0	0	0	1	0	0	0
Botu02116	Bacteria	Proteobacteria	Alphaproteobacteria	uncultured	uncultured_fa	uncultured_ge	NA	TN	1	0	0	0	1	0	0	0
Botu00082	Bacteria	Acidobacteria	Subgroup_6	Subgroup_6_or	Subgroup_6_fa	Subgroup_6_ge	NA	TN	1	0	0	0	1	0	0	0
Botu00124	Bacteria	Acidobacteria	Subgroup_6	Subgroup_6_or	Subgroup_6_fa	Subgroup_6_ge	NA	TN	1	1	1	1	1	1	1	1
Botu01099	Bacteria	Actinobacteria	Actinobacteria	Frankiales	Acidothermaceae	Acidothermus	NA	TN	1	0	0	0	1	0	0	0
Botu00068	Bacteria	Chloroflexi	AD3	AD3_or	AD3_fa	AD3_ge	NA	TN	0	1	1	0	0	1	1	0
Botu00103	Bacteria	Acidobacteria	Acidobacteriia	Acidobacteriales	Acidobacteriales_unclassified	Acidobacteriales_unclassified	NA	TN	0	1	1	1	0	1	1	1
Botu00178	Bacteria	Verrucomicrobia	Verrucomicrobiae	Chthoniobacterales	Chthoniobacteraceae	Candidatus_Udaeobacter	NA	TN	0	1	0	0	0	1	0	0
Botu00319	Bacteria	Proteobacteria	Gammaproteobacteria	Betaproteobacteriales	Burkholderiaceae	Burkholderia-Caballeronia-Parabu	NA	TN	0	1	1	0	0	1	1	0
Botu00320	Bacteria	Actinobacteria	Actinobacteria	Streptomycetales	Streptomycetaceae	Streptomyces	NA	TN	0	1	1	1	0	1	1	1
Botu00374	Bacteria	Actinobacteria	Thermoleophilia	Solirubrobacterales	Solirubrobacterales_unclassified	Solirubrobacterales_unclassified	NA	TN	0	1	0	1	0	1	0	1
Botu00785	Bacteria	Acidobacteria	Acidobacteriia	Solibacterales	Solibacteraceae_(Subgroup_3)	Bryobacter	NA	TN	0	1	1	1	0	1	1	1
Botu00942	Bacteria	Chloroflexi	Ktedonobacteria	C0119	C0119_fa	C0119_ge	NA	TN	0	1	0	0	0	1	0	0
Botu01060	Bacteria	Planctomycetes	Phycisphaerae	Tepidisphaerales	WD2101_soil_group	WD2101_soil_group_ge	NA	TN	0	1	0	0	0	1	0	0
Botu01227	Bacteria	Proteobacteria	Gammaproteobacteria	Betaproteobacteriales	SC-I-84	SC-I-84_ge	NA	TN	0	1	1	1	0	1	1	1
Botu01423	Bacteria	Chloroflexi	OLB14	OLB14_or	OLB14_fa	OLB14_ge	NA	TN	0	1	1	0	0	1	1	0

Table A.10. Continued (Page 2 of 2)

	Kingdom	Phylum	Class	Order	Family	Genus	Species	State	p0.00005.r0.6	p0.00001.r0.6	p0.000005.r0.6	p0.000001.r0.6	p0.00005.r0.8	p0.00001.r0.8	p0.000005.r0.8	p0.000001.r0.8
Botu02299	Bacteria	Actinobacteria	Acidimicrobiia	IMCC26256	IMCC26256_fa	IMCC26256_ge	NA	TN	0	1	0	0	0	1	0	0
Botu00005	Archaea	Thaumarchaeota	Nitrososphaeria	Nitrososphaerales	Nitrososphaeraceae	Nitrososphaeraceae_ge	NA	TN	0	1	1	1	0	1	1	1
Botu00035	Bacteria	Acidobacteria	Subgroup_6	Subgroup_6_or	Subgroup_6_fa	Subgroup_6_ge	NA	TN	0	1	1	0	0	1	1	0
Botu00436	Bacteria	Actinobacteria	Thermoleophilia	Gaiellales	Gaiellales_unclassified	Gaiellales_unclassified	NA	TN	0	1	0	0	0	1	0	0
Botu00041	Bacteria	Proteobacteria	Gammaproteobacteria	PLTA13	PLTA13_fa	PLTA13_ge	NA	TN	0	1	1	0	0	1	1	0
Botu00442	Bacteria	Actinobacteria	Thermoleophilia	Gaiellales	uncultured	uncultured_ge	NA	TN	0	1	1	1	0	1	1	1
Botu00098	Bacteria	Acidobacteria	Subgroup_6	Subgroup_6_or	Subgroup_6_fa	Subgroup_6_ge	NA	TN	0	1	0	0	0	1	0	0
Botu00797	Bacteria	Planctomycetes	Phycisphaerae	Tepidisphaerales	WD2101_soil_group	WD2101_soil_group_ge	NA	TN	0	1	0	0	0	1	0	0
Botu01403	Bacteria	Planctomycetes	Planctomycetacia	Pirellulales	Pirellulaceae	uncultured	NA	TN	0	0	1	0	0	0	1	0
Botu00252	Bacteria	Actinobacteria	Thermoleophilia	Solirubrobacterales	Solirubrobacteraceae	Conexibacter	NA	TN	0	0	1	0	0	0	1	0
Botu00614	Bacteria	Acidobacteria	Acidobacteriia	Acidobacteriales	Acidobacteriales_unclassified	Acidobacteriales_unclassified	NA	TN	0	0	1	1	0	0	1	1
Botu00998	Bacteria	Chloroflexi	Gitt-GS-136	Gitt-GS-136_or	Gitt-GS-136_fa	Gitt-GS-136_ge	NA	TN	0	0	1	0	0	0	1	0
Botu00814	Bacteria	Actinobacteria	Thermoleophilia	Gaiellales	uncultured	uncultured_ge	NA	TN	0	0	1	0	0	0	1	0
FOtu00051	k__Fungi	p__Ascomycota	c__Dothideomycetes	o__Pleosporales	f__Pleosporaceae	g__Alternaria	s__Alternaria_alternata	TN	0	0	1	1	0	0	1	1
Botu00259	Bacteria	Acidobacteria	Acidobacteriia	Acidobacteriales	uncultured	uncultured_ge	NA	TN	0	0	0	1	0	0	0	1
Botu00283	Bacteria	Proteobacteria	Alphaproteobacteria	Tistrellales	Geminicoccaceae	Candidatus_Alysiosphaera	NA	TN	0	0	0	1	0	0	0	1
Botu01579	Bacteria	Proteobacteria	Gammaproteobacteria	Betaproteobacteriales	SC-I-84	SC-I-84_ge	NA	TN	0	0	0	1	0	0	0	1
Botu00308	Bacteria	Actinobacteria	Thermoleophilia	Gaiellales	uncultured	uncultured_ge	NA	TN	0	0	0	1	0	0	0	1
Botu00642	Bacteria	Planctomycetes	Phycisphaerae	Tepidisphaerales	WD2101_soil_group	WD2101_soil_group_ge	NA	TN	0	0	0	1	0	0	0	1
FOtu00195	k__Fungi	p__Ascomycota	p__Ascomycota_unclassified	p__Ascomycota_unclassifie	p__Ascomycota_unclassified	p__Ascomycota_unclassified	p__Ascomycota_unclassified	WA	1	1	1	0	1	1	1	0
FOtu00529	k__Fungi	p__Ascomycota	c__Eurotiomycetes	c__Eurotiomycetes_unclass	c__Eurotiomycetes_unclassified	c__Eurotiomycetes_unclassified	c__Eurotiomycetes_unclassified	WA	1	1	1	1	1	1	1	1
FOtu00714	k__Fungi	p__Ascomycota	c__Eurotiomycetes	c__Eurotiomycetes_unclass	c__Eurotiomycetes_unclassified	c__Eurotiomycetes_unclassified	c__Eurotiomycetes_unclassified	WA	1	1	0	0	1	1	0	0
Botu00190	Bacteria	Acidobacteria	Blastocatellia_(Subgroup_4)	Blastocatellales	Blastocatellaceae	uncultured	NA	WA	1	0	0	0	1	0	0	0
Botu01450	Bacteria	Chloroflexi	Chloroflexia	Thermomicrobiales	JG30-KF-CM45	JG30-KF-CM45_ge	NA	WA	1	1	0	0	1	1	0	0
Botu00028	Archaea	Thaumarchaeota	Nitrososphaeria	Nitrososphaerales	Nitrososphaeraceae	Nitrososphaeraceae_ge	NA	WA	1	1	1	0	1	1	1	0
FOtu00073	k__Fungi	p__Ascomycota	c__Sordariomycetes	o__Hypocreales	o__Hypocreales_unclassified	o__Hypocreales_unclassified	o__Hypocreales_unclassified	WA	1	0	0	0	1	0	0	0
FOtu00151	k__Fungi	p__Ascomycota	c__Eurotiomycetes	o__Eurotiales	f__Aspergillaceae	g__Penicillium	s__Penicillium_pimiteouiense	WA	1	0	0	0	1	0	0	0
FOtu00079	k__Fungi	p__Ascomycota	c__Sordariomycetes	o__Chaetosphaeriales	f__Chaetosphaeriaceae	f__Chaetosphaeriaceae_unclassifi	f__Chaetosphaeriaceae_unclassifie	WA	1	0	0	1	1	0	0	1
Botu00009	Bacteria	Verrucomicrobia	Verrucomicrobiae	Chthoniobacterales	Chthoniobacteraceae	Candidatus_Udaeobacter	NA	WA	1	0	0	0	1	0	0	0
Botu00173	Bacteria	Acidobacteria	Acidobacteriia	Acidobacteriales	uncultured	uncultured_ge	NA	WA	1	0	0	1	1	0	0	1
Botu00222	Bacteria	Proteobacteria	Alphaproteobacteria	Rhizobiales	Rhizobiaceae	Rhizobiaceae_unclassified	NA	WA	1	0	0	0	1	0	0	0
Botu00253	Bacteria	Verrucomicrobia	Verrucomicrobiae	Chthoniobacterales	Chthoniobacteraceae	Candidatus_Udaeobacter	NA	WA	1	0	0	0	1	0	0	0
Botu00301	Bacteria	Actinobacteria	Thermoleophilia	Gaiellales	uncultured	uncultured_ge	NA	WA	1	1	1	1	1	1	1	1
Botu00126	Bacteria	Actinobacteria	Actinobacteria	Frankiales	Nakamurellaceae	Nakamurella	NA	WA	1	0	0	0	1	0	0	0
Botu00789	Bacteria	Bacteroidetes	Bacteroidia	Cytophagales	Microscillaceae	Ohtaekwangia	NA	WA	1	0	0	1	1	0	0	1
Botu00869	Bacteria	Proteobacteria	Alphaproteobacteria	Alphaproteobacteria_unclas	Alphaproteobacteria_unclassified	Alphaproteobacteria_unclassified	NA	WA	1	1	0	1	1	1	0	1
Botu00100	Bacteria	Actinobacteria	Actinobacteria	Micrococcales	Intrasporangiaceae	Intrasporangiaceae_unclassified	NA	WA	1	0	0	0	1	0	0	0
Botu00181	Bacteria	Proteobacteria	Gammaproteobacteria	PLTA13	PLTA13_fa	PLTA13_ge	NA	WA	1	0	0	0	1	0	0	0
Botu00270	Bacteria	Proteobacteria	Alphaproteobacteria	Rhizobiales	Rhizobiaceae	Rhizobiaceae_unclassified	NA	WA	1	0	0	0	1	0	0	0
Botu01897	Bacteria	Firmicutes	Bacilli	Bacillales	Planococcaceae	Planococcaceae_unclassified	NA	WA	1	0	0	0	1	0	0	0
Botu00280	Bacteria	Actinobacteria	Thermoleophilia	Gaiellales	Gaiellales_unclassified	Gaiellales_unclassified	NA	WA	1	0	1	0	1	0	1	0
Botu00399	Bacteria	Actinobacteria	Actinobacteria	Streptosporangiales	Thermomonosporaceae	Actinoallomurus	NA	WA	1	1	1	0	1	1	1	0
Botu00496	Bacteria	Actinobacteria	Thermoleophilia	Solirubrobacterales	67-14	67-14_ge	NA	WA	1	1	0	0	1	1	0	0
Botu00857	Bacteria	Latescibacteria	Latescibacteria_cl	Latescibacteria_or	Latescibacteria_fa	Latescibacteria_ge	NA	WA	1	0	0	0	1	0	0	0
Botu00382	Bacteria	Gemmatimonadetes	Gemmatimonadetes	Gemmatimonadales	Gemmatimonadaceae	uncultured	NA	WA	1	0	0	0	1	0	0	0
Botu00548	Bacteria	Proteobacteria	Deltaproteobacteria	Myxococcales	Archangiaceae	Anaeromyxobacter	NA	WA	1	0	0	0	1	0	0	0
Botu00070	Bacteria	Rokubacteria	NC10	Rokubacteriales	Rokubacteriales_fa	Rokubacteriales_ge	NA	WA	1	0	0	0	1	0	0	0
Botu00487	Bacteria	Firmicutes	Bacilli	Bacillales	Planococcaceae	Sporosarcina	NA	WA	1	1	0	0	1	1	0	0
Botu00403	Bacteria	Actinobacteria	Thermoleophilia	Solirubrobacterales	67-14	67-14_ge	NA	WA	1	0	0	0	1	0	0	0
Botu00394	Bacteria	Actinobacteria	Thermoleophilia	Gaiellales	uncultured	uncultured_ge	NA	WA	1	0	0	0	1	0	0	0
FOtu00657	k__Fungi	p__Ascomycota	c__Eurotiomycetes	o__Onygenales	f__Gymnoascaceae	g__unclassified_Gymnoascaceae	s__Gymnoascaceae_sp	WA	1	0	0	0	1	0	0	0
FOtu00339	k__Fungi	p__Ascomycota	c__Sordariomycetes	o__Sordariales	f__Lasiosphaeriaceae	g__Podospora	g__Podospora_unclassified	WA	1	0	0	0	1	0	0	0
Botu00256	Bacteria	Actinobacteria	Actinobacteria	Micromonosporales	Micromonosporaceae	Luedemannella	NA	WA	1	1	1	0	1	1	1	0
FOtu00261	k__Fungi	p__Ascomycota	c__Sordariomycetes	o__Hypocreales	f__Hypocreaceae	g__Trichoderma	g__Trichoderma_unclassified	WA	1	0	0	0	1	0	0	0
Botu00357	Bacteria	Proteobacteria	Gammaproteobacteria	Betaproteobacteriales	Nitrosomonadaceae	MND1	NA	WA	1	1	0	0	1	1	0	0
Botu00646	Bacteria	Latescibacteria	Latescibacteria	Latescibacterales	Latescibacteraceae	Latescibacteraceae_ge	NA	WA	1	0	0	0	1	0	0	0
Botu01284	Bacteria	Actinobacteria	Acidimicrobiia	Acidimicrobiia_unclassified	Acidimicrobiia_unclassified	Acidimicrobiia_unclassified	NA	WA	1	1	1	0	1	1	1	0
Botu00049	Bacteria	Actinobacteria	MB-A2-108	MB-A2-108_or	MB-A2-108_fa	MB-A2-108_ge	NA	WA	1	0	0	0	1	0	0	0
FOtu00774	k__Fungi	p__Ascomycota	c__Eurotiomycetes	o__Onygenales	f__Onygenaceae	g__Auxarthron	s__Auxarthron_umbrinum	WA	1	0	0	0	1	0	0	0
Botu02219	Bacteria	Gemmatimonadetes	Gemmatimonadetes	Gemmatimonadales	Gemmatimonadaceae	Gemmatimonadaceae_unclassifie	NA	WA	1	0	0	0	1	0	0	0
Botu00226	Bacteria	Acidobacteria	Subgroup_5	Subgroup_5_or	Subgroup_5_fa	Subgroup_5_ge	NA	WA	1	0	0	0	1	0	0	0
Botu00932	Bacteria	Planctomycetes	Planctomycetacia	Pirellulales	Pirellulaceae	uncultured	NA	WA	1	0	0	1	1	0	0	1
Botu00050	Bacteria	Acidobacteria	Subgroup_6	Subgroup_6_or	Subgroup_6_fa	Subgroup_6_ge	NA	WA	1	1	0	0	1	1	0	0
Botu00200	Bacteria	Actinobacteria	Thermoleophilia	Gaiellales	uncultured	uncultured_ge	NA	WA	1	0	0	0	1	0	0	0
Botu00068	Bacteria	Chloroflexi	AD3	AD3_or	AD3_fa	AD3_ge	NA	WA	1	0	0	1	1	0	0	1
Botu00451	Bacteria	Actinobacteria	Thermoleophilia	Gaiellales	uncultured	uncultured_ge	NA	WA	1	0	0	0	1	0	0	0
Botu00245	Bacteria	Latescibacteria	Latescibacteria_cl	Latescibacteria_or	Latescibacteria_fa	Latescibacteria_ge	NA	WA	1	0	0	0	1	0	0	0
FOtu00029	k__Fungi	p__Mortierellomycota	c__Mortierellomycetes	o__Mortierellales	f__Mortierellaceae	g__Mortierella	g__Mortierella_unclassified	WA	1	0	0	0	1	0	0	0
FOtu00245	k__Fungi	p__Ascomycota	c__Eurotiomycetes	o__Eurotiales	f__Aspergillaceae	g__Aspergillus	g__Aspergillus_unclassified	WA	0	1	0	0	0	1	0	0
Botu00430	Bacteria	Chloroflexi	Chloroflexia	Thermomicrobiales	JG30-KF-CM45	JG30-KF-CM45_ge	NA	WA	0	1	1	0	0	1	1	0
Botu01266	Bacteria	Armatimonadetes	uncultured	uncultured_or	uncultured_fa	uncultured_ge	NA	WA	0	1	0	0	0	1	0	0
Botu01278	Bacteria	Acidobacteria	Subgroup_25	Subgroup_25_or	Subgroup_25_fa	Subgroup_25_ge	NA	WA	0	1	0	0	0	1	0	0
Botu00625	Bacteria	Firmicutes	Bacilli	Bacillales	Bacillales_unclassified	Bacillales_unclassified	NA	WA	0	1	0	1	0	1	0	1
Botu02285	Bacteria	Proteobacteria	Alphaproteobacteria	Acetobacterales	Acetobacteraceae	uncultured	NA	WA	0	1	0	0	0	1	0	0
Botu00255	Bacteria	Proteobacteria	Gammaproteobacteria	Betaproteobacteriales	Nitrosomonadaceae	Ellin6067	NA	WA	0	1	0	0	0	1	0	0
FOtu00374	k__Fungi	p__Ascomycota	c__Eurotiomycetes	o__Chaetothyriales	f__Herpotrichiellaceae	g__Cladophialophora	s__Cladophialophora_sp	WA	0	1	0	0	0	1	0	0
Botu00087	Archaea	Thaumarchaeota	Nitrososphaeria	Nitrososphaerales	Nitrososphaeraceae	Candidatus_Nitrososphaera	NA	WA	0	1	0	0	0	1	0	0
Botu00092	Bacteria	Bacteroidetes	Bacteroidia	Chitinophagales	Chitinophagaceae	Chitinophagaceae_unclassified	NA	WA	0	1	1	0	0	1	1	0
Botu00024	Bacteria	Firmicutes	Bacilli	Bacillales	Bacillales_unclassified	Bacillales_unclassified	NA	WA	0	0	1	0	0	0	1	0
Botu00192	Bacteria	Chloroflexi	Gitt-GS-136	Gitt-GS-136_or	Gitt-GS-136_fa	Gitt-GS-136_ge	NA	WA	0	0	1	0	0	0	1	0
Botu00045	Bacteria	Nitrospirae	Nitrospira	Nitrospirales	Nitrospiraceae	Nitrospira	NA	WA	0	0	0	1	0	0	0	1
Botu00414	Bacteria	Planctomycetes	OM190	OM190_or	OM190_fa	OM190_ge	NA	WA	0	0	0	1	0	0	0	1
Botu00803	Bacteria	Acidobacteria	Acidobacteriia	Subgroup_2	Subgroup_2_fa	Subgroup_2_ge	NA	WA	0	0	0	1	0	0	0	1
Botu01055	Bacteria	Bacteroidetes	Bacteroidia	Cytophagales	Microscillaceae	uncultured	NA	WA	0	0	0	1	0	0	0	1
FOtu00088	k__Fungi	p__Ascomycota	c__Leotiomycetes	o__Helotiales	f__Helotiaceae	g__Tetracladium	s__Tetracladium_sp	WA	0	0	0	1	0	0	0	1
Botu00005	Archaea	Thaumarchaeota	Nitrososphaeria	Nitrososphaerales	Nitrososphaeraceae	Nitrososphaeraceae_ge	NA	WA	0	0	0	1	0	0	0	1
Botu00055	Bacteria	Actinobacteria	Actinobacteria	Micrococcales	Microbacteriaceae	Microbacterium	NA	WA	0	0	0	1	0	0	0	1
Botu00177	Bacteria	Proteobacteria	Gammaproteobacteria	Betaproteobacteriales	Nitrosomonadaceae	IS-44	NA	WA	0	0	0	1	0	0	0	1
Botu00272	Bacteria	Acidobacteria	Blastocatellia_(Subgroup_4)	Pyrinomonadales	Pyrinomonadaceae	RB41	NA	WA	0	0	0	1	0	0	0	1

APPENDIX B. SUPPLEMENTAL MATERIAL FOR CHAPTER 5

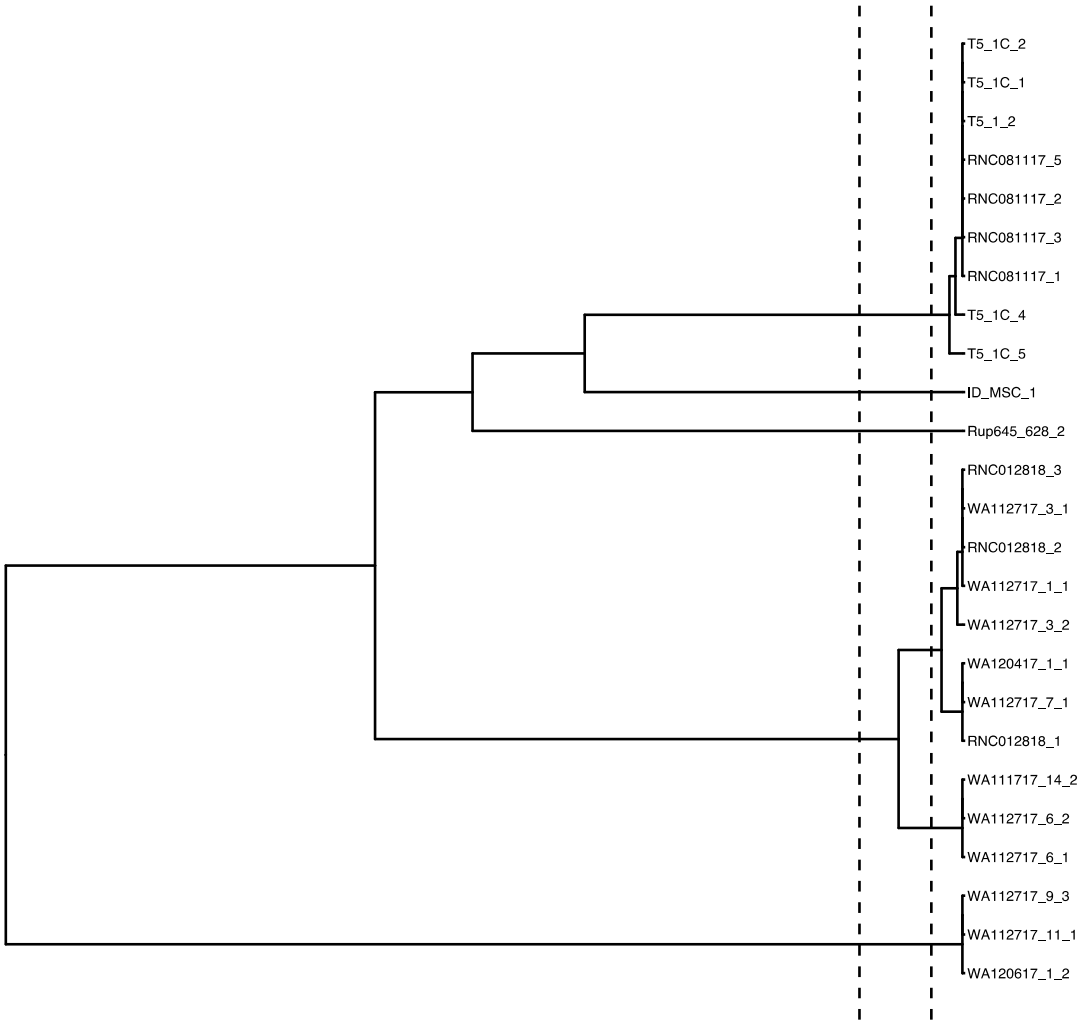

Fig B.1. Cytochrome oxidase *c* subunit 1-alpha mitochondrial DNA (COI-α mtDNA) UPGMA cluster analysis of pairwise nucleotide distances showing within-taxon population variation of *Bursaphelenchus juglandis* and *Panagrolaimus* sp. Vertical dashed lines represent 97 and 99% sequence similarity cutoff, left to right. From top to bottom, the five longest inner branches that circumscribe each major clade connect to *Panagrolaimus* sp. (n = 9), *Rhabditolaimus* sp. (n = 1), *Ditylenchus* sp. (n = 1), *B. juglandis* (n = 11), and cf. *Ektaphelenchus* sp. (n = 3).

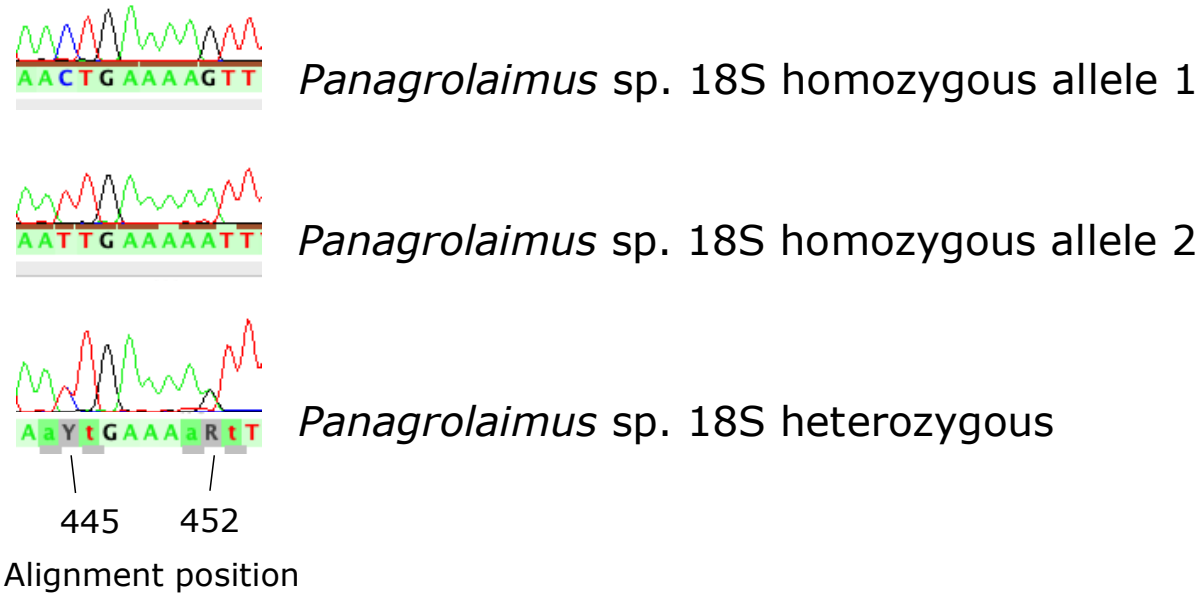

Fig S2. Alignments of 18S sequences from *Panagrolaimus* isolates showing sequences from individuals that were homo- and heterozygous for two alleles present in the population.